eman ta zabal zazu

Universidad del País Vasco
Euskal Herriko Unibertsitatea

FACULTAD DE FARMACIA

DEPARTAMENTO DE QUÍMICA ORGÁNICA I

Design and Synthesis of Novel Topoisomerase I Inhibitors. 1,5-Naphthyridine Derivatives with Antiproliferative Activity.

MEMORIA PRESENTADA POR

MARÍA GONZÁLEZ SÁENZ

PARA OPTAR AL GRADO DE DOCTOR CON MENCIÓN "DOCTOR INTERNACIONAL"

Vitoria-Gasteiz 2016

AGRADECIMIENTOS

Quisiera agradecer al Dr. Francisco Palacios Gambra, la Dra. Gloria Rubiales Alcaine y la Dra. Concepción Alonso Pérez por la dirección y supervisión de este trabajo, así como por darme la posibilidad de formar parte de este proyecto tan ambicioso y apasionante.

I am extremely grateful to Prof. Birgitta Ruth Knudsen for giving me the opportunity of joining her research group in Aarhus University, for encouragement and of course, for getting me involved in TopI world. I will never forget your generosity and our scientific discussions. Thank you for your patience when explaining me molecular biology, I will not forget those papers drawn with DNA substrates and that funny group meetings. In this adventure in Molecular Biology nothing would have been possible without my mentor Dr. Cinzia Tesauro. Cinzia, thank you for lend a hand even before we meet each other, I will always remember our long days at the lab and our happiness when results were successful. I still miss the coffee-times, cakes, walks and of course your home-made pizzas.

Agradecer al Dr. Jesús De los Santos (Delos) por haberse convertido en una persona tan especial para mí en este camino. He aprendido de tu rigurosidad y elegancia a la hora de trabajar en el laboratorio pero también de tú increíble forma de ser. Gracias por transmitirme esa tranquilidad que tantas veces he necesitado y ser mi mayor apoyo en los días más difíciles. Un placer trabajar y aprender contigo y espero tenerte cerca para siempre.

Y por supuesto y súper orgullosa, GRACIAS papá, GRACIAS mamá, GRACIAS tato y GRACIAS Maikel. Mis pilares fundamentales sin los cuáles esta etapa no habría podido llegar a su fin. Papá, en este momento tu serías el hombre más feliz de este mundo si me estuvieras viendo, pero el destino ha querido que lo estés disfrutando desde otro lugar pero igual de cerca que si estuvieras aquí. Gracias por trasmitirme siempre lo orgulloso que estabas de mí y por quererme incondicionalmente. Tú y mamá sois los verdaderos responsables de que haya llegado hasta aquí por vuestra implacable educación y por

anteponer pasar cada minuto libre a mi lado además de por darme siempre lo mejor. Mamá gracias por no permitirme quedarme atrás, trasmitirme esos valores tan necesarios como mujer y quererme tanto. Tato, no tengo palabras para agradecerte lo feliz que me hace tenerte tan cerca y compartirlo todo contigo. Gracias por escucharme cada vez que lo necesito, por sacar la mejor de mis sonrisas y por ser el mejor tato del mundo. Abuelita, gracias por esas lecciones de vida que me hacen cada día más fuerte, un claro ejemplo a seguir. Me encanta como disfrutas con mis logros y la ilusión con la que estás viviendo esta etapa y las ganas que tienes de ver la defensa de esta Tesis.

Y por supuesto mi chico, gracias Maikel por tu inmensa paciencia, por cuidarme cada día como si no hubiera un mañana y por hacerme tan feliz. Cerramos una etapa más juntos para abrir otras muchas llenas de buenos momentos. Gracias porque sin saber cómo funcionaba este mundillo, te has ido acostumbrando a todo lo que ha ido viniendo. Esto no habría sido posible sin tenerte tan cerca. Gracias Nieves y Jesús por acogerme desde el primer día como a una hija y compartir esta experiencia conmigo dándome siempre vuestro apoyo.

A todo el resto de mi familia y mis amig@s por interesaros y preocuparos siempre por mí. Gracias Amaya y Estibaliz por todos los momentos vividos desde los 3 añitos. Nere, espero que lo que la química ha unido no lo separe la distancia. Gracias por todo tu apoyo.

Por supuesto a todos mis compañeros de laboratorio, los ya doctores Guille, María y Ander, así como Zouhair, Annia y Endika. Al Dr. Javi Vicario por hacerme rabiar siempre que aparecía por el lab y a la Dra. Mirari Ayerbe por ese cariño con el que siempre me ha tratado. No puedo olvidarme de la Dra. Ane Garate y de Tania López, a las que me ha unido la biología. Gracias por enseñarme a evitar mal entendidos con los cultivos celulares, por tenderme una mano siempre que lo he necesitado y por todos los buenos ratos que me habéis hecho pasar. Anetxu, nunca olvidaré que esta tesis lleva un poquito de ti y espero que este sea el inicio de una bonita amistad.

Abbreviations, acronyms and symbols

Chapter 1

Introduction

Chapter 2

Synthesis of 1,5-naphthyridine derivatives

Chapter 3

Biological evaluation of the newly synthesized derivatives

4. Addenda

Leishmania and Topoisomerase I

5. Conclusions

Conclusions

5. Experimental section

Abbreviations, acronyms and symbols

aa	Amino acid(s)
AcOEt	Ethyl acetate
AcOH	Acetic Acid
AIBN	Azobisisobutyrinonitrile
Ar	Aryl
Aq.	Aqueous
Arg	Arginine
ATCC	American Type Culture Collection
ATP	Adenosine triphosphate
BA(s)	Brønsted acid(s)
BINOIL	1,1'-Bi-2-naphthol
°C	Celsius degree
Cat.	Catalyst
C_{arom}	Aromatic carbon
Cbz	Carboxybenzyl
CCK-8	Cell counting kit-8
cEPA	Conjugated eicosapentanoic acid
CL	Cutaneous leishmaniasis
COSY	Homonuclear correlation spectroscopy
CPT	Camptothecin
CPTs	Camptothecin derivatives
CSA	Camphorsulphonic acid
CTRL	Control
d	doublet
DBU	1,8-Diazabicyclo[5.4.0]undec-7-ene
DCE	1,2-Dichloroethane
DCL	Diffuse cutaneous leishmaniasis
dd	Doublet of doublets
ddd	Double doublet of doublets
DDQ	2,3-Dichloro-5,6-dicyano-1,4-benzoquinone
DFT	Density functional theory
DHBA	Dihydrobetulinic acid
DME	1,2-Dimethoxyethano
DMSO	Dimethylsulfoxide
DNA	Deoxyribonucleic acid

- **DSBs** Double strand breaks
- **E. coli** Escherichia coli
- **ee** Enantiomeric excess
- **e.g.** For example
- **Equiv.** Equivalent(s)
- **ERC** Electrocyclic ring closure
- **Et** Ethyl
- **EI** Electronic impact
- **FDA** Food and drug administration
- **g** Gram(s)
- **h** Hours
- **H_{arom}** Aromatic hydrogen
- **hCPT(s)** Homocamptothecin(s)
- **HDA** Hetero-Diels-Alder
- **HFIP** Hexafluoroisopropanol
- **His** Histidine
- **HIV** Human immunodeficiency virus
- **HMBC** Heteronuclear Multiple Bond Correlation
- **HMQC** Heteronuclear Multiple Quantum Correlation
- **HRMS** Hight resolution mass spectroscopy
- **Hz** Hertz
- **IC_{50}** Half maximal inhibitory concentration
- **IR** Infrared
- **I.S.** Selectivity index
- ***J*** Coupling constant
- **KDa** Kilo Dalton(s)
- **LC** Liquid Cromatography
- **LA(s)** Lewis acid(s)
- **LDA** Lithium diisopropylamine
- **L. donovani** Leishmania donovani
- **LdTopIL** Leishmania donovani topoisomerase I; large subunit
- **LdTopIS** Leishmania donovani topoisomerase I; small subunit
- **L. infantum** Leishmania infantum
- **Lys** Lysine
- **m** Multiplet
- **MCL** Mucocutaneous leishmaniasis
- **MCR(s)** Multicomponent reaction(s)
- **mg** Miligrams
- **min** Minute(s)
- **mL** Mililitre(s)

- **mmol** Milimol(s)
- **m.p.** Melting point
- **MS** Molecular sieves
- **MW** Microwave
- **NBS** *N*-bromosuccinimide
- **nm** Nanometers
- **NMR** Nuclear magnetic resonance
- **NOESY** Nuclear Overhauser effect spectroscopy
- **NTDs** Neglected tropical diseases
- **O.D**. Optical density
- **ORTEP** Oak Ridge Thermal Ellipsoid Plot
- **OXONE** Potassium peroxymonosulfate
- **PDB** Protein Data Bank
- **Ph** Phenyl
- **PKDL** Post Kala Azar leishmaniasis
- **Pos** Positive
- **q** Quadruplet
- **rt** Room temperature
- **s** Singlet, seconds
- **t** Triplet
- **T** Temperature
- **Tcc** Trans-2-(R-cumyl)cyclohexyl
- **TdpI** Tyrosyl DNA phosphodiesterase
- **TEA** Triethylamine
- **TFA** Trifluoroacetic acid
- **TFE** Trifluoroethanol
- **TfOH** Trifluoromethanosulfonic acid
- **THF** Tetrahydrofuran
- **THQ(s)** Tetrahydroquinoline(s)
- **TLC** Thin layer chromatography
- **TMS** Trimethylsylyl
- **TMSI** Trimethylsilyl iodide
- **TopI** Topoisomerase I
- **TopIcc** Topoisomerase I covalent complex
- **TPT** Topotecan
- **TS** Transition state
- **Tyr** Tyrosine
- **UV** Ultraviolet
- **VL** Visceral Leishmaniasis
- ***vs*** *versus*

- ***W*** watt
- **Y** Tyrosyl
- **Å** Amstrong
- **δ** Chemical shift
- **ν** frequency
- **λ** wavelength
- **µl** Microliters
- **µM** Micromolar

Chapter 1

Introduction

1.1. Cancer and Topoisomerases

Cancer is the name given to a collection of related diseases. In all types of cancer, some of the body cells begin to divide without stopping and spread into surrounding tissues. Cancer can start almost anywhere in the human body. Normally, human cells grow and divide to form new cells as the body needs them. When cells grow old or become damaged, they die, and new cells take their place. When cancer develops, however, this orderly process breaks down. As cells become more and more abnormal, old or damaged cells survive when they should die, and new cells are formed when they are not needed (Figure 1). These extra cells can divide without stopping and may form growths called tumors.

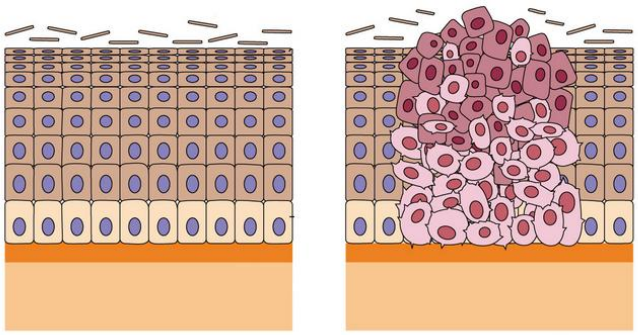

Figure 1. Normal cells *versus* cells forming a tumor.

Carcinogenesis (Figure 1) is the conversion of normal cells with control of the homeostatic feedback mechanism into cells capable of autonomous growth and invasion. The process by which normal cells become progressively transformed to malignancy is now known to require the sequential acquisition of mutations which arise as a consequence of damage to the genome. This damage can be the result of

endogenous processes such as errors in replication of DNA, the intrinsic chemical instability of certain DNA bases or from attack by free radicals generated during metabolism. DNA damage can also result from interactions with exogenous agents such as ionizing radiation, UV radiation and chemical carcinogens. Cells have evolved by means to repair such damage, but for several reasons errors occur and permanent changes in the genome, mutations, are introduced. The characterization of this mutational damage could lead to identify the basic causes of human cancer.[1] While cancer is clearly associated with an increase in cell number, alterations in mechanisms regulating new cell birth, or cell proliferation, are only one facet of the mechanism of cancer. Decreased rates of cell death, or apoptosis, are now known to contribute to certain types of cancer. Cancer is distinctive from other tumor forming processes because of its ability to invade neighboring tissues.

The adult human is composed of approximately 10^{15} cells, many of which are required to divide and differentiate in order to repopulate organs and tissues which require cell turnover. Obvious examples are cells in the basal layer of the skin which divide, differentiate and are finally sloughed, cells composing the epithelial layer of the intestines which turnover and must be replaced approximately every 10 days, and cells in the bone marrow which divide and differentiate to produce white and red cells whose life-time varies from 24 hours in the case of some leukocytes to 112 days for mature red cells. Cells which have the capacity for division and replenishment are called stem cells. It can be calculated that there are approximately 10^{12} divisions per day in these stem cells.[1] This exquisite control over cell multiplicity is achieved by a network of overlapping molecular mechanisms which govern cell proliferation on one hand and cell death, termed apoptosis when the result of a programmed event, on the other.

The cell cycle, or cell-division cycle[2] (Figure 2), is a series of events that take place in actively dividing eukaryote cells leading to its division and replication. In cells with a nucleus the cell cycle can be divided in four distinct phases: G_1 phase in which several

---

1 Bertram, J. S. *Mol. Aspects Med.* **2000**, *21*, 167-223.

2 Cooper, G. M. The Cell: A Molecular Approach. 2nd ed. Sunderland (MA): Sinauer Associates, **2000**.

metabolic changes prepare the cell for division, at a certain point, the restriction point, the cell is committed to division and moves into the S phase, where DNA synthesis is held, G_2 phase (collectively known as interphase) during which the cell grows, accumulates nutrients needed for mitosis and duplicates its DNA. M phase is itself composed of two tightly coupled processes: mitosis, during which the cell splits itself into two distinct cells, often called "daughter cells" which involves replication of the chromosomes and cytokinesis, in which the cell's cytoplasm divides in half forming distinct cells. Activation of each phase is dependent on the proper progression and completion of the previous one. Cells that have temporarily or reversibly stopped dividing are said to have entered into a state of quiescence called G_0 phase.

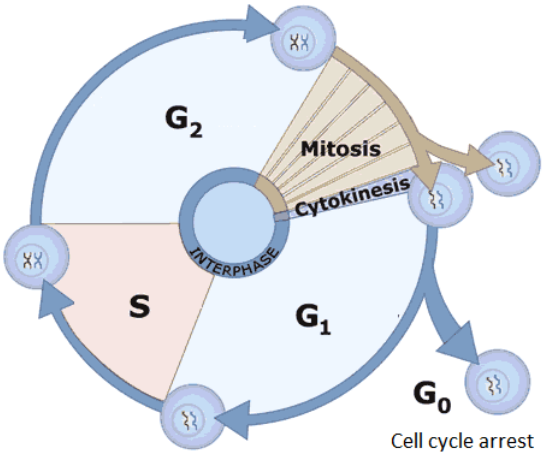

Figure 2. The cell cycle.

In normal cells, cell division only takes place when a chemical signal is received. These signals are interpretated in the nucleus, cells reproduce the genetic information and then they divide into two identical daughter cells through mitosis. Cancer cells however, do not obey this rule and they divide even if they don't receive the appropriate signals. In addition to the signal that normal cells receive telling them to divide they are also told when to stop dividing. This fact prevents too many cells from

being made. In fact, the cell division process is a highly ordered process; this is a critical issue in cancer since cancer cells don't answer to normal signals for division and thus, they grow uncontrollably and make tumors.

Cell cycle checkpoints[3] are regulatory pathways that control the order and timing of cell cycle transitions and ensure that critical events such as DNA replication and chromosome segregation are completed with high fidelity. In addition, checkpoints respond to damage by arresting the cell cycle to provide time for repair by inducing transcription of genes. Alterations in these checkpoints result in genomic instability and this fact has been implicated in the evolution of normal cells into cancer cells. Recent advances have revealed signal transduction pathways that transmit checkpoint signals in response to DNA damage and replication blocks.

Hanahan and Winberg,[4] defined six hallmarks of cancer and eleven years after they proposed[5] four additional ones that are involved in the pathogenesis of some and perhaps all cancers. Authors argue that all cancers share ten common traits ("hallmarks") that govern the transformation of normal cells into cancer (malignant or tumor) cells. These hallmarks are shown in the figure below (Figure 3).

[3] Elledge, S. J. *Science* **1996**, *274*, 1664-1672.
[4] Hanahan, D.; Weinberg, R. A. *Cell* **2000**, *100*, 57-70.
[5] Hanahan, D.; Weinberg, R. A. *Cell* **2011**, *144*, 646-674.

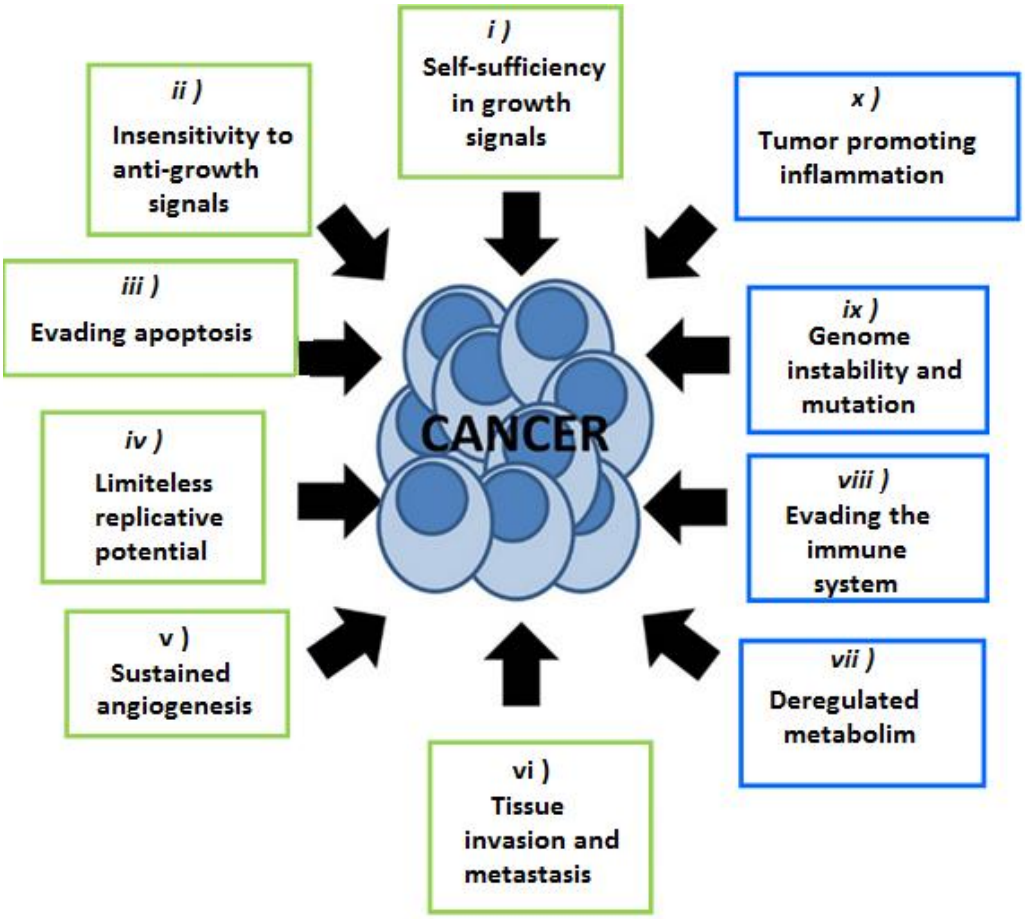

Figure 3. The hallmarks of cancer.

i) Self-sufficiency in growth signals

Normal cells require external growth signals (growth factors) to grow and divide. These signals are transmitted through receptors that pass through the cell membrane. When the growth signals are absent, they stop growing. Cancer cells do not need stimulation from external signals to multiply and this leads to an uncontrollable growth.

ii) Insensitivity to anti-growth signals

Cancer cells are generally resistant to growth preventing signals from the neighbors whereas normal cells answer to these inhibitory signals so as to maintain the homeostasis.

iii) Evading apoptosis

Apoptosis is a form of programmed cell death (cell suicide), the mechanism by which cells are programmed to die in the event they become damaged. Cancer cells characteristically are able to bypass this mechanism.

iv) Limitless replicative potential

Non-cancer cells die after a certain number of divisions.[6] Cancer cells escape this limit and are apparently capable of indefinite growth and division (immortality). But those immortal cells have damaged chromosomes, which can become cancerous.

v) Sustained angiogenesis

Angiogenesis is the process by which new blood vessels are formed. Cells before converting themselves into cancer cells lack from angiogenic ability[7] so as to the tumor to be expanded. Cancer cells appear to be able to initiate this process, ensuring that such cells receive a continuous supply of oxygen and other nutrients.

vi) Tissue invasion and metastasis

The newly formed metastasis arises as amalgams of cancer cells and normal supporting cells conscripted from the host tissue. Metastasis is responsible for the majority of cancer deaths.[8] The difference between benign tumor and malignant tumor

---

6 Hayflick, L. *Biochemistry* **1997**, *62*, 1180-1190.
7 Hanahan, D.; Folkman, J. *Cell* **1996**, *86*, 353-364.
8 Aplin, A. E.; Howe, A.; Alahari, S. K.; Juliano, R. L. *Pharmacol. Rev.* **1998**, *50*, 197-263.

arises from this concept. Benign tumors do not metastasize whereas malignant ones do metastasize.

vii) Deregulated metabolism

Most cancer cells have the ability to modify, or reprogram, cellular metabolism in order to most effectively support neoplastic proliferation.

viii) Evading the immune system

Cancer cells appear to be invisible to the body's immune system. They are able to evade immunological destruction, in particular by T and B lymphocytes, macrophages, and natural killer cells.

ix) Genome instability and mutations

Cancer cells generally have severe chromosomal abnormalities, which worsen as the disease progresses.

x) Tumor promoting inflammation

Pathologists have long recognized that some tumors are densely infiltrated by cells of both the innate and adaptive arms of the immune system and thereby mirror inflammatory conditions.[9]

The vast majority of mutations that give rise to cancer are not inherited, but arise spontaneously as a consequence of chemical damage to DNA resulting in altered function of crucial genes. It is important to note that chemical damage to DNA itself is not a mutagenic event. DNA replication and subsequent cell division is necessary to convert chemical damage to an inheritable change in DNA that is called mutation. Thus, proliferation is a virtual factor in the formation of mutations and in the expansion of clones of cells bearing these mutations.

[9] Dvorak, H. F. *N. Engl. J. Med*. **1986**, *315*, 1650-1659.

Chemical damage of DNA can be caused by both chemical and physical exogenous agents, most of which are now recognized as environmental carcinogens. For both types of agents, the most frequent chemical reaction giving rise to DNA damage can be characterized as an electrophilic attack upon a nucleophile tissue.[10] The most significant nucleophile tissue to be damaged by chemical attack is guanine, and the chemical changes induced are now known to interfere with base-pair recognition during replication. The earliest example of environmental carcinogenesis was reported in 1975 and involved tumor induction in workers exposed to coal tar. This led ultimately to the identification of the polycyclic aromatic hydrocarbon, benzo*[a]*pyrene, and other polycyclic hydrocarbons in coal tar and the discovery of their action as skin carcinogens in laboratory animals.[11]

One of the simplest chemical carcinogens is dimethylnitrosamine. This compound was widely used as a chemical solvent and was investigated because of suspicions that it caused liver damage in exposed workers. This suspicion was confirmed when laboratory rats developed a similar pathology after exposure. Its carcinogenic potential was discovered serendipitously when animals surviving acute doses were found to develop liver carcinomas later.[12] This discovery had major repercussions: not only was an industrial carcinogen discovered but this class of carcinogen, the *N*-nitrosamines, were found to be present in a large number of consumer items from beer, and tobacco smoke to cosmetics.[13] In addition, it was found that nitrosamines could be formed in the acid environment of the stomach after ingestion of primary and secondary amines, found in high levels in fish, and from sodium nitrite, also found in salted-fish. It is now believed that this endogeneous production of nitrosamines explains the particularly high incidence of gastric cancer in Japan and Iceland where salted-fish is a major dietary item.[14]

---

10 Miller, J. A.; Miller, E. C. *Mutat. Res*. **1975**, *33*, 25-26.
11 Doll, R.; Peto, R. *J. Natl. Cancer Inst.* **1981**, *66*, 1191-1308.
12 Magee, P. N. *Ann. Occup. Hyg.* **1972**, *15*, 19-23.
13 Hecht, S. S. *Proc. Soc. Exp. Biol. Med*. **1997**, *216*, 181-191.
14 Mirvish, S. S. *Cancer Lett*. **1995**, *93*, 17-48.

Regarding physical carcinogens both ionizing radiation and ultraviolet radiation can produce DNA damage which, as with chemical carcinogens, can lead to mutations. Ionizing radiation can cause direct damage to DNA by causing single and double-strand break of the DNA helix, and can also induce indirect damage as a consequence of radiolysis of water to yield free radicals.[15] Ultraviolet irradiation, though of insufficient energy to produce ions, is absorbed by DNA bases and is sufficiently energetic to induce chemical reactions. The most relevant of these occurs between two adjacent thymidines in the DNA helix and result in a covalent cross linking to form a cyclobutane-linked thymine dimer.

Since life began, the genome has been constantly exposed to chemical damage, both endogenous and exogenous. In order to protect against the immediate and long-term effects of excessive mutation rates, genes, such as p53 (tumor suppressor gene) have evolved to repair this damage.

The DNA damage response is essential for maintaining the genomic integrity[16] of the cell, and its disruption is one of the hallmarks of cancer.[4,5] This process evolved in response to the exposure of the genome to exogenous and endogenous genotoxins. Unless repaired in an error-free process, DNA damage can result in mutations and altered cellular behavior. Consequently, cells deploy a diverse repertoire of mechanism to maintain genetic integrity. These mechanisms involve the DNA repair processes themselves, and the systems that integrate DNA damage repair with the cell cycle.[17]

The helical and complementary nature of the DNA strands represents an elegant solution to the complicated task of housing the genetic blueprint in a way that allows accessibility for critical processes such as replication and transcription. After many trials and modifications, Watson and Crick[18] conceived an ingenious double helix model for the secondary structure of DNA. This achievement was accomplished with Rosalind

---

15 Hall, J.; Angele, S. *Mol. Med. Today* **1999**, *5*, 157-164.

16 Friedberg, E. C.; Aguilera, A.; Gellert, M.; Hanawalt, P. C.; Hays, J. B.; Lehmann, A. R.; Lindahl, T.; Lowndes, T.; Sarasin, A.; Wood, R. D. *DNA Repair* **2006**, *5*, 986-996.

17 Harper, J. W.; Elledge, S. J. *Mol. Cell* **2007**, *28*, 739-745.

18 Watson, J. D.; Crick, F. H. C. *Nature* **1953**, *171*, 964-967.

Franklin's X-ray experiments, which clearly demonstrated that DNA was a double helix. One of the most famous photographs demonstrating this fact is "Photo 51" (Figure 4), which was taken by Raymond Gosling in May 1952, working as a PhD student under the supervision of Rosalind Franklin.[19]

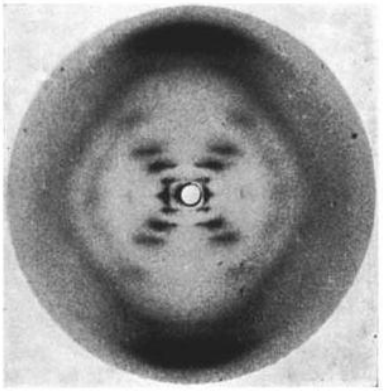

Figure 4. Photo 51, Rosalind Franklin.

Watson and Crick used characteristics and features of "Photo 51" to develop the chemical model of DNA molecule. This model proposed that the two strands of DNA were aligned anti-parallel to each other, i.e. with opposite 3' and 5' ends, as shown in figure 5a. Complementary primary nucleotide structures for each strand allowed intra-strand hydrogen bonding between each pair of bases. These complementary strands are colored red and green in figure 5b. The coiling of these coupled strands leads to a double helix structure, shown as cross-linked ribbons in figure 5b. The double helix is further stabilized by hydrophobic attractions and π-stacking of the bases.

[19] Sayre, A. Rosalind Franklin and DNA. New York. W. W. Norton and Company, **1975.**

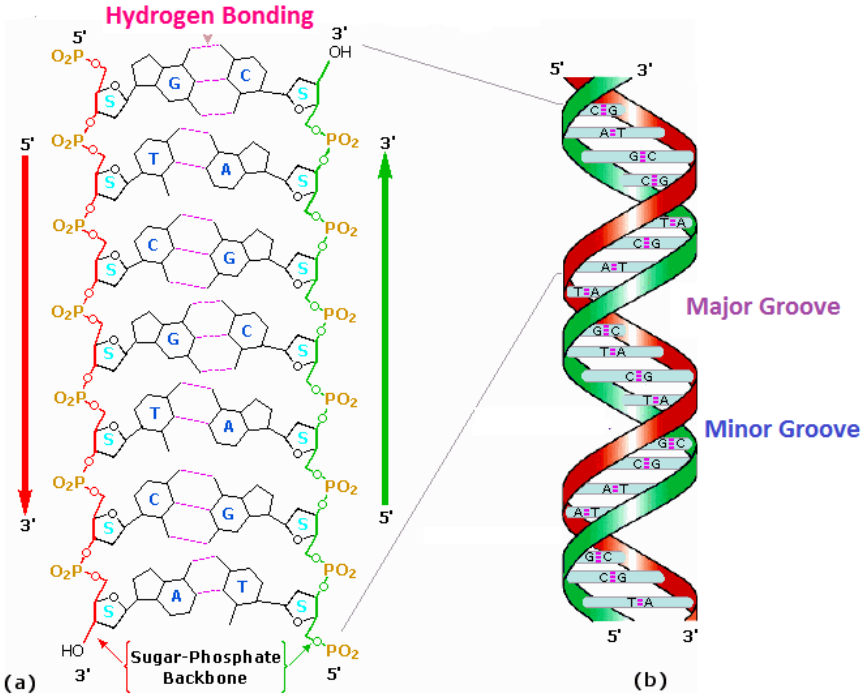

Figure 5. The double helix structure of DNA.

As the DNA strands wind around each other, they leave gaps between each set of phosphate backbones. Two alternating grooves result, a wide and deep "major groove" (22Å wide), and a shallow and narrow "minor groove" (12Å wide, Figure 5b). Other molecules, including polypeptides, may insert into these grooves, and in so perturbing the chemistry of DNA.

However, since the end of eukaryotic chromosomes are essentially fixed due to their large size, accessing the information contained in the double helix presents a significant topological problem for cells to overcome.[20] More specifically, the superhelical tension and other topological consequences resulting from the separation

[20] Leppard, J. B.; Champoux, J. J. *Chromosoma* **2005**, *114*, 75-85.

of the two strands must be resolved in order for DNA metabolic processes such as replication, transcription, and recombination to be completed.[21] Topoisomerases are the enzymes involved in resolving these problems; these enzymes accomplish their task by breaking the DNA backbone to facilitate the necessary changes in DNA topology, followed by the resealing of the DNA.[20]

The discovery of several DNA topoisomerases has brought a deep understanding of their important roles in living cells. The mammalian genome encodes seven topoisomerases genes: four that encode type I topoisomerases and three that encode type II topoisomerases. The name is derived from the action in breaking (-ase) the DNA into an isomer with different topological form.

The biological functions of DNA topoisomerases are deeply rooted in the double-helical structure of DNA.[22] There are two classes of topoisomerases, type I (Table 1, entries 1-10) and type II (Table 1, entries 11-16). Type I enzymes cleave only one strand of duplex DNA, whereas type II enzymes cleave both strands.[23] Topoisomerases have been described in the three cellular domains of life (Archaea, bacteria and eukaryote), as well as, in viruses infecting eukaryotes or bacteria. DNA topoisomerases are further classified as either type IA subfamily if the protein link is to 5' phosphate or type IB subfamily if the protein is attached to a 3' phosphate. In addition, they are named from I to VI according to their discovery. A broad classification[21] of the different subfamilies of topoisomerases in different organisms is represented in table 1.

[21] Champoux J. J. *Annu. Rev. Biochem.* **2001**, *70*, 369-413.
[22] Wang, J. C. *Biol. Chem*. **1991**, *266*, 6659-6662.
[23] Wang, J. C. A*nnu. Rev. Biochem.* **1996**, *65*, 635-692.

Table 1. Classification of topoisomerases.

Entry	Topoisomerase	Organism	Subfamily	Subunit structure
1	TopI	Eubacterial DNA *(E.coli)*	IA	monomer
2	TopIII	Eubacterial DNA (E.coli)	IA	monomer
3	TopIII	Yeast DNA (S.cerevisae)	IA	monomer
4	ToPIIIα	Mammalian DNA (human)	IA	monomer
5	ToPIIIβ	Mammalian DNA (human)	IA	monomer
6	gyrase	Eubacterial and archaeal reverse DNA (Sulfolobus acidocaldarius)	IA	monomer
7	gyrase	Eubacterial reverse (Methanopyrus kandleri)	IA	monomer
8	TopI	Eukaryotic DNA (human)	IB	monomer
9	TopI	(Poxvirus DNA) vaccinia	IB	monomer
10	TopV	Hyperthermophilic eubacterial DNA (Mehtanopyrus kandleri)	IB	monomer
11	gyrase	Eubacterial DNA (E.coli)	IIA	Heterotetramer
12	TopIV	Eubacterial DNA (E.coli)	IIA	Heterotetramer
13	TopII	Yeast DNA (S. cerevisae)	IIA	Homodimer
14	TopIIα	Mammalian DNA (human)	IIA	Homodimer
15	TopIIβ	Mammalian DNA (human)	IIA	Homodimer
16	TopVI	Archaeal DNA (Sulfolobus shibatae)	IIB	Heterotetramer

1.1.1. Topoisomerase I

DNA topoisomerases relax DNA torsional strain generated during replication, transcription, recombination, repair, and chromosome condensation, and are therefore vital to all cells undergoing division.

Topoisomerases[21] catalyze the cleavage and religation of the DNA with the formation of an intermediate that is covalently bound to DNA through a phosphotyrosine bond. DNA cleavage by all topoisomerases is accomplished by the formation of a transient phosphodiester bond between a tyrosine residue in the protein and one of the ends of the broken strand. DNA topology can be modified during the lifetime of the covalent intermediate and the enzyme is released as the DNA is religated.

Type I enzymes are monomeric and pass a single-stranded region of DNA through a break in the opposite strand. Type I topoisomerase has several unusual features. Unlike type II topoisomerases, topoisomerase I does not require ATP hydrolysis to catalyze the complex topological rearrangements of DNA for which it is responsible.

One of the best studied human topoisomerases is DNA topoisomerase I and it has been subdivided into two groups, type IA and IB, on the basis of the side of DNA to which the enzyme becomes covalently bound. Type IA subfamily attaches covalently to the 5' end of the cleaved DNA, whereas the type IB subfamily attaches to the 3' end during the catalytic cycle. Eukaryotic TopI[24] is classified as type IB because of two key differences with *E. coli* Top IA. First, it relaxes both negative and positive supercoils, whereas *E. coli* Top I only relaxes negative supercoils. Second, it cleaves DNA by forming a tyrosyl (Y)-DNA covalent catalytic intermediate at the 3' end of the break (3'-P-Y), whereas *E. coli* TopI forms a 5'-P-Y intermediate.

Human DNA topoisomerase I is a 91-kDa enzyme (765 amino acids, aa) that can be divided into four domains based on limited proteolysis studies and crystal structure analysis.[20,21] The three dimensional structure of the human topoisomerase I complex with DNA molecules shows the enzyme organized in multiple domains which "clamp on" the DNA molecules (Figure 6)[25] named the *N*-terminal domain (aa 1-214), a core domain (aa 215-635), a linker (aa 636-712), and the *C*-terminal domain that contains the active site Tyr723 (aa 713-765)[21] (Figure 6 and 7). Core subdomain I, II and III are colored in light blue, dark blue and green, respectively. The linker and *C*-domain are shown in yellow and orange, respectively.

[24] Champoux, J. J.; Dulbecco, R. *Proc. Natl. Acad. Sci. USA* **1972**, *69*, 143-146.

[25] Redinbo, M. R.; Stewart, L.; Kuhn, P.; Champoux, J. J.; Hol, W. G. J. *Science* **1998**, *279*, 1504-1513.

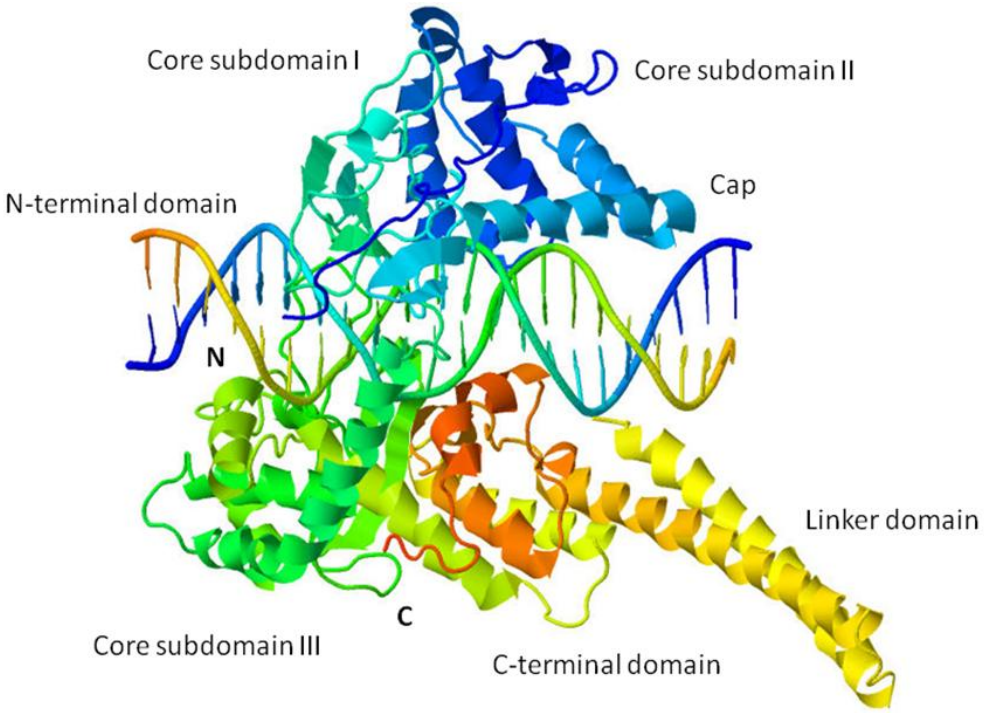

Figure 6. Human TopI complex with DNA molecules (PDB: 1A36).

The core and the *C*-terminal domains represent the minimal requirement for DNA relaxation *in vitro*, as the combination of two fragments corresponding to these domains can reconstitute enzymatic activity.[26]

The most complete analysis of the crystallographic studies revealed[27] a bilobed clamp like protein that completely envelopes the DNA duplex and contains four discrete domains (Figure 7). The *N*-terminal domain which has no significance to the enzyme function. Adjacent to the *N*-terminal domain is the core subdomain that it is highly conserved and consist of subdomain I (highlighted in yellow), II (highlighted in blue) and

[26] Stewart, L.; Ireton, G. C.; Champoux, J. J. *J. Mol. Biol*. **1997**, *269*, 355-372.
[27] Lesher, D. T.; Pommier, Y.; Stewart, L.; Redinbo, M. R. *Proc. Natl. Acad. Sci. USA* **2002**, *99*, 12102-12107.

III (highlighted in red). Subdomains I and II make up the upper lob of the enzyme and it is called the capping lobe. The last two domains are the linker domain and the *C*-terminal domain. These two domains along with subdomain III form the lower lobe called the catalytic lobe.[28]

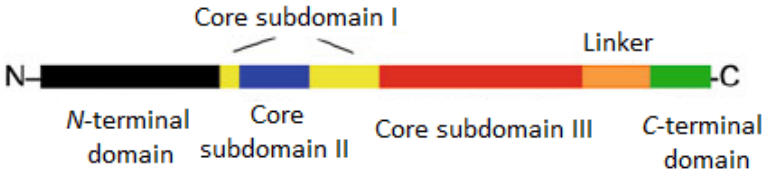

Figure 7. Core domain organization of human TopI.

The sequence of events that lead to the relaxation of one or more turns of a superhelical DNA molecule are represented schematically in figure 8. Currently, the most attractive model for DNA relaxation by topoisomerase I proposes that relaxation proceeds by a controlled rotation mechanism.[29]

When binding to DNA, topoisomerase I cleaves one strand of the DNA through a tyrosine residue attacking a phosphate. Once the strand has been cleaved, it rotates in a controlled manner around the other strand. The reaction is completed by religation of the cleaved strand. This process results in partial or complete relaxation of a supercoiled plasmid.

[28] Carey, J. F.; Schultz, S. J.; Sisson, L.; Fazzio, T. G.; Champoux, J. J. *Proc. Natl. Acad. Sci. USA* **2003**, *100*, 5640-5645.

[29] Stewart, L.; Redinbo, M. R.; Qiu, X.; Hol, W. G. J.; Champoux, J. J. *Science* **1998**, *279*, 1534-1541.

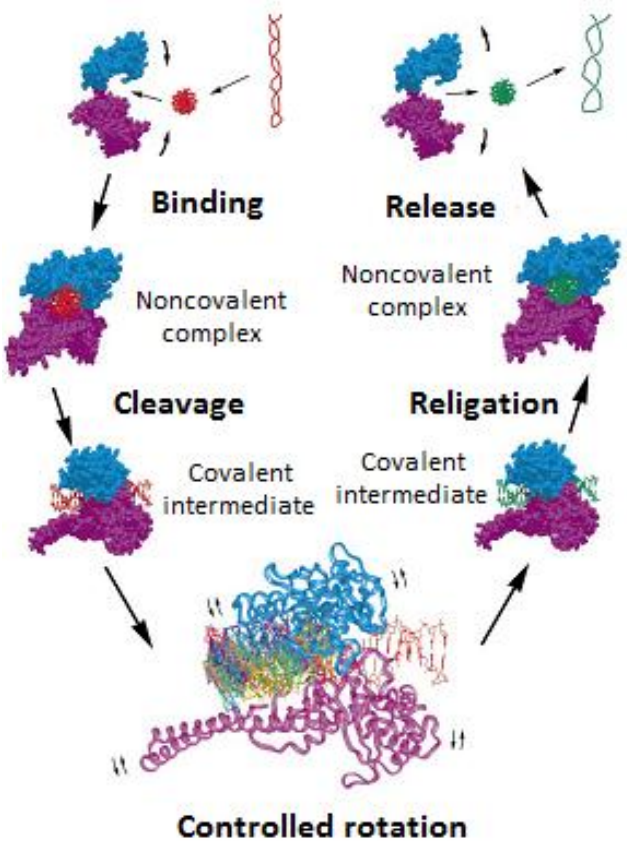

Figure 8. TopI catalytic mechanism.

In the topoisomerization reaction, once the enzyme clamps around the DNA, four of the five active site residues (Arg488, Lys532, Arg590, and His632) act to position the phosphate group during nucleophilic attack.[25] The active site tyrosine (Tyr723) starts the catalytic cycle through a nucleophilic attack on the 3'-phosphate group to form the TopI-DNA covalent complex (TopIcc, Scheme 1). Stabilization of the transition state of the reaction is achieved through interactions in the active site. For instance, Arg 590 may act to enhance the nucleophilicity of Tyr 723 by stabilizing the phenolate anion.

The religation reaction is essentially the reverse of the cleavage reaction. The oxygen on the 5' end of the cleaved strand acts as the nucleophile that attacks the phosphate to break the bond between DNA and enzyme.[30] After changing the linking number, a second nucleophilic attack, driven by the 5'-hydroxy DNA end, restores an intact double-stranded DNA, and the enzyme is released (Scheme 1).

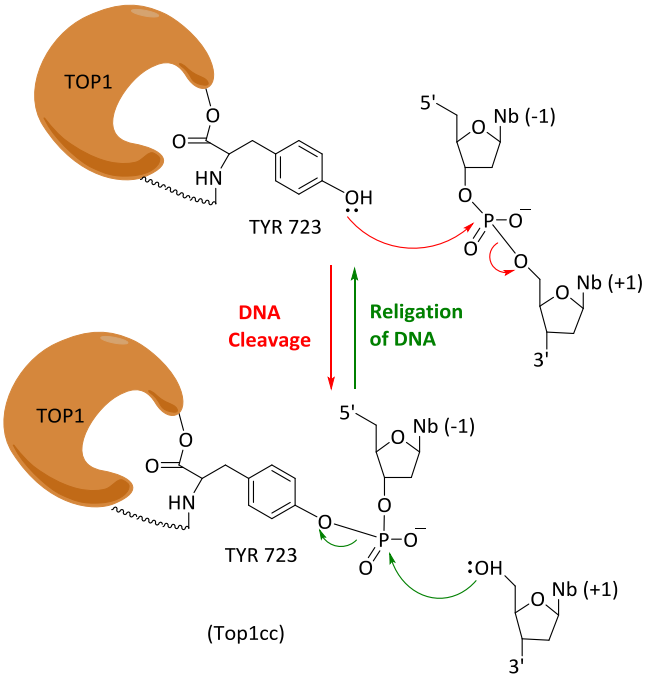

Scheme 1. Formation of the TopI-DNA cleavable complex (TopIcc).

Due to its essentiality and its crucial role in transcription and replication, TopI is an attractive clinical molecular target. Moreover, as it has been mentioned before, topoisomerase I is over-expressed in tumor cells. For such these reasons, it is extremely important to develop new drugs with the aim of selectively hitting this enzyme.

[30] Champoux, J. J. Cold Spring Harbor Monograph Series **1990**, *20*, 217-242.

1.1.2. Targeting human Topoisomerase IB in cancer therapy

When targeting topoisomerases[31] it must be taken in mind the difference between inhibiting the activity *versus* 'poisoning' or 'trapping' the enzyme in an inactive state on DNA. DNA topoisomerase IB can be inhibited by several compounds that act through different mechanism such as prevention of DNA-topoisomerase binding, inhibition of DNA cleavage, stabilization of the covalent complex (TopIcc) or inhibition of religation process. TopI inhibitors are classified as inhibitors when they impede the cleavage reaction and as poisons when they impede the religation process.[32] Poisons include drugs approved by the FDA for clinical use, such as the derivatives of the natural compound camptothecin (CPT) **1**, whose systematic name is (*S*)-4-ethyl-4-hydroxy-1*H*-pyrano[3',4',6,7]indolizino[1,2-*b*]quinoline-3,14-(4*H*,12*H*)-dione,[33] (Figure 9) and two water soluble CPT derivatives (CPTs), topotecan (TPT) **2** and irinotecan **3**.

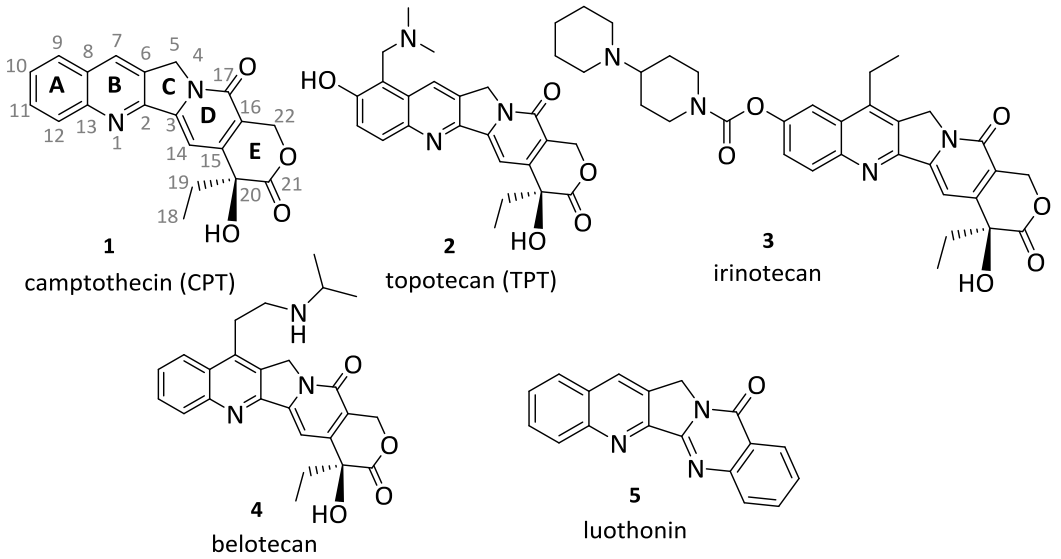

Figure 9. CPT, its derivatives (CPTs) and luothonin.

[31] Pommier, Y. *ACS Chem. Biol*. **2013**, *8*, 82-95
[32] Pommier, Y. *Chem. Rev*. **2009**, *109*, 2894-2902.
[33] Systematic IUPAC name. However, in literature it is often numbered as shown in figure 9.

These CPT derivatives reversibly bind to the covalent TopI-DNA complex, slowing down the religation of the cleaved DNA strand and thus, inducing cell death.

Belotecan **4** (CKD-602, Figure 9) is another popular derivative used in cancer treatment and it has been approved for the clinical treatment of ovarian, small-cell lung and refractory colorectal cancers.[34] Preliminary studies have revealed this drug as a potent topoisomerase I inhibitor.

A CPT-like mechanism has been demonstrated for luothonin **5** (Figure 9), a pyrroloquinazoquinoline alkaloid extracted from the Chinese plant *Peganum nigellastrum*. Luothonin **5** is cytotoxic towards leukemia cell lines and produces an effect similar to CPT, as tested by a cleavage/religation equilibrium assay and by the effect observed in a *Saccharomyces cerevisae* strain lacking yeast TopI, but harboring human TopI.[35]

The great number of natural compounds targeting TopI that have been isolated or modified in the past few years is in agreement with the fact that the area of TopI-targeted drugs is very active. The most relevant compounds are the ones acting at enzyme-DNA covalent complex level. Nevertheless, compounds directly interacting with the enzyme may rapidly reveal themselves to be useful since they provide a valuable scaffold that can be modified or mimicked through chemical synthesis.

Although CPT **1** (Figure 9) first isolation was five decades ago,[36] CPT-based drugs remain appealing to many researchers worldwide and more CPT analogs are emerging as promising chemotherapeutic agents. The discovery of topoisomerase I as CPT's therapeutic target opened a new area for anticancer drug development. The

---

[34] Ahn, S. K.; Choi, N. S.; Jeong, B. S.; Kim, K. K.; Journ, D. J.; Kim, J. K. *J. Heterocycl. Chem*. **2000**, *37*, 1141-1144.

[35] Cagir, A.; Jones, S. H.; Gao, R.; Eisenhauer, B. M.; Hecht, S. M. *J. Am. Chem. Soc*. **2003**, *125*, 13628-13629.

[36] Wall, M. E.; Wani, M. C.; Cook, C. E.; Palmer, K. H.; McPhail, A. T.; Slim, G. A. *J. Am. Chem. Soc.* **1966**, *88*, 3888-3890.

tremendous effort in this field included the total synthesis or semisynthesis of several CPTs that has been crucial to make new anticancer drugs.

1.1.2.1.a Camptothecin (CPT) and derivatives

Camptothecin **1** (CPT)[33] is the best well known target towards TopI. CPT is an alkaloid that was first isolated and identified from the *Chinese tree Camptotheca acuminate.* It was discovered and initially studied[36] in the 1960s by Wall, Wani, and colleagues and only about 20 years later it was demonstrated that it was able to specifically target TopI.[37] This compound attracted great interest as a potential cancer chemotherapeutic agent due to its impressive activity against leukemia and various solid tumors in experimental systems. It reversibly binds to the TopI-DNA cleaved complex, inhibiting the religation process. There are some experimental evidences that CPT **1** selectively poisons TopI:

- Natural CPT isomer is active against TopI;[38]
- Genetically modified yeast deleted for TopI is immune to CPT **1**;[39]
- Cells selected for CPT **1** resistance show a point mutation in TopI gene;[40]
- CPT-producing plants have a point mutation in TopI (N722S) that renders the enzyme immune to CPT **1**.[41]

---

37 Hsiang, Y. H.; Hertzberg, R.; Hecht, S.; Liu, L. F. *J. Biol. Chem*. **1985**, *260*, 14873-14878.
38 Jaxel, C.; Kohn, K. W.; Wani, M. C.; Wall, M. E.; Pommier, Y. *Cancer Res*. **1989**, *49*, 1465-1469.
39 Eng, W. K.; Faucette, L.; Johnson, R. K.; Sternglanz, R. *Mol. Pharmacol*. **1988**, *34*, 755-760.
40 Pommier, Y.; Pourquier, P.; Urasaki, Y.; Wu, J.; Laco, G. S. *Drug Resistance Updates* **1999**, *2*, 307-318.
41 Sirikantaramas, S.; Yamazaki, M.; Saito, K. *Proc. Natl. Acad. Sci*. **2008**, *105*, 6782-6786.

The cytotoxicity of CPT **1** is because the TopI-DNA cleavage complex is trapped, inhibiting the resealing of the cleaved strand and transforming the enzyme into something poisonous to the cell. During the S phase of the cell cycle, collision of the replication fork with the drug stabilized complexes converts a transient single-strand break into an irreversible double-helix break, resulting in cell death.[42,43]

CPT does not bind to DNA nor to TopI by itself, it requires the presence of both TopI and DNA associated in a cleavage complex (Figure 10).[37,44]

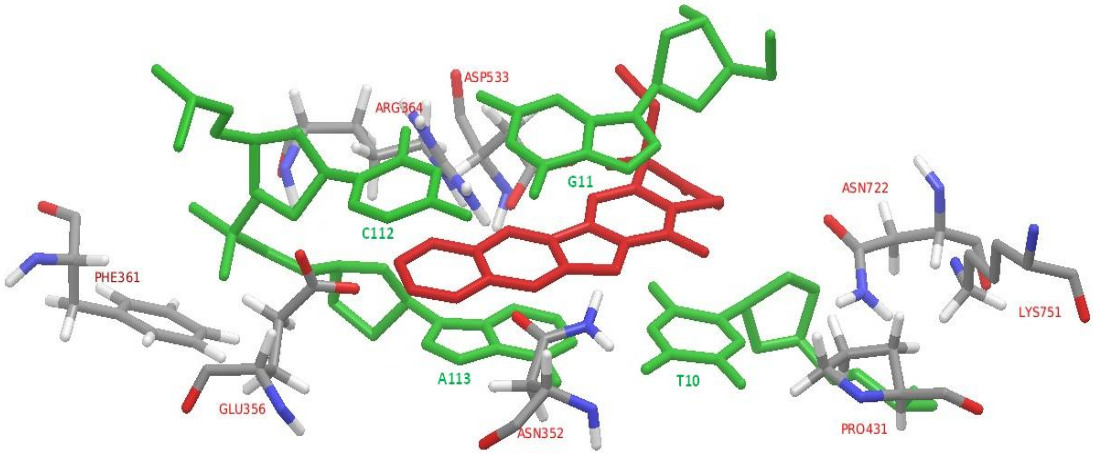

Figure 10. Cleavable complex TopI-DNA-CPT crystal structure partial view (PDB 1T81). Residues around the cleavage site in the ternary TopI cleavage complex, CPT (in red) and DNA base pairs (in green) are shown.

---

42 Liu, L. F.; Desai, S. D.; Li, T. K.; Mao, Y.; Sun, M.; Sim, S. P. *Ann. N. Y. Acad. Sci*. **2000**, *922*, 1-10.

43 Hsiang, Y. H.; Lihou, L. F. *Cancer Res*. **1989**, *49*, 5077-5082

44 Jaxel, C.; Capranico, G.; Kerrigan, D.; Kohn, K. W.; Pommier, Y. *J. Biol. Chem.* **1991**, *266*, 20418-20423.

This observation led to the hypothesis that CPT binds at the interface of both TopI and DNA in a ternary complex.[44,45] This hypothesis was confirmed 13 years later by the determination of the crystal structure of a ternary TopI cleavage complex with topotecan, the clinically used CPT analogue.[46] After that, it was possible to obtain the crystal of the ternary complex with CPT and thus confirm the mechanism of action of this drug.[47]

Camptothecins (CPTs) are the only clinically approved TopI inhibitors. In spite of their activity in colon, lung and ovarian cancers[48] camptothecins have several limitations,[40,49] that are enumerated bellow:

i.) CPTs are chemically unstable at physiological pH due to the lactone ring that rapidly transformates into the carboxylate inactivated form in blood (Scheme 2);

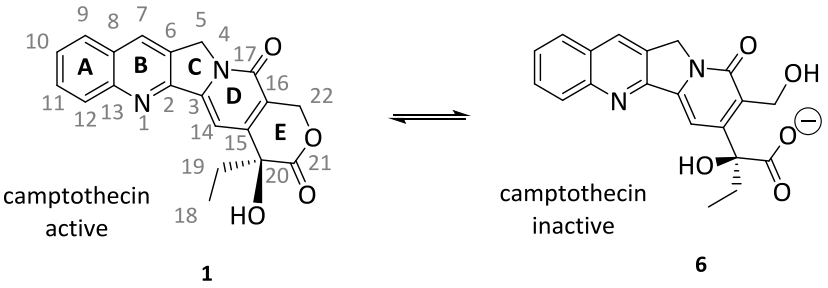

Scheme 2. Lactone ring hydrolysis at physiological pH.

45 Kerrigan, J. E.; Pilch, D. S. *Biochemistry* **2001**, *40*, 9792-9798.
46 Staker, B. L.; Hjerrild, K.; Feese, M. D.; Behnke, C. A.; Burgin, A. B. Jr.; Stewart, L. *Proc. Natl. Acad. Sci.* **2002**, *99*, 15387-15392.
47 Staker, B. L.; Feese, M. D.; Cushman, M.; Pommier, Y.; Zembower, D.; Stewart, L.; Burgin, A. B. *J. Med. Chem*. **2005**, *48*, 2336-2345.
48 Teicher, B. A. *Biochem. Pharmacol*. **2008**, *75*, 1262-1271.
49 Pommier, Y. *Nat. Rev. Cancer* **2006**, *6*, 789-802.

The ternary complex (TopI-DNA-CPT) reverses within minutes after drug removal.

ii.) Side-effects of CPTs such as diarrhea and neutropenia are potentially severe and dose-limiting.

iii.) The discovery that the primary cellular target of CPT **1** is DNA topoisomerase I (TopI) created renewed interest in this compound and lead to synthesize more water soluble analogs[50] so as to overcome CPT limitations previously mentioned.[49]

1.1.2.1.b Synthesis of CPT and its analogues

There are plenty of approaches to overcome CPT **1** synthesis and some of the reaction types used to synthesize this compound will be discussed in the next lines.

Following the structure of CPT **1**, numerous synthetic methods were reported employing a wide range of approaches.[51] The first successful total synthesis of the racemic form of the molecule was reported by Stork and Schultz[52] in 1971 (Scheme 3).

---

[50] (a) Rothenberg, M. L. *Ann. Oncol*. **1997**, *8*, 837-855. (b) Pommier, Y.; Pourquier, P.; Fan, Y.; Strumberg, D. *Biochim. Biophys. Acta* **1998**, *1400*, 83-105.

[51] (a) Wenkert, E.; Dave, K. G.; Lewis, R. G.; Sprague, P. W. *J. Am. Chem. Soc*. **1967**, *89*, 6741-6745. (b) Shamma, M.; Novak, L. *Tetrahedron* **1969**, *25*, 2275-2279. (c) Kepler, J. A.; Wani, M. C.; McNaul, J. N.; Wall, M. E.; Levine, S. G. *J. Org. Chem.* **1969**, *34*, 3853-3858. (d) Shamma, M.; Novak, L. Collect. *Czech*. *Chem. Commun*. **1970**, *35*, 3280-3286.

[52] Stork, G.; Schultz, A. G. *J. Am. Chem. Soc*. **1971**, *93*, 4074-4075.

The initial key step in this synthesis was B-ring formation. For this purpose, the quinolinic acid **9** was obtained by the condensation of *o*-aminobenzaldehyde **7** and the pyrrolidone **8** in the presence of diluted sodium hydroxide. The hydrolysis of **9** yields the amino ester **10a** that reacts with half acid chloride of diethyl malonate to afford the diesteramide **10b** which was cyclized upon heating to the tetracyclic compound **11a**.

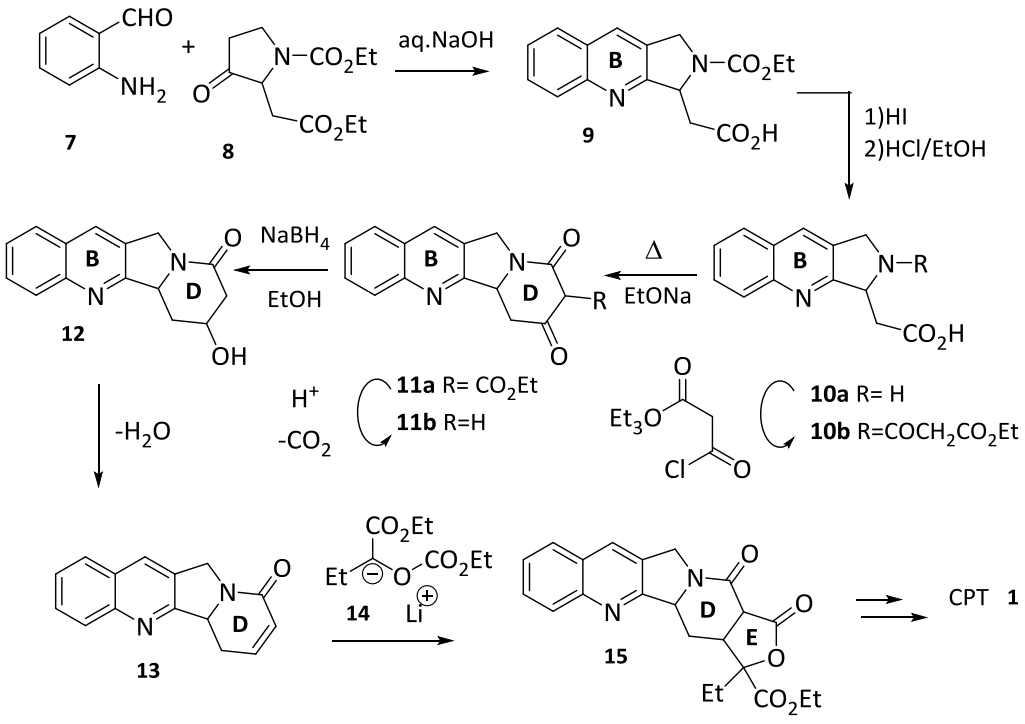

Scheme 3. Stork and Schultz total synthesis to CPT **1**.

Hydrolysis and decarboxylation of **11a** afforded compound **11b** which upon reduction gave the β-hydroxy lactam **12** that is converted to the corresponding unsaturated lactam **13** that reacts with the anion **14** to form CPT **1** pentacyclic lactone precursor **15**.

The first asymmetric synthesis of (20*S*)-CPT **1** was reported by Tagawa and coworkers[53] in 1989 (Scheme 4), using a functionalized pyridine **16** and the *N*-tosyl-(*R*)-proline derivative **17** as the chiral auxiliary to induce the stereocontrol in the diastereoselective ethylation to form products **18** and **19**, that after several steps yield lactone **20** in which the E-ring is formed. This lactone **20** reacts with amine **21** resulting in the B-ring formation and thus CPT **1** formation.

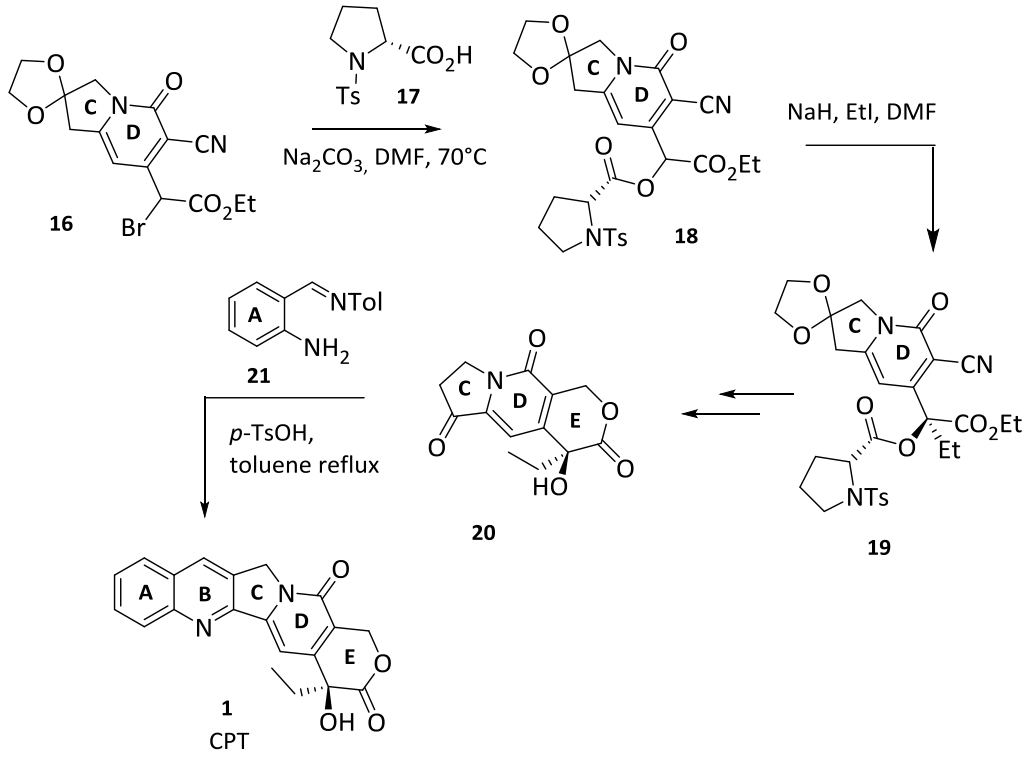

Scheme 4. First asymmetric synthesis of CPT **1**.

[53] Ejima, A.; Terasawa, H.; Sugimori, M.; Tagawa, H. *Tetrahedron Lett*. **1989**, *30*, 2639-2640.

Since the discovery of the first synthetic approach, lots of strategies have been described. Representative summary of some of the strategies used for the synthesis of CPT **1** showing relevant intermediates are shown in figure 11, pathways A-D.

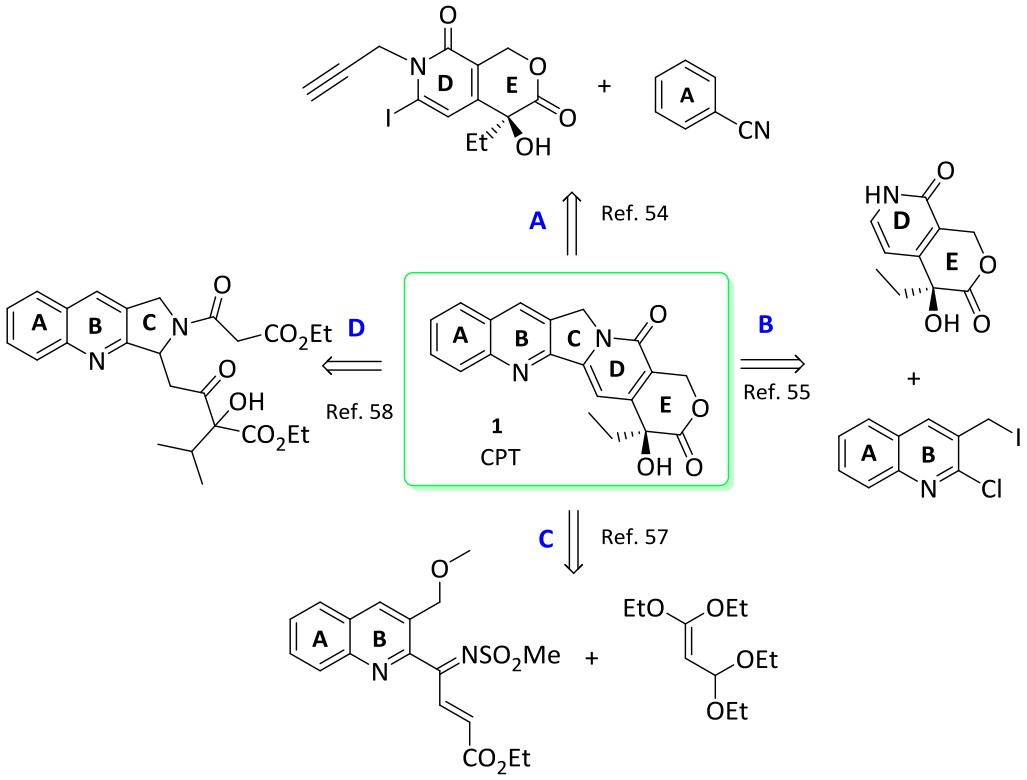

Figure 11. Diverse strategies used for the synthesis of CPT **1**.

Curran and coworkers[54] designed an interesting strategy in which the appropriately functionalized A and D/E-fragments (Figure 11, pathway A, Scheme 5) participate in a free-radical cascade, which led to the formation of B and C rings of CPT. The formation of the D/E fragment is the key target in this synthesis. The synthesis of the D/E fragment was accomplished by directed lithiation of pyridine **22** followed by

[54] Josien, H.; Ko, S. B.; Bom, D.; Curran, D. P. *Chem. Eur. J*. **1998**, *4*, 67-83.

addition of *N*-formyl-*N*,*N*,*N*'-trimethylethylenediamine to yield an intermediate that was trapped with iodine to afford the iodoaldehyde **23**. A reductive estherification of **23** with crotyl alcohol **24**, triethylsilane (Et_3SiH), and trifluoroacetic acid (TFA) provided the crotyl ether **25**. After an intramolecular Heck reaction, the enol ether **27** was obtained and it was then subjected to a Sharpless asymmetric dihydroxylation, further oxidation, iododesilylation and functionalization to give the iodolactone **28** which reacted with phenyl nitrile **29** through a radical cascade reaction to form the B and C-rings of the CPT **1**.

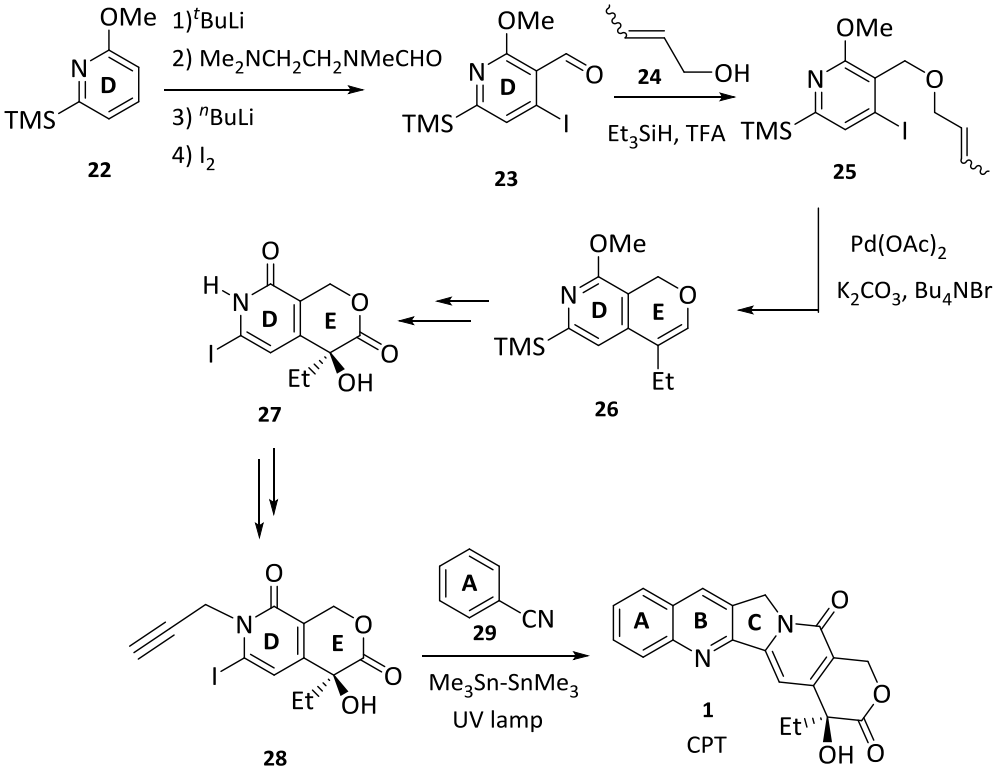

Scheme 5. Curran and coworkers approach to CPT **1**.

The shortest asymmetric synthesis of CPT **1** was described by Comins and Nolan[55] and involves the formation of the C-ring by connecting the A/B and D/E fragments (Figure 11, Pathway B, Scheme 6). In order to prepare the D/E-ring fragments alcohol **30** that was converted to 1,3-dioxane **31** on treatment with NaI, TMSCl and paraformaldehyde. Conversion of **31** to intermediate **33** was carried out through a lithium-halogen exchange with n-BuLi followed by the addition of the ketoester **32**, bearing the chiral auxiliary TCC.[56] For the formation of the A/B-ring, reaction of quinoline **34**, Et_3SiH, and TMSI in $CHCl_3$ yielded the desired transformation to afford iodide **35**. The reaction of **33** with **35** in the presence of ^{t}BuOK in DME provides compound **36**. The C-ring closure was achieved through a Heck reaction.

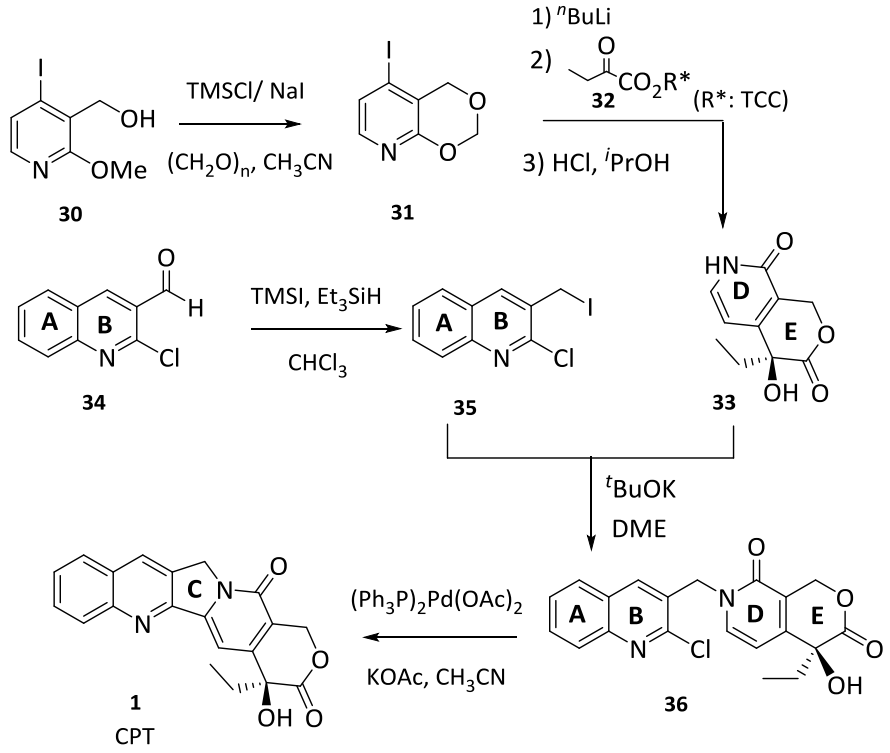

Scheme 6. Comins and Nolan synthetic approach to CPT **1**.

[55] Comins, D. L.; Nolan, J. M. *Org. Lett*. **2001**, *3*, 4255-4257.
[56] TCC: *trans*-2-(*R*-cumyl)cyclohexyl.

However, Blagg and Boger[57] focused on the construction of D-ring as the first key step in their synthesis (Figure 11, Pathway C and Scheme 7). The synthesis of (20*S*)-CPT **1** is based on an inverse electron demand hetero-Diels-Alder cycloaddition of the *N*-sulfonylimine **37** with the electron rich dienophile **38** for the formation of the pyridine D-ring. The ethyl ketone **40** was formed by addition of EtMgBr in the presence of TEA. The vinyl ether **41** was formed by a Wittig reaction of the ethyl ketone **40** and the ylide generated from methoxymethylenetriphenylphosphonium salt.

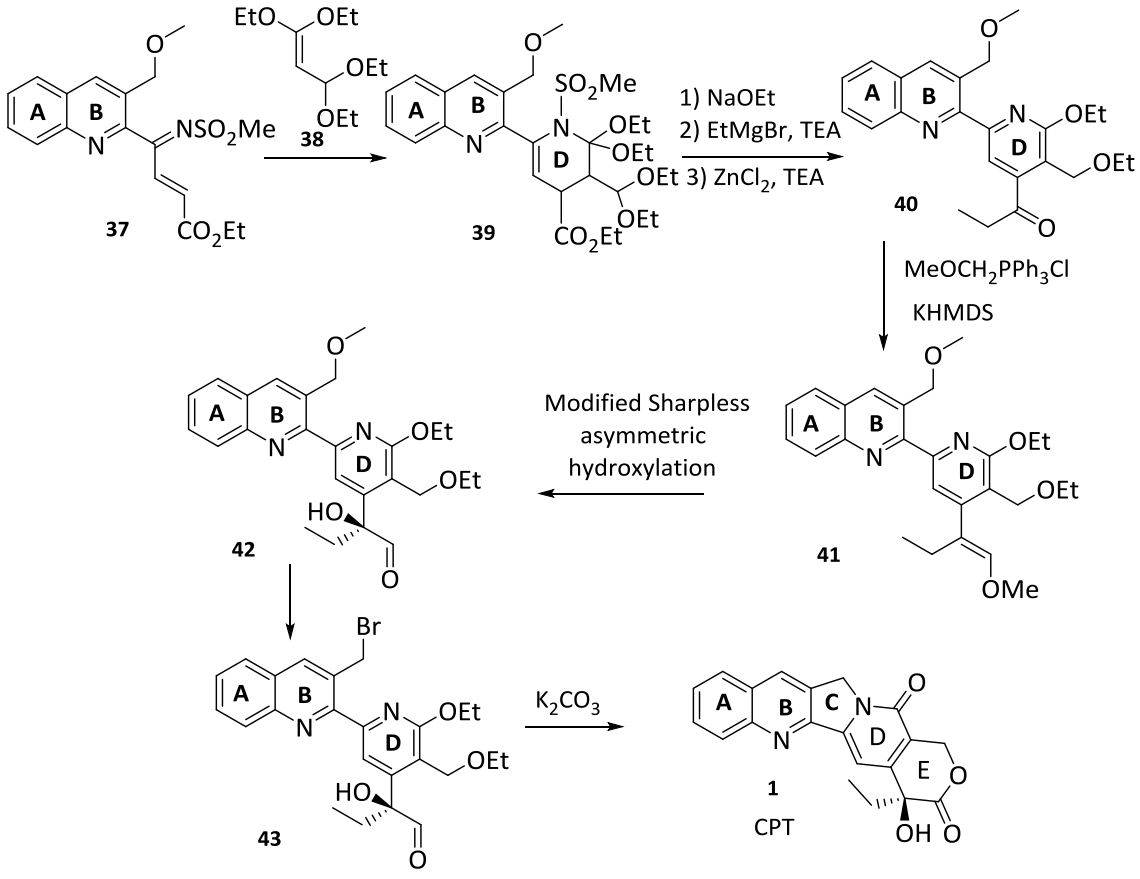

Scheme 7. Blagg and Boger strategy for the synthesis of CPT **1**.

[57] Blagg, B. S. J.; Boger, D. L. *Tetrahedron* **2002**, *58*, 6343-6349.

Then through a modified Sharpless asymmetric hydroxylation, the benzylic ether **42** was obtained. Conversion of **42** into the corresponding benzylic bromide **43** followed by intramolecular displacement upon addition of the base (K_2CO_3) furnished CPT **1**.

Although there are several syntheses of (20*S)*-CPT **1**, there is a great interest in developing short, direct and practical routes that can be scaled up for drug preparation.

The most relevant step in CPT **1** synthesis described by Chavan's[58] group is the introduction of an intramolecular aldol reaction of an α-hydroxy ketone **49** (Figure 11, Pathway D, Scheme 8) to generate the pyridine D-ring with functionality for manipulating the lactone E-ring.

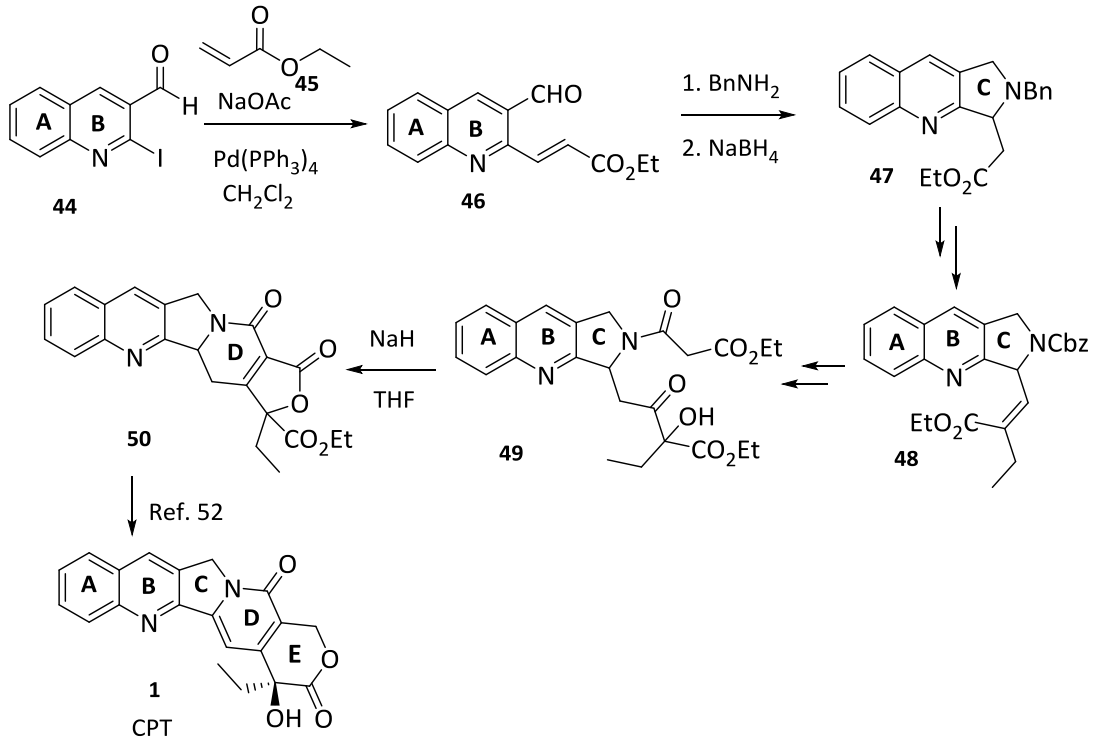

Scheme 8. Chavan approach to (20*S)*-CPT **1**.

[58] Chavan, S. P.; Sivappa, R. *Tetrahedron Lett*. **2004**, *45*, 3113-3115.

Thus, condensation of **46** with benzylamine in methanol formed tricyclic amine **47** and consequently, the C-ring. Through several steps, Cbz protected amine **48** was obtained, after that, it was deprotected and converted into α-hydroxy ketone **49** *via* $KMnO_4$ oxidation. Intramolecular aldol condensation of **49** with NaH in THF afforded compound **50**, CPT **1** precursor.[52]

Not only CPT **1** synthesis, but also the synthesis of its analogues has been studied due to the importance of their biological properties. Some derivatives such as topotecan[59] **2** and irinotecan[60] **3** (Figure 9) have been prepared by semi-synthesis from CPT **1**, by functionalization of its A, B-rings.

Modifications in A- and B-ring

The semi-synthesis of topotecan **2** is shown in scheme 9.[61] Platinum-catalyzed hydrogenation of CPT **1** yields tetrahydroquinoline **51**, which is oxidized with $PhI(OAc)_2$ in one pot to give 10-hydroxycamptothecin **52** which condensation with formaldehyde and dimethylamine yields topotecan **2**.

[59] Curran, D. P.; Ko, S. B.; Josien, H. *Angew. Chem. Int. Ed.* **1996**, *34*, 2683-2684.

[60] Kehrer, D. F. S.; Soepenberg, O.; Loos, W. J.; Verweij, J.; Sparreboom, A. *Anti-Cancer Drugs* **2001**, *12*, 89-105.

[61] Kingsbury, W. D.; Boehm, J. C.; Jakas, D. R.; Holden, K. G.; Hecht, S. M.; Gallagher, G.; Caranfa, M. J.; McCabe, F. L.; Faucette, L. F.; Johnson, R. K.; Hertzberg, R. P. *J. Med. Chem*. **1991**, *34*, 98-107.

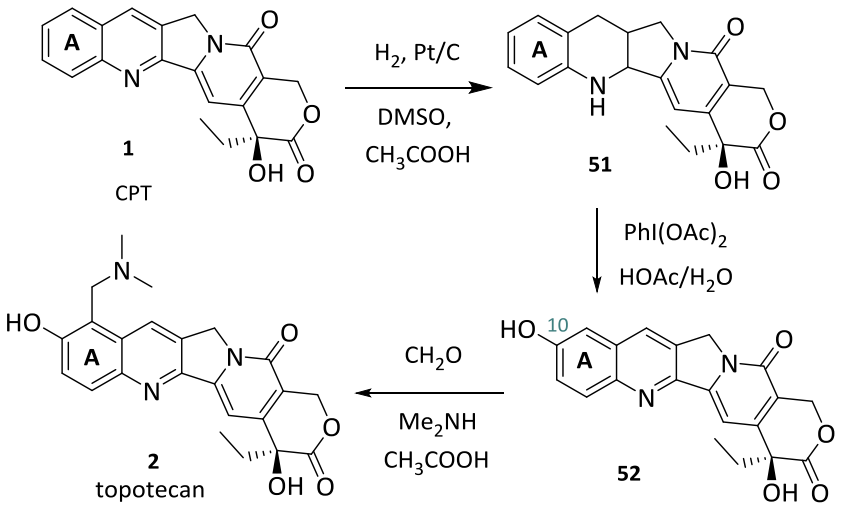

Scheme 9. Semi-synthesis of topotecan **2**.

Simultaneously, another CPT derivative, irinotecan **3**, was synthesized in 1991 by the Sawada[62] group (Scheme 10) by reaction of CPT **1** and propanal in the presence of $FeSO_4$ and H_2O_2 in aqueous acidic medium. An ethyl radical is generated and added to the 7-position of camptothecin **1** to yield 7-ethylcamptothecin **53**. Oxidation of **53** to its *N*-oxide **54** followed by photo irradiation in the presence of acid gave the corresponding 7-ethyl-10-hydroxy camptothecin **55** (SN-38). Treatment of SN-38 **55** with 1,4'-bipiperidinyl-1'-carbonyl chloride **56** provided irinotecan **3**.

[62] Sawada, S.; Okajima, S.; Aiyama, R.; Nokata, K. I.; Furata, T.; Yokokura, T.; Sugimo, E.; Yamaguchi, K.; Miyasaka, T. *Chem. Pharm. Bull*. **1991**, *39*, 1446-1454.

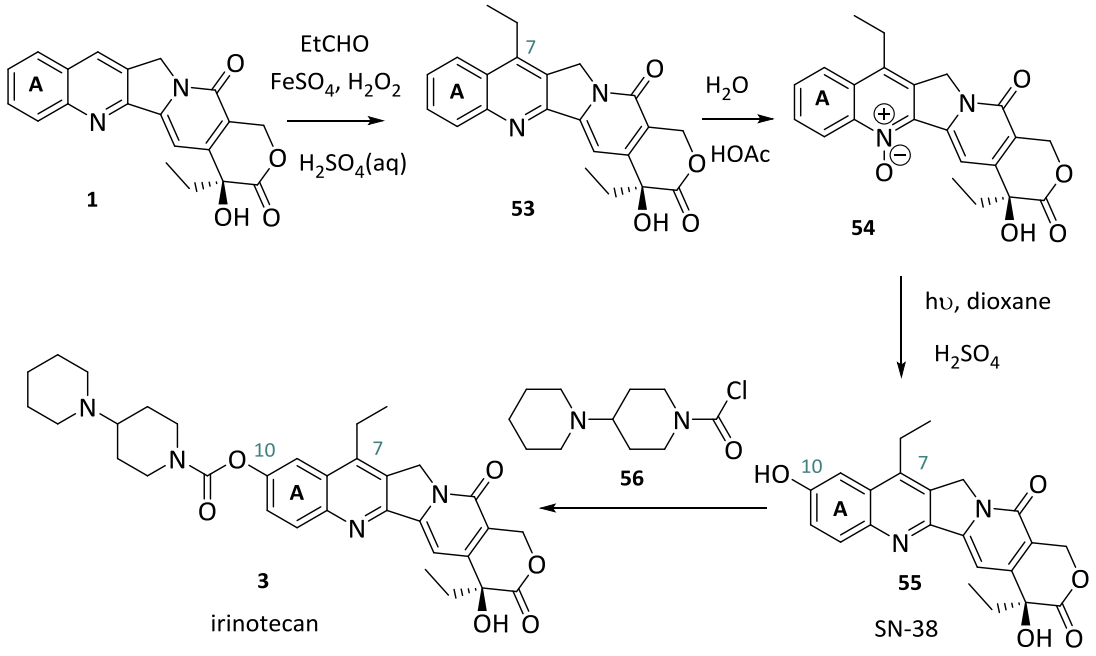

Scheme 10. Semi-synthesis of irinotecan **3**.

CPT derivatives with modification in A and B ring have been studied too. You and coworkers[63] reported a series of 7-cycloalkylcamptothecin derivatives **57** (Figure 12). Many of these compounds exhibited IC_{50} values in the low micromolar to nanomolar level and were up to 40 fold more potent than topotecan **2**.

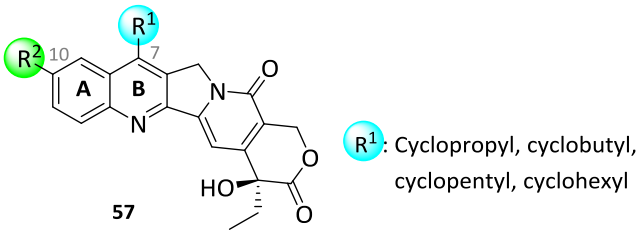

Figure 12. 7-(Cycloalkyl)-CPT derivatives **57**.

[63] Li, M. Z.; Jin, W.; Jiang, C.; Zheng, C.; Tang, W. D.; You, T. P.; Lou, L. G. *Bioorg. Med. Chem. Lett.* **2009**, *19*, 4107-4109.

7-Trifluoromethylated camptothecin derivatives **58** (Figure 13) were synthesized by Zhu and coworkers.[64] Some of them presented higher *in vitro* antitumor activity than topotecan **2**. Further *in vivo* and *in vitro* studies showed that the 7-position of CPTs is a favorable site for the introduction of a trifluoromethyl group.

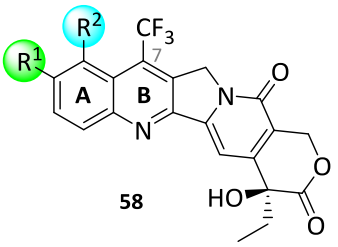

Figure 13. Structure of 7-trifluoromethylated camptothecin derivatives **58**.

In addition, some 10-arylcamptothecins **59** and **60** (Figure 14) were synthesized by Suzuki cross coupling[65] chemistry, some of them showing high cytotoxicity in preliminary *in vitro* assays.

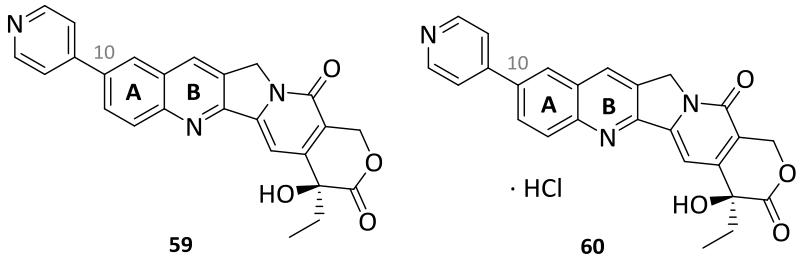

Figure 14. 10-Arylcamptothecins **59** and **60** as TopI inhibitors.

[64] Zhu, L.; Miao, Z.; Sheng, C.; Guo, W.; Yao, J.; Liu, W.; Che, X.; Wang, W.; Cheng, P.; Zhang, W. *Eur. J. Med. Chem*. **2010**, *45*, 2726-2732.

[65] Jiao, Y.; Liu, H. C.; Geng, M. Y.; Duan, W. H. *Bioorg. Med. Chem. Lett.* **2011**, *21*, 2071-2074.

CPTs with lipophilic moieties at position 9 have been synthesized, including compounds with various substituted C=N groups linked to CPT scaffold *via* oxyiminomethyl moieties (Figure 15). These compounds **61-63** exhibited potent cytotoxic activity *in vitro* and *in vivo* comparable or superior to TPT **2**.[66]

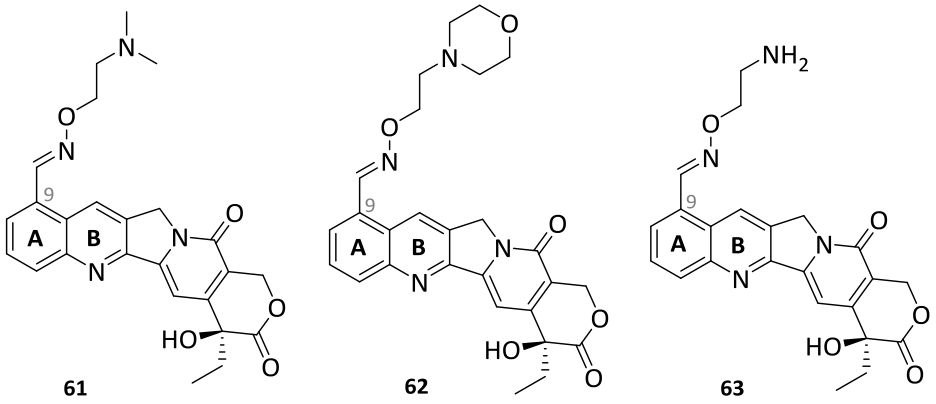

Figure 15. Structures of 9-substituted CPTs **61-63**.

Modifications in E-ring substitution

As it has been already mentioned, one of the most important limitations of the CPT due to its chemical instability is the lactone ring opening (see Scheme 2, page 25). To date, different approaches have been adopted to overcome this limitation.

The strategy based on the extension of the E-ring by one carbon atom, avoids ring opening reaction.[67,68] This enlargement is achieved by the insertion of a methylene

[66] De Cesare, M.; Beretta, G. L.; Tinelli, S.; Benedetti, V.; Pratesi, G.; Penco, S.; Dallavalle, S.; Merlini, L.; Pisano, C.; Carminati, P.; Zunino, F. *Biochem. Pharmacol.* **2007**, *73,* 656-664.

[67] Lavergne, O.; Lesueur-Ginot, L.; Pla Rodas, F.; Kasprzyk, P. G.; Pommier, J.; Demarquay, D.; Prevost, G.; Ulibarri, G.; Rolland, A.; Schiano-Liberatore, A. M.; Harnett, J.; Pons, D.; Camara, J.; Bigg, D. C. H. *J. Med. Chem*. **1998**, *41*, 5410-5419.

[68] Tangirala, R. S.; Antony, S.; Agama, K.; Pommier, Y.; Anderson, B. D.; Bevins, R.; Curran, D. P. *Bioorg. Med. Chem*. **2006**, *14*, 6202-6212.

spacer between C-20 moiety and the carbonyl group of the classical six-membered α-hydroxyl lactone ring. These compounds are named homocamptothecins (hCPTs) and the first hCPT to enter clinical trials with promising results is diflomotecan **64** (Scheme 11). This derivative, which showed more stable E-ring, hydrolyzes less rapidly to the carboxylate form **65** than the classical α-hydroxylactone present in CPTs and so, it has revealed to be a stronger TopI poison.

Another modification in this ring consisted on converting the E-ring from 6 to a 5-membered ring and it was achieved with the synthesis of α-keto derivatives exemplified by S 39625 **66** (Scheme 11). The remarkable potency of this novel drug class against purified TopI and in cells, with selective targeting of TopI indicates the tight binding of S 39625 **66** to TopIcc.[69]

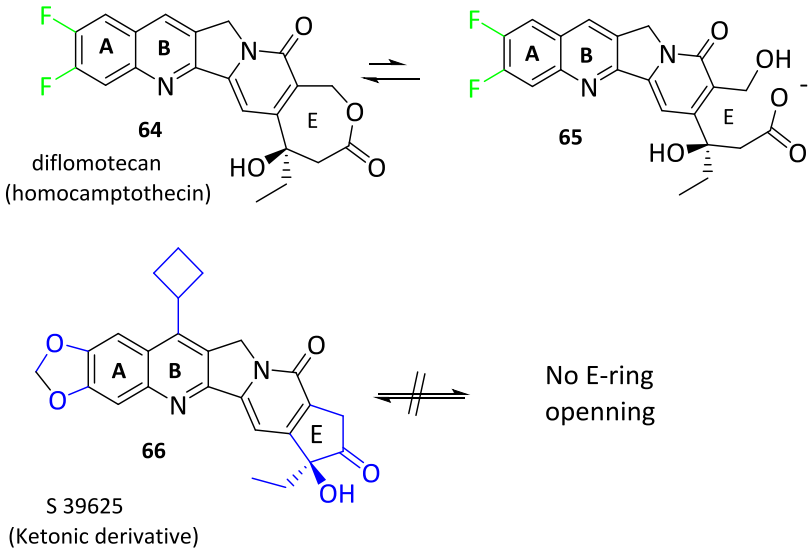

Scheme 11. Synthetic E-ring camptothecin analogs.

[69] Takagi, K.; Dexheimer, T. S.; Redon, C.; Sordet, O.; Agama, K.; Lavielle, G.; Pierre, A.; Bates, S. E.; Pommier, Y. *Mol. Cancer Ther.* **2007**, *6*, 3229-3938.

For the synthesis of diflomotecan **64**, 2-methoxy-4-isopropylamide **69** is the suitable intermediate for the metalation of the 3-pyridine position (Scheme 12).[70] Compound **69** was prepared from 2-chloroisonicotinic acid **67**. The 2-chloro substituent in **68** was subsequently substituted by a methoxy group. Compound **69** was reduced by $NaBH_4$ in ^{i}propanol/water and cyclized in the same pot by addition of aqueous HCl furnishing lactone **70** and transformed into **71** that reacts with the auxiliary **72** to give **73**. The chiral dihydroxy acid **74** was transformed to lactone **75** with the subsequent formation of the D/E-ring. Following Comins and Nolan methodology[55] D/E fragment **75** was coupled with A/B ring fragment **76** *via* Mitsunobu alkylation followed by Heck cyclization forming C-ring of the pentacyclic derivative **64**.

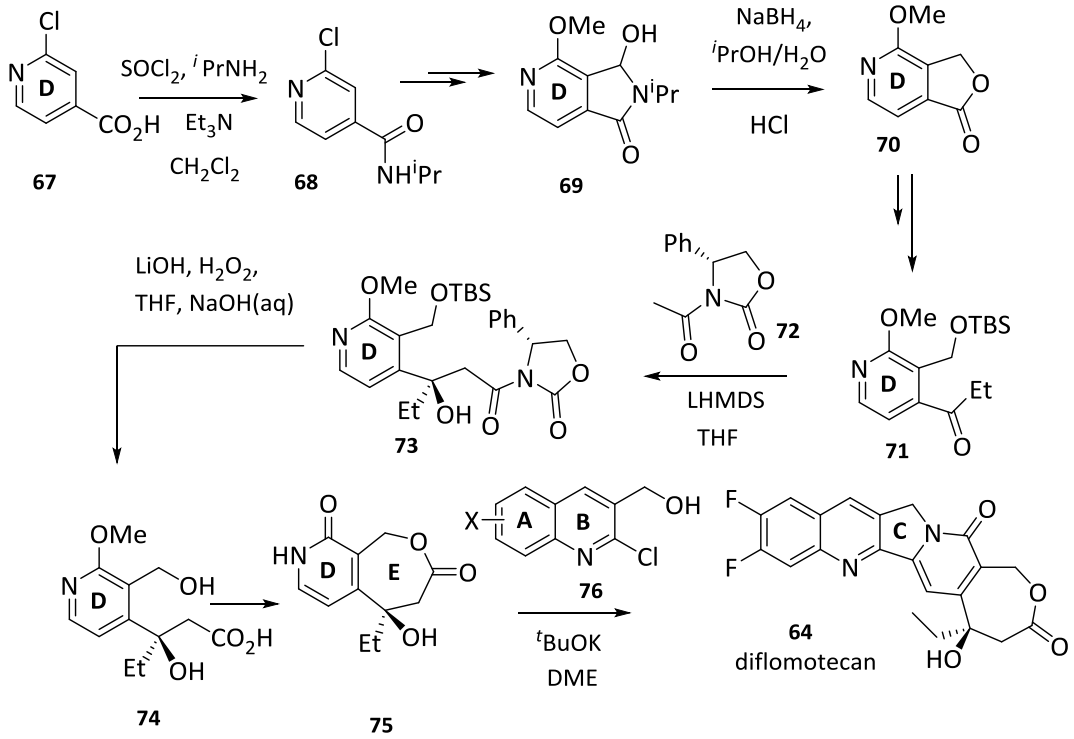

Scheme 12. Diflomotecan **64** synthesis.

[70] Peters, R., Althaus, M.; Diolez, C.; Rolland, A.; Manginot, E.; Veyrat, M. *J. Org. Chem.* **2006**, *71*, 7583-7595.

Apart from modifications in E-ring size, modifications in E-ring substitutions have also been performed so as to improve the activity. There are studies which are focused on designing ester prodrugs at C-20 position particulary aimed as new form of administration, especially on a nanoscale administration so as to optimize drug delivery.

For example, Deshmukh and coworkers,[71] synthesized a series of α-amino acid ester prodrugs of CPT. A successful example from this work is afeletecan **77**, a clinical prodrug (Figure 16).

In a similar way, 20-sulfonylamidine CPT derivatives have been studied as TopI inhibitors. These derivatives displayed potent antitumor activity with drug-resistance profiles significantly different from those of CPT **1**. Compound **78** shown in figure 16 was evaluated in mouse xenograft models and the results demonstrated significant activity without overt adverse effects at low doses.[72]

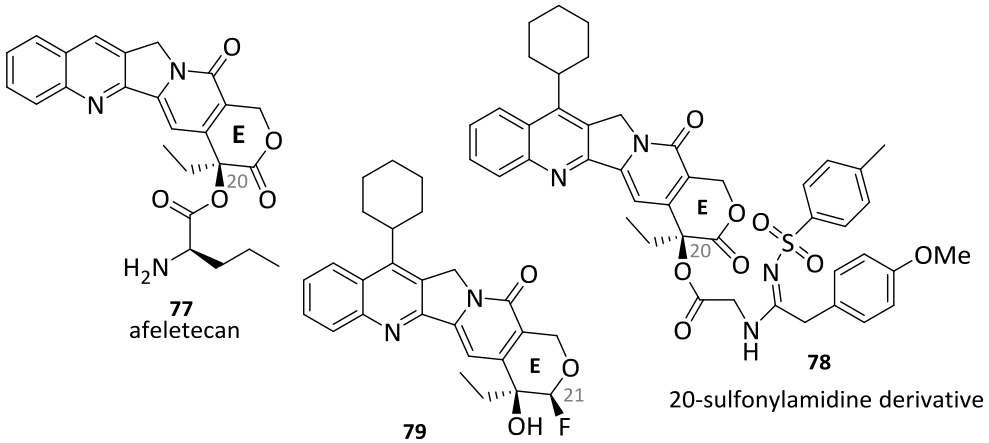

Figure 16. Different E-ring modifications in CPT structure.

[71] Deshmukh, M.; Chao, P.; Kutscher, H. L.; Gao, D. Y.; Sinko, P. J. *J. Med. Chem*. **2010**, *53*, 1038-1047.

[72] Wang, M. J.; Liu, Y. Q.; Chang, L. C.; Wang, C. Y.; Zhao, Y. L.; Zhao. X. B.; Qian, K. D.; Nan, X.; Yang, L.; Yang, X. M.; Hung, H. Y.; Yang, J. S.; Kuo, D. H.; Goto, M.; Morris-Natschke, S. L.; Pan, S. L.; Teng, C. M.; Kuo, S. C.; Wu, T. S.; Wu, Y. C.; Lee, K. H. *J. Med. Chem.* **2014**, *57*, 6008-6018.

Recently, due to the important role of fluorine substitution in drug design,[73] a series of (20*S*,21*S*)-21-fluorocamptothecins were designed and synthesized. All these analogs showed potent *in vitro* antitumor activity and were strong TopI inhibitors with increased hydrolytic stability.[74] The best results were shown in 7-cyclohexyl-21-fluoro-camptothecin **79** (Figure 16).

1.1.2.2.a Non-camptothecin derivatives

Non-camptothecin TopI inhibitors may possess better chemical stability, different therapeutic activities and antitumor spectrum, improved pharmacokinetics and lower toxicity.

Heterocyclic derivatives

Some heterocyclic compounds have been isolated from natural sources. For instance, the benzophenanthridine nitidine **80** (Figure 17) has shown to be good topoisomerase I inhibitor. This alkaloid isolated from Chinese plant *Zanthoxylum nitidum* and from the *Toddalia asiatica* found in Kenya, is more effective than CPT **1** in inhibiting the relaxation of supercoiled plasmid DNA by TopI.[75] Cellular studies suggest that TopI is the major cytotoxic target for nitidine **80**.[76] However, it is known that

[73] Alonso, C.; Martínez de Marigorta, E.; Rubiales, G.; Palacios, F. *Chem. Rev*. **2015**, *115*, 1847-1935.
[74] Miao, Z. Y.; Zhu, L. J.; Dong, G. Q.; Zhuang, C. L.; Wu, Y. L.; Wang, S. Z.; Guo, Z. Z.; Liu, Y.; Wu, S. C.; Zhu, S. P.; Fang, K.; Yao, J. Z.; Li, J.; Sheng, C. Q.; Zhang, W. N. *J. Med. Chem*. **2013**, *56*, 7902-7910.
[75] Wang, L. K.; Johnson, R. K.; Hecht, S. M. *Chem. Res. Toxicol*. **1993**, *6*, 813-818.
[76] Makhey, D.; Gatto, B.; Yu, C.; Liu, L. F.; Lavoie, E. J. *Bioorg. Med. Chem*. **1996**, *4*, 781-791.

benzophenanthridine alkaloids have been reported to mediate a variety of biological activities,[77] so that the main cause of its toxicity is still unclear.

The analog coralyne **81** (Figure 17) and its derivatives also inhibit TopI.[78] Despite the strong activity of several of these coralyne derivatives as TopI poisons, these compounds were generally less potent than CPT **1** in cellular systems.

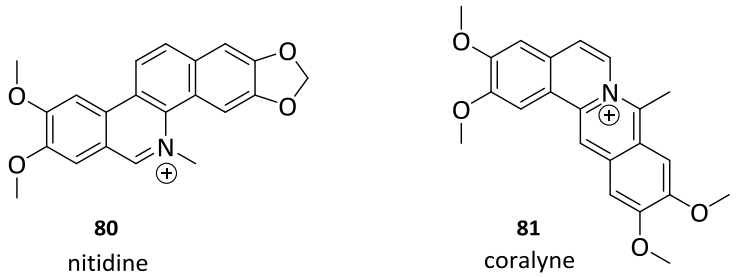

80
nitidine

81
coralyne

Figure 17. Benzophenantridine derivatives.

Another natural compound thaspine **82** (also referred to as taspine, Figure 18) is an alkaloid present in the cortex of the South American tree *Crotonlechleri* used in traditional medicine for different purposes. It was shown to induce apoptosis in HCT116 colon carcinoma cells.[79] In the same study thaspine was shown to induce a gene expression profile similar to that induced by CPT **1**, suggesting a similar cytotoxic mechanism. Thaspine is unambiguously targeting human topoisomerase IB sharing characteristics with poisons and catalytic inhibitors of topoisomerase I, being able to inhibit both the cleavage and the religation steps.

---

77 Herbert, J. M.; Augereau, J. M.; Gleye, J.; Maffrand, J. P. *Biochem. Biophys. Res. Commun.* **1990**, *172*, 993-999.

78 Gatto, B.; Sanders, M. M.; Yu, C.; Wu, H. Y.; Makhey, D.; Lavoie, E. J.; Liu, L. F. *Cancer Res*. **1996**, *56*, 2795-2800.

79 Castelli, S.; Katkar, P.; Vassallo, O.; Falconi, M.; Linder, S.; Desideri, A. *Anti-cancer Agents Med. Chem.* **2013**, *13*, 356-363.

In the case of liriodenin **83** (Figure 18), an oxoaporphine alkaloid isolated from the traditional Chinese herb *Nitidium it* has also been reported to be cytotoxic and to target TopI when chelated to gold (III).[80]

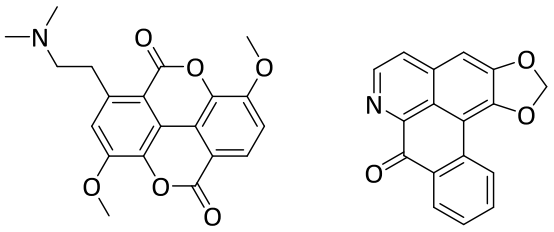

82
thaspine

83
liriodenin

Figure 18. Other natural compounds showing TopI inhibitory effect.

Lamellarins, a family of hexacyclic pyrrole alkaloids originally isolated from marine invertebrates,[81] display promising anti-tumor activity. They induce apoptotic cell death through multi-target mechanisms, including inhibition of topoisomerase I,[82] interaction with DNA and direct effects on mitochondria. Lamellarin D **84** (Figure 19) is one of the most active derivatives of this family that contains hydroxyl and methoxy groups that interact with important residues in the active site of the enzyme.

[80] Chen, Z. F.; Liu, Y. C.; Peng, Y.; Hong, X.; Wang, H. H.; Zhang, M. M.; Liang, H. *J. Biol. Inorg. Chem.* **2012**, *17*, 247-261.

[81] Raymond, J.; Andersen, D.; Faulkner, J.; He, C. H.; Van Duyne, G. D. *J. Am. Chem. Soc*. **1985**, *107*, 5492-5495.

[82] Facompre, M.; Tardy, C.; Bal-Mahieu, C.; Colson, P.; Perez C.; Manzanares, I.; Cuevas, C.; Bailly, C. L. *Cancer Res.* **2003**, *63*, 7392-7399.

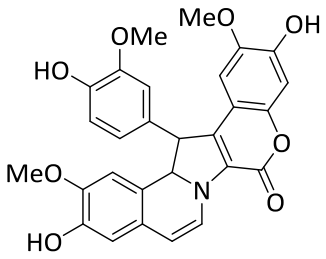

84
lamellarin D

Figure 19. Pyrrole alkaloid poisoning TopI.

In addition, heterocyclic derivatives with naphtoquinone structure such as lapachol **85**[83] (Figure 20) isolated from plants of the *Bignoniaceae* family, has been shown to be cytotoxic against tumor cells. However, it has been demonstrated that β-lapachone **86**, obtained by simple sulfuric treatment of the natural lapachol **85**, does not induce formation of the TopI-DNA cleaved complex, as CPT **1** does, but it binds directly to the enzyme preventing DNA unwinding.[84]

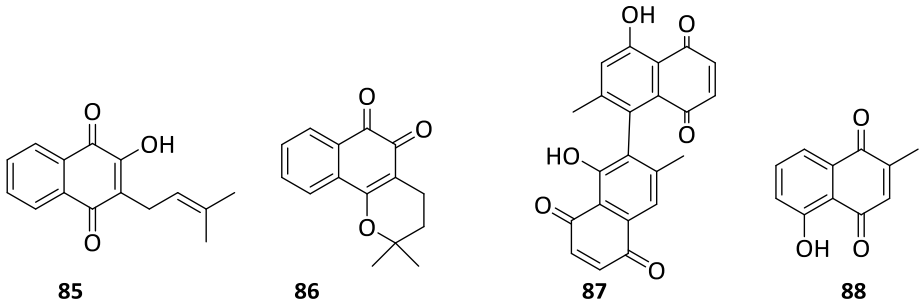

85 lapachol | **86** β-lapachone | **87** isodiospyrin | **88** plumbagin

Figure 20. Naphtoquinone derivatives as TopI inhibitors.

[83] Paterno, E. *Gazz. Chim. Ital*. **1882**, *12*, 337-392.
[84] Li, C. J.; Averboukh, L.; Pardee, A. B. *J. Biol. Chem*. **1993**, *268*, 22463-22468.

A similar mechanism occurs with isodiospyrin **87** an asymmetrical 1,2-binaphthoquinone (Figure 20), isolated from *Diospyros morrisiana*. This compound displays cytotoxic activity to tumor cell lines and it inhibits TopI by directly binding to it and limiting the access of the enzyme to the DNA substrate.[85] There is no evidence for the formation of the TopI-DNA covalent complex.

Another naphtoquinone-like derivative, plumbagin **88** (Figure 20) extracted from *Plumbago zelyanica,* has been shown to be cytotoxic and to target TopI when chelated to copper (II).[86] Nevertheless, this compound only inhibits relaxation process, suggesting that it mainly interferes with the cleavage mechanism of the enzyme.

Heterocyclic compounds with flavonoid skeleton have shown TopI inhibitory activity. For instance, quercetin **89**,[87] luteolin **90**,[88] myricetin **91**[89] and related flavonoids **92** (Figure 21) are known to inhibit tumor cells proliferation and to increase the cytotoxicity of anticancer drugs such as cisplatin **93**.[90]

---

85 Ting, C. Y.; Hsu, C. T.; Hsu, H. T.; Su, J. S.; Chen, T. Y.; Tarn, W. Y.; Kuo, Y. H.; Whang-Peng, J.; Liu, L. F.; Hwang, J. *Biochem. Pharmacol*. **2003**, *66*, 1981-1991.

86 Chen, Z. F.; Tan, M. X.; Liu, L. M.; Liu, Y. C.; Wang, H. S.; Yang, B.; Peng, Y.; Liu, H. G.; Liang, H.; Orvig, C. *Dalton Trans*. **2009**, *28* , 10824-10833.

87 Yoshida, M.; Yamamoto, M.; Nikaido, T. *Cancer Res.* **1992***, 52*, 6676-6681.

88 Chowdhury, A. R.; Sharma, S.; Mandal, S.; Goswami, A.; Mukhopadhyay, S.; Majumder, H. K. *Biochem. J*. **2002**, *366*, 653-661.

89 Lopez-Lazaro, M.; Martin-Cordero, C.; Toro, M. V.; Ayuso, M. J. *J. Enzyme Inhib. Med. Chem.* **2002**, *17*, 25-29.

90 Scambia, G.; Ranelletti, F. O.; Benedetti Panici, P.; Bonanno, G.; DeVincenzo, R.; Piantelli, M.; Mancuso, S. *Anti-cancer Drugs* **1990**, *1*, 45-48.

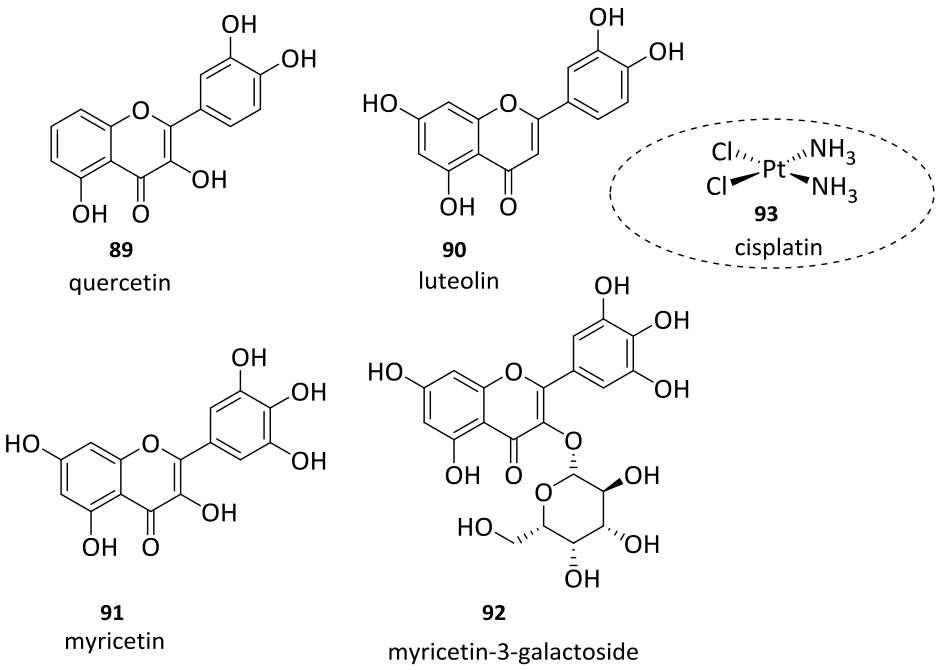

Figure 21. Flavonoids derivatives as TopI inhibitors.

A dual inhibition activity is displayed by erybraedin-C **94** (Figure 22), a natural pterocarpan, purified from the plant *Bituminaria bituminosa*, that is able to interact with the enzyme alone or with the DNA-enzyme cleavable complex in both cases inhibiting the enzyme active site.[91] Molecular docking provides an explanation for this dual activity, showing that with the enzyme alone, the preferential drug binding site is localized in the proximity of the active Tyr723 residue, with one of the two isoprene groups close to the active-site residues Arg488 and His632, essential for the catalytic reaction. When interacting with the covalent complex, erybraedin-C **94** interacts with both the enzyme and DNA in a similar way to topotecan **2**.

[91] Tesauro, C.; Fiorani, P.; D 'Annessa, I.; Chillemi, G.; Turchi, G.; Desideri, A. *Biochem. J*. **2010**, *425*, 531-539.

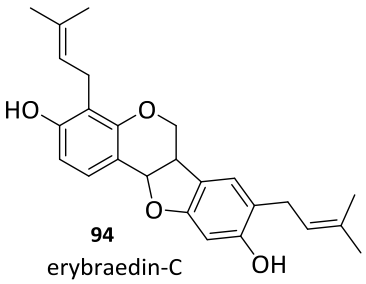

94
erybraedin-C

Figure 22. TopI cleavage and religation inhibitor.

Other non-natural heterocyclic compounds can act as topoisomerase I inhibitors. For instance, indenoisoquinolinones have been investigated and optimized for therapeutic development and a wide scope of them have been synthesized and tested.[92] These indenoisoquinolines are chemically stable, they trap TopIcc at differential sites than CPTs, which is indicative of potentially different gene targeting, their antiproliferative activity is similar or greater than that of CPTs in some cell lines and they selectively target TopI in cells. This particular binding mode is also common among other non-CPT TopI inhibitors such as the indenoisoquinolines, norindenoisoquinolines, and indolocarbazoles.

Derivatives with a carbonyl group in position 11 of the indenoisoquinoline ring show both; inhibitory activity towards TopI and cytotoxic effect in five different cell lines. One of the most promising indenoisoquinolinones that shows cytotoxicity values

[92] (a) Antony, S.; Jayaraman, M.; Laco, G.; Kohlhagen, G.; Kohn, K. W.; Cushman, M.; Pommier, Y. *Cancer Res*. **2003**, *63*, 7428-7435. (b) Antony, S.; Kohlhagen, G.; Agama, K.; Jayaraman, M.; Cao, S.; Durrani, F. A.; Rustum, Y. M.; Cushman, M.; Pommier, Y. *Mol. Pharmacol*. **2005**, *67*, 523-530. (c) Antony, S.; Agama, K. K.; Miao, Z. H.; Hollingshead, M.; Holbeck, S. L.; Wright, M. H.; Varticovski, L.; Nagarajan, M.; Morrell, A.; Cushman, M.; Pommier, Y. *Mol. Pharmacol*. **2006**, *70*, 1109-1120. (d) Nagarajan, M.; Morrell, A.; Ioanoviciu, A.; Antony, S.; Kohlhagen, G.; Agama, K.; Hollingshead, M.; Pommier, Y.; Cushman, M. *J. Med. Chem*. **2006**, *49*, 6283-6289. (e) Antony, S.; Agama, K. K.; Miao, Z. H.; Takagi, K.; Wright, M. H.; Robles, A. I.; Varticovski, L.; Nagarajan, M.; Morrell, A.; Cushman, M.; Pommier, Y. *Cancer Res*. **2007**, *67*, 10397-10405.

similar to CPT is NSC 314622 **96** (Figure 23).[93] Several substitution modifications in the indenoisoquinolinones have been made so as to stabilize TopI-DNA complex.[94] Some examples **95-99** are represented in figure 23.

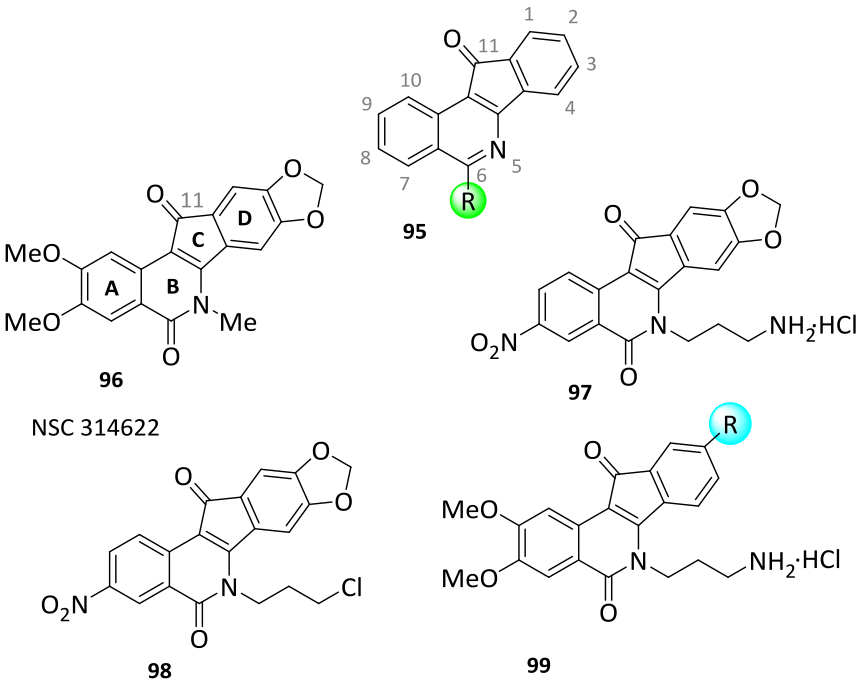

Figure 23. Indenoisoquinolinone derivatives.

Modifications in the indenoisoquinoline A, B and D rings have been extensively studied in order to optimize TopI inhibitory activity and cytotoxicity. To improve the understanding of the forces that stabilize drug-TopI-DNA ternary complexes, the five-membered cyclopentadienone C-ring of the indenoisoquinoline system was replaced by

[93] (a) Kohlhagen, G.; Paull, K.; Cushman, M.; Nagafuji, P.; Pommier, Y. *Mol. Pharmacol*. **1998**, *54*, 50-58. (b) Song, Y.; Shao, Z.; Dexheimer, T. S.; Scher, E. S.; Pommier, Y.; Cushman, M. *J. Med. Chem*. **2010**, *5*, 1979-1989.

[94] Khadka, D. B.; Cho, W. J. *Bioorg. Med. Chem*. **2011**, *19*, 724-734.

six-membered nitrogen heterocyclic rings, resulting in dibenzo[*c*,*h*][1,6]naphthyridines **100** and **101** that were synthesized by a novel route and tested as TopI inhibitors (Figure 24).[95] This resulted in several compounds that had unique DNA cleavage site selectivities and potent antitumor activities in a number of cancer cell lines. The novel chloronaphthyridinones **100** represent promising lead compounds with TopI inhibitory activities and low micromolar to submicromolar cytotoxicity GI_{50} values.

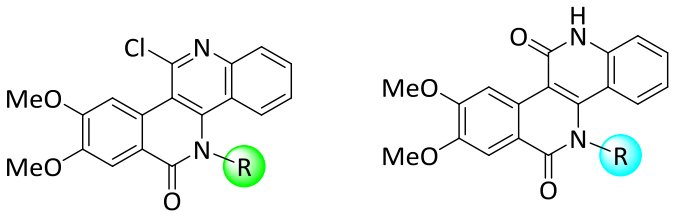

100 **101**

Figure 24. Examples of [1,6]-naphthyridine derivatives **100** and **101**.

Non-Heterocyclic derivatives

Apart from heterocyclic derivatives, it is possible to find non-heterocyclic derivatives in literature as topoisomerase I inhibitors. Condensed carbocycles such as acetyl-boswellic acid **102** (acetyl-BA), a pentacyclic triterpene (Figure 25) derived from the gum resin of *Boswellia serrata*, are effective cytotoxic agents, acting through a mechanism that appears to involve the inhibition of TopI activity.[96] The inhibition does not involve stabilization of the cleaved complex or the intercalation of DNA, but competition with DNA for binding to the enzyme.[97] Fomitellic acid **103** (Figure 25), found in the higher plants *Tabebuia caraiba* and *Campsis radicans*, has been also reported as

[95] Kiselev, E.; Dexheimer, T.; Pommier, Y.; Cushman, M. *J. Med. Chem*. **2010**, *53*, 8716-8726.
[96] Hoernlein, R. F.; Orlikowsky, T.; Zehrer, C.; Niethammer, D.; Sailer, E. R.; Simmet, T.; Dannecker, G. E.; Ammon, H. P. *J. Pharmacol. Exp. Ther*. **1999**, *288*, 613-619.
[97] Syrovets, T.; Buchele, B.; Gedig, E.; Slupsky, J. R.; Simmet, T. *Mol. Pharmacol.* **2000***, 58*, 71-81.

TopI inhibitor through a direct acid-enzyme interaction mechanism.[98] Additionally, it has also been observed an inhibitory effect on the growth of cancer cells in the case of ganoderic acid **104** (Figure 25), isolated from the fruit bodies of *Ganoderma amboinense*.[99]

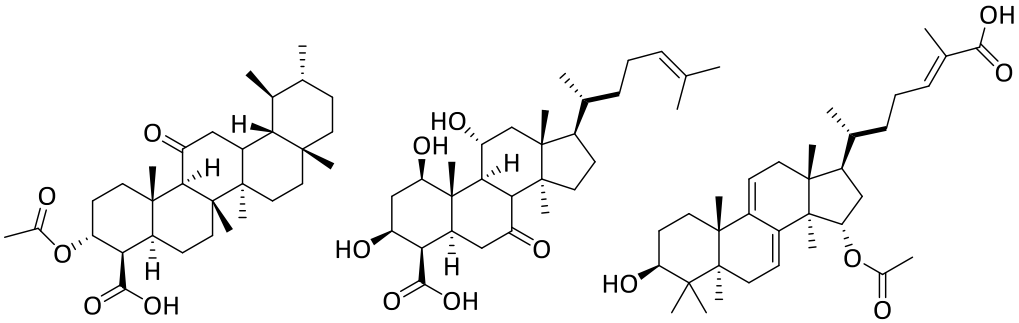

102 acetyl-boswellic acid

103 fomitellic acid

104 ganoderic acid

Figure 25. Triterpene derivatives **102-104** as TopI inhibitors.

Finally, there are acyclic compounds that have also shown TopI inhibitory effect. Conjugated Eicosapentaenoic Acid (cEPA) **105** (Figure 26), which is found in seaweeds such as red and green algae, has an inhibitory effect on human cancer cells and it inhibits supercoiled DNA relaxation by TopI.[100] The acid **105** inhibits the cleavage reaction and it is not able to stabilize the enzyme-DNA covalent complex.[101]

---

98 Mizushina, Y.; Iida, A.; Ohta, K.; Sugawara, F.; Sakaguchi, K. *Biochem. J*. **2000**, *350*, 757-763.

99 Li, C. H.; Chen, P. Y.; Chang, U. M.; Kan, L. S.; Fang, W. H.; Tsai, K. S.; Lin, S. B. *Life Sci*. **2005**, *77*, 252-265.

100 Yonezawa, Y.; Tsuzuki, T.; Eitsuka, T.; Miyazawa, T.; Hada, T.; Uryu, K.; Murakami-Nakai, C.; Ikawa, H.; Kuriyama, I.; Takemura, M. *Arch. Biochem. Biophys*. **2005**, *435*, 197-206.

101 Castelli, S.; Campagna, A.; Vassallo, O.; Tesauro, C.; Fiorani, P.; Tagliatesta, P.; Oteri, F.; Falconi, M.; Majumder, H. K.; Desideri, A. *Arch*. *Biochem. Biophys*. **2009**, *486*, 103-110.

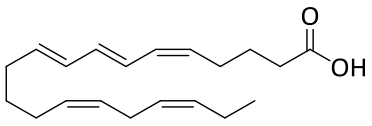

105

Conjugated Eicosapentaenoic Acid (cEPA)

Figure 26. Fatty acid **105** as Top I inhibitor.

1.1.2.2.b Synthesis of non-camptothecin derivatives

Strategies for the preparation of non-CPT derivatives with isoquinoline or indenoisoquinoline core have been widely studied. The Pictet-Spengler condensation,[102] (Scheme 13) also known as Pictet-Spengler tetrahydroisoquinoline synthesis, is one of the most relevant strategies available to the modern chemist for the synthesis of isoquinoline containing heterocycles.

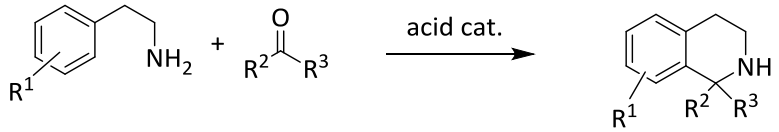

106 **107** **108**

Scheme 13. The Pictet-Spengler reaction.

[102] (a) Pictet, A.; Spengler, T. *Ber. Dtsch. Chem. Ges*. **1911**, *44*, 2030-2036. (b) Cox, E. D.; Cook, *J. M. Chem. Rev*. **1995**, *95*, 1797-1842.

In 2010, the synthesis of new anticancer norindenoisoquinoline TopI inhibitors was reported.[103] The general strategy is based on the classical Pomeranz-Fritsch reaction[104] (Scheme 14) and the improved versions include the Bobbit[105] and Jackson modifications.[106,107]

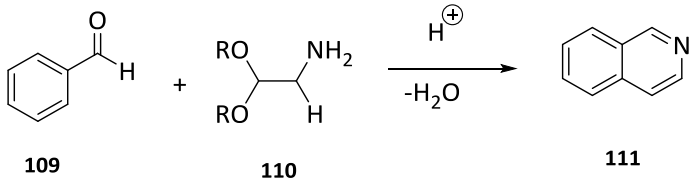

Scheme 14. Pomeranz-Fritsch reaction.

In such this way, 2-methylpiperonal **112** is converted to its oxime **113** with subsequent radical bromination with NBS and AIBN affording the benzyl bromide **114** (Scheme 15). Displacement of the bromide with various amines and condensation of the oxime **116** with the intermediate **117** yielded the final products **118**. The intermediate **117** that is the isoquinolinic ring precursor was synthesized following the methodology previously described by the same authors.[107]

[103] Song, Y.; Shao, Z.; Dexheimer, T. S.; Scher, E. S.; Pommier, Y.; Cushman, M. *J. Med. Chem.* **2010**, *53*, 1979-1989.
[104] Gensler, W. J. *Org. React.* **1951**, *6*, 191-206.
[105] Bobbitt, J. M.; Winter, D. P.; Kiely, J. M. *J. Org. Chem.* **1965**, *30*, 2459-2460.
[106] Birch, A. J.; Jackson, A. H.; Shannon, P. V. R. *J. Chem. Soc. Perkin Trans.* **1974**, *1*, 2185-2190.
[107] Ioanoviciu, A.; Antony, S.; Pommier , Y.; Staker, B. L.; Stewart, L.; Cushman, M. *J. Med. Chem.* **2005**, *48*, 4803-4814.

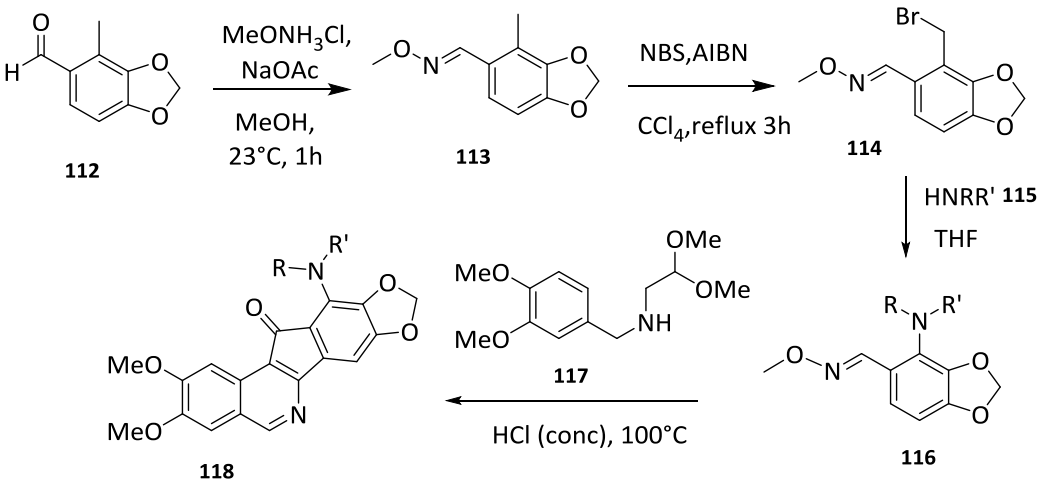

Scheme 15. Indenoisoquinole derivatives **106** synthesis

These indenoisoquinolines **118** present an indenone fragment in its structure that could be interesting in terms of the biological activity since this fragment is present in compounds with very interesting biological properties including topoisomerase I inhibitory effect. This is the case of indotecan[108] **119** (Figure 27) currently in Phase I trials.

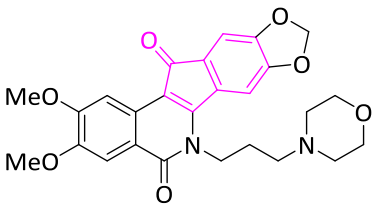

119
indotecan

Figure 27. Indenoisoquinoline derivative, indotecan **119**.

[108] Beck, D. E.; Agama, K.; Marchand, C.; Chergui, A.; Pommier, Y.; Cushman, M. *J. Med. Chem*. **2014**, *57*, 1495-1512.

To date, the most frequently used synthetic approach to various indenoisoquinolines substituted on the indenone D-ring has been the condensation of homophthalic anhydrides **120** (Scheme 16) with various Schiff bases **121**, followed by cyclization of the resulting *cis* isoquinolonic acids **122** into indenoisoquinolinediones **123** *via* intramolecular acylation, forming the central C-ring.[109]

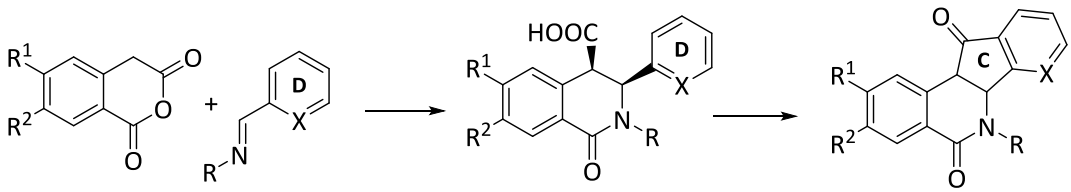

Scheme 16. Synthetic approach to indenoisoquinolines.

The presence of an additional nitrogen atom in the aromatic ring improves the cytotoxic properties with respect to the structures that lack this extra nitrogen atom. This fact could be due to an improvement in π-π* stacking interactions with the base pairs in the ternary complex drug-TopI-DNA.[110] For this reason, in order to prepare 7-azaindenoisoquinolinones (X=N) **123**, a 2-pyridyl Schiff base **121** needs to be used as the precursor for the D-ring (Scheme 16). Due to extremely low reactivity of pyridines in reactions of electrophilic aromatic substitution, cyclization of **122** into the corresponding **123** would be very difficult. Therefore, Kiselev and coworkers[111] designed an alternative protocol in which the commercially available 2-cyano-3-picoline **124** was treated with *N*-bromosuccinimide (NBS) in refluxing 1,2-dichloroethane in presence of the radical

[109] (a) Nagarajan, M.; Xiao, X. S.; Antony, S.; Kohlhagen, G.; Pommier, Y.; Cushman, M. *J. Med. Chem*. **2003**, *46*, 5712-5724. (b) Morrell, A.; Placzek, M. S.; Steffen, J. D.; Antony, S.; Agama, K.; Pommier, Y.; Cushman, M. *J. Med. Chem*. **2007**, *50*, 2040-2048.

[110] Kiselev, E.; Agama, K.; Pommier, Y.; Cushman, M. *J. Med. Chem.* **2012**, 55, 1682-1697.

[111] Kiselev, E.; DeGuire, S.; Morrell, A.; Agama, K.; Dexheimer, T. S.; Pommier, Y.; Cushmam, M. *J. Med. Chem*. **2011**, *54*, 6106-6116.

initiator AIBN (Scheme 17). Crude bromide **125** was subsequently treated with homophthalic anhydride **126** to provide compounds **127**. Treatment of **127** with selenium dioxide in refluxing 1,4-dioxane provided indenoisoquinolines **128**.

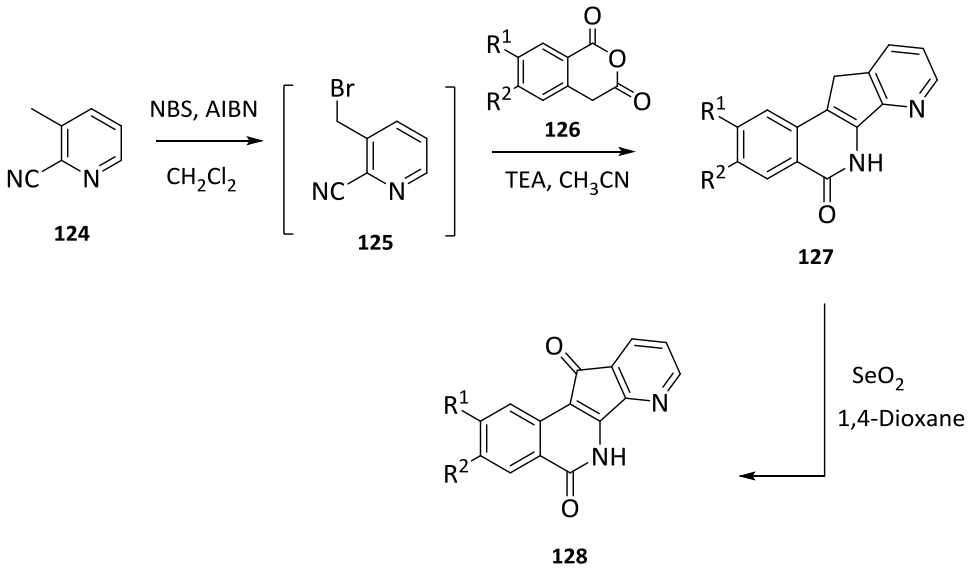

Scheme 17. 7-Azaindenoisoquinolines synthesis

Cushman and coworkers,[112] bearing in mind the importance of compounds with dual tyrosyl-DNA phosphodiesterase I (Tdp1)-topoisomerase I (TopI) inhibitory activity, reported in 2012 the synthesis of the first dual inhibitor Tdp1-TopI which is based on the indenoisoquinoline chemotype.

[112] Nguyen, T. X.; Morrell, A.; Conda-Sheridan, M.; Marchand, C.; Agama, K.; Bermingham, A.; Stephen, A. G.; Chergui, A.; Naumova, A.; Fisher, R.; O'Keefe, B. R.; Pommier, Y.; Cushman, M. *J. Med. Chem.* **2012**, *55*, 4457-4478.

The key starting material in the synthesis of these inhibitors is the lactone **132** obtained from lactones **129** and **130** which upon reaction with aminoalcohols **133** yields the indenoisoquinolines **134** that are further transformed to the desired indenoisoquinoline sulfonamides **135** (Scheme 18).

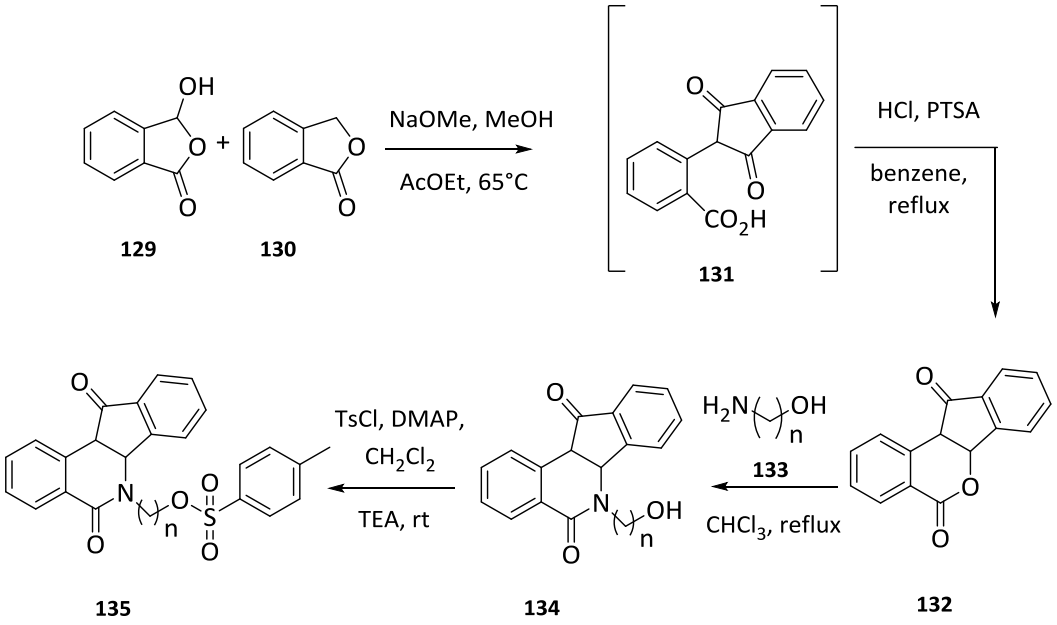

Scheme 18. Indenoisoquinoline derivatives synthesis.

In order to optimize TopI inhibitory activity and cytotoxicity, Cushman and coworkers[95] introduced modifications in the five-membered cyclopentadienone C-ring of the indenoisoquinoline system replacing it by six-membered nitrogen heterocyclic rings resulting in dibenzo[*c,h*][1,6]-naphthyridinones **143**. Thus, the *N*-protected *o*-aminobenzaldehyde **136** was converted to imine **137** (Scheme 19), which reacted with **138** to give the mixture of *cis*/*trans* derivatives **139/140**. This mixture **139/140** was esterified to produce the more stable *trans* ester **141** followed by dehydrogenation and acidification with acetic acid to provided product **143**. In the same work, authors

prepared a variety of analogues that presents TopI inhibitory activities and low micromolar to submicromolar cytotoxicity IC_{50} values.

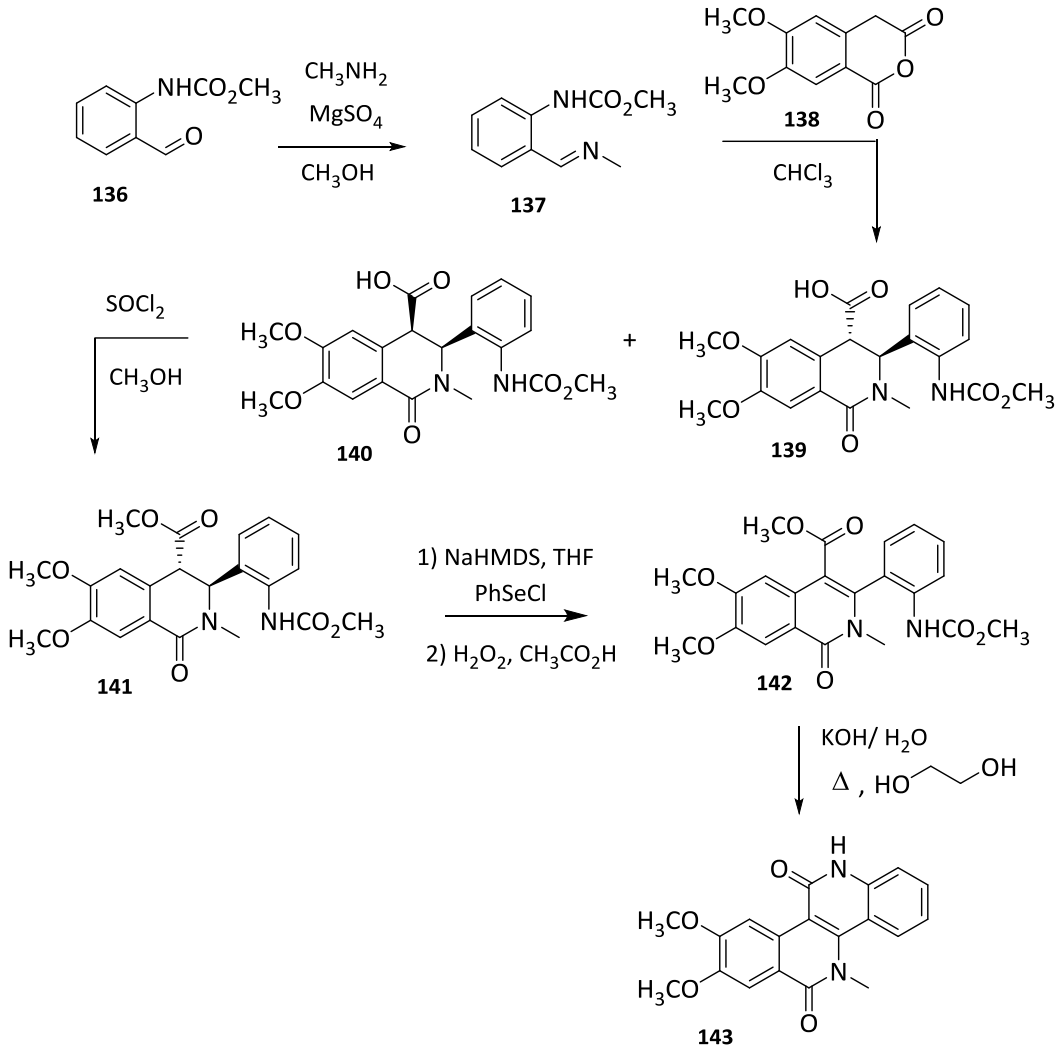

Scheme 19. Synthesis of dibenzo[*c,h*][1,6]-naphthyridines.

In the search of a novel chemotype to develop TopI inhibitors, Taliani and coworkers[113] designed some phenylpyrazolo[1,5-*a*]-quinazoline core derivatives **145** (Figure 28) that are structurally related to the indenoisoquinoline systems. In fact, the core of these pyrazoloquinazolines **145** would mimic the A, B and C rings of the indeno-isoquinoline structure **144**, while the phenyl hanging from the pyrazole portion of **145** could mimic the substituted D ring of **144**.

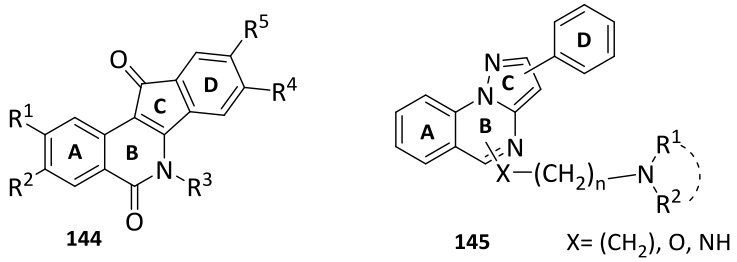

Figure 28. Indenoisoquinoline structures **144** *vs* pyrazoloquinazolines **145**.

The phenylpyrazolo[1,5-*a*]-quinazoline derivatives **153** were synthesized as shown in scheme 20. The commercially available 2-hydrazinobenzoic acid hydrochloride **146** and ethylbenzoylacetate **147** were reacted in water to yield the hydrazone **148** that was then transformed into the lactone **149**. The 2-phenyl-5*H*-pyrazolo[1,5-*a*][3,1]-benzoxazin-5-one **149** was obtained by an improved microwave procedure and then reacted with the appropriate dialkylaminoalkylamine **150** or **152** to obtain compounds **151** or **153**, respectively.

[113] Taliani, S.; Pugliesi, I.; Barresi, E.; Salerno, S.; Marchand, C.; Agama, K.; Simorini, F.; La Motta, C.; Marini, A. M.; Saverio Di Leva, F.; Marinelli, L.; Cosconati, S.; Novellino, E.; Pommier, Y.; Di Santo, R.; Da Settimo, F. *J. Med. Chem*. **2013**, *56*, 7458-7462.

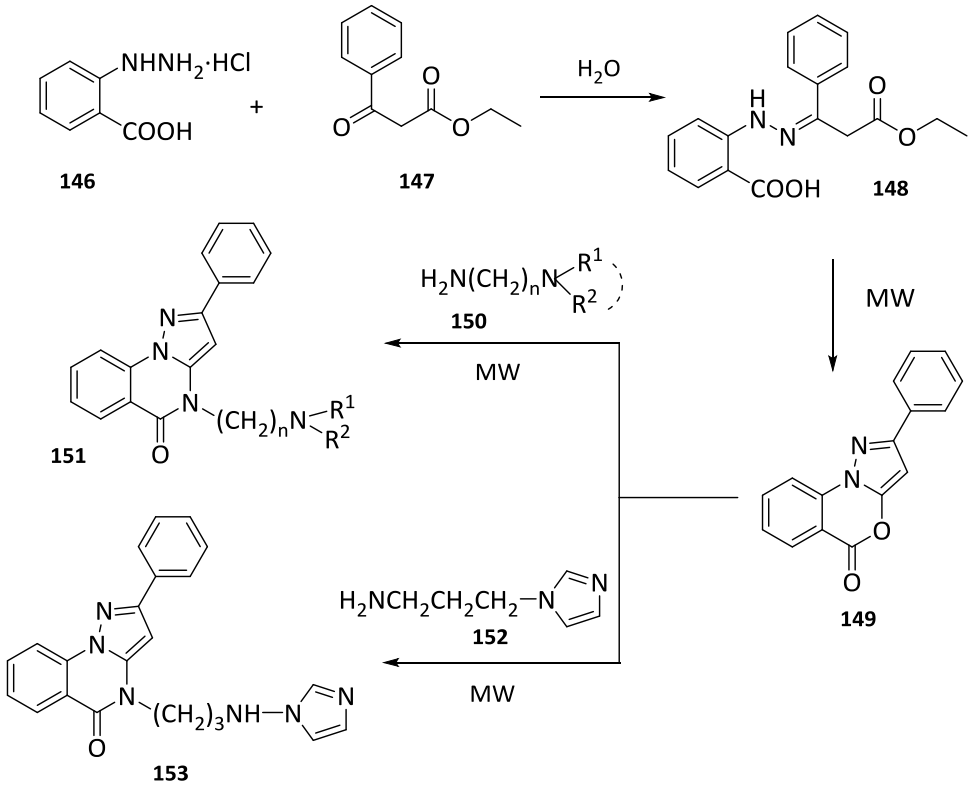

Scheme 20. 7-Phenylpyrazolo[1,5-*a*]-quinazoline synthesis.

Some of these compounds are in fact able to target not only the TopI present in cancer processes but also TopI found in diverse widespread parasites such as *Plasmodium falciparum* and *Leishmania donovani*.[114]

With these antecedents in mind we explored the design of new topoisomerase I inhibitors that do not present CPT **1** limitations and with good stabilities. Our aim was to synthesize polinuclear flat heterocyclic derivatives that could act *via* a comparable

[114] Roy, A.; Das, B. B.; Ganguly, A.; Bose Dasgupta, S.; Khalkho, N. V.; Pal, C.; Dey, S.; Giri, V. S.; Jaisankar, P.; Dey, S. *Biochem. J*. **2008**, *409*, 611-622.

mechanism to that of CPT **1** by forming a ternary TopI covalent complex between TopI-DNA and the synthesized derivatives.

Chapter 2

Synthesis of 1,5-naphthyridine derivatives

2.1. Povarov reaction

The six-membered nitrogen-containing heterocyclic compounds play a major role in organic chemistry through their widespread presence in nature and in their consequent biological activity. These compounds are also frequently found in synthetic pharmaceuticals and drugs.[115] Clear examples of this relevance are some chemotherapeutic agents used in cancer treatment previously described in chapter 1. The vast majority of these molecules present several fused heterocycles in their structure.

Heteroaromatic flat compounds are particularly effective as antitumoral agents.[116] Among them some remarkable structures are tetrahydroquinoline derivatives, isoquinoline analogs and naphthyridine structure that are known to display several biological activities including antimalarials, antitumorals, antioxidants and anti-inflammatory properties.[117]

Many strategies have been developed in order to facilitate the synthesis of various complex natural products; nevertheless, most of them are time-consuming and in some cases might also lack structural variability. Nowadays, it is highly desirable to achieve diversity oriented molecules in a simple way.

One of the major challenges in modern organic synthesis is to develop highly selective methodologies to provide efficient and fast access to biologically important

[115] (a) Michael, J. P. *Nat. Prod. Rep*. **2008**, *25*, 166-187. (b) Stefani, H. A.; Amaral, M. F. Z.; Reyes-Rangel, G.; Vargas-Caperati, J.; Juaristi, E. *Eur. J. Org. Chem*. **2010**, 6393-6403. (c) Kaur, K.; Jain, M.; Reddy, R. P.; Jain, R. *Eur. J. Med. Chem.* **2010**, *45*, 3245-3264. (d) Nahed, F.; Abdel, G. *Nature and Science* **2011**, *9*, 190-201. (e) Pham, H. T.; Chataigner, I.; Renaud, J. L. *Curr. Org. Chem.* **2012**, *16*, 1754-1775. (f) Tseng, C. H.; Chen, Y. L.; Yang, C. L.; Cheng, C. M.; Han, C. H.; Tzeng, C. C. *Bioorg. Med. Chem*. **2012**, *20*, 4397-4404. (g) Luniewski, W.; Wietrzyk, J.; Godlewska, J.; Switalska, M.; Piskozub, M.; Peczynska-Czoch, W.; Kaczmarek, L. *Bioorg. Med. Chem. Lett*. **2012**, *22*, 6103-6107.

[116] Thapa, U.; Thapa, P.; Karki, R.; Yun, M.; Choi, J. H.; Jahng, Y.; Lee, E.; Jeon, K. H.; Na, Y.; Ha, E. M.; Cho, W. J.; Kwon, Y.; Lee, E. S. *Eur. J. Med. Chem.* **2011**, *46*, 3201-3209.

[117] Martins, P.; Jesus, J.; Santos, S.; Raposo, L. R.; Roma-Rodrigues, C.; Baptista, P. V.; Fernandes, A. R. *Molecules* **2015**, *20*, 16852-16891.

molecules found in natural products and scaffolds for pharmaceutical development. The hetero-Diels-Alder reaction (HDA) is among the most useful strategies used for the synthesis of six-membered nitrogen heterocycles[118] and it is a highly atom-economic alternative for carbon-carbon and carbon-heteroatom bond construction[119] to generate molecular complexity efficiently and with industrial applications.[120] Among them, the Povarov reaction[121,122] could be considered as an example of HDA reaction and represents an excellent method for the preparation of nitrogen-containing heterocyclic compounds, where aldimines derived from aromatic amines and aldehydes react with electron-rich alkenes in the presence of a Lewis acid catalyst. In this sense, Povarov reaction can be considered as a potential tool for the synthesis of several nitrogen containing heterocycles and thus, we think that it could be an appropriate synthetic strategy for the preparation of the desired 1,5-indenonaphthyridine and 1,5-naphthyridine derivatives that can behave as topoisomerase I inhibitors.

In the Povarov reaction, originally reported in 1963,[121a] arylaldimines **156**, obtained from condensation of aromatic aldehydes **155** and aniline **154**, reacts with electron-rich olefins, in the presence of $BF_3{\cdot}Et_2O$ as Lewis acid (LA) catalyst yielding 2,4-disubstituted tetrahydroquinolines **158** which were further oxidized to the corresponding quinolines **159** (Scheme 21). The reaction can be considered as a

[118] (a) Nicolaou, K. C.; Snyder, S. A.; Montagnon, T.; Vassilikogiannakis, G. *Angew. Chem. Int. Ed*. **2002**, *41*, 1668-1698. (b) Fringuelli, F.; Taticchi, A. *The Diels–Alder Reaction: Selected Practical Methods*; Wiley, Chichester: UK, **2002**. (c) Ess, D. H.; Jones, G. O.; Houk, K. N. *Adv. Synth. Catal*. **2006**, *348*, 2337-2361.

[119] Shea, K. M. Name Reactions for Carbocyclic Ring Formations, Li, J. J. Ed, Wiley, Hoboken: NJ, **2010**, pp. 275-308.

[120] Funel, J. A.; Abele, S. *Angew. Chem. Int. Ed.* **2013**, *52*, 3822-3863.

[121] (a) Povarov, L. S., Mikhailov, B. M. *Izv. Akad. Nauk SSR, Ser. Khim.* **1963**, 953-956. (b) Povarov, L. S. *Russ. Chem. Rev*. **1967**, *36*, 656-670. (c) Vicente-Garcia, E.; Ramon, R.; Lavilla, R. *Synthesis* **2011**, 2237-2246. (d) Kouznetsov, V. V. *Tetrahedron* **2009**, *65*, 2721-2750.

[122] For recent contributions see: (a) Zanwar, M. R.; Gawande, S. D.; Kavala, V.; Kuo, C. W.; Yao, C. F. *Adv. Synth. Catal*. **2014**, *356*, 3849-3860. (b) Galvez, J.; Castillo, J. C.; Quiroga, J.; Rajzmann, M.; Rodriguez, J.; Coquerel, Y. *Org. Lett*. **2014**, *16*, 4126-4129. (c) Bunescu, A.; Wang, Q.; Zhu, *J. Org. Lett.* **2014**, *16*, 1756-1759. (d) Muthukrishnan, I.; Vinoth, P.; Vivekanand, T.; Nagarajan, S.; Maheswari, C. U.; Menendez, J. C.; Sridharan, V. *J. Org. Chem.* **2015**, *6*, 32317-32338. (e) Bello, F.; Josue, S.; Jones, J, Jr.; Da Silva, F. M. *Curr. Org. Synth.* **2016***, 13,* 157-175.

powerful tool for generating three contiguous stereogenic centers in a single step with excellent regioselectivity.

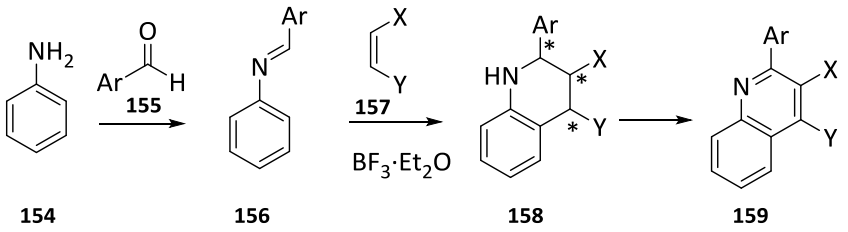

Scheme 21. Lewis-Acid catalyzed Povarov reaction.

Since the pioneering work of Povarov and coworkers, relevant interest and enormous efforts have been implicated in this particular research area to achieve more efficient synthetic routes to directly access tetrahydroquinolines and other interesting heterocyclic scaffolds employing Povarov reaction as the key step.

There are a lot of publications coming out each year on this particular issue, describing new mechanistic features and discovering novel synthetic applications. In 2009 Kouznetsov[121d] reviewed this topic. This author mainly focused on the various applications of Povarov reaction, especially, the intramolecular strategy allowing a straightforward access to various heterocycles.

In 2010, Lavilla and coworkers[123] outlined different mechanistic variations of this reaction including the multicomponent version. The asymmetric version of Povarov reaction has been reviewed by Fochi and Bernardi's group.[124]

In general, for Diels-Alder reactions, the electronic features on the substituents at the diene and the dienophile should be opposite. This type of substitution favors an asynchronous concerted mechanism. In this sense, adequate substitution on the diene

[123] Bello, D.; Ramón, R.; Lavilla, R. *Curr. Org. Chem*. **2010**, *14*, 332-356.
[124] Fochi, M. F.; Caruana, L.; Bernardi, L. *Synthesis* **2014**, *46*, 135-157.

and the dienophile, which can favor the stabilization of charges of opposite sign, can produce a stepwise mechanism with highly polar character.[125]

Azabutadienes might be electrophilically activated by the coordination with an LA to participate in the Diels-Alder reaction towards alkenes. In addition, *N*-arylimines bear an aromatic ring, being of poor reactivity when participating along the cycloaddition, a behavior that could reverse the addition reaction. These two behaviors demand a strong electrophilic activation of the *N*-arylimine. For this purpose, it is necessary to use strong LAs, and even Brønsted acids (BAs) able to activate the heterodiene moiety.

The use of Lewis acid catalysis can be considered as the standard method for the Povarov reaction. The most popular LAs include among others, the original boron trifluoride, iodine,[126] cerium ammonium nitrate,[127] bismuth[128] and indium salts,[129] lanthanide chlorides[130] and triflates.[131] In 1967, Hagihara[132] demonstrated that quinoline derivatives could be synthesized using dicobalt ortocarbonyl as the catalyst instead of $BF_3{\cdot}Et_2O$. Kobayashi and coworkers[131] studied this reaction using lanthanide (III) triflates as excellent catalyst for three-component Povarov reaction between *N*-aryl aldimines and alkenes, potentially replacing the stoichiometric use of other LAs. As a result of the smaller ionic radius of lanthanide (III) triflates, they are more effective towards Lewis bases such as imines. Xia and Lu,[133] demonstrated that molecular iodine could also be employed as inexpensive and readily available catalyst for the Povarov reaction.

[125] Domingo, L. R.; Sáez, J. A. *Org. Biomol. Chem.* **2009**, *7*, 3576-3583.
[126] Das, B.; Reddy, M. R.; Reddy, V. S.; Rammu, R. *Chem. Lett*. **2004**, *33*, 1526-1527.
[127] Sridharan, V.; Avendaño, C.; Menéndez, J. C. *Synthesis **2008**, 7*, 1039-1044.
[128] Rogers, J. L.; Ernat, J. J.; Yung, H.; Mohan. R. S. *Catal. Commun*. **2009**, *10*, 625-626.
[129] Baby, G.; Perumal, P. T. *Tetrahedron Lett*. **1998**, *39,* 3225-3228.
[130] Ma, Y.; Quian, C.; Xie, M.; Sun, J. *J. Org. Chem*. **1999**, *64*, 6462-6467.
[131] Kobayashi, S.; Ishitani, H.; Nagayama, S. *Synthesis* **1995**, 1195-1202.
[132] John, T.; Hagihara, H. *Tetrahedron Lett.* **1967**, *8*, 4199-4200.
[133] Xia, M.; Lu, Y. *Synlett* **2005**, *15*, 2357-2361.

Gutiérrez and coworkers[134] synthesized several tetrahydroquinolines (THQs) **164**, **167** as acetylcholinesterase/ butyrylcholinesterase inhibitors using the Povarov reaction in the presence of $BiCl_3$ (Scheme 22).

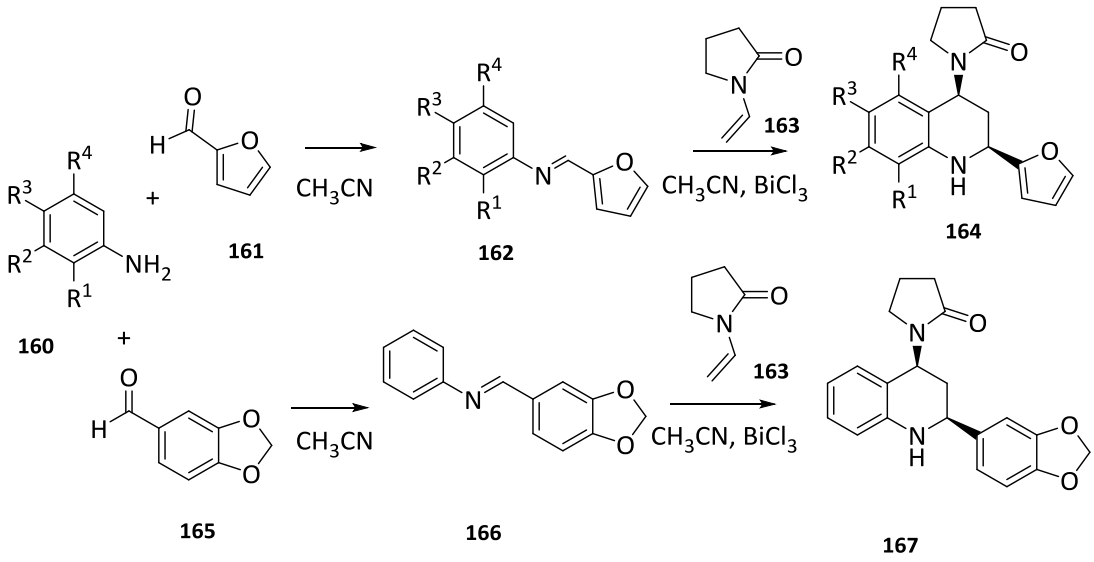

160 **161** **162** **163** **164**

165 **166** **163** **167**

Scheme 22. THQs synthesis through Povarov reaction.

Generally, the hetero-Diels−Alder reaction (Povarov reaction) of *N*-arylimines is subjected to react with activated, electron-rich alkenes. Moderately strained bicyclo[2.2.1]heptenes as norbornene **170** have been used, Batey's group,[135] in the Povarov reaction with *in situ* formation of *N*-arylimines under Lewis acid ($BF_3{\cdot}Et_2O$) catalyzed conditions (Scheme 23) to give the polycyclic derivative **171** in a stereoselective fashion.

[134] Gutiérrez, M.; Arévalo, B.; Martínez, G.; Valdés, F.; Vallejos, G.; Carmona, U.; San Martin, A. *J. Chem. Pharm. Res.* **2015**, *7*, 351-358.

[135] Smith, C. D.; Gavrilyuk, J. I.; Lough, A. J.; Batey, R. A. *J. Org. Chem*. **2010**, *75*, 702-715.

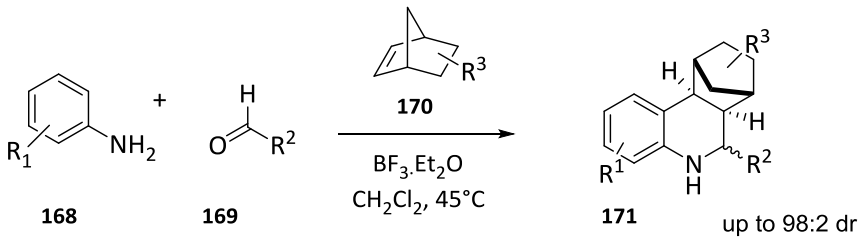

Scheme 23. Povarov reaction of *N*-arylimines with norbornene **170**.

In addition to LAs, several Brønsted acids are also known to catalyze the Povarov reactions. The reaction of *N*-phenyl-*C*-methoxycarbonylimine **172** with methylenecyclopropane **173** was reported [136] in the presence of several LAs ($Yb(OTf)_3$, $Cu(OTf)_2$, $Sn(OTf)_2$, $La(OTf)_3$, $Zr(OTf)_4$, $Zn(OTf)_2$ and $Yb(OTf)_3$) and BAs ($C_8F_{17}SO_3H$ and TfOH). However, the best yields were obtained using trifluoromethanosulphonic acid (TfOH) as catalyst (Scheme 24).

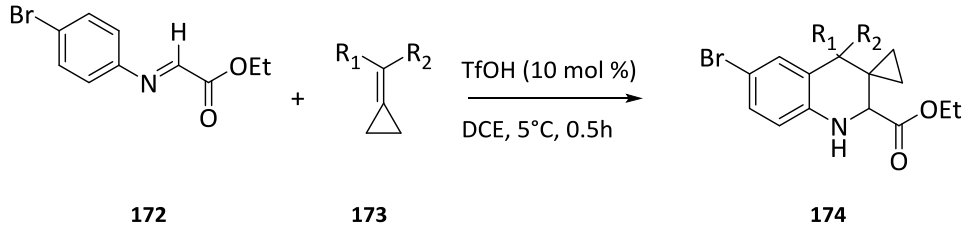

Scheme 24. TfOH catalyzed reaction.

In this sense, Povarov reaction can be considered as a potential tool for the total synthesis of several nitrogen containing heterocycles, as for example, tetrahydroquinolines present in several natural products, and naphthyridines. The first

[136] Zhi-Bin, Z.; Li-Xiong, S.; Min, S. *Eur. J. Org. Chem*. **2009**, 15, 2576-2580.

example of biomimetic Povarov reaction was described by Batey and coworkers.[137] They synthesized the unprecedented martinelline **180** and martinellic acid **181** heterocyclic pyrroloquinoline core using methyl-4-aminobenzoate **175** with 2 equivalents of *N*-Cbz-2-pyrroline **176** in the presence of camphorsulphonic acid (CSA, Scheme 25).

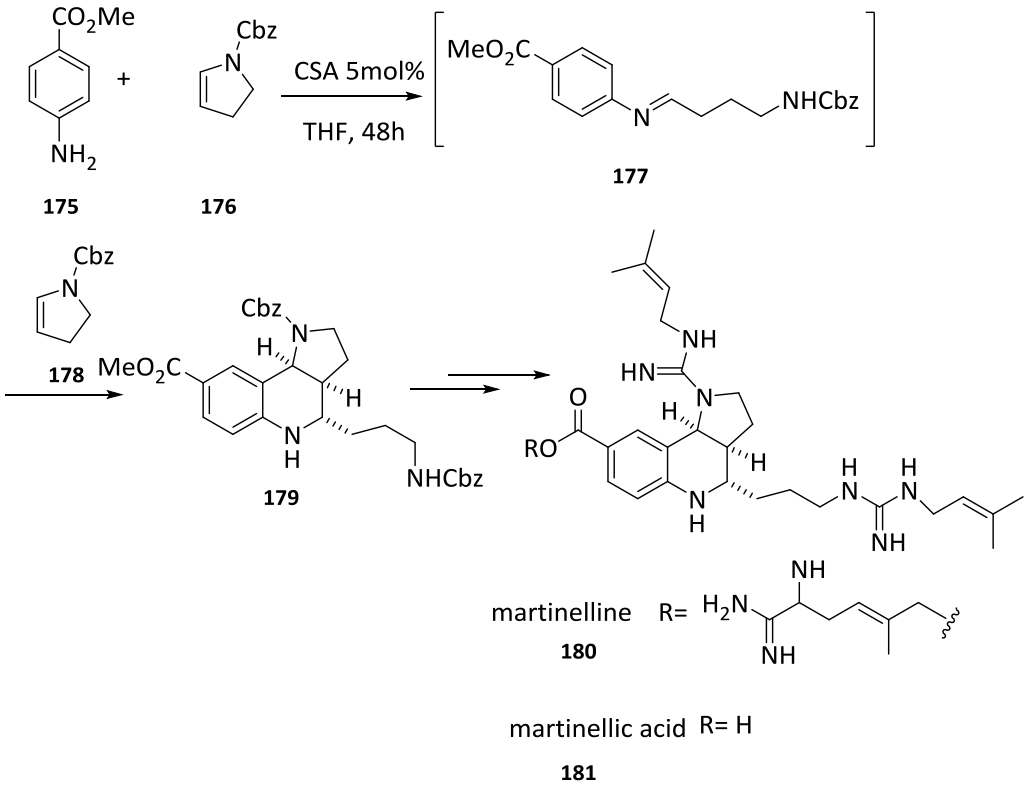

Scheme 25. Total synthesis of martinelline **180** and martinellinic acid **181**.

Despite the fact that hetero-Diels-Alder reaction (Povarov reaction) is a very useful tool to synthesize nitrogen-containing heterocycles both chemo- and stereoselectively, little attention has been paid to theoretical studies and mechanism

[137] Powell, D. A.; Batey, R. A. *Org. Lett.* **2002**, *4*, 2913-2916.

features. In pioneer studies,[131] a stepwise mechanism was suggested for the lanthanide triflate catalyzed imino-Diels-Alder reaction of imines derived from anilines with alkenes.

Domingo and coworkers,[138] studied the molecular mechanism of the BF_3 catalyzed Povarov reaction between *N*-phenyl-*C*-arylimine **182** and methyl vinyl ether **183** as the dienophile (Scheme 26). The formation of the corresponding zwitterionic intermediates **184** and **186** is endothermic. Nevertheless, the generation of the second C-C single bond along the ring-closure process has very low activation energy and the formation of the formal [4+2] cycloadducts **185** and **187** is exothermic. This process is completely *endo* selective and it occurs through a two-step mechanism due to the large stabilization of the corresponding zwitterionic intermediates **184** and **186**.

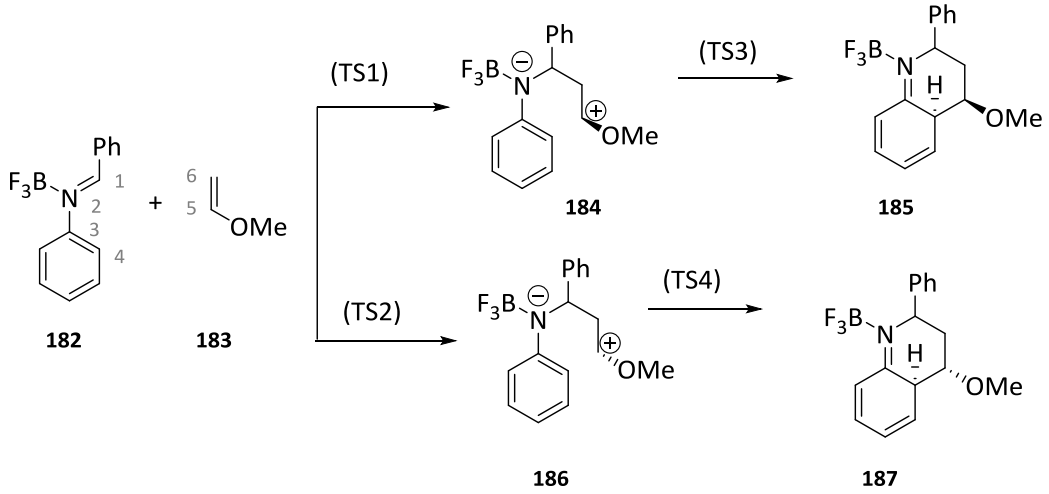

Scheme 26. LA catalyzed Povarov reaction mechanistic features.

The mechanism of Brønsted acid catalyzed Povarov reactions was explored by the same group.[139] For this purpose, they studied the BA catalyzed Povarov reaction of *N*-

[138] Domingo, L. R.; Aurell, M. J.; Sáez, J. A.; Mekelleche, S. M. *RSC Adv*. **2014**, *4*, 25268-25278.
[139] Ríos-Gutiérrez, M.; Layeb, H.; Domingo, L. R. *Tetrahedron* **2015**, *71*, 9339-9345.

phenyl-*C*-methoxycarbonylimine **188** with methylcyclopropene **189** using DFT methods (Scheme 27). They proposed that BAs catalyzed Povarov reactions start by the nucleophilic attack of compound **189** on the protonated imine **188** with the formation of a cationic intermediate **190**, which undergoes a fast intramolecular Friedel-Crafts reaction.[138]

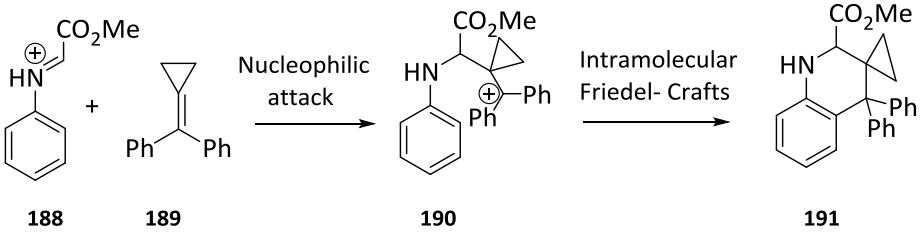

188 **189** **190** **191**

Scheme 27. BA catalyzed Povarov reaction.

In our research group,[140] we performed some theoretical studies to understand the mechanism of the Povarov reaction between aldimines **192** derived from 3-aminopyridine and benzaldehyde (R= Ph), acetaldehyde (R= Me) and formaldehyde (R= H) with different olefins **194**. In this case, we studied the most favorable orientation of the pyridine ring in the cycloaddition reaction, the influence of the $BF_3{\cdot}Et_2O$ and if this Lewis acid preferentially coordinates to the pyridinic nitrogen or to the iminic nitrogen. In addition, we extended the computational calculations to study the regio- and diastereoselectivity of the reaction towards simple olefins **194** as styrene, cylopentadiene and indene (Scheme 28).

[140] Palacios, F.; Alonso, C.; Arrieta, A.; Cossío, F. P.; Ezpeleta, J. M.; Fuertes, M.; Rubiales, G. *Eur. J. Org. Chem*. **2010**, 2091-2099.

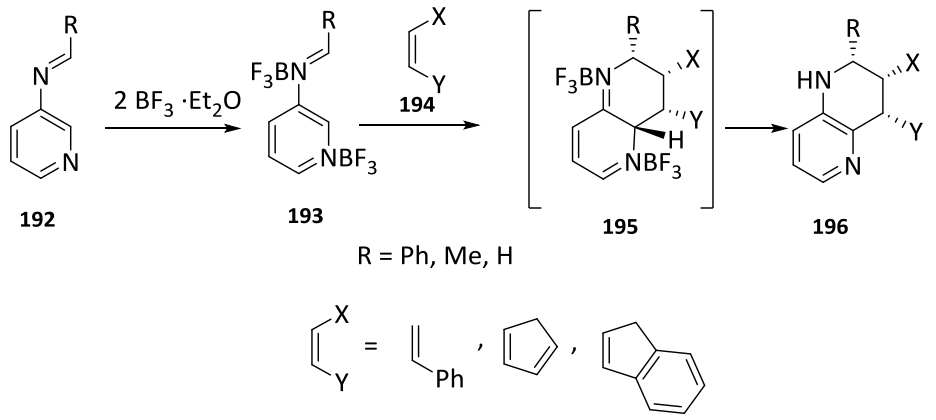

Scheme 28. Povarov reaction between aldimines **192** and simple olefins **194**.

The results of this study showed that the use of 2 equivalents of $BF_3{\cdot}Et_2O$ activates the azadienic system, making this process faster than when 1 equivalent of $BF_3{\cdot}Et_2O$ was used, due to a double coordination of the two nitrogen atoms. Moreover, the lower activation barriers correspond to the *endo* transition-state structures that lead to the formation of the *endo* adducts **195** (Scheme 28) in a regio- and stereoselective way with the control of two or three stereocenters. The mechanism may be explained through an exothermic, concerted and asynchronous process yielding the corresponding tetrahydro-1,5-naphthyridines **196** (Scheme 28). As a representative example, in figure 29 it can be observed the transition structures **TSa** for the reactions corresponding to the imine **192** derived from benzaldehyde (R = Ph) with styrene and **TSb** for the imine **192** derived from acetaldehyde (R = Me) with indene.

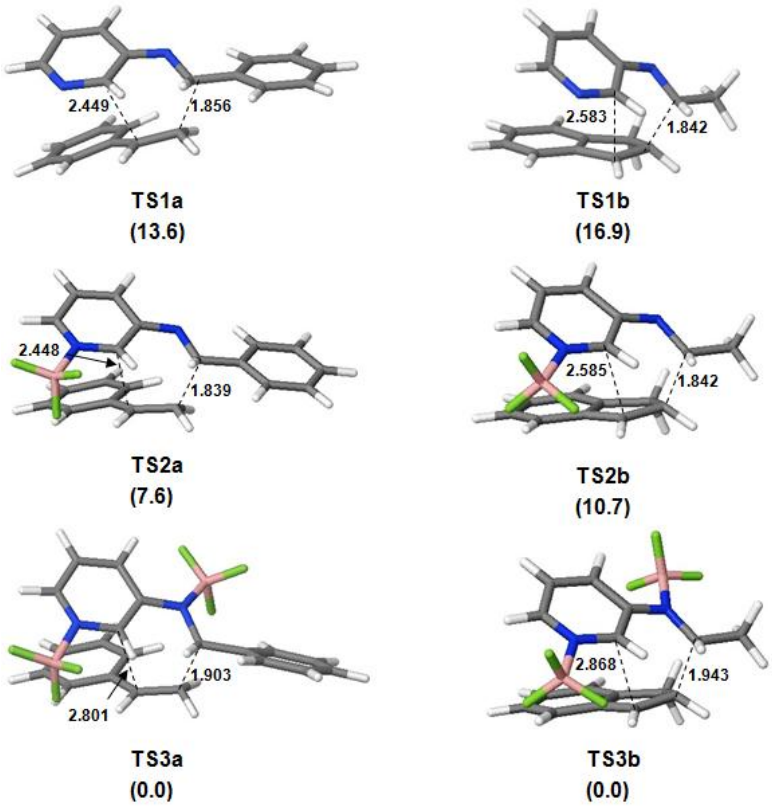

Figure 29. Transition-state structures TS1, TS2 (with BF_3 coordinated to the pyridinic nitrogen) and TS3 (with BF_3 coordinated to both nitrogen atoms), with selected bond lengths given in Å. The relative energy differences numbers given in parentheses (in kcal/mol) for the reaction between the imine derived from benzaldehyde (R= Ph) with styrene and for the reaction between the imine derived from acetaldehyde (R= Me) with indene fully optimized at the B3LYP/6-31G*+ΔZPVE level of theory.

Not only olefins can be used as dienophiles in the Povarov reaction but also terminal alkynes,[141] although it is much less common. Baudelle and coworkers[141b] used propoxyacetylene **198** to obtain the aromatic quinoline **199** (Scheme 29).

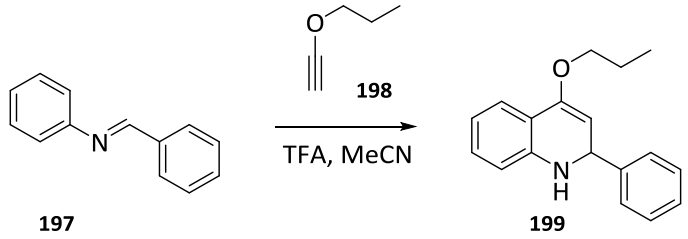

Scheme 29. Povarov reaction between imine **197** and acetylene **198**.

Muthusubramanian and coworkers[141f] recently reported an efficient synthesis of various azaindole substituted quinoline derivatives **204** by Povarov reaction employing acetylenes **203**, using inexpensive and commercially available $SnCl_2$ as a Lewis acid catalyst in good yields and diastereoselectivity (Scheme 30). This reaction was demonstrated to be chemo- and regioselective with good atom economy.

[141] For a Povarov reaction with alkynes as dienophiles, see: (a) Leardini, R.; Nanni, D.; Tundo, A.; Zanardi, G.; Ruggieri, F. *J. Org. Chem*. **1992**, *57*, 1842-1848. (b) Baudelle, R.; Melnyk, P.; Deprez, B.; Tartar, A. *Tetrahedron* **1998**, *54*, 4125-4140. (c) Heather Twin, H.; Batey, R. A. *Org. Lett*. ***2004***, *6*, 4913-4916. (d) Zhao, Y.; Zhang, W.; Wang, S.; Liu, Q. *J. Org. Chem*. **2007**, *72*, 4985-4988. (e) Gaddam, V.; Ramesh, S.; Nagarajan, R. *Tetrahedron* **2010**, *66*, 4218-4222. (f) Suresh, R.; Muthusubramanian, S.; Senthilkumaran, R.; Manickam, G. *J. Org. Chem*. ***2012***, *77*, 1468-1476. (g) Pericherla, K.; Kumar, A.; Jha, A. *Org. Lett*. **2013**, *15*, 4078-4081.

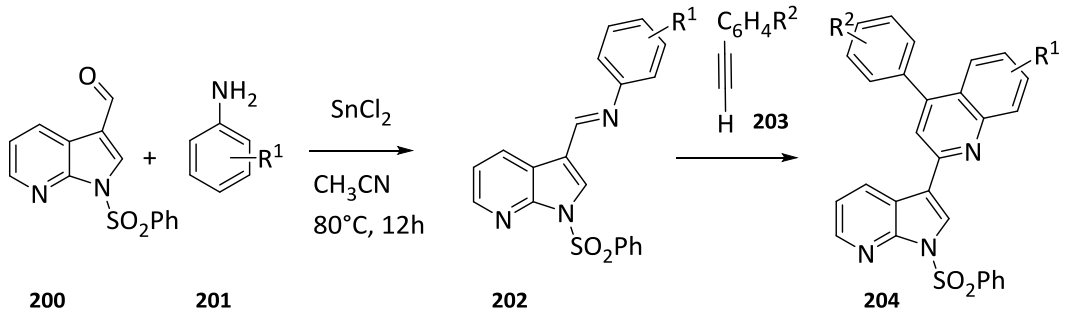

Scheme 30. $SnCl_2$ catalyzed Povarov reaction.

Povarov reaction can take place intramolecularly when the molecule bears both the diene and the dienophile moieties connected by a chain. As a result, fused bicyclic adducts and bridged bicyclic compounds are obtained. This alternative is a valuable tool since it allows the generation of heterocycles where the size of the second ring depends on the chain lengthening of adequately functionalized aldehydes with an alkenyl or alkynyl group.

Bodwell and coworkers[142] reported the use of the intramolecular Povarov reactions to obtain pentacyclic heterocycles from 3-aminocoumarin **205** (Scheme 31). In one case they used the aldehyde **206** with an alkenyl group in the presence of catalytic amount of $Yb(OTf)_3$. No reaction was observed at room temperature. Upon heating the non-aromatized Povarov adduct **208** was isolated in a *cis* relative stereochemistry. In an effort to obtain the desired aromatized product, they also used 2-(propargyloxy)benzaldehyde **209** in the presence of 5 mol% $Yb(OTf)_3$ in acetonitrile at reflux to yield the aromatized product **211**.

[142] Kudale, A.; Miller, D. O.; Dawe, L. N.; Bodwell, G. J. *Org. Biomol. Chem.* **2011**, *9*, 7196-7206.

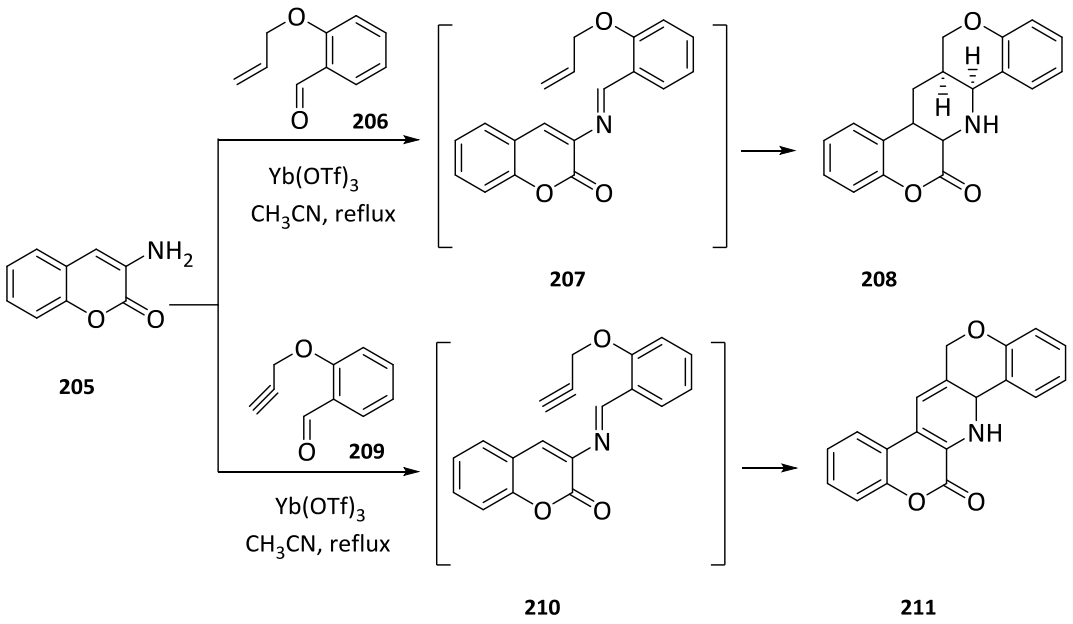

Scheme 31. Intramolecular Povarov reactions to obtain 3-aminocoumarins.

Recently, Belal's group[143] improved the methodology to synthesize pyrido[2,3-*c*]coumarin derivatives **214** by an intramolecular Povarov reaction (Scheme 32) using triflic acid as catalyst. With this methodology they have shorten reaction times, improved yields and there is no need to do column chromatographic separation.

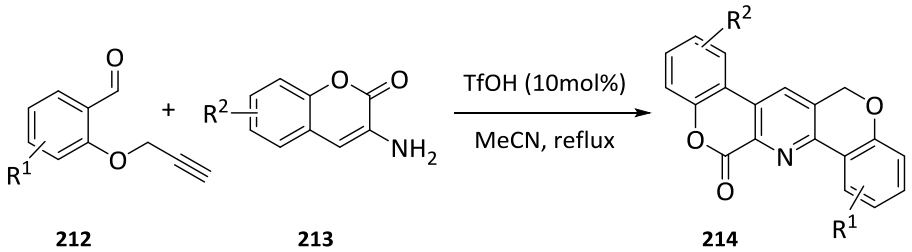

Scheme 32. Synthesis of pyrido [2,3-*c*]coumarin derivatives **214**.

[143] Belal, M.; Dasa, D. K.; Khan, A. T. *Synthesis* **2015**, *47*, 1109-1116.

Batey and coworkers[144] described an intramolecular Povarov reaction for the formal synthesis of the camptothecin core **218**. This approach consisted on the employment of a pyridone precursor **215** (Scheme 33) for the key Povarov intramolecular reaction. Heating precursor **215** with aniline **216** in the presence of catalytic amount of $Dy(OTf)_3$ afforded quinoline **218** through intramolecular hetero-Diels-Alder reaction of functionalized imine **217** to give the tetracyclic compound **218**.[145]

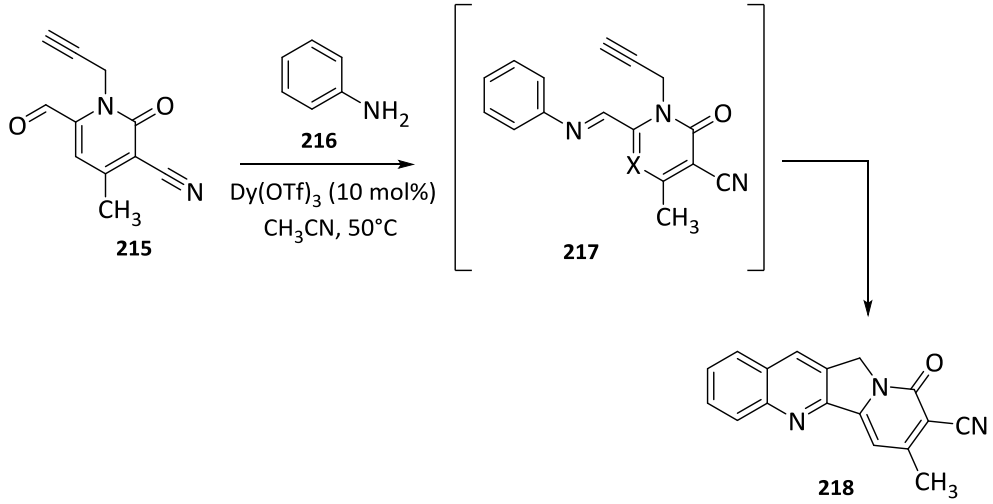

Scheme 33. Intramolecular Povarov reaction for the synthesis of CPT core **218**.

Liu and coworkers[146] developed a new methodology to synthesize indeno[1,2-*b*]quinolines **221** using *o*-propargylbenzaldehydes **219** with *N*-arylamines **220** based on an intramolecular Povarov reaction (Scheme 34). This method offers several advantages such as no requirement for an oxidant, high efficiency, and a wide reaction scope. Aromatization was achieved by elimination of the leaving group and isomerization. Similarly, Almansour and coworkers have designed several pyrrolo[3,4-*b*]quinolines

[144] Twin, H.; Batey, R. A. *Org. Lett*. **2004**, *6*, 4913-4916.
[145] Eckert, H. *Angew. Chem. Int. Ed. Engl*. **1981**, *20*, 208-210.
[146] Chen, M.; Sun, N.; Liu, Y. *Org. Lett*. **2013**, *15*, 5574-5577.

through intramolecular Povarov reactions using boron trifluoride diethyl etherate as catalyst.[147]

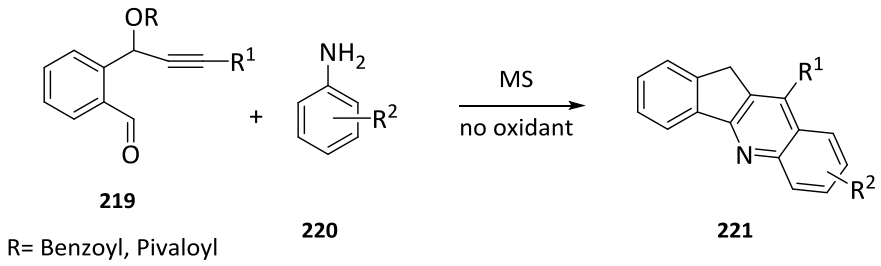

219 **220** **221**

R= Benzoyl, Pivaloyl

Scheme 34. Synthesis of indeno[1,2-b]quinolines **221**.

Reactions combining three or more different components in one reaction vessel, leading to the formation of a single product, are denoted under the term multicomponent reactions (MCRs). After almost three decades of Povarov's original work,[121a,b] the reaction was upgraded into a multicomponent reaction (MCR).[148] The multicomponent version of the Povarov reaction has attracted great interest in the last years since it has some advantages over classic divergent reaction strategies.[149] These include lower costs, shorter reaction times and energy, as well as environmentally friendlier aspects, diversity with atom-economy and enantiocontrol.

[147] Almansour, A. I.; Arumugam, N.; Kumar, R. S.; Menéndez, J. C.; Ghabbour, H. A.; Fun, H. K.; Kumar, R. R. *Tetrahedron Lett.* **2015**, *59*, 6900-6903.

[148] Brzozowski, Z.; Czewski, F. S.; Gdaniec, M. *Eur. J. Med. Chem*. **2000**, *35*, 1053-1064.

[149] For books and reviews see: (a) Brauch, S.; Van Berkel, S. S.; Westermann, B. *Chem. Soc. Rev*. **2013**, *42*, 4948-4962. (b) Multicomponent Reactions in Organic Synthesis; Zhu, J.; Wang, Q.; Wang, M. (Eds.); Wiley: Chichester, **2014**. (c) Muticomponent Reactions; Müller, T. J. J. (Ed.) Science of Synthesis. Vols 1 and 2; Thieme: Stuttgart, **2014**.

Legros and coworkers[150] reported the use of fluorinated alcohols as trifluoroethanol (TFE) or hexafluoroisopropanol (HFIP) as both solvent as well as catalyst for three-component Povarov reaction of 8-aminoquinolines **225** (Scheme 35). This route lies on a Povarov/oxidation sequence from simple reagents; 1,2-phenylenediamines **222**, aldehydes **223** and ethyl vinyl ether **224**.

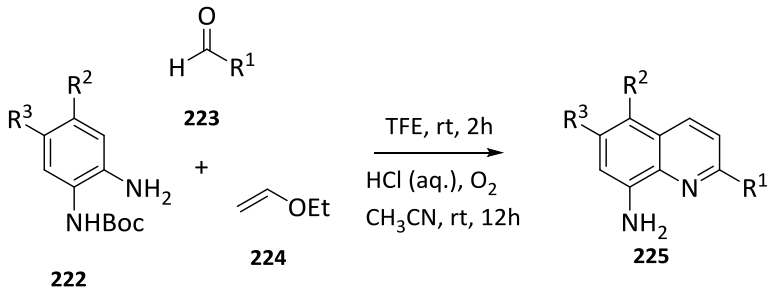

Scheme 35. MCR of 2-substituted 8-aminoquinolines **225**.

Di Pietro and coworkers,[151] recently designed tricyclic heterofused quinolines **230** through 2-4 step synthetic sequences that involve as the key step an initial Povarov multicomponent reaction between a cyclic enamide or enol ether **226** as an activated olefin and a properly substituted aniline **227** and aromatic aldehyde **228** (Scheme 36). The oxidation of adduct **229** with DDQ gave quinolines **230**.

[150] De, K.; Legros, J.; Crousse, B.; Chandrasekaran, S.; Bonnet-Delpon, D. *Org. Biomol. Chem.* **2011**, *9*, 347-350.

[151] Di Pietro, O.; Vicente-García, E.; Taylor, M. C.; Berenguer, D.; Viayna, E.; Lanzoni, A.; Sola, I.; Sayago, H.; Riera, C.; Roser, F.; Clos, M. V.; Pérez, B.; Kelly, J. M.; Lavilla, R.; Muñoz-Torrero, D. *Eur. J. Med. Chem.* **2015**, *105*, 120-137.

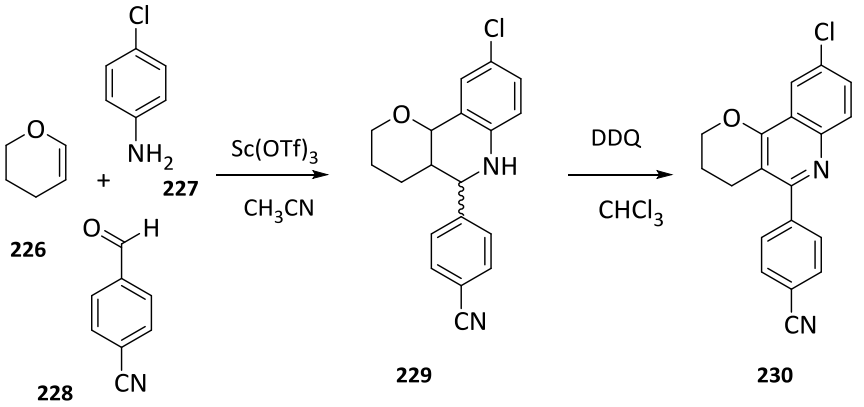

Scheme 36. Tricyclic heterofused quinolines synthesis.

Zhao and Liu[152] reported the three-component version of anilines **231**, aromatic aldehydes **232**, and enynes **233** to synthesize 4-substituted quinolines **234** using a Brønsted acid catalyst, trifluoromethanosulfonic acid (Scheme 37).

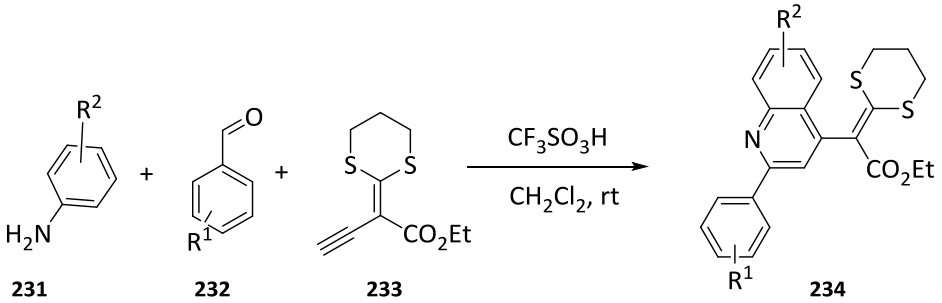

Scheme 37. Brønsted acid-catalyzed Povarov reaction

Alkyl-substituted quinolines **238** described by Larsen and coworkers[153] are formed directly from commercially available anilines **235**, aldehydes **236**, and alkynes **237**

[152] Wang, S.; Zhao, Y. L.; Zhang, W.; Liu, Q. *J. Org. Chem.* **2007**, *72*, 4985-4988.

bearing a variety of substituents (Scheme 38). In this case, catalytic amount of copper (II) triflate (5mol %) catalyzes this three-component coupling without ligand, cocatalyst, solvent, or inert atmosphere.

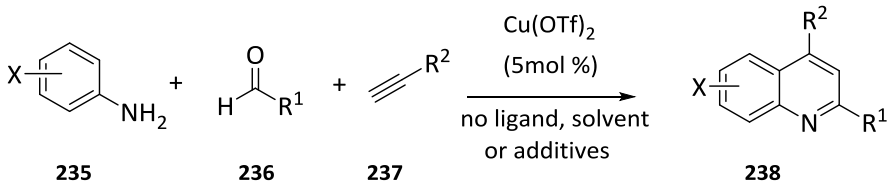

235 **236** **237** **238**

Scheme 38. 2,4-dialkyl quinolines **238** synthesis.

Asymmetric variants of the reaction have also been achieved with a great success, leading to the synthesis of enantiomerically pure tetrahydroquinolines in presence of chiral catalysts. In this work, we are going to describe few examples of this Povarov version since we are not going to use this asymmetric version in this PhD work.

The first example[154] of the asymmetric Povarov reaction was reported in 1996 (Scheme 39) using (*R*)-BINOL as the chiral source for the formation of quinoline derivatives **241**. Only 2-aminophenol-derived imines **239**, that are able to form a bidentate coordination to the chiral Lewis acids, yielded measurable enantioselectivities. The need of the hydroxyl group at the imine was overcome some years later by Sundararajan and coworkers[155] using a titanium complex catalyst.

[153] Meyet, C. E.; Larsen, C. H. *J. Org. Chem*. **2014**, *78*, 9835-9841.
[154] Ishitani, H.; Kobayashi, S. *Tetrahedron Lett*. **1996**, *37*, 7357-7362.
[155] Sundararajan, G.; Prabagaran, N.; Varghese, B. *Org. Lett*. **2001***, 3*, 1973-1976.

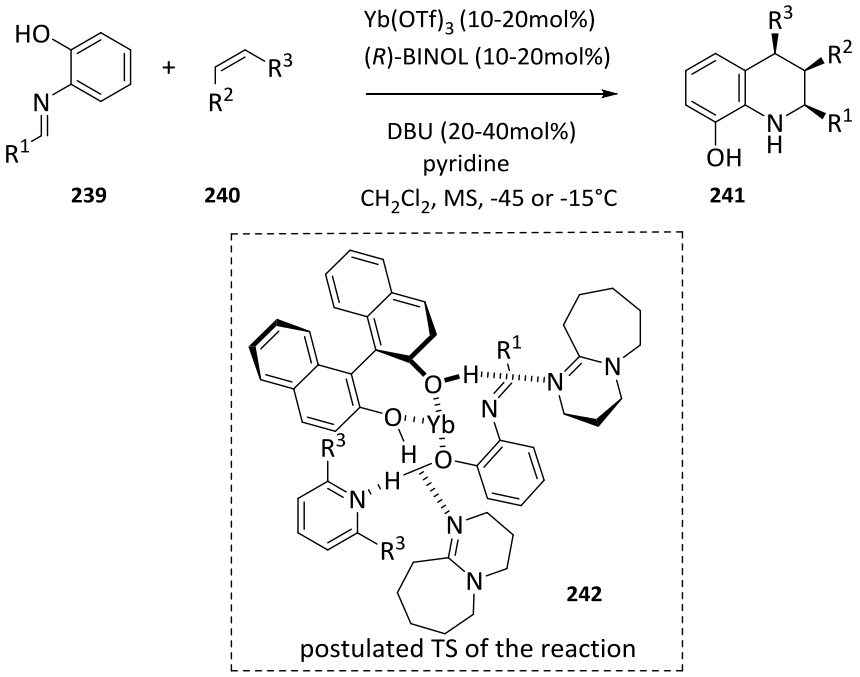

Scheme 39. First Povarov enantioselective reaction.

Around 2009 the scenery changed and nowadays it is possible to find a lot of catalytic asymmetric Povarov reaction examples.[124] It was not until 2011 that Feng and coworkers described a truly efficient asymmetric Povarov reaction (Scheme 40) using metal complexes bearing *N*,*N'*-dioxide ligands **248** as catalyst[156] and using cyclopentadiene **245** as dienophile. [157] The same authors, one year after, extended the methodology to alkylstyrenes.[158]

[156] Lihu, X.; Lin, L.; Feng, X. *Acc. Chem. Res*. **2011**, *44*, 574-580.
[157] Xie, M.; Liu, X.; Zhu, Y.; Gao, B.; Lin, L.; Liu, X.; Feng, X. *Angew. Chem. Int. Ed.* **2010**, *49*, 3799-3802.
[158] Xie, M.; Liu, X.; Zhu, Y.; Zhao, X.; Xiao, Y.; Lin, L.; Feng, X. *Chem. Eur. J.* **2011**, *17*, 13800-13805.

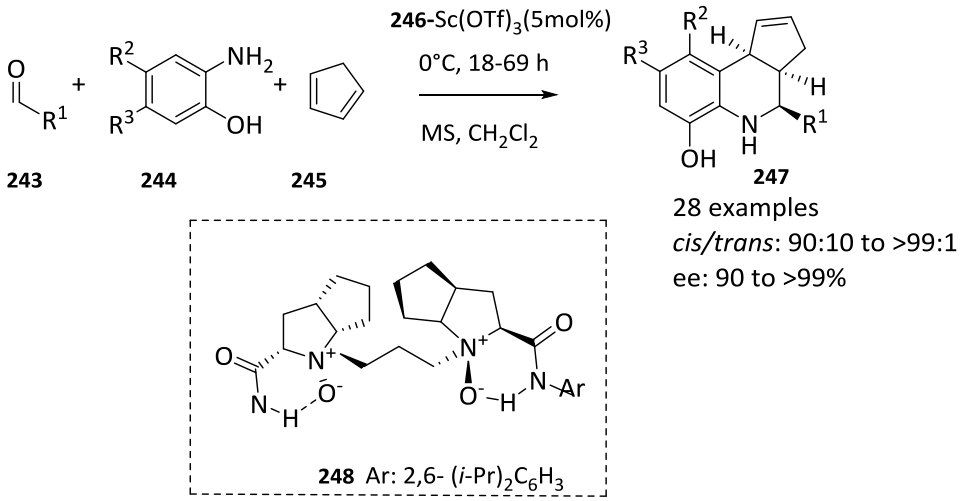

Scheme 40. Asymetric Povarov reaction with cyclopentadiene **245**.

A detailed mechanism study on three-component Povarov reaction was reported by Masson and Zhu.[159] Depending on the polarized nature of the enecarbamate double bond of the dienophile, a stepwise mechanism could be initiated by the Mannich-type reaction. They were able to trap the *N*-acyliminium intermediate generated after the Mannich-type reaction by an alcohol as an external nucleophile (Scheme 41). Utilization of benzaldehyde **250** and 4-methoxyaniline **249** in the presence of the dienophile **251** and a Povarov terminator, EtOH (17 equivalents), afforded the Mannich adduct **252** in low yield, together with the tetrahydroquinoline **253** as the major product. With electron deficient anilines such as 4-nitroaniline **249** (R^1= NO_2), Mannich adduct **252** was isolated. These results provided direct evidence of a stepwise mechanism for this catalytic Povarov reaction.

[159] Dagousset, G.; Zhu, J.; Masson, G. *J. Am. Chem. Soc*. **2011**, *133*, 14804-14813.

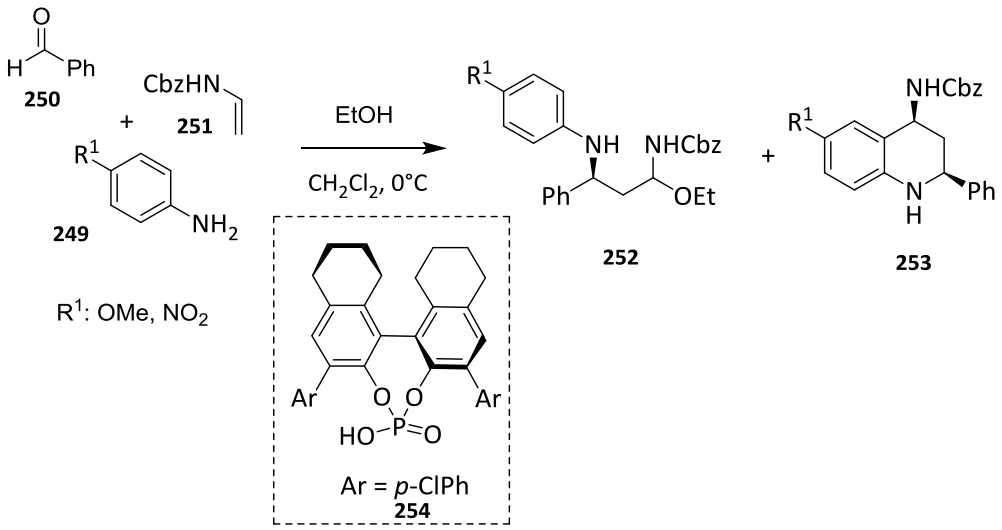

Scheme 41. Asymmetric three-component Povarov reaction.

A recent work published by Feng's group[160] describes the first application of 3-methyl-2-vinylindoles **255** in catalytic asymmetric Povarov reactions *via* the three-component reaction of aldehydes **257** and anilines **256** in the presence of chiral phosphoric acid (CPA) **258** (Scheme 42). Both, the aldimine and 3-methyl-2-vinylindoles **255** would be simultaneously activated by CPA **258** *via* dual hydrogen bonding interaction favoring the formation of the tetrahydroquinoline **259** enantioselectively. This strategy provides an easy access to chiral indole-derived tetrahydroquinolines **259** with three contiguous stereogenic centers and excellent diastereo- and enantioselectivities.

[160] Wei, D.; Xiao-Li, J.; Ji-Yu, T.; Feng, S. *J. Org. Chem*. **2016**, *81*, 185-196.

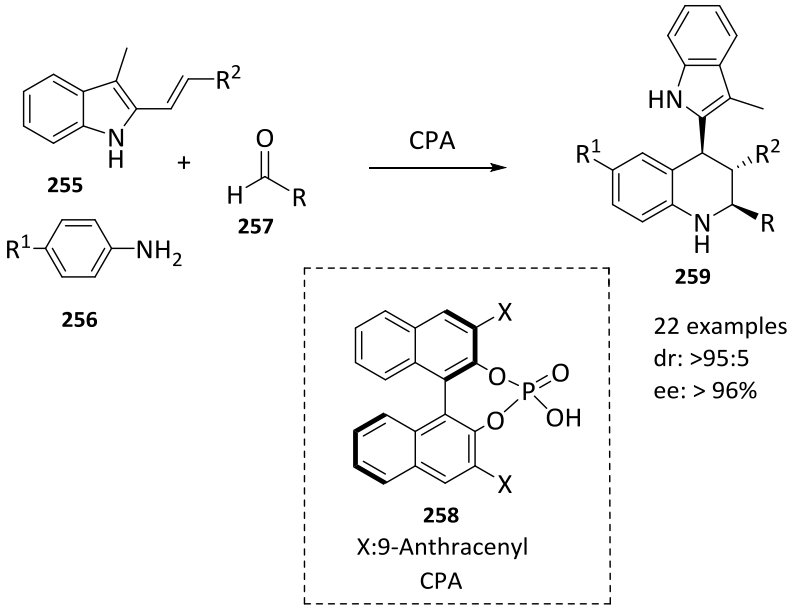

Scheme 42. Enantioselective tetrahydroquinolines **259** synthesis.

It can be concluded that asymmetric Povarov reactions could be performed with a broad set of olefins and not only in a one-pot version but also in multicomponent reactions as it has been shown in the previous example.

In general, the Povarov reaction is extremely useful with a broad set of anilines and carbonyl derivatives. It is important to state that not only aromatic Schiff bases like *N*-benzylidenaniline, but also *N*-alkylaldimines can be utilized as aza-dienes in this type of reactions.[161] However, the addition reaction towards these aldimines is difficult to develop, because of their tendency to hydrolysis and polimerization under acidic conditions.

[161] (a) Narasaka, K.; Shibata, T. *Heterocycles* **1993**, *35*, 1039-1053. (b) Powell, D. A.; Batey, R. A. *Tetrahedron Lett.* **2003**, *44*, 7569-7573.

Further efforts have also been extensively devoted to expand the range of activated olefin input for this reaction. Initially, cyclic enol ethers, as for 2,3-dihydrofuran and 3,4-2*H*-dihydropyran were used as more popular dienophiles to obtain the corresponding *cis*-fused furo[3,2,*c*]- and pyrano[3,2,*c*]-quinoline derivatives. Among other dienophiles, vinyl enol ethers and vinyl and silyl enol ethers, vinyl sulfides and analogues were significantly used in the cycloaddition of *N*-arylaldimines to obtain trisubstituted tetrahydroquinolines.

With this background in mind and with the aim of developing new heteroaromatic derivatives as topoisomerase I inhibitors, we study the use of the Povarov reaction as the synthetic tool for the preparation of 1,5-indenophthyridine and 1,5-naphthyridine scaffolds (Figure 30).

Generally speaking heteroaromatic flat compounds are particularly effective as antitumoral agents.[162] Moreover, these types of compounds have demonstrated being more active than the non-aromatized compounds.[163]

Regarding topoisomerase I inhibitors,[32] it has been reported that flat compounds could be particularly effective against topoisomerase I due to the fact that they could be placed between the DNA base pairs and stabilize the covalent complex (TopIcc) through π-π stacking interactions.[110] This effect is known as the interfacial paradigm inhibition.[164]

[162] A. Begouin, A.; Hesse, S. 10th Electronic Conference on Synthetic Organic Chemistry, 2006.
[163] Kumar, R. S.; Rajesh, S.M.; Perumal, S.; Banerjee, D.; Yogeeswari, P.; Sriram, D. *Chem. Pharm. Bull.* **2010**, *58*, 602-610.
[164] Pommier, Y.; Marchand, C. *Nat. Rev. Drug Discov.* **2011**, *11*, 25-36.

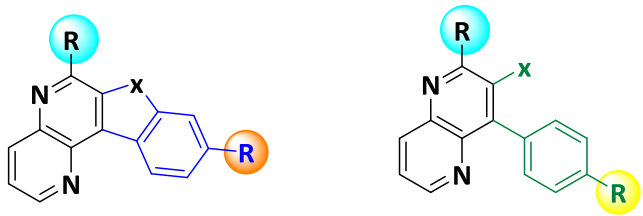

Figure 30. Polycyclic 1,5-indenonaphthyridine and 1,5-naphthyridine derivatives.

The synthetic strategy based on the hetero-Diels-Alder reaction between *N*-arylimines and electron rich dienophiles is a very interesting and practical methodology for the preparation of 6-membered heterocyclic compounds. We considered that this strategy may be adequate for the preparation of the goal molecules showed in figure 30. In addition, as far as we know, there are no precedents in literature in the use of Povarov reaction for the synthesis of 1,5-naphthyridines.

In particular, the aims of this PhD work are:

- The study of the Povarov reaction between pyridylaldimines derived from aromatic aldehydes and 3-aminopyridine with olefins using $BF_3{\cdot}Et_2O$ as Lewis acid for the synthesis of 1,2,3,4-tetrahydroindenonaphthyridines.
- Structural modifications of the previously synthesized 1,2,3,4-tetrahydroindenonaphthyridines in order to increase the diversity of the naphthyridine scaffolds.

- The study of the Povarov reaction between pyridylaldimines, derived from the condensation between aromatic aldehydes and 3-aminopyridine, with acetylenes using $BF_3{\cdot}Et_2O$ as Lewis acid for the synthesis of 1,5-naphthyridines.

- The study of the biological activity of the synthesized derivatives including the inhibitory effect toward topoisomerase I, as well as, the cytotoxic effect in three different cancer cell lines (A549, BT20, SKOV3).

Note:

Compounds, figures, schemes and tables numeration in next section will start with number 1.

2.2. Synthesis of 6-aryltetrahydroindeno-1,5-naphthyridines

Naphthyridines are very interesting molecules containing two nitrogen atoms in their structure and they are related to pyridine as naphthalene is to benzene. The opportunities of ring fusion lead to 6 isomeric structures, the 1,5-, 1,6-, 1,7-, 1,8-, 2,6-, 2,7-naphthyridines (Figure 1).

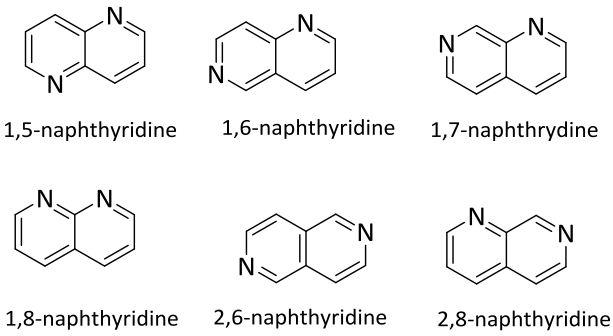

Figure 1. Naphthyridine isomeric structures.

These heterocyclic compounds are less studied than quinolines or isoquinolines, but they are likely to see a resurgence of interest with respect to their applications in medicinal chemistry.[165]

Taking as reference the synthetic methodology previously discussed, the Povarov reaction, we are going to design and synthesize new 1,5-naphthyridine derivatives that may act as topoisomerase I inhibitors.

[165] (a) Wang, Y.; Xu, Z. L.; Ai, J.; Peng, X.; Lin, J. P.; Ji, Y. C.; Geng, M. Y.; Long, Y. Q. *Org. Biomol. Chem*. **2013**, *11*, 1545-1562. (b) Kumpan, K.; Nathubhai, A.; Zhang, C.; Wood, P. J.; Lloyd, M. D.; Thompson, A. S.; Haikarainen, T.; Lehtiö, L.; Threadgill, M. D. *Bioorg. Med. Chem*. **2015**, *23*, 3013-3032.

2.2.1. Povarov reaction between aldimines derived from 3-aminopyridine and olefins

As previously mentioned, it is well-known that the use of Lewis acid as catalyst in the Povarov reaction is a very useful tool. In fact, the first example of Povarov reaction was described in the presence of $BF_3{\cdot}Et_2O$.[121] Bearing in mind that there were no precedents for the use of aminopyridines in this process, our research group[140] in a previous work, studied experimentally and computationally the hetero-Diels-Alder reaction between different *N*-(3-pyridyl) aldimines **3** with olefins **4** as dienophiles for the preparation of 1,5-naphthyridine derivatives **6** (Scheme 1).

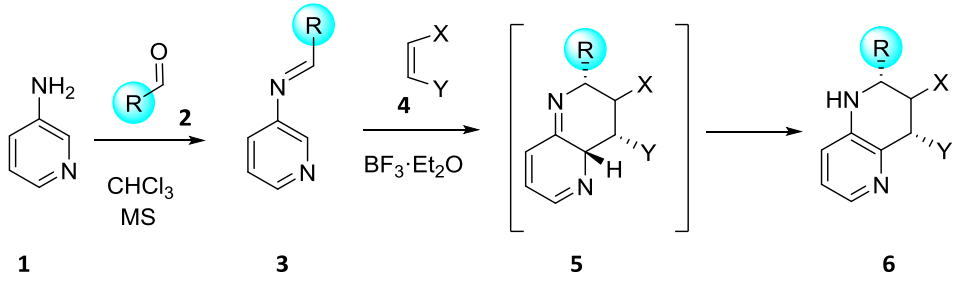

Scheme 1. Povarov reaction between aldimines **3** and olefins **4**.

No reaction was observed in the absence of Lewis acid at room temperature or in chloroform at reflux. In contrast, when the reaction was performed at room temperature in the presence of 1 equiv. of $BF_3{\cdot}Et_2O$, bicyclic *endo* compound **6** was regioselectively obtained after long reaction times. When the reaction was carried out in chloroform at reflux at 60°C, the same compound was obtained but in a shorter reaction time. The use of 1.2 equiv. $BF_3{\cdot}Et_2O$ was not enough to give the optimal conditions, the reaction time decreases but not as much as with the use of 2.0 equiv.

Theoretical studies previously detailed (Figure 29, page 75), revealed that the use 2 equivalents of $BF_3{\cdot}Et_2O$ instead of one, accelerates the reaction by double coordination

with both nitrogen atoms. Pathways involving *endo* transition states exhibited the lowest activation barriers. All the reactions took place in a concerted manner, but the bond formation seems to be quite asynchronous with the C (dienophile)-C (imine) bond being more advanced in all cases.

2.2.1.1. Povarov reaction between aldimines derived from 3-aminopyridine and indene

With these antecedents in mind, in the present work, we will start the discussion with the study of the Povarov reaction of aldimines **3**. Thus, the corresponding aldimines **3** were obtained using 3-aminopyridine **1** and aromatic aldehydes **2** in chloroform as solvent and in the presence of molecular sieves (Scheme 2, Table 1).

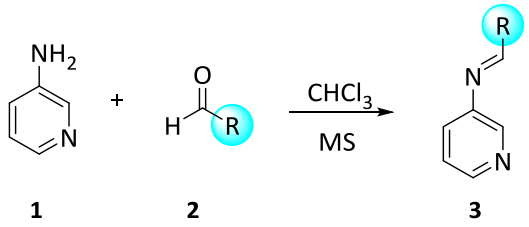

Scheme 2. Synthesis of the corresponding aldimines **3**.

In all cases total conversion of the starting materials was observed. The corresponding aromatic aldimines **3** were isolated by filtration to remove the molecular sieves. However, when imines **3** were isolated, we observed a decrease in the final yield due to imines **3** instability. Consequently, aldimines **3** were used without isolation for subsequent cycloaddition reactions.

Table 1. Aldimines **3** obtained.

Entry	Compound	R	t(h)	T(°C)
1	**3a**	Ph	48	20
2	**3b**	1-Naphthyl	30	20
3	**3c**	2-Naphthyl	24	20
4	**3d**	4-$NO_2C_6H_4$	12	60
5	**3e**	Pyridyl	30	60
6	**3f**	2,4-F_2-C_6H_3	20	60
7	**3g**	3,4-F_2-C_6H_3	24	60
8	**3h**	4-$CF_3C_6H_4$	30	20
9	**3i**	4-FC_6H_4	36	60
10	**3j**	3-$NO_2C_6H_4$	16	60
11	**3k**	3-$OMeC_6H_4$	30	60
12	**3l**	2-MeO_2C-C_6H_4	24	60

Aldimines **3** were characterized by means of ^{1}H-NMR and ^{13}C-NMR spectroscopy. As an example, ^{1}H-NMR and ^{13}C-NMR spectra of imine **3j** are shown (Figure 2). The most characteristic signals in both spectra are the iminic proton (δ = 8.5-9.0 ppm) and carbon (δ = 160-165 ppm). For compound **3j** these signals are pointed out with a green arrow.

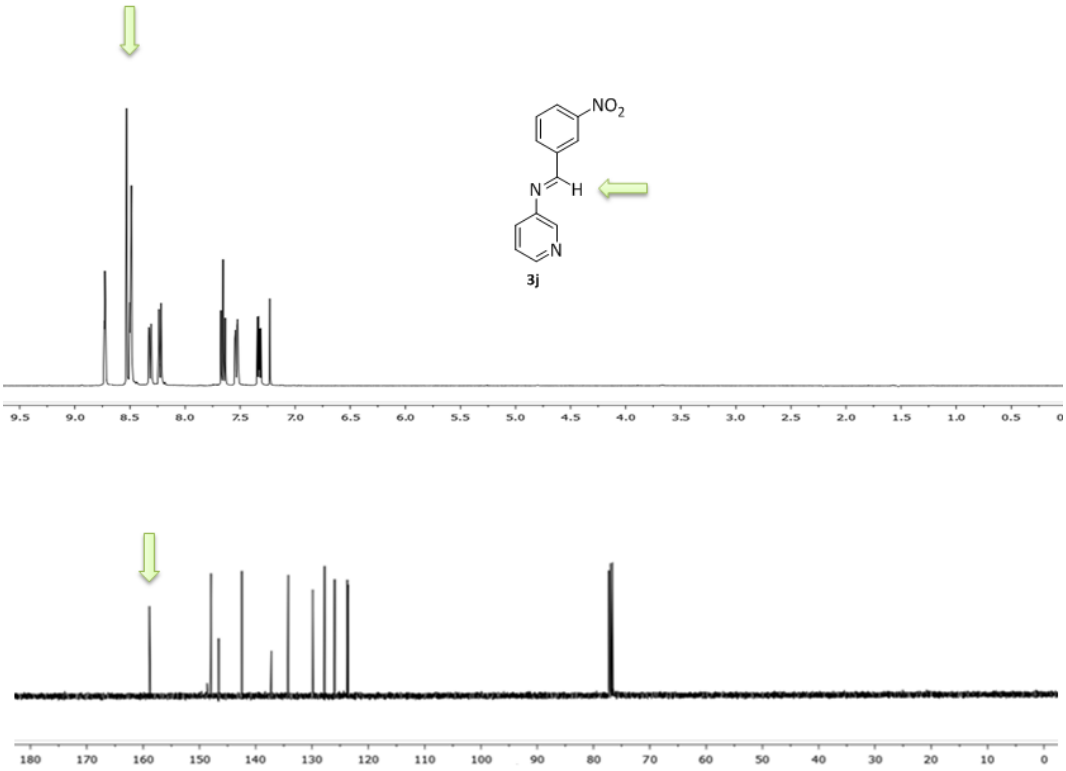

Figure 2. ^{1}H-NMR and ^{13}C-NMR spectra of compound **3j**.

Once the heteroaromatic imines **3** were prepared, the aim was to study the reactivity of these imines **3** in [4+2] cycloaddition reactions with indene **7** as dienophile. The reactions were performed in the presence of 2.0 equivalents of $BF_3{\cdot}Et_2O$ and chloroform as solvent (Scheme 3) to yield tetracyclic *endo* tetrahydro-7*H*-indeno[2,1-*c*][1,5]-naphthyridines **9**.

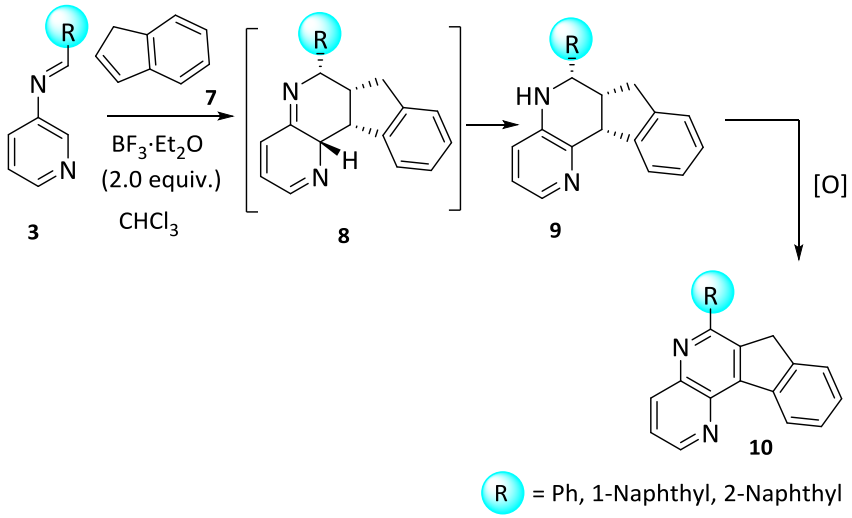

Scheme 3. Reaction between aldimines **3** and indene **7**.

The reaction conditions used to carry out the hetero-Diels-Alder reaction between imines **3** and indene **7** as dienophile, as well as, the yields after chromatographic purification are summarized in table 2.

Table 2. Synthesis of 1,2,3,4-tetrahydronaphthyridines **9**.

Entry	Prod.	R	t(h)	T(°C)	Yield[a](%)
1	**9a/10a**	Ph	21	60	75/13[b]
2	**9b/10b**	1-Naphthyl	48	60	12/60[b]
3	**9c/10c**	2-Naphthyl	48	60	20/55[b]
4	**9d**	4-$NO_2C_6H_4$	36	60	70
5	**9e**	4-Pyridyl	30	60	60
6	**9f**	2,4-F_2-C_6H_3	24	60	75
7	**9g**	3,4-F_2-C_6H_3	36	60	70

[a] Isolated yields [b] Percentage of compounds **10** obtained.

In some cases (Table 2, entry 1), a small proportion (13%) of dehydrogenated naphthyridine **10a** was also obtained. Likewise, the presence of a naphthyl group (R=1-Naphthyl or R= 2-Naphthyl) in 6 position yielded the corresponding dehydrogenated naphthyridines **10b** and **10c** (Table 2, entries 2 and 3) as the major product. Compounds **10** may be generated through dehydrogenation of heterocycles **9** under the reaction and purification conditions.

The structure of tetrahydro-7*H*-indeno[2,1-*c*][1,5]-naphthyridine derivatives **9** was determined by means of 1D and 2D NMR spectra and High Resolution Mass Spectra (HRMS). Taking as example ^{1}H NMR spectrum of compound **9f** (Figure 3), in the aliphatic region it can be seen a doublet of doublets (dd) at δ_H= 2.35 ppm with coupling constants $^{2}J_{HH}$ = 15.0 Hz, $^{3}J_{HH}$ = 8.0 Hz, that corresponds to one of the methylenic protons, a multiplet at δ_H= 3.12-3.19 that corresponds to the other methylenic proton and 6a proton appears as another multiplet at δ_H = 3.26-3.33 ppm. The proton of the amino group appears as a singlet at δ_H = 3.55 ppm, a doublet at δ_H = 4.60 ppm with a coupling constant of $^{3}J_{HH}$ = 8.6 Hz corresponding to proton 11b-H and at δ_H = 4.89 ppm another doublet corresponding to proton 6-H with a coupling constant of $^{3}J_{HH}$ = 3.0 Hz.

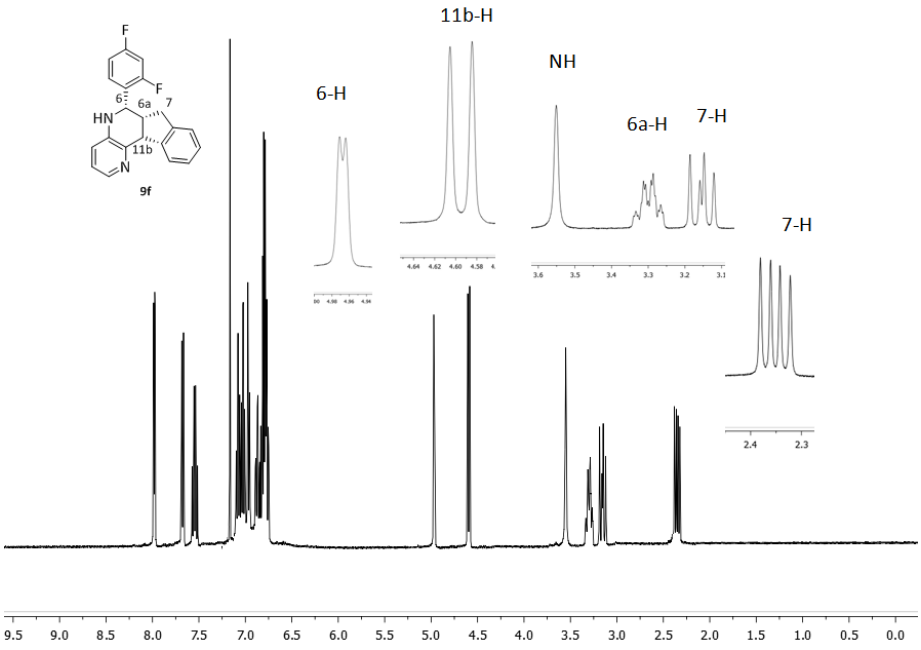

Figure 3. ^{1}H-NMR spectrum for compound **9f**.

In the same way, some representative signals in ^{13}C-NMR spectrum for **9f** derivative are pointed out (Figure 4). At δ= 31.7 ppm appears the methylenic carbon and at δ= 45.4, 48.7 and 50.7 ppm the rest of the aliphatic carbons. Likewise, for **9f**, it can be observed the aromatic carbon C-3 of the benzene ring in 6 position at δ= 104.2 ppm as a doublet of doublets with two coupling constants of $^{2}J_{CF}$ = 25.4 Hz. The carbons directly bonded to the fluorine atoms appear at δ= 159.8 ppm and 162.3 ppm as doublet of doublets with coupling constants of $^{1}J_{CF}$ = 249.2 Hz, $^{3}J_{CF}$ = 11.7 Hz and $^{1}J_{CF}$ = 248.4 Hz, $^{3}J_{CF}$ = 12.3 Hz respectively (See spectroscopic data for compound **9f** in the experimental section).

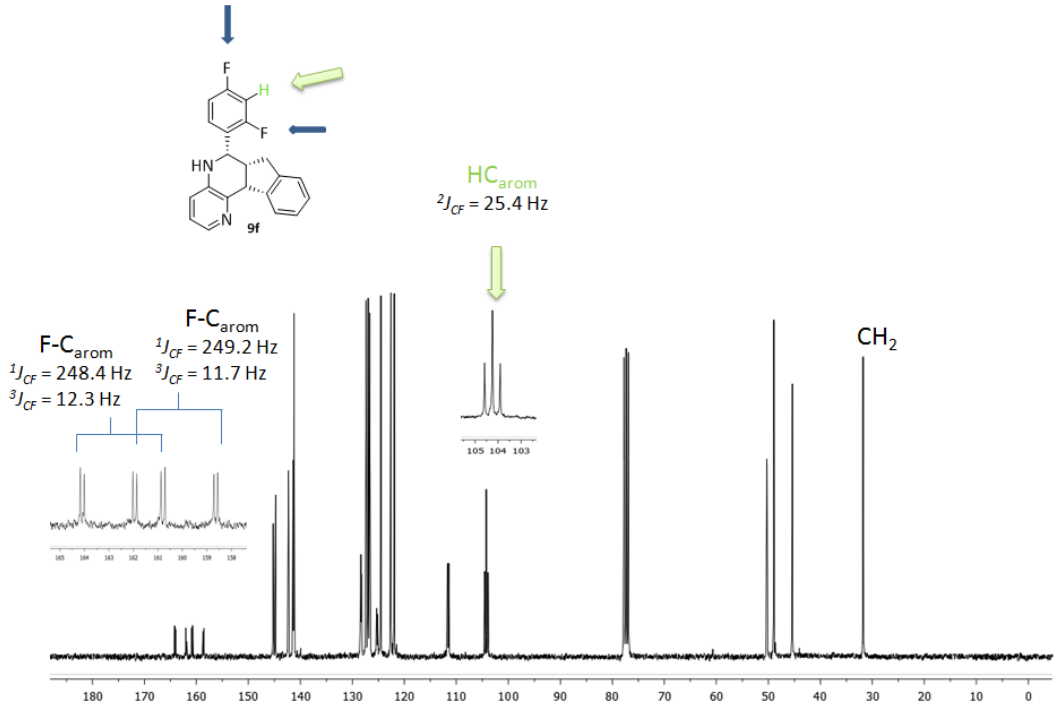

Figure 4. ^{13}C-NMR spectrum for compound **9f**.

Moreover, the structure of the resulting tetrahydroindenonaphthyridines **9** was unambiguously confirmed by comparison with the spectra of compound **9a** (R = Ph), whose structure was previously confirmed by X-Ray analysis (Figure 5).[140]

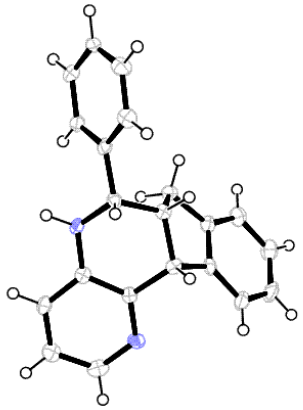

Figure 5. ORTEP view of compound **9a**.

The formation of polycylic compounds **9** could be explained by a [4+2] cycloaddition reaction of double activated imine **3** with indene **7** via *endo* cycloadducts **8** followed by prototropic tautomerization under the reaction conditions in a similar way to that previously reported.[140] Compounds **9** were obtained with control of three stereocenters in a regio- and stereoselective manner (Scheme 3).

Thus, with this methodology we are able to prepare compounds **9** not only with a pyridine group (R = 4-Pyridyl), but also with a broad range of aromatic substrates containing electron-withdrawing groups, including fluorine substituents.

With these results in hand, we then focused our attention on three-component synthetic protocol. Multicomponent reactions (MCR)[149b] have some advantages over classic divergent reaction strategies. These include lower costs, shorter reaction times, and energy, as well as environmentally friendlier aspects, diversity with atom-economy and enantiocontrol. This strategy has been widely applied in medicinal chemistry.

In order to optimize this Povarov type reactions and increase its efficiency and diversity we explored the scope and versatility of the muticomponent (MCR) strategy in the synthesis of tetrahydro-7*H*-indeno[2,1-*c*][1,5]-naphthyridine derivatives **9**.

Therefore, we studied the three-component synthetic protocol using 3-pyridylamine **1**, aromatic aldehydes **2** and indene **7** as dienophile in the presence of 2 equivalents of $BF_3{\cdot}Et_2O$ in refluxing chloroform (Scheme 4). All the reactions afforded in a regiospecific and stereospecific way the corresponding *endo* tetrahydro-7*H*-indeno[2,1-*c*][1,5]-naphthyridines **9** in good yields (Scheme 4, Table 3).

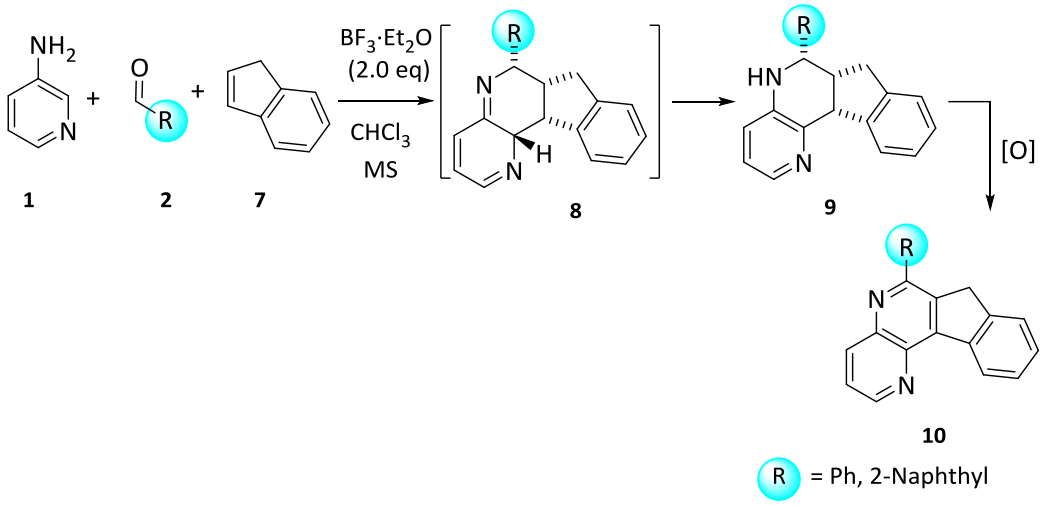

Scheme 4. Multicomponent Povarov reaction.

Table 3. MCR conditions and compounds **9**/**10** obtained.

Entry	Product	R	Reaction time (h)	Yield (%)[a]
1	**9a/10a**	Ph	21	70/7[b]
2	**9c/10c**	2-Naphthyl	24	50/10[b]
3	**9d**	4-$NO_2C_6H_4$	36	67
4	**9e**	4-pyridyl	60	70
5	**9f**	2,4-$F_2C_6H_3$	24	80
6	**9g**	3,4-$F_2C_6H_3$	36	73

[a] Isolated yields. [b] Percentage of naphthyridines **10** obtained.

In all cases we were able to obtain the desired naphthyridine derivatives **9** in good yields and in shorter reaction times than in the two step version. In the case of compounds **9a** (R = Ph) and **9c** (R = 2-Naphthyl) a small proportion of the dehydrogenated compounds **10a** and **10c** were observed in the crude mixture (Table 3, entries 1 and 2).

The formation of polycyclic derivatives **9** can be explained in the same way as when performing the reaction in the two step procedure. Initial condensation reaction between amine **1** and aldehydes **2** may give the corresponding imines **3**, followed by [4+2] cycloaddition reaction of aldimines **3** with indene **7** and subsequent prototropic tautomerization of **8** under the reaction conditions to give polycyclic compounds **9** (Scheme 4).

The scope of these processes, as two-step or MCR protocol, is very wide and can tolerate aldehydes with aromatic, heteroaromatic and naphthyl groups as well as electron-withdrawing groups including fluorine containing substituents, which may be interesting compounds in medicinal chemistry.[73]

2.2.1.2. Povarov reaction of the aldimine derived from 3-aminopyridine and methyl 2-formylbenzoate with olefins

In order to extend the synthetic applications of this strategy, we thought that the presence of a carboxylate group in the *ortho* position of the imine **3l** might open new access to polycyclic indenonaphthyridines containing an additional lactam group in its structure. In this way, we could not only increase the diversity of this family of heterocycles, but also access to new molecules with potentital biological activity.

Consequently, aldimine **3l** derived from methyl 2-formylbenzoate was reacted under the same reaction conditions as those previously used with indene **7** and the

corresponding lactam **14** was obtained as the major product. In a similar way, we explored the reaction using styrene **11** as the dienophile. In this case, the corresponding lactam **15** was also obtained (Scheme 5).

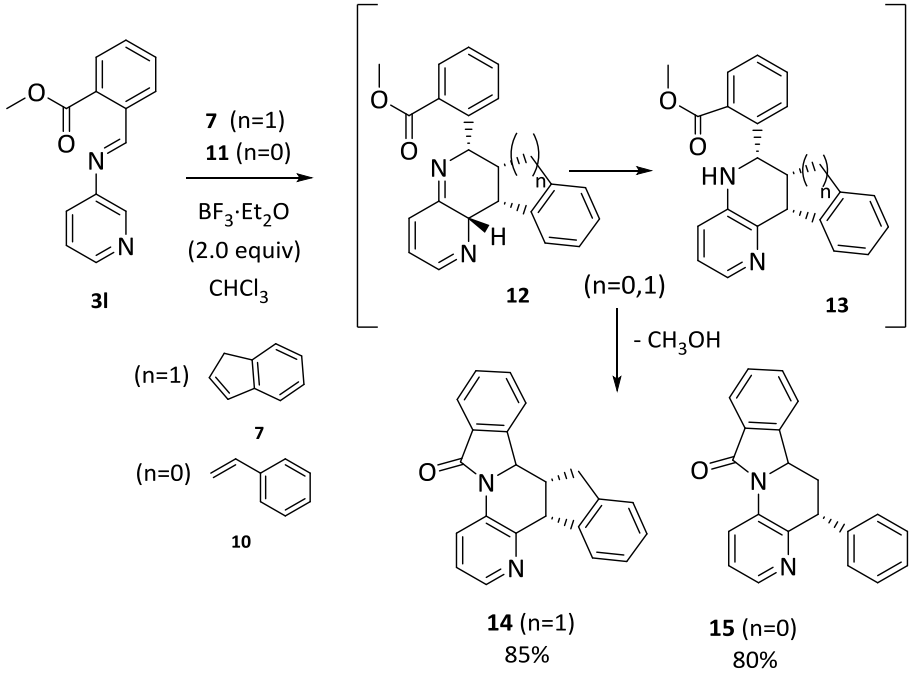

Scheme 5. Povarov reaction between aldimines **3l** and olefins **7** and **11**.

These products were characterized by means of 1D and 2D NMR experiments. As an example, in ^{1}H-NMR spectrum of compound **15** (Figure 6) it can be seen a doublet of doublets (dd) at δ_H = 4.90 ppm with coupling constants $^{3}J_{HH}$ = 12.4 Hz and $^{3}J_{HH}$ = 2.5 Hz, that corresponds to proton 6a-H, another doublet of doublets at δ_H = 4.46 ppm with coupling constants of $^{3}J_{HH}$ = 12.4 Hz y $^{3}J_{HH}$ = 6.3 Hz corresponding to proton 5-H. Moreover, it can be seen two doublet of doublets at δ_H = 2.86 ppm which coupling constants are $^{3}J_{HH}$ = 2.5 Hz y $^{3}J_{HH}$ = 6.3 Hz and $^{2}J_{HH}$ = 12.4 Hz, corresponding to one of the methylenic protons 6-Ha. Finally the other methylenic proton 6-Hb appears as a double doublet of doublets at δ_H = 1.85 ppm with coupling constants $^{2}J_{HH}$ = 12.4 Hz, $^{3}J_{HH}$ = 12.4 Hz and $^{3}J_{HH}$ = 12.4 Hz.

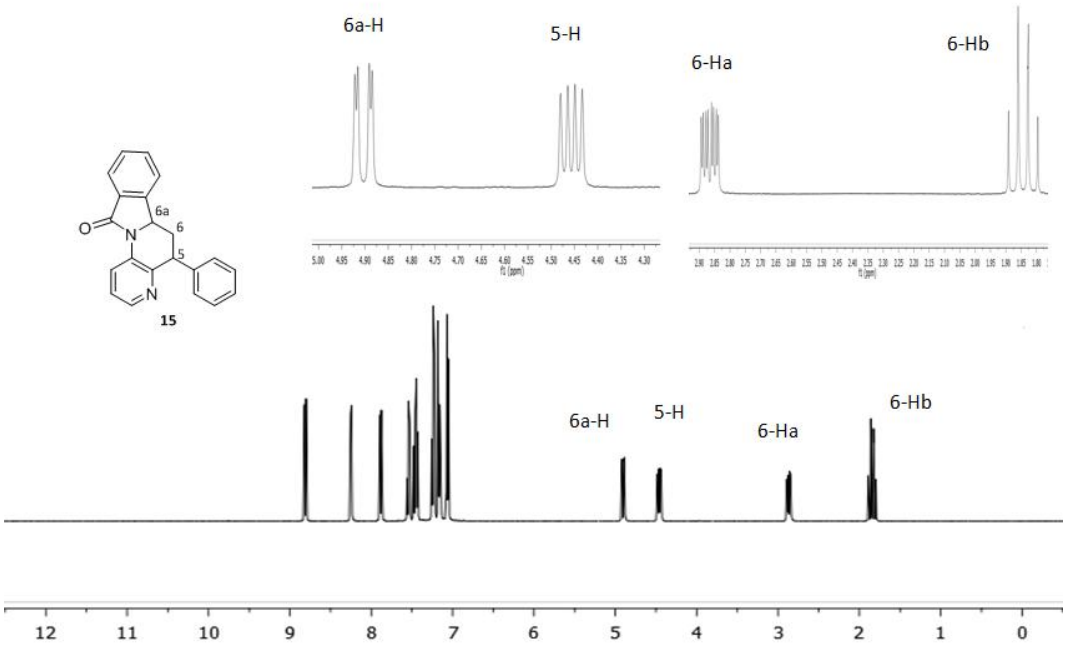

Figure 6. Compound **15** ^{1}H-NMR spectrum.

In the 1D-NOESY spectrum of compound **15** (Figure 7), the selective saturation of 6-Ha (δ_H= 2.86 ppm) afforded a positive NOESY with protons 5-H (3.6%), 6a-H (2.5%) and 6-Hb (16.2%). Likewise, the selective saturation of 6a-H (δ_H= 4.90 ppm) afforded a positive NOESY with proton 5-H (2.3%) and 6-Ha (1.8%). In the case of selective saturation of 5-H (δ_H= 4.46 ppm), positive NOESY can be observed with 6a-H (1.3%) and 6-Ha (2.9%). However, very small NOESY effect was observed with 6-Hb (0.45%). These interactions together with the coupling constants observed in the ^{1}H-NMR spectrum of compound **15** are consistent with the relative *cis* configuration (Figure 7) between 5-H, 6a-H and 6-Ha protons. These results suggest that the cycloaddition reaction between the aldimines **3l** and styrene **11** occurs through an *endo* transition state.

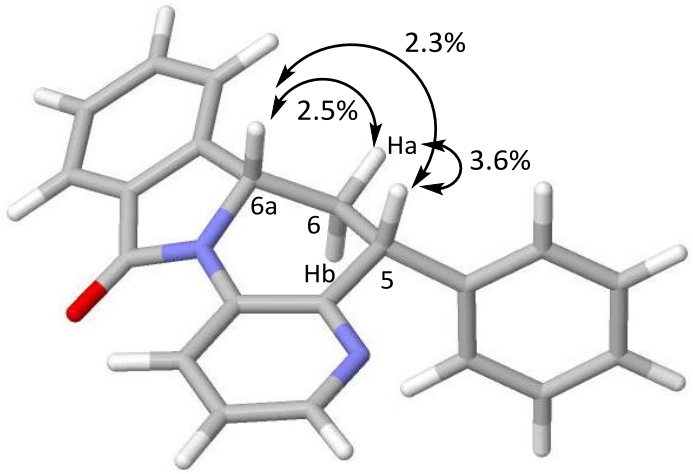

Figure 7. Relative configuration *cis* for compound **15** assigned by 1D-NOESY.

The formation of these compounds **14** and **15**, could be explained through an initial [4+2] cycloaddition between aldimines **3l** and olefins **7** or **11** respectively, and subsequent intramolecular cyclization of **13** followed by a loss of methanol (Scheme 5).

2.2.2. Dehydrogenation of tetrahydro-7H-indeno[2,1-c][1,5]-naphthyridine derivatives

Polycyclic heterocyclic compounds with quasi-planar structure are very effective as chemotherapeutic drugs.[166,167] Among them, some remarkable structures are

[166] (a) Xiao, X.; Cushman, M. *J. Am. Chem. Soc.* **2005**, *127*, 9960-9961. (b) Xiao, X.; Antony, S.; Pommier, Y.; Cushmann, M. *J. Med. Chem.* **2005**, *48*, 3231-3238.

[167] Thapa, U.; Thapa, P.; Karki, R.; Yun, M.; Choi, J. H.; Jahng, Y.; Lee, E.; Jeon, K. H.; Na, Y.; Ha, E. M.; Cho, W.; Kwon, Y.; Lee, E. S. *Eur. J. Med. Chem.* **2011**, *46*, 3201-3209.

tetrahydroquinoline derivatives, isoquinoline analogs and naphthyridine structures that are known to display several biological activities.[117] In the case of topoisomerase I inhibitors, this fact is especially important since flat compounds can establish π-π stacking interactions with different base pairs and stabilize the covalent complex.[168] For these reasons, we explored the transformation of tetrahydro-7*H*-indeno[2,1-*c*][1,5]-naphthyridines **9** into the corresponding 7*H*-indeno-[1,5]-naphthyridines **10** by means of the dehydrogenation of the tetrahydropyridine ring (Scheme 6).

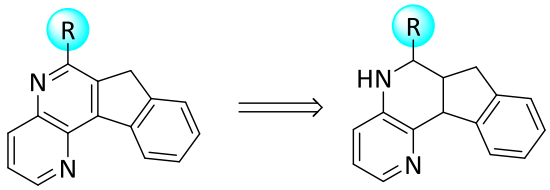

10 **9**

Scheme 6. Dehydrogenation of the tetrahydropyridine ring.

Varma and Kumar[169] developed a general procedure to carry out 1,4-dihydropyridine oxidation using a mild oxidant as it is manganese triacetate.[170] Moreover, it is well-known that microwave-assisted reactions often enhances reaction rates and allows shorter reaction times. With these concepts in mind, we performed several experiments so as to get the conditions for the dehydrogenation of the 1,2,3,4-tetrahydronaphthyridine derivatives **9** previously obtained.

In this way, we explored the reaction with manganese (III) acetate dihydrate and acetic acid as solvent (Scheme 7). The dehydrogenation was studied by using different stoichiometric amounts of oxidant (2, 3 or 5 equivalents) and at different temperatures

[168] Pommier, Y., Merchand, C. *Nature Rev. Drug Discov.* **2012**, *11*, 25-36.
[169] Varma, R. S.; Kumar, V. *Tetrahedron Lett.* **1999**, *40*, 21-24.
[170] (a) Snider, B. B. *Chem. Rev*. **1996**, *96*, 339-363. (b) Criegee, R. *Angew*. Chem. **1958**, *70*, 173-179.

(room temperature, reflux) and under microwave irradiation with 1,2,3,4-tetrahydronaphthyridine derivative **9g.**

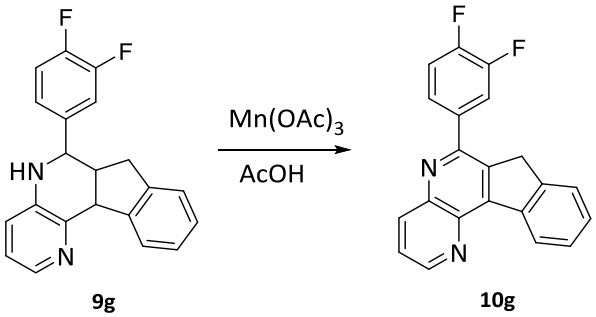

9g **10g**

Scheme 7. Dehydrogenation reaction of derivative **9g**.

The results of the dehydrogenation reaction experiments with tetrahydroindenonaphthyridine **9g** are summarized in table 4.

Table 4. Dehydrogenation condition studies with compound **9g**.

Entry	Reaction conditions	Time(h)	9g/10g[a]
1	$Mn(OAc)_3$, (2 equiv), rt	24	24/59
2	$Mn(OAc)_3$, (5 equiv), reflux	13	30/35
3	$Mn(OAc)_3$, (3 equiv), MW	0.75	35/51
4	$Mn(OAc)_3$, (3 equiv), MW	2	48/42

[a]Proportion of compounds **9**/**10** obtained.

As it can be observed in table 4, we were not able to get full conversion of the 1,2,3,4-tetrahydronaphthyridine **9g**. Moreover, the presence of other over-oxydized derivatives was detected. Due to these results, we investigated another alternative

route to perform this dehydrogenation with the purpose of obtaining full conversion and the dehydrogenated product as the unique reaction product.

It is known the use of quinones as electron acceptor species in the oxidation of 1,4 dihydropyridines[171] and that microwave-assisted synthesis enhances the reaction rates and allows shorter reaction times. In this context, we studied the dehydrogenation of the tetrahydronaphthyridines **9** with 2,3-dichloro-5,5-dicyanobenzoquinone (DDQ) under microwave irradiation (Scheme 8). It was necessary to make optimization studies under various reaction conditions so as to get the best dehydrogenation rates (Table 5).

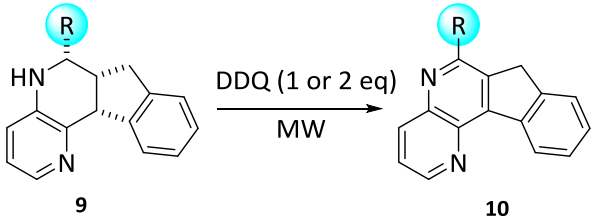

9 **10**

Scheme 8. Dehydrogenation reaction of tetrahydronaphthyridines **9** with DDQ.

We first studied the dehydrogenation reaction of **9a** (R= Ph) in the presence of 2 equivalents of DDQ in four different solvents (chloroform, dioxane, acetonitrile and toluene) and at two different temperatures (25°C and 80°C) under microwave irradiation for 15 minutes (Table 5, entries 1-8). The results indicated that toluene at 25°C (Table 5, entry 7) is able to produce 7*H*-indeno[2,1-*c*][1,5]naphthyridine derivative **10a** in higher yields, and less secondary products are observed in the ^{1}H-NMR crude spectrum.

[171] (a) Gordeev, M. F.; Patel, D. V.; Gordon, E. M. *J. Org. Chem.* **1996**, *61*, 924-928. (b) Janis, R. A.; Triggle, D. J. *J. Med. Chem*. **1983**, *26*, 775-785.

Table 5. Optimization studies for the dehydrogenation with DDQ.

Entry	Reaction Conditions	Conversion 10a (%)
1	Chloroform, 2 equiv of DDQ, 25°C, 15 min	53
2	Chloroform, 2 equiv of DDQ, 80°C, 15 min	53
3	Dioxane, 2 equiv of DDQ, 25°C, 15 min	30
4	Dioxane, 2 equiv of DDQ, 80°C, 15 min	24
5	Acetonitrile, 2 equiv of DDQ, 25°C, 15 min	12
6	Acetonitrile, 2 equiv of DDQ, 80°C, 15 min	54
7	Toluene, 2 equiv of DDQ, 25°C, 15 min	56
8	Toluene, 2 equiv of DDQ, 80°C, 15 min	43
9	Toluene, 1 equiv of DDQ, 25°C, 15 min	60
10	Toluene, 1 equiv of DDQ, 25°C, 60 min	72
11	Toluene, 1 equiv of DDQ, 25°C, 120 min	100

Once the best solvent conditions were chosen, we studied this process with only one equivalent of DDQ (Table 5, entries 9-11) and at longer reaction times. These results were interpreted by means of ^{1}H-NMR crude spectra, in which we could observe that using 1.0 equivalent of DDQ, toluene as solvent, 25°C and during 120 min, the conversion of the starting material **9a** with respect to the dehydrogenated compound **10a** was quantitative (Table 5, entry 11).

The formation of compound **10a** was determined by ^{1}H-NMR spectroscopy where signals corresponding to the tetrahydronaphthyridine ring **9a** protons disappeared, while a sole signal at δ= 4.11 ppm, corresponding to the methylene group of the dehydrogenated derivative **10a**, appeared as a singlet (See experimental section).

Using these optimized conditions, the scope of the reaction was extended to different tetrahydronaphthyridines **9**, and the results obtained are shown in table 6. In all cases, we were able to obtain the desired 1,5-indenonaphthyridines **10**.

Table 6. Dehydrogenation reaction of tetrahydronaphthyridines **9**.

Entry	Product	R	Yield (%)[a]
1	**10a**	Ph	68
2	**10b**	1-Naphthyl	60
3	**10c**	2-Naphthyl	60
4	**10d**	4-$NO_2C_6H_4$	45
5	**10e**	Pyridyl	40
6	**10f**	2,4-$F_2C_6H_3$	54
7	**10g**	3,4-$F_2C_6H_3$	69

[a]Isolated yields after chromatographic purification.

The indenonaphthyridine derivatives **10** were characterized by means of ^{1}H-NMR and ^{13}C-NMR. As an example, in the ^{1}H-NMR spectrum of compound **10g** (Figure 8) appears a characteristic singlet at δ=4.12 ppm corresponding to the methylenic protons.

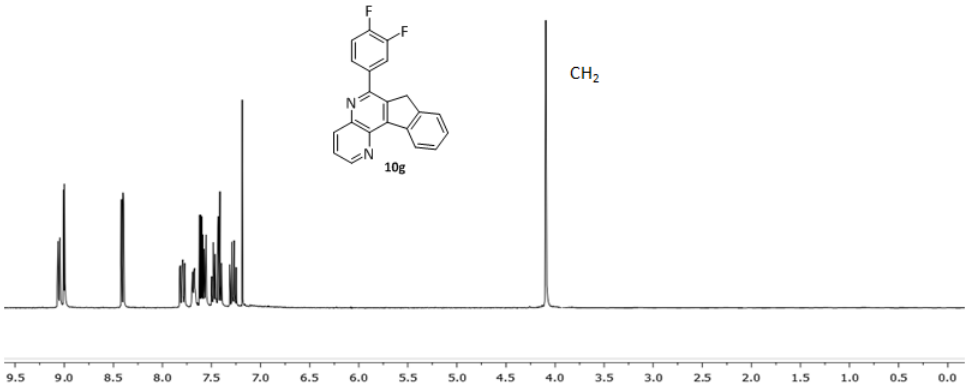

Figure 8.^{1}H-NMR spectrum of **10g** derivative.

The transformation of 1,2,3,4-tetrahydronaphthyridines **9** into the corresponding indenonaphthyridines **10** can be explained by means of the dehydrogenation of the dihydropyridine ring of the 1,2,3,4-tetrahydronaphthyridines **9**.

We found that the reaction conditions tolerated substituted aromatic substrates including fluorine substituents as well as naphthyl groups.

2.2.3 Methylene oxidation of 7H-indeno[2,1-c] [1,5]naphthyridine derivatives

Some indenoisoquinolines that present an indenone fragment in its structure are interesting in terms of the biological activity (Figure 9). This is the case of indotecan,[108] that is a novel selective and potent topoisomerase I inhibitor with potential anticancer activity. If we are able to transform the methylene group in the indeno-1,5-naphthyridine core into a carbonyl group, we are opening new possibilities of interaction between the lone pairs in the oxygen atom and some interesting amino acids in the protein. This carbonyl group will be sensitive to form H bonds with some amino acid and this could be translated as a positive effect by means of enzymatic inhibition.

However, it is noteworthy that methylene oxidation of C-H bonds is a difficult task[172] from a chemical point of view. Even so, this transformation deserves a deeper study since this modification increases the diversity of these polycyclic heterocycles.

[172] Chen, M. S.; White, M. C. *Science* **2010**, *327*, 566-571.

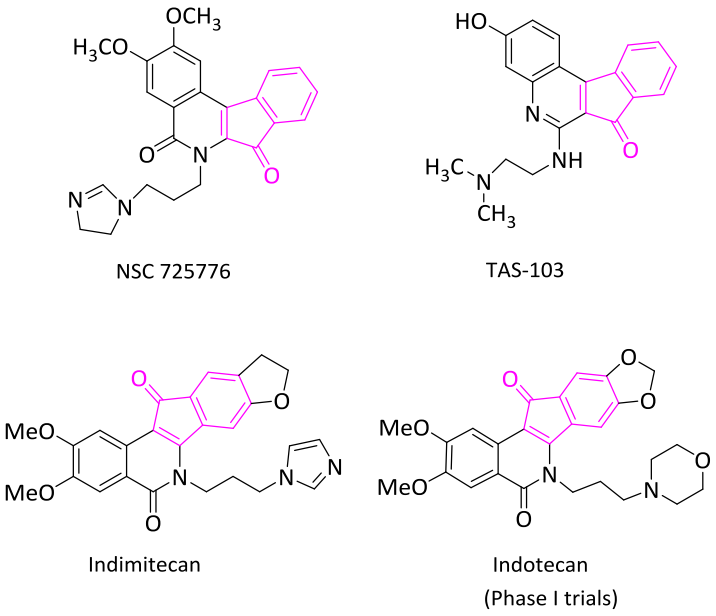

Figure 9. Biologically active compounds with indenone fragment in their structure.

Methylene carbonylation of 1,5-naphthyridines **10** (Scheme 9) was studied by using different oxidant reagents such as $FeCl_3$, $KMnO_4$, potassium peroxymonosulfate (OXONE) and manganese(III) acetate. However, the only oxidizing agent that yielded the desired naphthyridinones **16** was manganese(III) acetate.

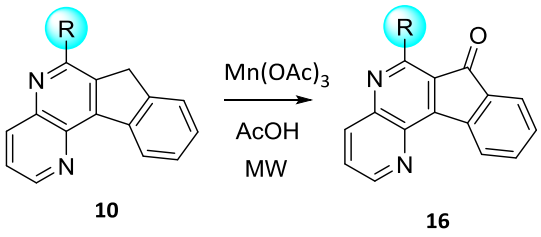

Scheme 9. Methylene carbonylation of *7H*-indeno[2,1-*c*] [1,5]naphthyridines **10**.

In this sense, the reaction between 7*H*-indeno[1,5]naphthyridines **10** with 3 equivalents of $Mn(OAc)_3$ in a microwave reactor in acetic acid during 30 minutes generated 7*H*-indeno[2,1-*c*][1,5]-naphthyridine-7-ones **16** in moderate yields (Scheme 9, Table 7).

Table 7. Compounds **16** obtained.

Entry	Product	R	Yield (%)[a]
1	**16a**	Ph	51
2	**16c**	2-Naphthyl	30
3	**16f**	2,4-$F_2C_6H_3$	35

[a]Isolated yields after chromatographic purification.

The transformation of the indenonaphthyridine derivatives **10** into the corresponding carbonyl derivatives **16** was confirmed by ^{1}H and ^{13}C-NMR. As an example, in the ^{13}C-NMR spectrum of indeno[2,1-*c*][1,5]naphthyridin-7-one **16c** (Figure 10), the signal of the methylenic carbon (CH_2) at δ = 38.3 ppm disappeared and instead a carbonylic carbon signal at δ= 192.6 ppm appeared confirming that the oxidation occurred.

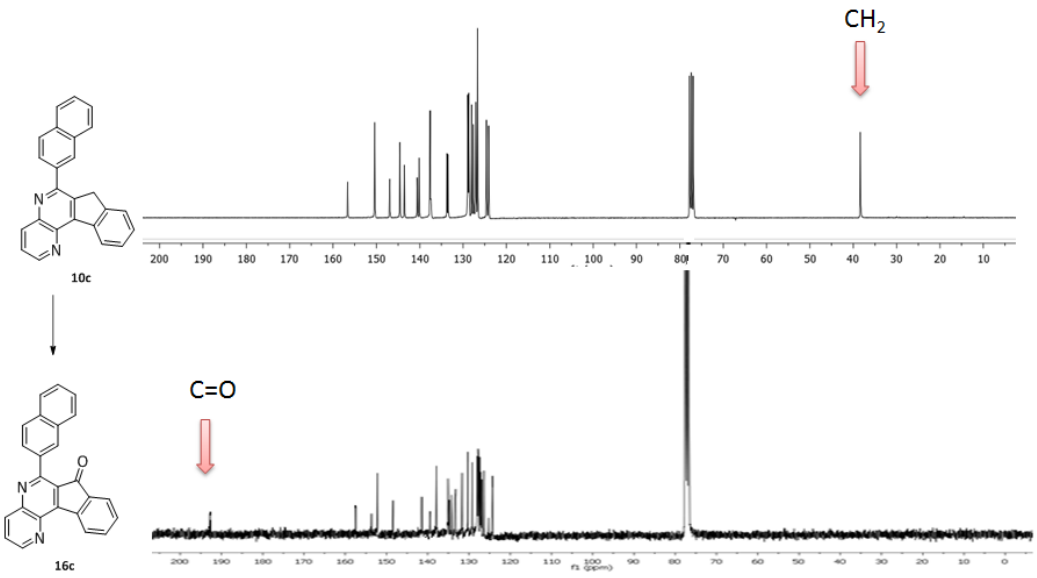

Figure 10. Transformation of derivative **10c** into the carbonyl derivative **16c**.

These results demonstrated that substituents with electron-withdrawing groups including fluorine substituents, as well as, naphthyl groups could be appropriate candidates to participate in this process.

2.2.4. Reduction of 7H-indeno[2,1-c][1,5]naphthyridinone derivatives

The presence of OH groups in a molecule makes possible the formation of hydrogen bonds with some interesting amino acids in the enzymes and can improve the solubility and the biological activity.[173]

Several hydroxylated steroids derivatives have been studied as possible cytotoxic agents.[174] Some of the most representative examples of steroids used in the cancer treatment are shown below (Figure 11). Danazole and RU38486 have shown efficacy in different breast cancers. 9 β-fluoro-11β-hydroxi-17 α-metiltestosterone showed high inhibition in prostatic tumor and in breast cancer.

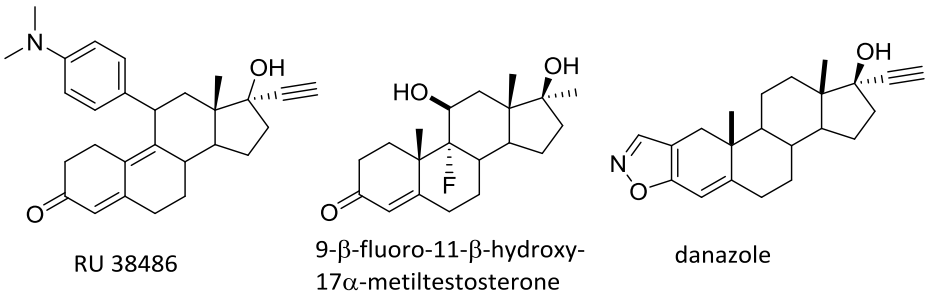

Figure 11. Representative steroids used in cancer therapy.

It can be remarkable to remind that not only camptothecin but also most of the camptothecin derivatives inhibiting TopI activity bear a hydroxyl group in their structure (see Figure 9, Chapter 1).

[173] Nagy, V.; Benltifa, M.; Vidal, S.; Berzsényi, E.; Teilhet, C.; Czfrak, K.; Batta, G.; Docsa, T.; Gergely, P.; Somsák, L.; Praly, J. P. *Bioorg. Med. Chem*. **2009**, *17*, 5696-5707.

[174] Poza, J.; Regam, M.; Paz, V.; Alonso, B.; Rodriguez, J.; Salvador, N.; Fernández, A.; Jiménez, C. *Bioorg. Med. Chem*. **2007**, *15*, 4722-4740.

For these reasons and due to the fact that the reduction of the carbonyl group from a chemical point of view it is not often a difficult transformation, we decided to make some derivatives bearing the OH group in order to increase the diversity of the polycyclic derivatives and evaluate the effect of this group in terms of the biological effect towards topoisomerase I.

Sodium borohydride is among the most used reagent to reduce C=O groups to CH-OH. For instance, the reduction of some indenones to the corresponding hydroxyindenopyridinones has been achieved with this reagent.[175] In this way, we tackle the reduction of some of the indenonaphthyridinones **16** using sodium borohydride in methanol (Scheme 10).

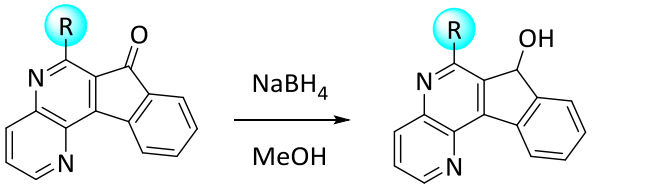

16

17a R = Ph (90%)
17b R= 2-Naphthyl (30%)

Scheme 10. Formation of the hydroxylated derivatives **17**.

Compounds **17** were characterized by means of ^{1}H and ^{13}C-NMR experiments. In the ^{1}H-NMR spectrum of compound **17a** (Figure 12), it can be seen at δ= 2.14 ppm a broad singlet corresponding to the proton of the hydroxyl group and at δ= 6.15 ppm another singlet corresponding to the methine adjacent to the hydroxyl group as characteristic signals for this derivatives **17**.

[175] Tolkunov, S. V.; Khyzhan, A. I.; Suikov, S. Y.; Dulenko, V. I. *Chem*. *Heterocycl. Comp*. **2005**, *41*, 379-386.

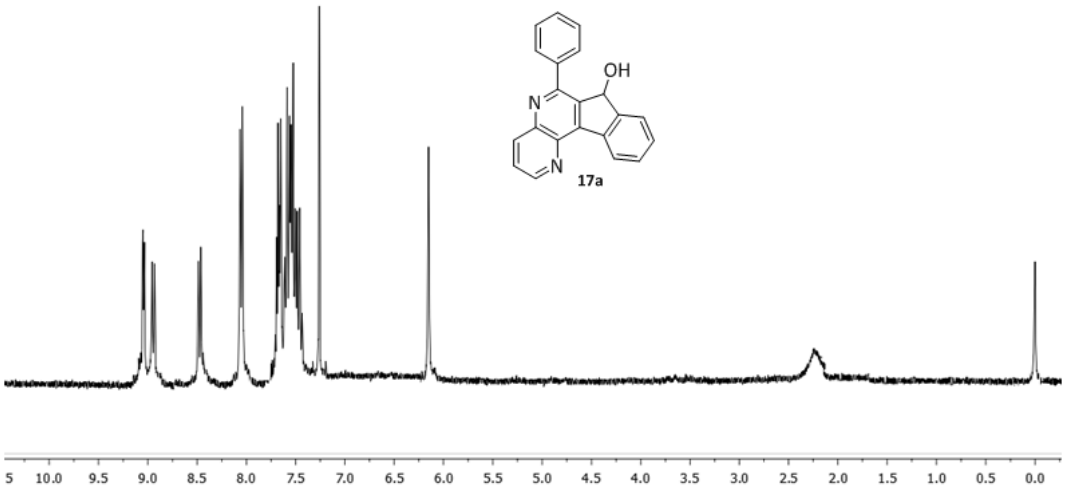

Figure 12. ^{1}H-NMR spectrum of compound **17a**.

All the synthesized derivatives were subjected to biological evaluation as topoisomerase I inhibitors and to *in vitro* cytotoxicity experiments in different cancer cell lines (See chapter 3).

In conclusion, the [4+2] cycloaddition reaction via *endo* transition state of aldimines **3** with indene **7** as dienophile allows the preparation of tetrahydro-7*H*-indeno[2,1-*c*][1,5]-naphthyridines **9** with a regio-and stereoselective control of the three stereocenters (Figure 13). The dehydrogenation of the tetrahydro-7*H*-indeno[2,1-*c*][1,5]-naphthyridine derivatives **9** with DDQ yields the corresponding 7*H*-indeno[2,1-*c*][1,5]naphthyridines **10**. The methylene group in these derivatives **10** can be transformed into a carbonyl group to yield the corresponding 7*H*-indeno[1,5]naphthyridin-7-ones **16** in which the carbonyl group can be reduced to the hydroxyl group to obtain the hydroxylated derivatives **17**.

In the special case of using methyl 2-formylbenzoate as the starting aldehyde for the imine formation **3l** (R=2-MeO_2C-C_6H_4), the product obtained from the [4+2] cycloaddition reaction with indene **7** is the polycyclic lactam **14** (Figure 13).

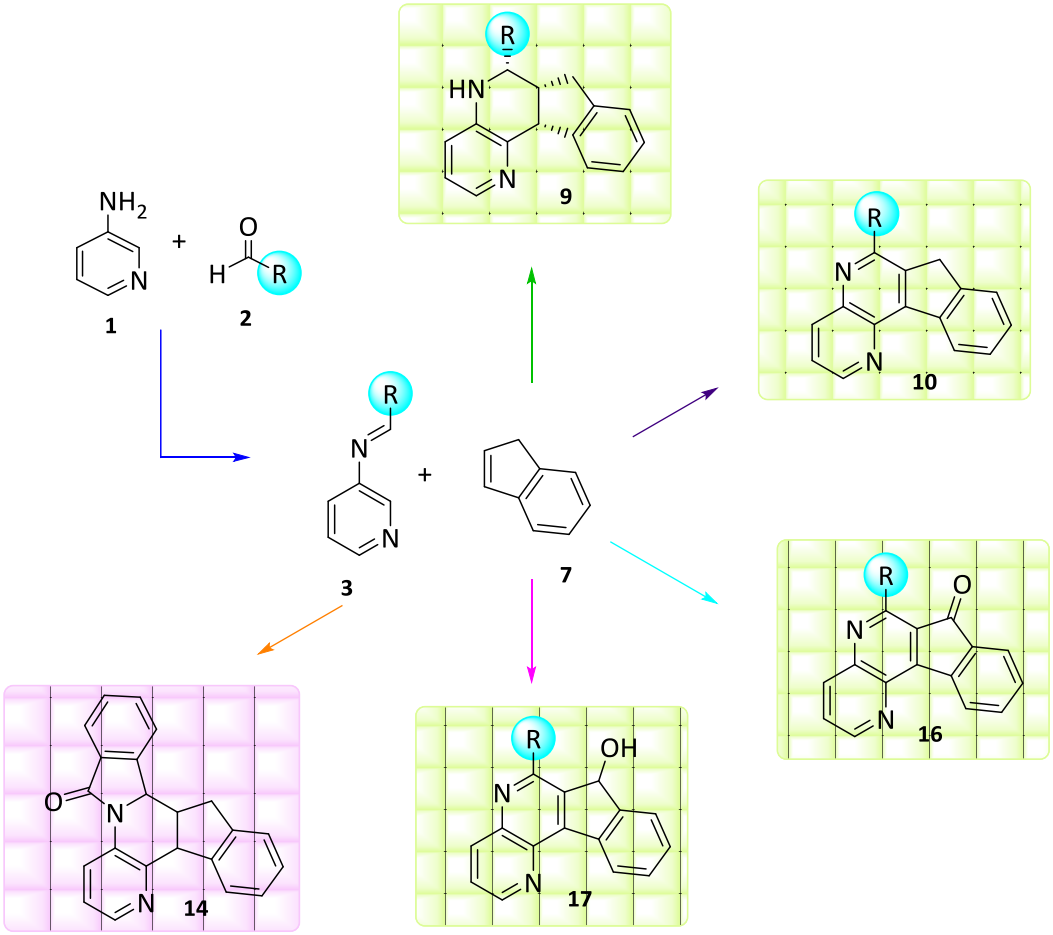

Figure 13. Summary of the synthesized derivatives.

2.3. Synthesis of 2,4-diaryl-1,5-naphthyridines

It was previously mentioned when explaining the Povarov methodology that apart from olefins it is possible to use acetylenes as dienophiles. Thus, once we explored the Povarov reaction between aldimines and different olefins we pose the challenge of performing the Hetero Diels-Alder reaction between aldimines **3**, derived from 3-aminopyridine **1** and aromatic aldehydes **2**, with acetylenes as dienophiles. The use of acetylenes in this Povarov reaction might afford molecules with a wide diversity in their structures.

2.3.1. Povarov reaction between aldimines derived from 3-aminopyridine and acetylenes

Pyridylaldimines **3** previously synthesized (Table 1, page 94) for its use in the Povarov reaction with indene were used to study the optimal reaction conditions for the Povarov reaction with acetylenes.

As in the Povarov reaction with olefins, when acetylenes were used the reaction without catalyst didn't work and the starting products were recovered. However, the use of trifluor boro etherate as Lewis acid catalyst gave us excellent results with indene.

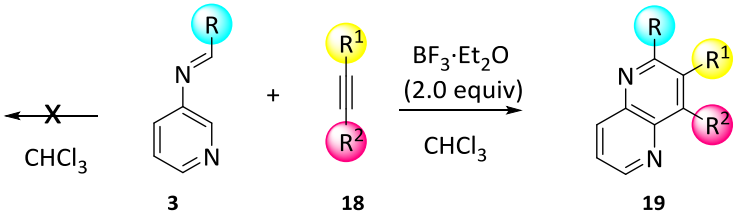

Scheme 11. Povarov reaction with acetylenes **18**.

Therefore, we explored the reaction in the same conditions using 2.0 equivalents of $BF_3{\cdot}Et_2O$ and acetylenes **18** (Scheme 11) and we obtained a wide variety of 1,5-naphthyridine derivatives **19** in one single step and in good yields. Results are summarized in table 8.

Table 8. Povarov reaction between aldimines **3** and acetylenes **18**.

Entry	Product	R	R^1	R^2	Reaction Conditions		Yield[a](%)
					t(h)	T(°C)	
1	**19a**	Ph	H	Ph	48	60	75
2	**19b**	3,4-F_2-C_6H_3	H	Ph	24	60	60
3	**19c**	4-CF_3-C_6H_4	H	Ph	18	60	60
4	**19d**	4-F-C_6H_4	H	Ph	36	60	75
5	**19e**	4-NO_2-C_6H_4	H	Ph	48	20	50
6	**19f**	3-NO_2-C_6H_4	H	Ph	15	60	35
7	**19g**	3-OMe-C_6H_4	H	Ph	20	60	50
8	**19h**	4-CF_3-C_6H_4	H	C_6H_4Ph	48	20	65
9	**19i**	4-F-C_6H_4	H	C_6H_4Ph	36	60	55
10	**19j**	4-NO_2-C_6H_4	H	C_6H_4Ph	24	20	50
11	**19k**	3-NO_2-C_6H_4	H	C_6H_4Ph	24	60	30
12	**19l**	3-OMe-C_6H_4	H	C_6H_4Ph	48	60	55
13	**19m**	4-F-C_6H_4	H	6-OMe-Naphtyl	24	60	50
14	**19n**	4-CF_3-C_6H_4	H	4-OMe-C_6H_4	36	60	60
15	**19o**	4-F-C_6H_4	H	4-OMe-C_6H_4	24	60	40
16	**19p**	4-NO_2-C_6H_4	H	4-OMe-C_6H_4	18	60	60
17	**19q**	3-OMe-C_6H_4	H	4-OMe-C_6H_4	26	60	40
18	**19r**	4-CF_3-C_6H_4	H	4-CF_3-C_6H_4	36	60	60
19	**19s**	4-CF_3-C_6H_4	H	3-Thienyl	40	60	50
20	**19t**	4-F-C_6H_4	H	3-Thienyl	48	20	30
21	**19u**	4-CF_3-C_6H_4	Me	Ph	48	60	50

[a]Isolated yields after chromatographic purification.

Compounds **19** were characterized by means of ^{1}H and ^{13}C-NMR experiments. As an example, ^{1}H-NMR spectrum of compound **19n** is shown in figure 14. The most characteristic signal in these derivatives **19** corresponds to the 3-H proton that appears as a singlet at around 8.0 ppm. In the case of **19n** derivative it can be observed at δ = 3.84 ppm a singlet corresponding to the protons of the methoxy group, the singlet corresponding to 3-H proton at δ= 8.04 ppm and finally the characteristic naphthyridine protons 8-H at δ= 8.44 and 6-H at 8.95 ppm as doublet of doublets.

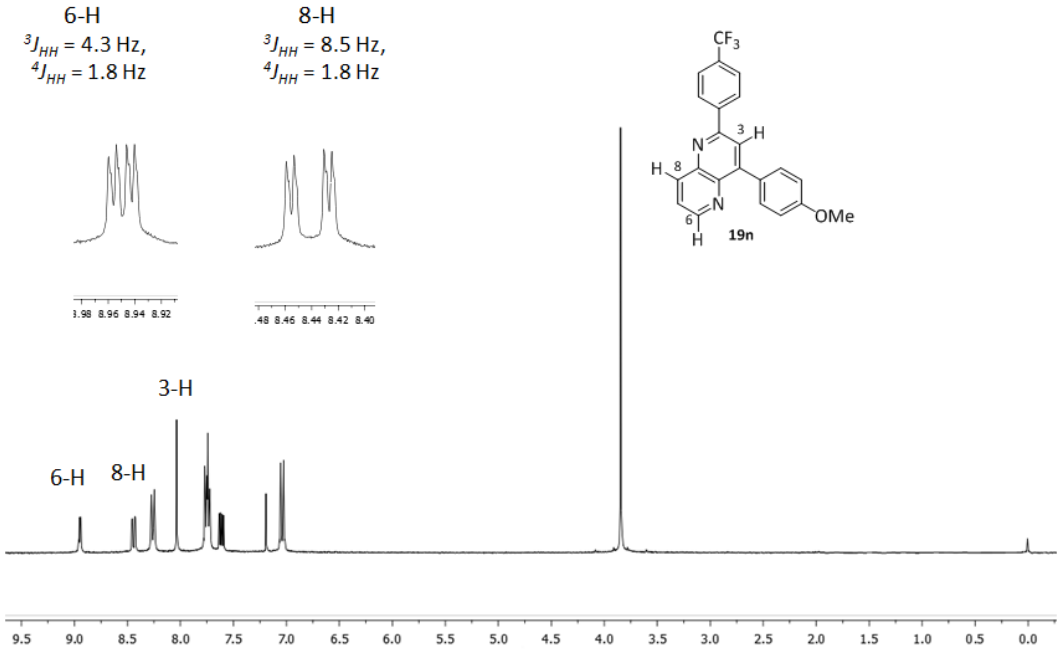

Figure 14. ^{1}H-NMR spectrum of compound **19n**.

The structure of **19n** was fully confirmed by means of X-Ray experiment (Figure 15). This data revealed that the formation of compounds **19** takes place *via* a regioselective process.

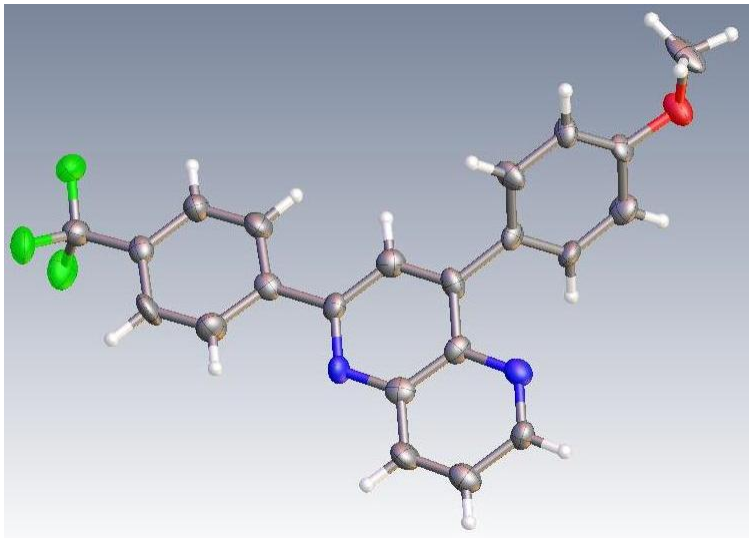

Figure 15. ORTEP view of compound **19n**.

The formation of these functionalized compounds **19** could be explained by means of a [4+2] cycloaddition between the pyridylaldimines **3** and acetylenes **18** and subsequent aromatization by a loss of hydrogen under the reaction conditions.

The scope of this Povarov type reaction using acetylenes as dienophiles is very wide and can tolerate electron-releasing substituents in position 2 including fluorine substituents and a broad range of electron-withdrawing group . Moreover, it is possible to use not only mono substituted acetylenes **18a-f** (Table 8, entries 1-20) but also disubstituted ones **18g** (Table 8, entry 21).

It has been already mentioned that multicomponent reactions (MCRs) have several advantages over classical reactions. In the same way as done when using indene in the Povarov reaction, in the case of using acetylenes we thought that studying the multicomponent version of the reaction would be interesting because we could reduce reaction time and in some cases improve yields.

For this purpose, we performed the multicomponent reaction (MCR) between the amine **1**, aldehydes **2** and acetylenes **18** in the presence of $BF_3{\cdot}Et_2O$ (2 equivalents) in refluxing chloroform (Scheme 12).

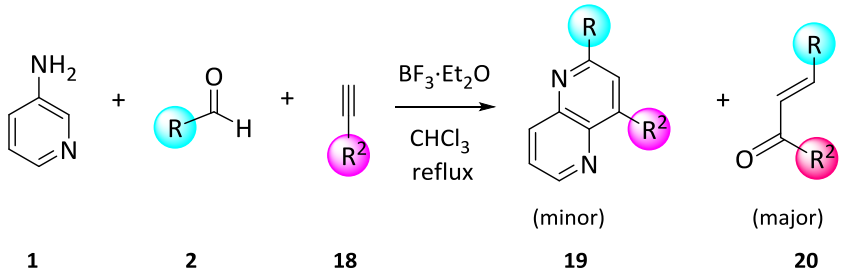

Scheme 12. MCR Povarov reaction with acetylenes **18**.

For our surprise we were able to observe little amount of the desired naphthyridines **19** in the crude mixture and the corresponding spectra were more complexes indicating that there were another products formed. The major product in the MCR version was the α,β-unsaturated carbonyl derivative **20**. The results of this multicomponent version are summarized in table 9.

Table 9. MCR conditions and compounds **19/20** obtained.

Entry	Products	R	R^2	Reaction time (h)	Yield 19/20(%)[a]
1	**19c/20c**	4-CF_3-C_6H_4	Ph	24	7/50
2	**19e/20e**	4-$NO_2C_6H_4$	Ph	30	4/55
3	**19n/20n**	4-CF_3-C_6H_4	4-$OMeC_6H_4$	30	6/50
4	**19p/20p**	4-$NO_2C_6H_4$	4-$OMeC_6H_4$	36	4/55

[a]Isolated yields after chromatographic purification.

The reaction between aldehydes and acetylenes to obtain α-β-unsaturated ketones is already known.[176] Thus, we decided to perform the reaction between aldehydes **2** and acetylenes **18** in the presence of $BF_3{\cdot}Et_2O$ (Scheme 13), and in these conditions compounds **20** were obtained in good yields (Table 10).

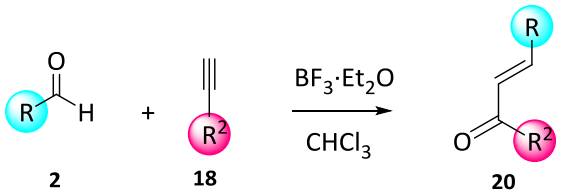

Scheme 13. Reaction between aldehydes **2** and acetylenes **18**.

Table 10. α-β-unsaturated ketones **20** obtained.

Entry	Product	R	R^2	t (h)	T (°C)	Yield[a] (%)
1	**20e**	4-$NO_2C_6H_4$	Ph	20	60	85
3	**20n**	4-$CF_3C_6H_4$	4-$OMeC_6H_4$	24	60	75
2	**20p**	4-$NO_2C_6H_4$	4-$OMeC_6H_4$	24	60	55

[a]Isolated yields after chromatographic purification.

The structure of all the derivatives **20** were confirmed by NMR spectroscopy and High Resolution Mass Spectrometry (HRMS). With these experiments we were able to confirm that the major product in the multicomponent crude mixture was the α-β-unsaturated ketone **20** derived from reaction between aldehydes **2** and the acetylenes **18**.

[176] Rueping, M.; Bootwicha, T.; Baars, H.; Sugiono, E. *Beilstein J. Org. Chem*. **2011**, *7*, 1680-1687.

Keeping in mind these results, we conclude that the multicomponent version of the Povarov reaction when using acetylenes **18** is not a good choice for the synthesis of the desired 1,5-naphthyridine derivatives **19** due to the competence between aldehydes **2** and acetylenes **18**.

2.3.2. Povarov reaction between the aldimine derived from 3-aminopyridine and methyl 2-formylbenzoate and acetylenes

It has been previously reported that when using the imine **3l**, derived from condensation reaction between 3-aminopyridine **1** and methyl 2-formylbenzoate, with indene **7**, polycyclic lactam **14** (Scheme 5) was obtained. In the same way, we decided to explore the reaction between pyridylaldimine **3l** and acetylenes **18** (Scheme 14). Initially, we studied the reaction of **3l** with phenylacetylene **18a** (R^2 = Ph) in refluxing chloroform, with 2 equivalents of $BF_3{\cdot}Et_2O$ and after 48h of reaction the expected tetracyclic lactam **22** was not obtained (Scheme 14). Instead, the *N*-pyridyl lactam **21a** (R^2 = Ph) was isolated (Table 11, entry 1). Then, the process was extended to other acetylenes, therefore the reaction was carried out with biphenylacetylene **18b** (R^2= C_6H_4Ph) and 4-methoxyphenylacetylene **18d** (R^2= 4-$OMeC_6H_4$) and compounds **21b** and **21c** were obtained, respectively (Table 11, entries 2 and 3).

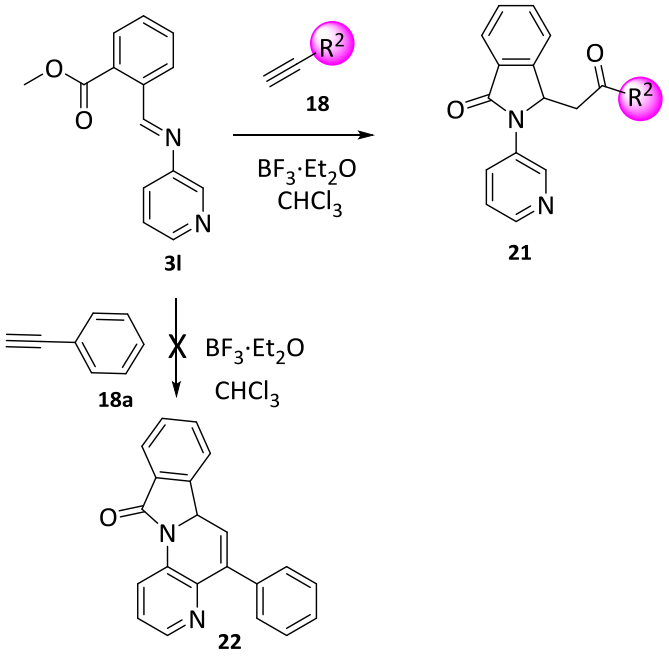

Scheme 14. Povarov reaction between imine **3l** and acetylenes **18**.

Table 11. Compounds **21** obtained.

Entry	Product	R^2	Reaction time (h)	Yield (%)[a]
1	**21a**	Ph	48	50
2	**21b**	C_6H_4Ph	60	50
3	**21c**	4-$OMeC_6H_4$	24	55

[a]Isolated yields after chromatographic purification.

Products **21** were characterized by means of 1D and 2D NMR experiments and confirmed by HRMS. For instance, in the ^{1}H-NMR spectrum of compound **21a** (Figure16) appear three different doublet of doublets (dd).

The first one at δ_H = 3.18 ppm with coupling constants $^2J_{HH}$ = 17.5 Hz and $^3J_{HH}$ = 9.8 Hz, that corresponds to one of the methylenic protons, the second doublet of doublets corresponding to the other methylenic proton appears at δ_H = 3.44 ppm with coupling constants $^2J_{HH}$ = 17.5 Hz and $^3J_{HH}$ = 3.0 Hz, and the third doublet of doublets at δ_H = 5.95 ppm with coupling constants $^3J_{HH}$ = 9.8 Hz and $^3J_{HH}$ = 3.0 Hz, corresponds to the methyne proton of the lactam skeleton.

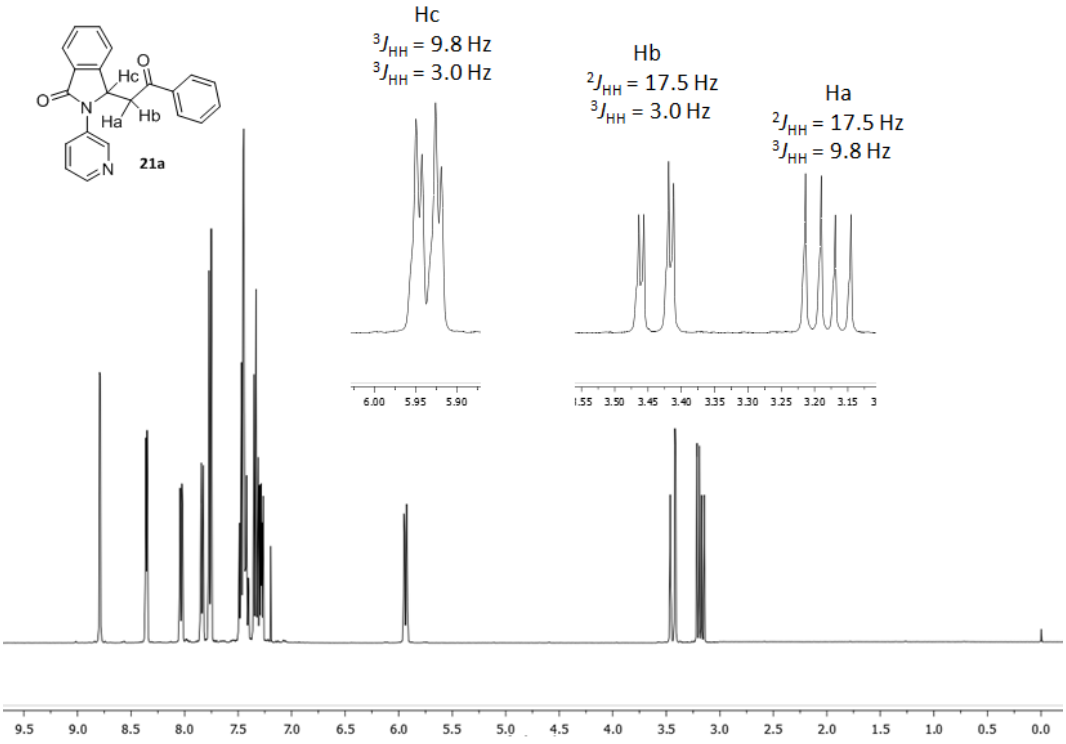

Figure 16. ^{1}H-NMR spectrum of compound **21a**.

COSY experiment results (Figure 17) are in agreement with this structure **21a** showing coupling relationship between methylenic protons and the adjacent proton at three bond distance.

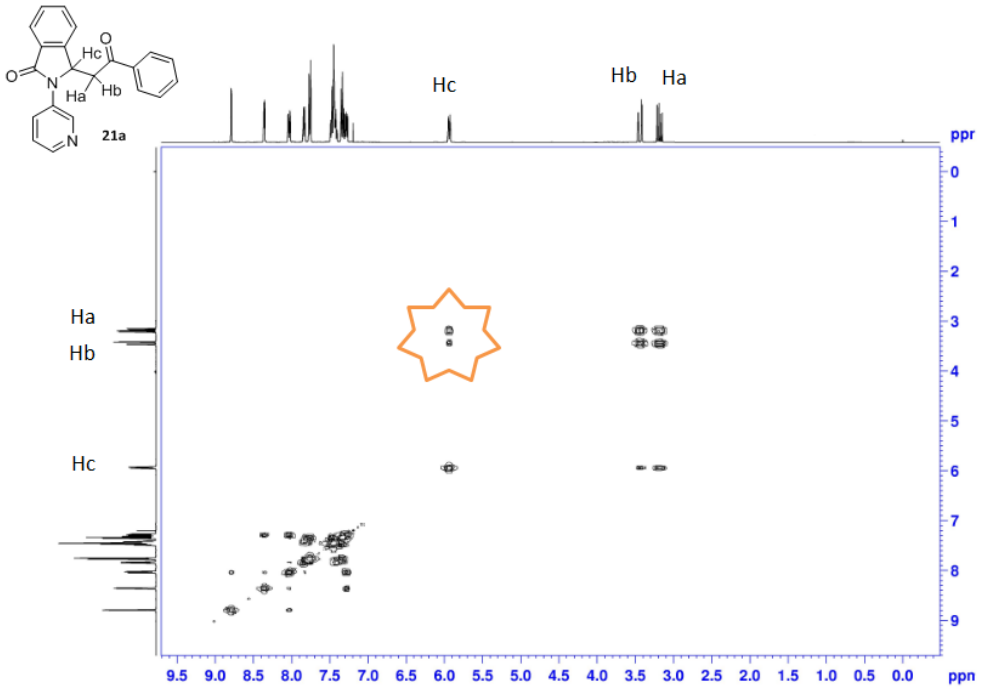

Figure 17. COSY experiment of compound **21a**.

The formation of products **21** could be explained by means of the addition of the acetylene **18** to the iminic double bond of the imine **3l** with the subsequent formation of the zwitterion **23** that cyclize to give the intermediate **24** (Scheme 15). Finally, in the presence of NaOH, the functionalized enol **25** may be formed and subsequent keto-enol tautomerization yields compound.

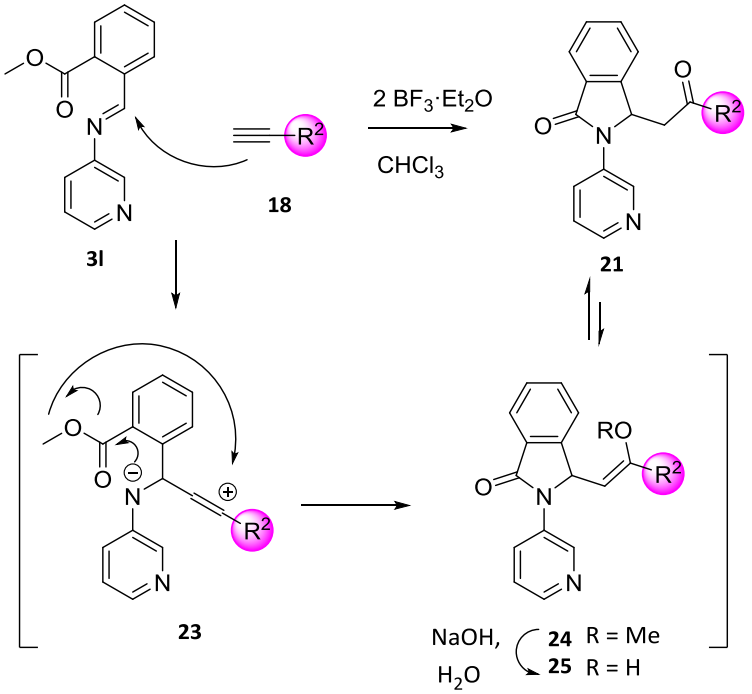

Scheme 15. Possible mechanism for the formation of compounds **21**.

With these results, it is possible that the Povarov reaction when using acetylenes **18** as dienophiles might take place through a stepwise mechanism instead of a concerted process.

2.3.3. Mechanistic study of the reaction between aldimines derived from 3-aminopyridine and acetylenes

As it has been previously mentioned, in our research group, we carried out theoretical studies (Figure 29, page 75) of the aldimines derived from 3-aminopyridine with different olefins in the presence of $BF_3{\cdot}Et_2O$. In these studies we exposed that in this case the Povarov reaction took place through a concerted, asyncronous process, regio- and stereoselectively to yield 1,5-indenonaphthyridine derivatives. However, it is possible to find theoretical studies for the Povarov reaction between aldimines derived from anilines with olefins using Brønsted acids as catalyst in which it is said that the reaction goes through a step-by-step mechanism.[139] In this case, the process starts with the nucleophilic attack of the alkene to the protonated imine with the formation of a cationic intermediate that undergoes an intramolecular Friedel-Crafts reaction to give the corresponding quinolines.

In this way, and with the aim of understanding the mechanism through which the Povarov reaction between aldimines **3** derived from 3-aminopyridine with acetylenes **18** takes place, we decided to use a Brønsted acid such as diphenylphosphonic acid **26** (Scheme 16) as catalyst knowing that, the behavior of Lewis acid could be different to that of Brønsted acids.

Thus, when the reaction of imine **3h** with *p*-methoxy-phenylacetylene **18d** (R^3= 4-$OMeC_6H_4$) was performed in the presence of 2.0 equivalents of phosphonic acid, the propargylamine **27** was isolated.

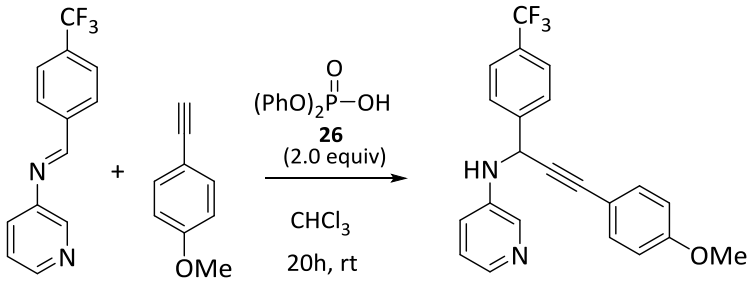

3h **18 d** **27**

Scheme 16. Povarov reaction in the presence of a phosphonic acid.

The structure of compound **27** was assigned by means of 1D and 2D NMR experiments and confirmed by HRMS. In the ^{1}H-NMR spectrum of compound **27** (Figure 18) appears a doublet at δ = 5.55 ppm with a coupling constant of $^{3}J_{HH}$ = 7.2 Hz corresponding to the hydrogen adjacent to the amino group.

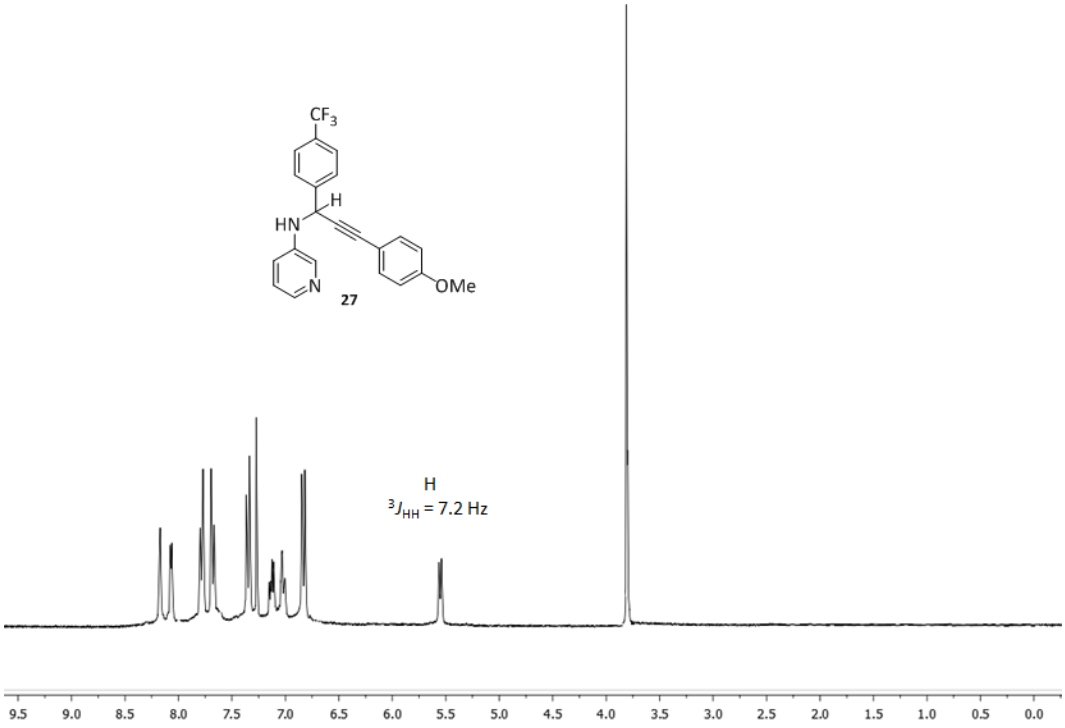

Figure 18. ^{1}H-NMR spectrum of compound **27**.

In the ^{13}C-NMR spectrum of compound **27** (Figure 19), signals corresponding to the quaternary carbons at δ = 85.1 ppm and δ = 86.3 ppm of the acetylene group present in the structure are the most characteristic ones.

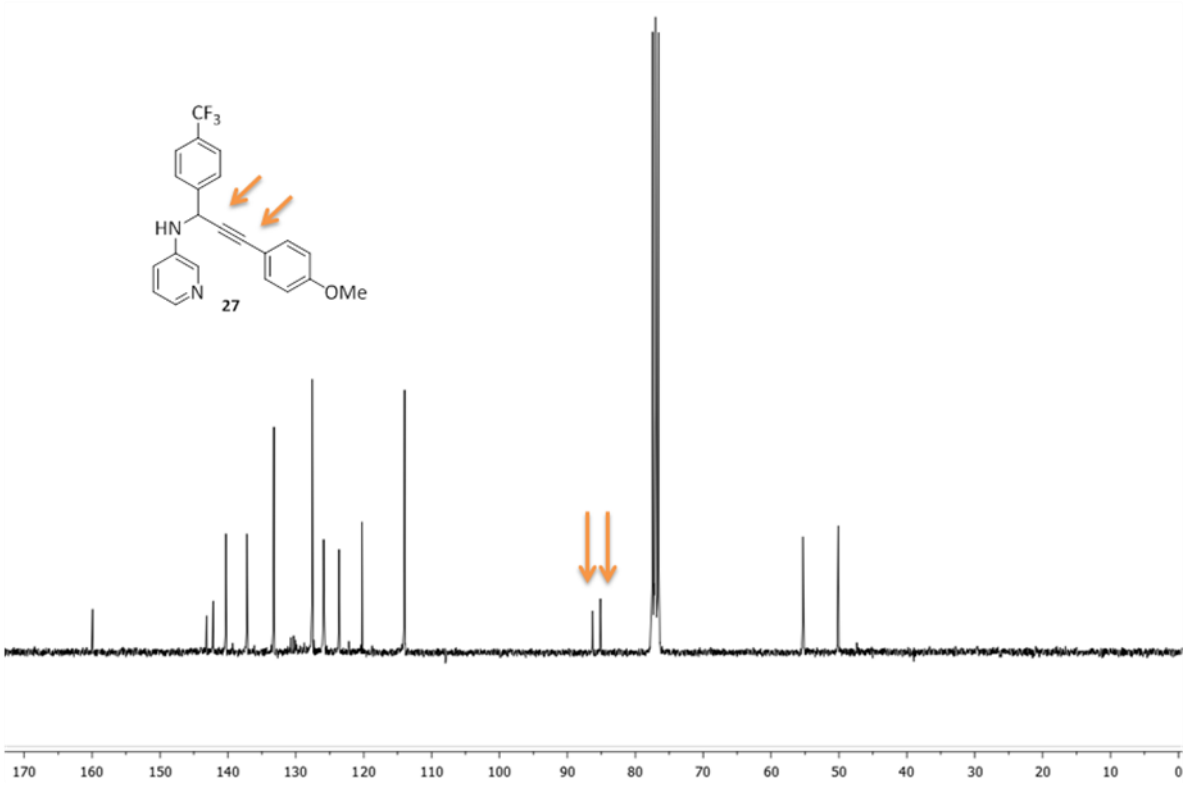

Figure 19. ^{13}C-NMR spectrum of compound **27**.

The formation of compound **27** could be explained by an initial attack of the acetylene **18d** (R^3= 4-OMeC_6H_4) to the iminic carbon of the double protonated imonium salt **28** to form intermediate **29** that through a loss of a proton, it is transformed in the pyridinium salt **30**. Finally, this salt **30** is converted into compound **27** under the reaction conditions (Scheme 17).

On the other hand, posterior heating of the propargyl amine **27** in the presence of BF_3·Et_2O did not cyclize to form the 1,5-naphthyridine **19n**.

These results together with that obtained for the reaction of imine **3l** with methyl 2-formylbenzoate (Section 2.3.2, page 124) seem to suggest that the Povarov reaction between aldimines **3** derived from 3-aminopyridine and acetylenes **18** takes place through a step-by-step mechanism.

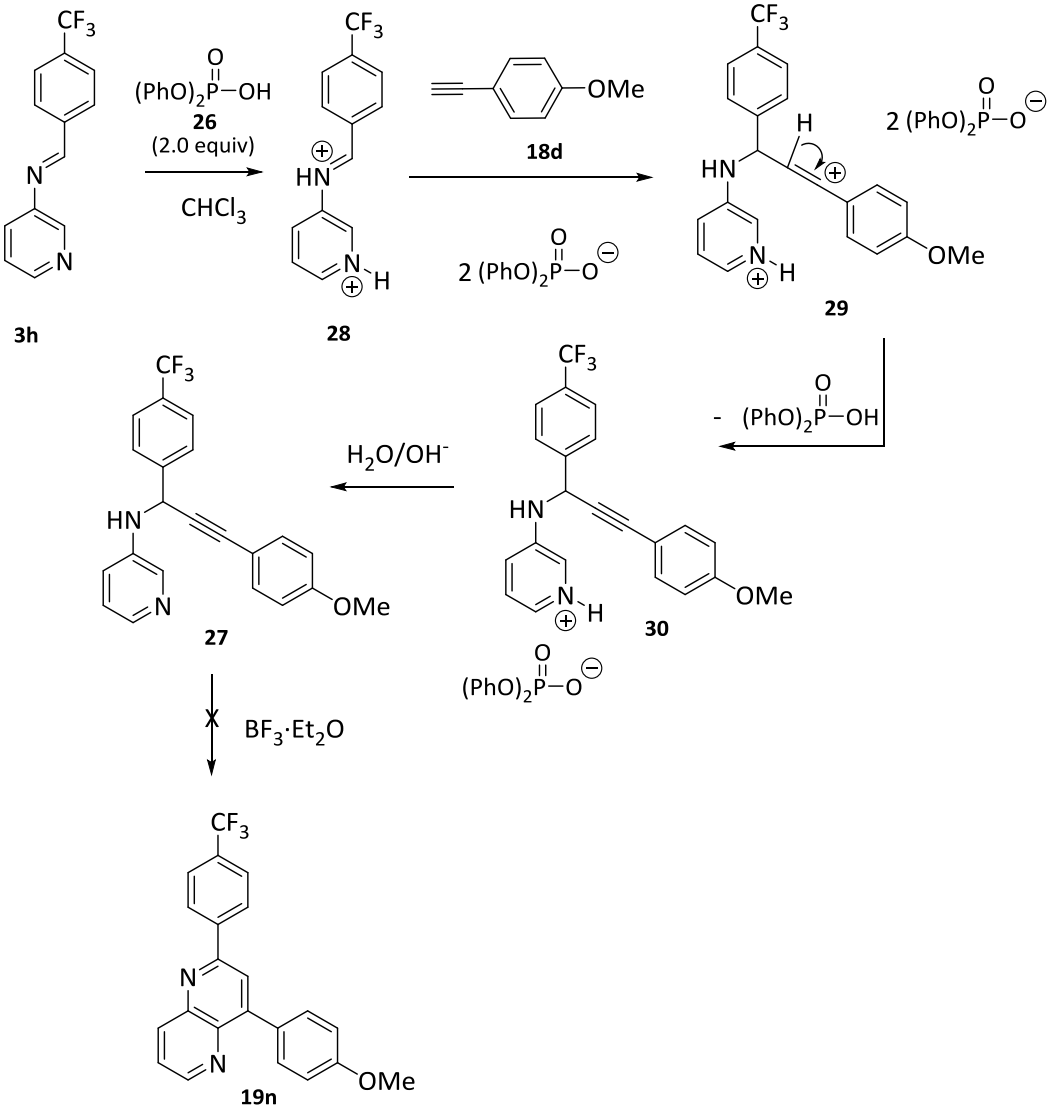

Scheme 17. Possible mechanism for the propargylamine **27** formation.

These results with diphenylphosphonic acid **26** as Brønsted acid (Scheme 16), as well as, the isolation of lactams **21** (Scheme 14) in the reaction of imine **3l** with acetylenes **18** allow us to reconsider the possible mechanisms for this process with Lewis acids ($BF_3{\cdot}Et_2O$, Scheme 18). Firstly, the double activated imine **31** may suffer a nucleophilic attack from the acetylene **18** with the formation of a zwitterionic intermediate **32**. On one hand, the intermediate **32** could undergo a 1,3 proton transfer to form the propargylamine **27**, that is not able to cyclize to form naphthyridines **19**, because pyridine ring is not activated towards an electrophilic substitution and specially in α and γ positions with respect to the pyridinic nitrogen. Nevertheless, the zwitterion **32** through a 1,3-hydride shift may form the 3-azatriene **33**, which by means of an electrocyclic ring closure (ERC) may give the byciclic compound **34**. This intermediate **34**, under the reaction or purification conditions could afford the 1,5-naphthyridines **19**.

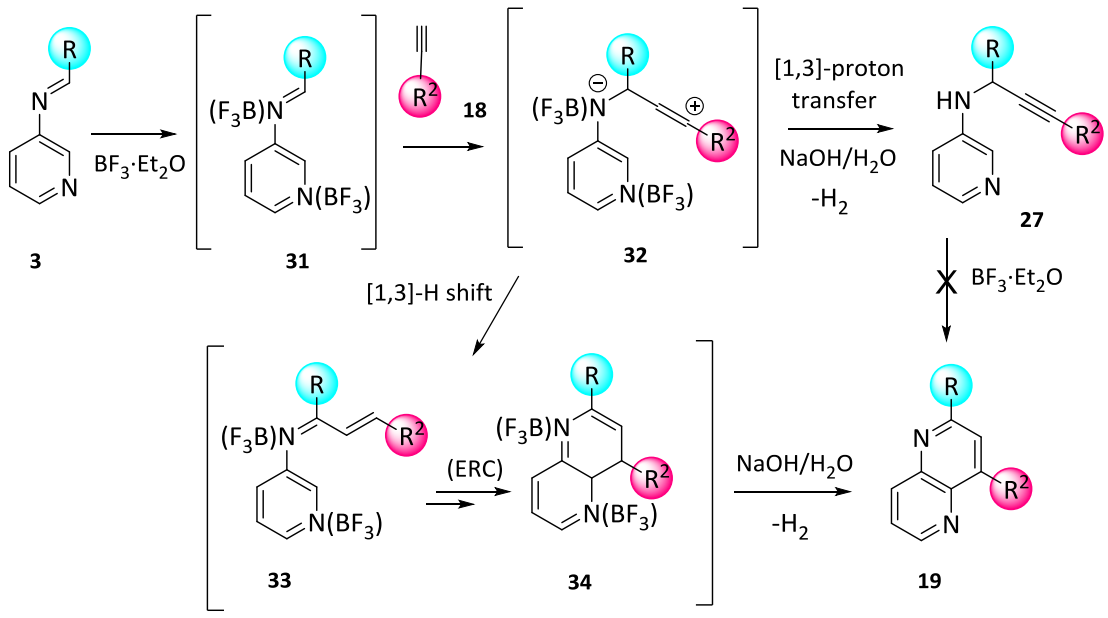

Scheme 18. Possible mechanism for the Povarov reaction with acetylenes **18**.

To sum up, the [4+2] cycloaddition reaction between aldimines **3** and acetylenes **18** as dienophiles yields the desired 1,5-naphthyridines **19** (Scheme 19) in good yields with the clear advantage of obtaining aromatic flat derivatives in only one step. However, if the process is performed in the presence of a Bronsted acid (phosponic acid) the reaction of imine **3h** (R = 4-CF_3-C_6H_4) with acetylene **18** (R^1 = H, R^2 = 4-OMe-C_6H_4) led to the formation of the propargylamine **27**.

In the special case of using the functionalized imine **3l** (R=2-MeO_2C-C_6H_4) for the Povarov reaction with acetylenes **18**, the product formed is not a tetracyclic lactam, instead a *N*-pyridylactam **21** is obtained (Scheme 19). These results may suggest a step-by-step mechanism instead of a concerted one, as happened in the case of employing olefins as the dienophiles for the Povarov reaction.

It is noteworthy that, this is the first time that this pyridylaldimines **3** are used in the Povarov reaction with acetylenes to reach 1,5-naphthyridines **19**.

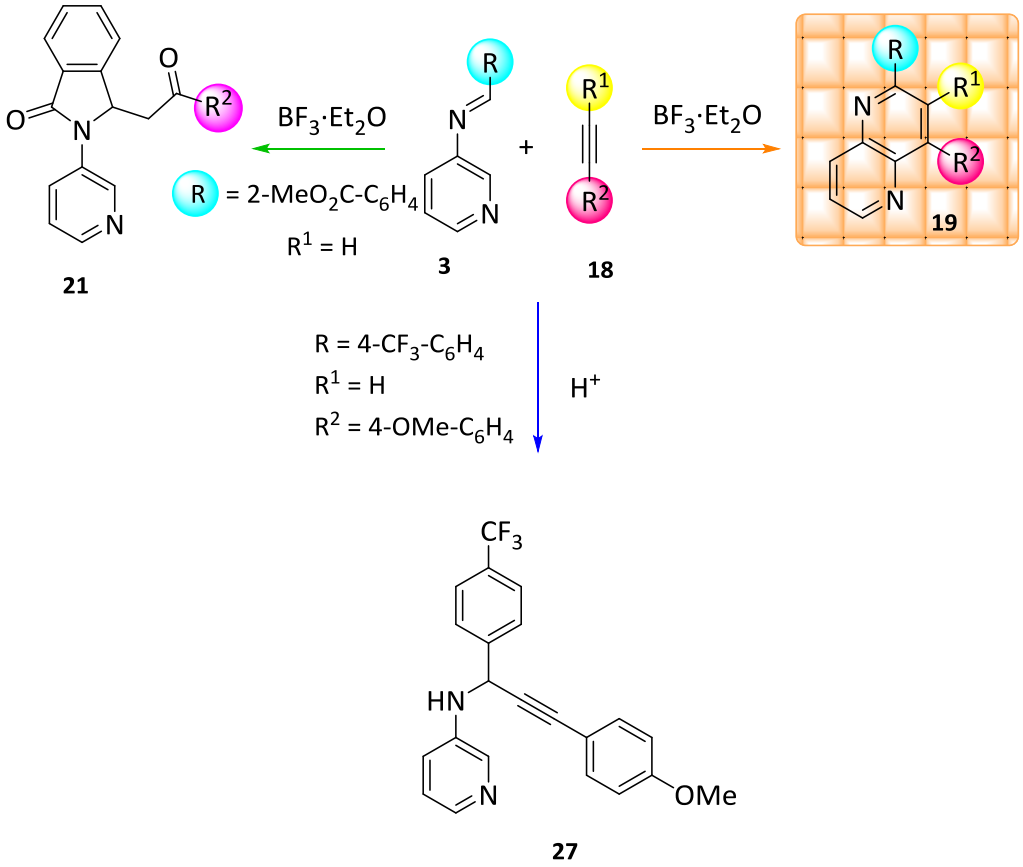

Scheme 19. Summary of the synthesized derivatives.

Note:

Compounds, figures and schemes numeration in the next chapter will start with number 1.

Chapter 3

Biological evaluation of the newly synthesized derivatives

3.1. Topoisomerase I inhibitory activity of the newly synthesized derivatives

DNA topoisomerases are DNA modifying enzymes involved in removing the DNA topological problems which occur during replication, transcription, and recombination of DNA in cells.[21,23] Topoisomerase I accomplishes this task by breaking one strand of the DNA double helix so as to release the stress.

Beside its biological role, human DNA Topoisomerase I (TopI) is also the sole cellular target of a family of anticancer compounds namely camptothecins (CPTs). It must be reminded that CPT (Figure 1)[32] stabilizes the covalent TopI-DNA complex through inhibition of the religation step in the TopI catalytic mechanism.[177]

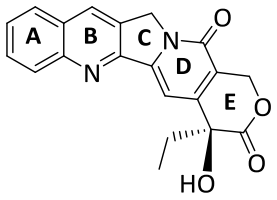

Figure 1. CPT structure.

Supercoiled DNA has a different electrophoretic mobility than DNA that is completely relaxed.[178] DNA plasmid isolated from *E. coli* is negatively supercoiled and can be used to assay TopI activity. TopI is capable of relaxing supercoiled DNA thus; based on this ability it is possible to evaluate its activity. TopI from eukaryotic cells is an ATP independent enzyme, and it does not require any divalent cation (e.g., Mg^{2+}) for activity, however, Mg^{2+} stimulates activity 3- to 5 fold.[178] In order to evaluate the behavior of the previously synthesized derivatives as TopI inhibitors, the time

[177] Porter, S. E.; Champoux, J. J. *Nucleic Acids Res*. **1989**, *21*, 8521-8532.
[178] Nitiss, J. L.; Soans, E.; Rogojina, A.; Seth, A.; Mishina, M. *Curr. Protoc. Pharmacol.* ***2012****, 3,* 1-34.

dependent inhibition (15s, 50s and 3 min for and DMSO and 15s, 40s, 1 min and 3 min for CPT and the synthesized derivatives) of TopI relaxation activity will be investigated and resolved by electrophoresis on agarose gel. CPT has been chosen as positive control for all the experiments meaning that the inhibition ability and cytotoxic effect of the 1,5-naphthyridine derivatives will be always compared to CPT.

The result of the relaxation experiment with the supercoiled DNA (pUC18, lane 8), DMSO (lanes 1-3) and CPT (lanes 4-7) is shown in figure 2. The upper bands of the gel correspond to the relaxed DNA, in the middle part of the gel we can observe different bands representing molecules of DNA plasmid having different mobility due to their different linking number[179] and called topoisomers whereas the lower bands correspond to the supercoiled DNA (not relaxed).

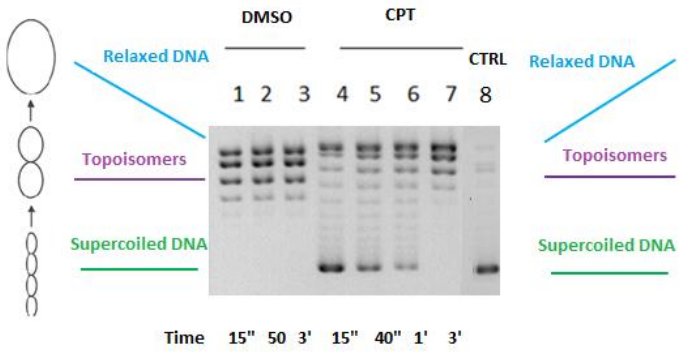

Figure 2. Relaxation experiment with DMSO and CPT**.**

When performing the relaxation with DMSO (the solvent of CPT and all tested compounds) known not to be inhibitor of TopI (Figure 2, lanes 1-3), we are not able to see lower bands corresponding to supercoiled DNA meaning that topoisomerase I is fully active in these experimental conditions. However, when using CPT (Figure 2, lanes 4-7), the natural inhibitor, bands corresponding to the supercoiled DNA are observed because

[179] Levene, S. D. *Methods Mol. Biol*. **2009**, *582*, 27-37.

CPT inhibits TopI role. Lane 8 corresponds to the negative supercoiled DNA control (pUC18), consequently DNA alone runs as a single band, the supercoiled band.

We synthesized different families of 1,5-naphthyridine derivatives which are going to be evaluated as potential TopI inhibitors. These families are named 1,5-indenonaphthyridine derivatives **9**, **10**, **16** and **17** (Figure 3), lactams **14** and **15** and 1,5-naphthyridines **19**. In this chapter, the biological activity of 1,5- indenonaphthyridines **9**, **10**, **16** and **17** and lactams **14** and **15** results will be discussed together and separately from 1,5-naphthyridines **19**.

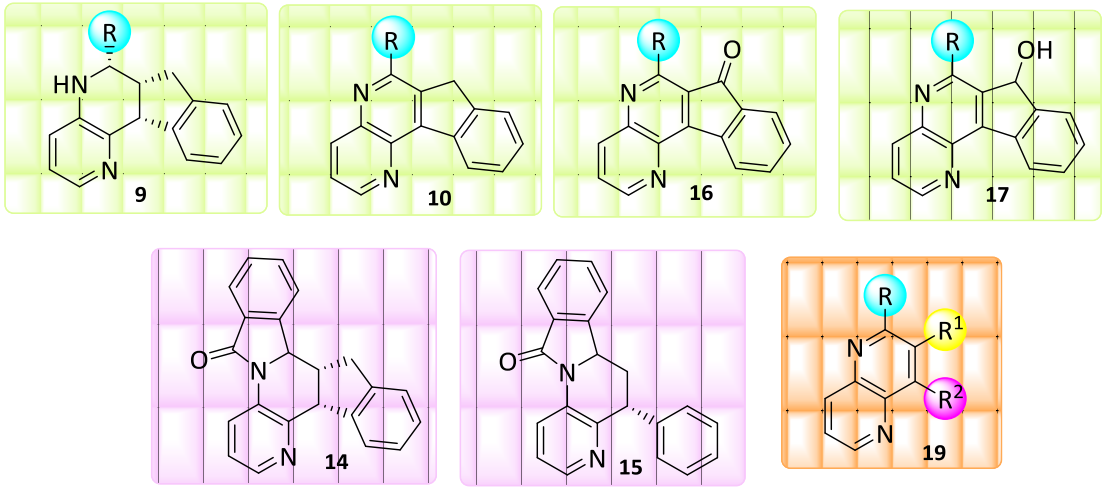

Figure 3. Synthesized 1,5-naphthyridine derivatives.

3.1.1. Inhibition of Topoisomerase I relaxation activity of indeno-1,5-naphthyridine derivatives 9, 10, 16 and 17 and lactams 14 and 15

First of all, we carried out a dose-dependent relaxation experiment so as to explore the effect of the concentration on the inhibition (Figure 4) and for these purpose, we performed the relaxation experiments with CPT and compound **16c** at different concentrations and at a fixed time point, 3 minutes. In this case, we added a sample with DNA and TopI (Pos, Figure 4, lane 2), in order to check TopI activity. In this way, we can conclude that both CPT and **16c** exhibit a dose-dependent inhibition. For CPT, the strongest inhibition is observed at 80 µM (lane 7) whereas for **16c** the strongest inhibition is at 120 µM (lane 13). Moreover, in CPT results (lanes 4-8) seems that there is a fall in inhibition at 120 µM, this could be due to precipitation of CPT at high concentrations since it has been previously reported that CPT solubility is one of the main drawbacks of this inhibitor. Based on these results we have decided to use 80 µM concentration for the following experiments.

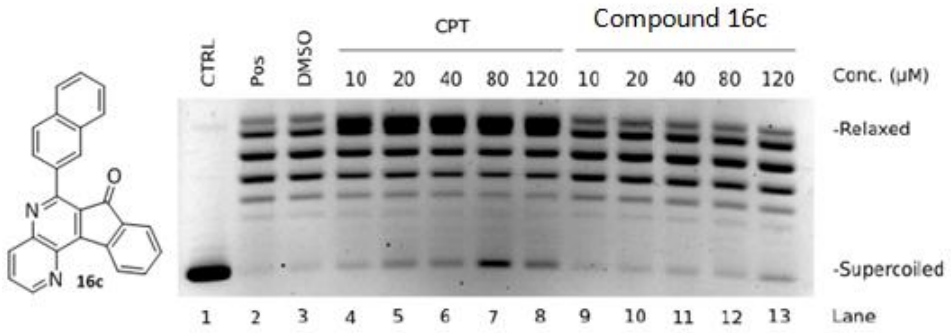

Figure 4. Dose-dependent relaxation with **16c**.

An additional experiment was performed with the indenonaphthyridinone **16c** at 80 µM and longer reaction times (0.5-60 min) to see the effect of the inhibition along

the time (Figure 5). Samples were incubated at 37°C, without a previous preincubation, at a maximum of 60 min. From this experiment we can conclude that, **16c** (lanes 17-24) is an inhibitor but the inhibition decreases with the time faster than in the case of CPT (lanes 9-16).

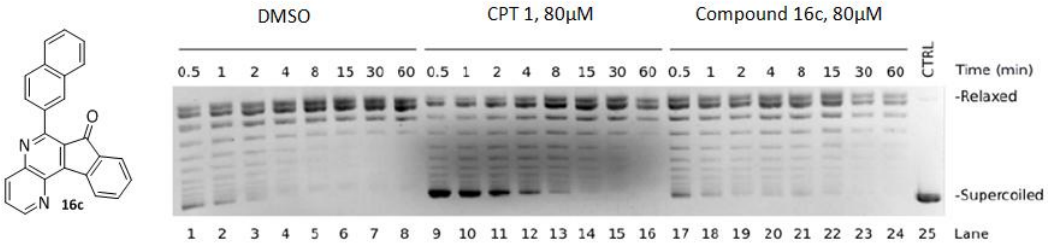

Figure 5.

Once the compound concentration was fixed, the next relaxation experiments are based on kinetics experiments in which we observe the evolution of the inhibition along the time in different reaction conditions. We first evaluated tetrahydro-7*H*-indeno[2,1-*c*][1,5]-naphthyridine derivatives **9** as possible TopI inhibitors at 80 µM.

The activity of the compounds will be evaluated in three different reaction conditions in each gel. First, we are going to perform relaxation experiments without any preincubation between DNA or TopI with the compounds, second by preincubating compounds with DNA and third by preincubating TopI with the compounds (Figure 6). Preincubations are carried out during 15 min at 37°C. When preincubating with the plasmid (pUC18), the reaction between pUC18 and compounds will be initiated by addition of TopI and incubated at 37°C at the selected time points (0.25, 0.7, 1 and 3 min). In the case of preincubating compounds with TopI, the reactions will be initiated by addition of the plasmid (pUC18) after 15 minutes and incubated at 37°C at the selected time points (0.25, 0.7, 1 and 3 min). In addition, a sample without TopI and with the plasmid was included as negative control (CTRL).

It should be noted that preincubation of CPT with either DNA or TopI does not affect the inhibition with this compound. [180]

In figure 6, the inhibitory effect of DMSO (lanes 1-3), CPT (lanes 4-7) and compound **9f** (lanes 8-19) is shown (Table 1, entry 7). The preincubation of the enzyme with compound **9f** (lanes 16-19) enhances the inhibition of TopI (compare lanes 16-19 with lanes 8-11) being stronger than in the case of CPT (compare lanes 16-19 with lanes 4-7). The preincubation of the compound **9f** with the DNA (lanes 12-15) does not have any effect in terms of inhibition. These results indicate that **9f** inhibits topoisomerase I activity in the relaxation process.

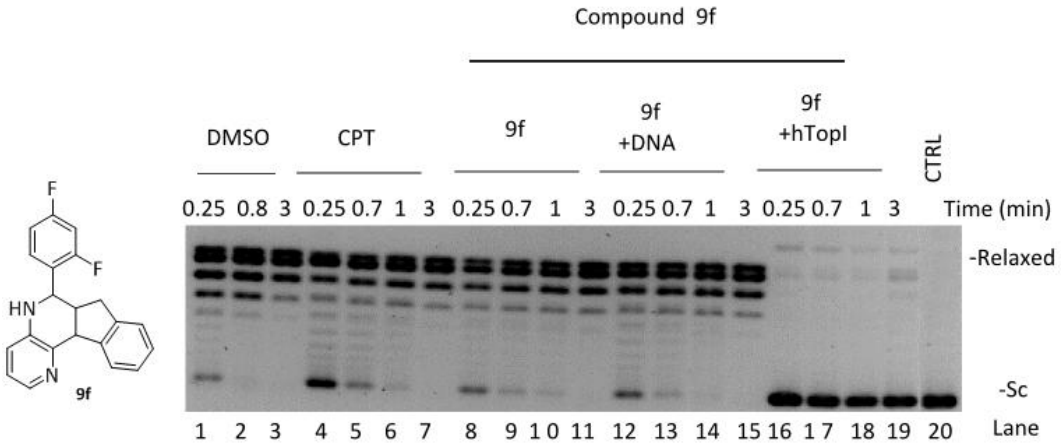

Figure 6

[180] Pommier, Y. *Nat. Rev. Cancer* **2006**, *6*, 789-802.

Table 1. Inhibitory effect of derivatives **9** towards TopI.

Entry	Compound	R	% Inhibition[a]			
			15 s	40 s	1 min	3 min
1	CPT		++	++	++	Θ
2	**9a**	Ph	+++	+++	+++	+++
3	**9b**	1-Naphthyl	+++	+++	+++	+++
4	**9c**	2-Naphthyl	+++	+++	+++	+++
7	**9d**	4-NO_2-C_6H_4	+++	+++	+++	+++
8	**9e**	4-Pyridyl	+++	+++	+++	+++
5	**9f**	2,4-F_2-C_6H_3	+++	+++	+++	+++
6	**9g**	3,4-F_2-C_6H_3	+++	+++	+++	+++

[a] TopI inhibitory activity was expressed semiquantitatively as follows: Θ, no activity; +, weaker activity than CPT; ++ similar activity to CPT; +++ stronger activity than CPT.

The same experiments were carried out with all the tetrahydro-7*H*-indeno[2,1-*c*][1,5]-naphthyridines **9** so as to check if these derivatives behave as TopI inhibitors or not (Table 1, experimental section). In all cases, CPT was used as positive control and the results obtained for the synthesized compounds were compared to this inhibitor.

In a similar way compounds **10** were evaluated (Table 2 and experimental section). Thereby, in figure 7 the relaxation experiment with the dehydrogenated derivatives **10e** (lanes 7-15) and **10c** (lanes 16-24) are shown. In both cases, it is clear that the preincubation of the compounds **10e** (Table 2, entry 6) and **10c** (Table 2, entry 4) with the enzyme (lanes 13-15 and lanes 22-24) potentiates the inhibitory effect (compare lanes 13-15 and 22-24 with 7-12 and 16-21, respectively). Moreover, the inhibiton in these cases is stronger than in the case of CPT (compare lanes 13-15 and 22-24 with lanes 4-6) and the inhibitory pattern in the different reaction conditions is completely different. Thus, when preincubating with the enzyme it is not possible to observe topoisomers in the middle part of the gel and in the case of preincubating with

the plasmid it is possible to see the different topoisomers formed in the topoisomerization reaction. We can conclude that, in general when preincubating with the enzyme, full inhibition of the enzyme is observed in contrast to CPT that has a reversible inhibition mechanism.[181] Therefore, compounds **10e** and **10c** are TopI inhibitors and the inhibition is persistent even at 3 minutes of incubation (compares lanes 15 and 24 with lane 6).

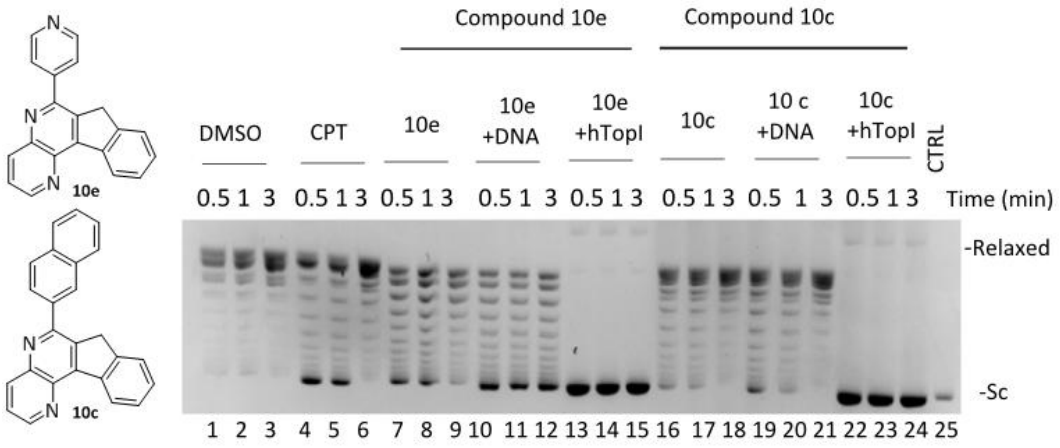

Figure 7.

The inhibitory activity of compounds **10** is displayed in table 2.

[181] Hertzberg, R. P.; Caranfa, M. J.; Hecht, S. M. *Biochemistry* **1989**, *28*, 4629-4638.NO exsite antes

Table 2. Inhibitory effect of derivatives **10** towards TopI.

Entry	Compound	R	% Inhibition[a]			
			15 s	40 s	1 min	3 min
1	CPT		++	++	++	Θ
2	**10a**	Ph	+++	+++	+++	+++
3	**10b**	1-Naphthyl	+++	+++	+++	+++
4	**10c**	2-Naphthyl	+++	+++	+++	+++
5	**10d**	4-NO_2-C_6H_4	+++	+++	+++	+++
6	**10e**	4-Pyridyl	+++	+++	+++	+++
7	**10f**	2,4-F_2-C_6H_3	+++	+++	+++	+++
8	**10g**	3,4-F_2-C_6H_3	+++	+++	+++	+++

[a] TopI inhibitory activity was expressed semiquantitatively as follows: Θ, no activity; +, weaker activity than CPT; ++ similar activity to CPT; +++ stronger activity than CPT.

The inhibitory effect of the two synthesized lactams **14** and **15** (Figure 8) was evaluated in the same reaction conditions as for the indenonaphthyridine derivatives **9** and **10** previously described.

On one hand, the lactam **14** that has the indene moiety presents the same inhibition pattern that the indenonaphthyridine derivatives **9** and **10**. The inhibition in this case is potentiated by preincubation of the compound and the enzyme (compare lanes 13-15 with lanes 7-12). On the other hand, in the lactam with the phenyl moiety **15** there is not any effect neither preincubating with the enzyme (lanes 22-24) nor with the supercoiled plasmid (lanes 19-21). In fact, the inhibitory effect of **15** comparing with CPT is weaker (compare lanes 16-24 with lanes 4-6). The results for these compounds are very interesting since we can observe a different behavior for **14** and **15** (Table 3 entries 2 and 3).

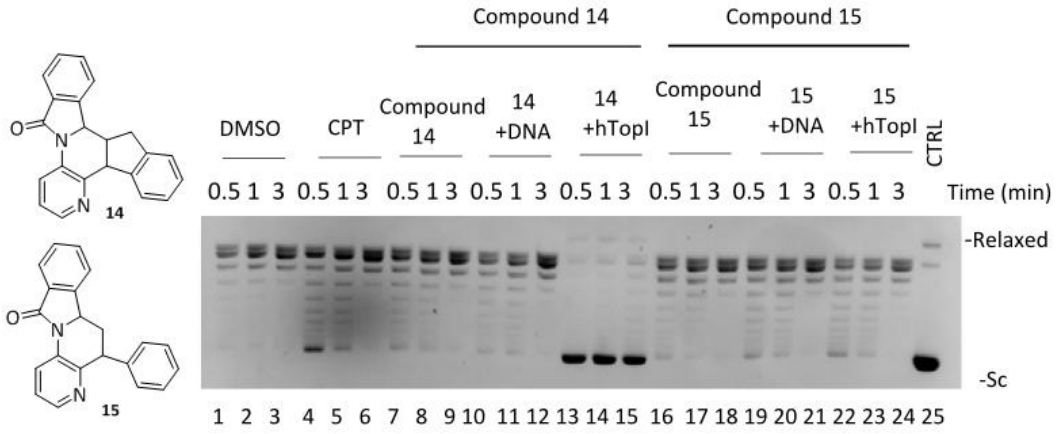

Figure 8.

Looking at the behavior of the carbonyl derivatives **16**, we found similar results as for the previous derivatives (Table 3, entries 4-7, and experimental section). When indenonaphthyridinones **16** were preincubated with TopI during 15 minutes the inhibition of the enzyme was complete. As an example of the inhibitory effect of these derivatives **16**, indenonaphthyridinone **16c** behavior is shown in figure 9. Complete inhibition in TopI activity is achieved when preincubating **16c** (Table 3, entry 5) with the enzyme (lanes 13-15). In such this way, the inhibition when preincubating **16c** and DNA (lanes 10-12) seems to be more stable along the time than that of CPT (compare lanes 4-6 with 10-12).

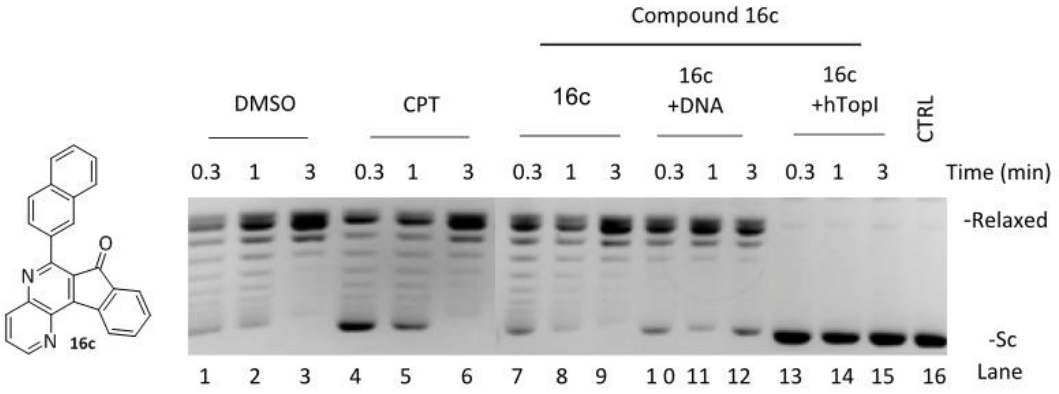

Figure 9.

Table 3. Inhibitory effect of derivatives **14**, **15**, **16** and **17** towards TopI.

Entry	Compound	R	% Inhibition[a]			
			15 s	40 s	1 min	3 min
1	CPT		++	++	++	Θ
2	**14**	---	+++	+++	+++	+++
3	**15**	---		+	+	Θ
4	**16a**	Ph	+++	+++	+++	+++
5	**16c**	2-Naphthyl	+++	+++	+++	+++
6	**16f**	2,4-F_2-C_6H_3	+++	+++	+++	+++
7	**17a**	Ph	++	++	++	++
8	**17c**	2-Naphthyl	+++	+++	+++	+++

[a] TopI inhibitory activity was expressed semiquantitatively as follows: Θ, no activity; +, weaker activity than CPT; ++ similar activity to CPT; +++ stronger activity than CPT.

Finally, the hydroxyl derivative **17c** inhibitory effect was evaluated (Figure 10, Table 3 entry 8, experimental section). Again, when preincubating compound **17c** with

the enzyme for 15 minutes, complete inhibition is observed (lanes 16-19) stronger than in the case of CPT (lanes 4-7). The preincubation with the plasmid (lanes 12-15) instead of with the enzyme has no effect and the inhibition is weaker than in the case of CPT (Table 3, entry 8, experimental section)

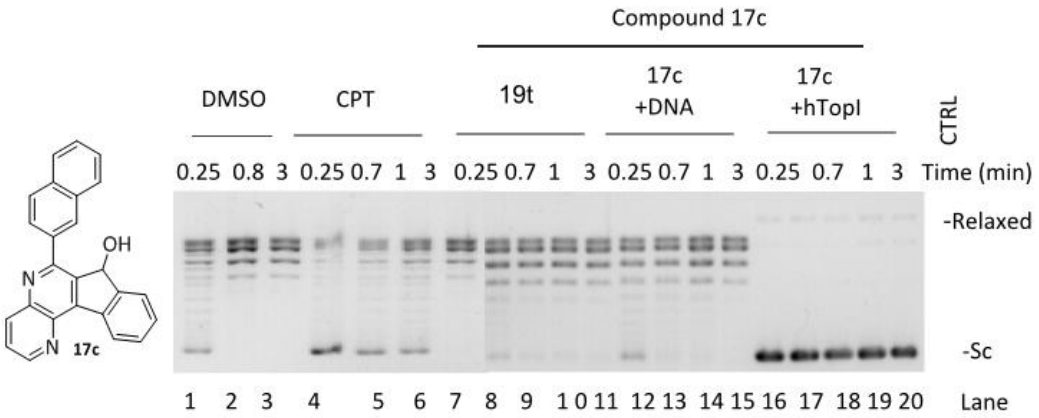

Figure 10.

To sum up, the 1,5-indenonaphthyridine derivatives **9** including the dehydrogenated forms **10**, the carbonyl derivatives **16** and hydroxyl derivatives **17** (See experimental section) act as Topoisomerase I inhibitors and their effect is stronger when preincubating compounds with the enzyme during 15 minutes prior to the addition of the plasmid. This behavior reflects some kind of interaction between the enzyme and the compound that blocks the relaxation process.

Despite the fact that we have only shown some relaxation examples the experiments were done for all the synthesized indenonaphthyridine derivatives (**9**, **10**, **14**, **15**, **16** and **17**, Tables 1-3). The reaction conditions for all the experiments were fixed preincubating the compounds with the enzyme since the strongest inhibitory effect was obtained in this situation.

Therefore, we can conclude that all the synthesized indenonaphthyridine derivatives **9**, **10**, **14**, **16** and **17** (Figure 3) are topoisomerase I inhibitors. Furthermore, we demonstrated that when we preincubated the compounds with the enzyme for 15 minutes the inhibitory effect is stronger than in the case of CPT. These results indicate that these compounds interact with the enzyme and make it incapable of relaxing supercoiled plasmid DNA. Therefore, this mechanism of action seems to be different to the mechanism by which CPT inhibits TopI activity.

3.1.2. Topoisomerase I mechanism studies with derivative 16c

It was described in the first chapter (Figure 8) that relaxation of supercoiled DNA by TopI is divided in different stages: 1) non-covalent binding between DNA and TopI; 2) cleavage and formation of the covalent complex TopI-DNA; 3) supercoiled DNA relaxation through a controlled strand rotation; 4) religation of the nicked strand; 5) release of the relaxed substrate. In order to explain the mechanism of action[29] of the synthesized compounds, it is necessary to investigate the different stages in the catalytic cycle separately.

It is known that the most interesting inhibitors from a clinical point of view are those that inhibit the religation step and thus cause cell death. These kinds of religation inhibitors are called poisons.[32] Compounds that inhibit the cleavage step are termed as inhibitors.

During my internship at Aarhus University in the group of Prof. Birgitta Knudsen (Department of Molecular Biology and Genetics), we investigated cleavage and religation steps separately. For this purpose, we use a suicide DNA substrate (Figure 11).

This substrate consists of two synthetic DNA strands (AS88 and AS90). AS88 represents the cleavable strand and AS90 represents the non-cleavable strand. Prior to hybridization, AS88 was 5'-^{32}P-radiolabelled (pink star, Figure 11) and AS90 was phosphorylated with unlabeled ATP at the 5'end in order to prevent ligation of the 5'OH. The non-cleavable strand (AS90) contains a highly preferred TopI cleavage site (small arrow, Figure 11).

In solution two suicide substrates will dimerize due to a palindromic sequence on the protruding single stranded DNA end of the substrate generating regions of double stranded DNA on both sites of the hTopI cleavage site. TopI is then able to bind and cleave at one of the cleavage sites. Upon cleavage, TopI will remain covalently attached to the 3'-end of the cleaved strand (cleavage) and the 3 nucleotide fragment (light blue, Figure 11) containing the 5'-OH generated by cleavage will diffuse preventing religation of the single stranded end.

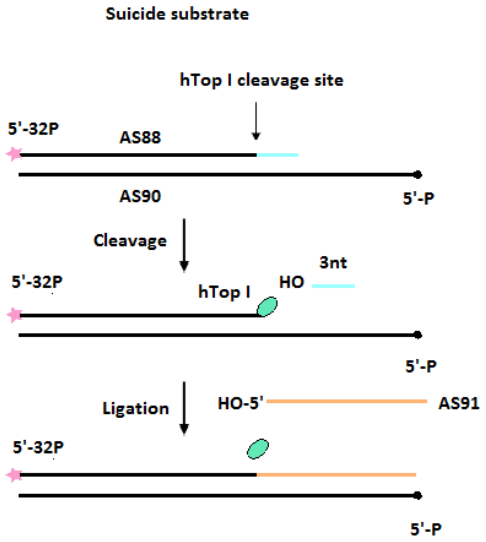

Figure 11. Suicide substrate for detection of cleavage and ligation by TopI.

Cleavage experiments were made with DMSO, TopI and **16c** derivative (Figure 12). Lanes 1-3 show the cleavage in the presence of DMSO, lane 4 is the suicide substrate alone (control), and lanes 5-7 show the cleavage reaction with **16c**. Samples were analyzed in a 12 % denaturing polyacrilamide gel and radiolabelled DNA was visualized via PhosphorImaging. The intensities of the bands are similar to that of the DMSO ones indicating that the cleavage step is not inhibited by the compound **16c**.

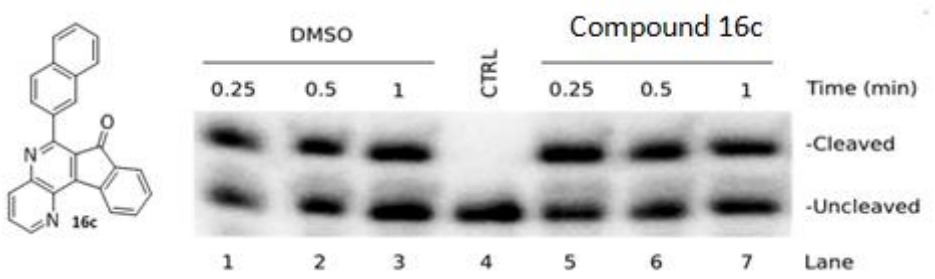

Figure 12. Cleavage activities of TopI by **16c**.

The intensities of the bands were measured using the QuantityOne software from Bio-Rad and the degree of cleavage was calculated as the ratio between cleaved and uncleaved substrate. The results were normalize to 100% cleavage for the reaction performed in the presence of DMSO after 1 minute of incubation and these results are outlined in figure 13. The results are plotted as the average of three experiments and error bars indicate standard deviations.

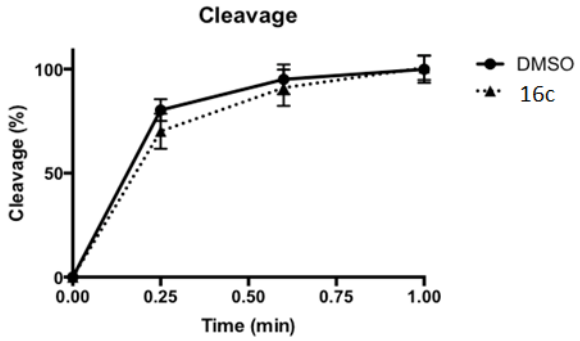

Figure 13. Cleavage result by **16c**.

Both figures, the gel (Figure 12) and the graph (Figure 13) showed that indenonaphthyridinone **16c** does not inhibit the cleavage step of TopI catalytic cycle.

These results may indicate that **16c** is a religation inhibitor as CPT.[182] Consequently, the next step was to explore if **16c** inhibits the religation step. For the evaluation of the religation step it was necessary to generate the active cleavage complex (TopI-DNA-compound). The religation reaction was initiated by addition of the ligator strand (AS91, Figure 11) in molar excess and incubated for increasing time periods as indicated in figure 14. CPT was used as positive control of religation. Samples were analyzed in a 12 % denaturing polyacrilamide gel as previously described for cleavage experiment. The shape of the religation activity gel of **16c** is outlined in figure 14. Lane 1: time =0, lanes 2-4 show the religation in the presence of DMSO, lanes 5-7 religation in the presence of 80μM CPT, lanes 8-10 religation in the presence of 80μM **16c**.

[182] Porter, S.E.; Champoux. J. J. *Nucleic Acids Res*. **1989**, *17*, 8521-8532.

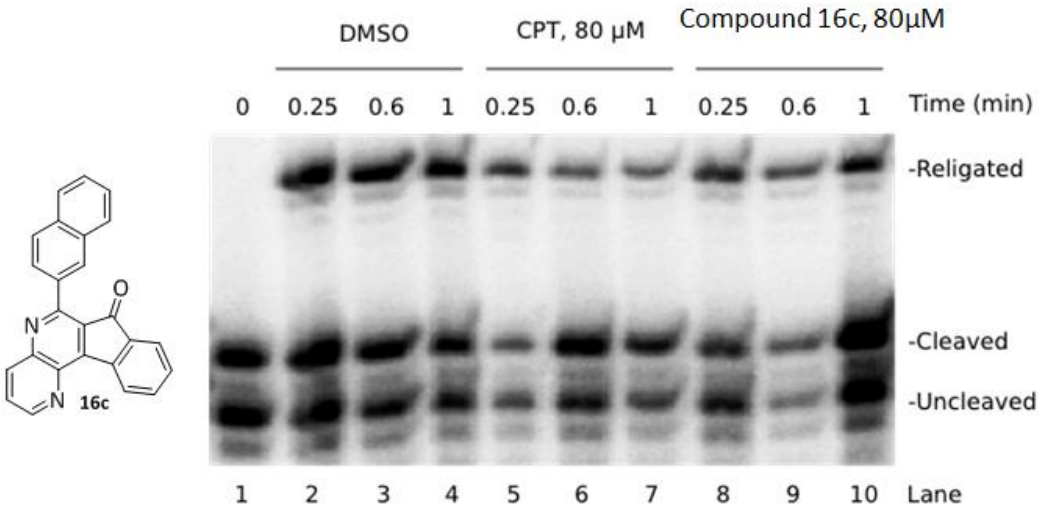

Figure 14. Religation activity of TopI in the presence of **16c** derivative.

The results were normalized to 100 % religation for the reaction carried out in the presence of DMSO after 1 min of incubation. Results are represented as the average of religation percentage with standard deviation of 5 experiments (Figure 15).

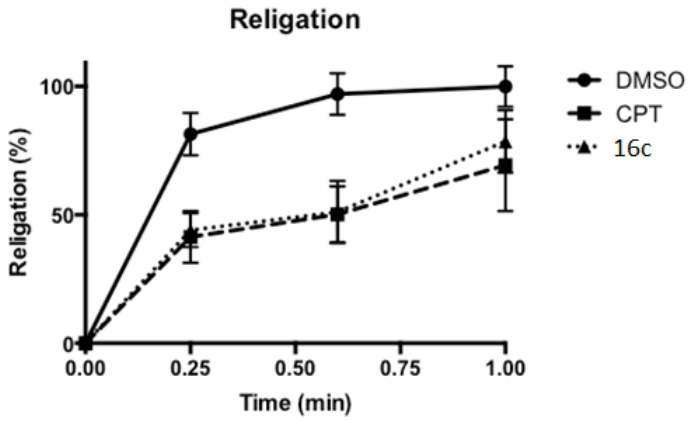

Figure 15.

The inhibitory capacity of **16c** (lanes 8-10) is comparable to the capacity of CPT as evident from graph in figure 15. With these experiments we showed that **16c** derivative inhibits the religation of TopI (Figure 14) in the same way as CPT (lanes 5-7) does compared to DMSO (lanes 2-4).

At this point it seems that **16c** is a novel TopI targeting compound that inhibits the religation step but it does not inhibit cleavage. In this way, this derivative could be able to generate stabilized TopI cleavage complex as CPT does but these results are in contrast with the relaxation results in which **16c** has a strong inhibition when preincubating with the enzyme. So it is possible that we are facing a compound with different mechanism of action to that of CPT.

In order to investigate whether **16c** generates stabilized cleavage complexes *in vitro* a nicking assay was performed. This assay takes advantage of the fact that a nicked open plasmid has a slower migration in agarose gel electrophoresis with ethidium bromide compared to an intact plasmid, which will appear positively supercoiled due to intercalation with ethidium bromide. CPT stabilizes the cleavage complexes generated by hTopI leading to an increase in nicked plasmid DNA.

Nicking experiment was performed using negatively supercoiled pUC18 plasmid DNA in the presence of 80 μM CPT and **16c** derivative at 80 μM (Figure 16). It can be observed that in the presence of CPT (lanes 7-11) nicked plasmid DNA is generated in *vitro* as a consequence of stabilization of cleavage complexes. It is not possible, however, to see any nicked band upon incubation with **16c** (see lanes 12-16).

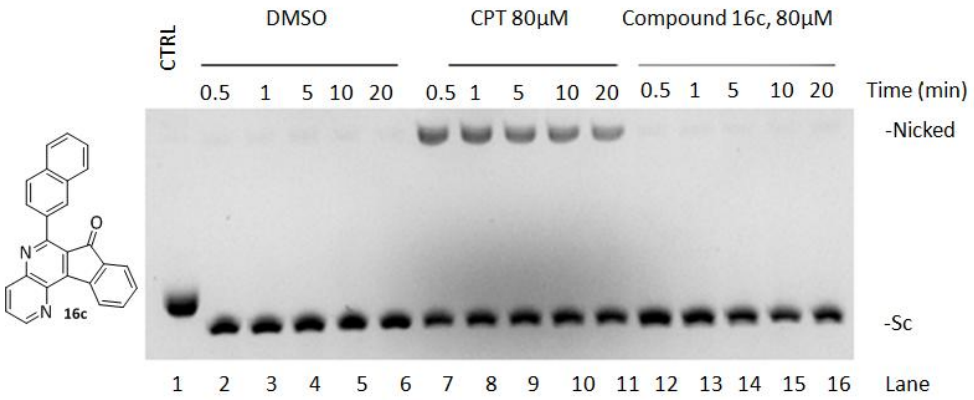

Figure 16.

Although **16c** derivative is unable to generate detectable stabilized cleavage complexes using the nicking assay, it might still be possible that the compound is able to generate double strand breaks (DSBs) *in vivo*. Although big efforts were made to investigate the generation of DSBs in $CaCo_2$ (colorectal cancer) and HeLa (cervical cancer), results were not conclusive.

In conclusion, from a mechanistic point of view, the experimental results show that derivative **16c** does not inhibit cleavage step of the TopI catalytic cycle but it inhibits the religation step pointing to a CPT-like mechanism of action where stabilized cleavage complexes are generated. However, apparently this is not the case because the nicking experiment reflects that **16c** is not able to generate stabilized Topoisomerase I cleavage complexes *in vitro.* DSB experiments were not conclusive.

3.1.3. Inhibition of Topoisomerase I relaxation activity of 1,5-naphthyridine derivatives 19

As it has been previously explained, we have also synthesized 1,5-naphthyridine derivatives **19** (Figure 17). These derivatives present quite a planar structure and in this sense we thought that 1,5-naphthyridine could act as topoisomerase I inhibitors. Likewise, in the same way that we performed the relaxation experiments for the indenonaphthyridines **9**, **10**, **16** and **17**, we evaluated TopI activity. Relaxation experiments for these derivatives **19** were carried out at 80 μM.

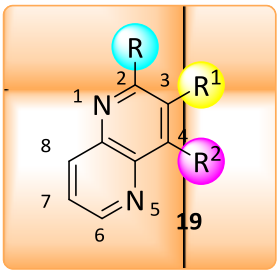

Figure 17. 1,5-naphthyridine derivatives **19**.

In this manner, the inhibitory effect of compound **19n** (lanes 7-15) and **19r** (lanes 16-24) is shown in figure 18. Derivative **19n** (Table 4, entry 15) with an electron-donating group, has a similar inhibitory effect than CPT (compare lanes 10-15 with lanes 4-6). However, derivative **19r** (Table 4, entry 19) with an electron-withdrawing group, when preincubating with the DNA (lanes 19-21) or the enzyme (22-24) presents a stronger inhibitory effect comparing to CPT (compare lanes 19-24 with lanes 4-6).

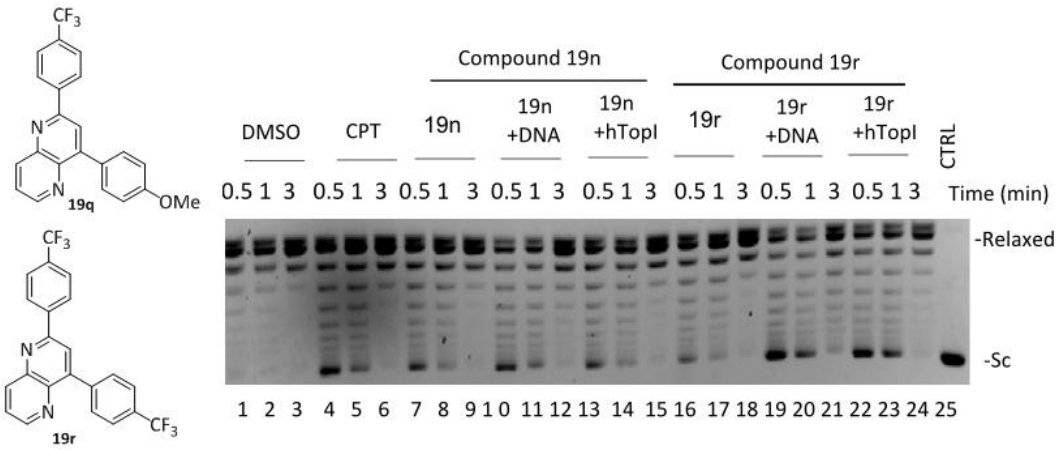

Figure 18.

It can be deduced from the relaxation experiments that this family of compounds show a different behavior comparing with indenonaphthyridine derivatives **9**, **10**, **16** and **17**. In this case, for 1,5-naphthyridines **19n** and **19r**, there is not a strong effect neither when preincubating with the enzyme nor with the supercoiled plasmid. Apparently, this relaxation pattern is more in agreement with the possibility of this compound to act as a poison and not as an inhibitor.

Regarding the inhibitory effect of derivative **19t** (Figure 19, lanes 8-19, Table 4, entry 21) containing an heteroaromatic group, the preincubation of **19t** with the enzyme during 15 minutes (lanes 16-19) enhances the inhibitory effect towards the preincubation with DNA (lanes 12-15) or without preincubation (lanes 8-11).

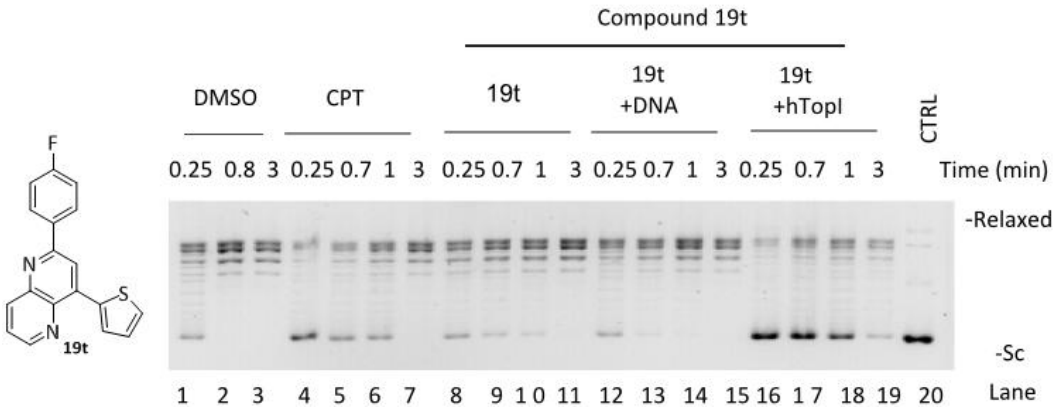

Figure 19.

Similarly, the relaxation experiment (Figure 20, lanes 8-11) for compounds **19p**, **19f** (lanes 12-15, Table 4, entries 17 and 7) and **19q** (lanes 16-19, Table 4, entry 18) were performed preincubating compounds with the enzyme for 15 min. The results suggest that the *metha* substitution of the aromatic ring in the position 2 of the naphthyridine **19f** (lanes 12-15) and **19q** (lanes 16-19) have a positive effect in terms of inhibition. On the other hand, the *para* substitution present in compound **19p** derivative has a similar effect to that CPT (compare lanes 4-7 with lanes 8-11).

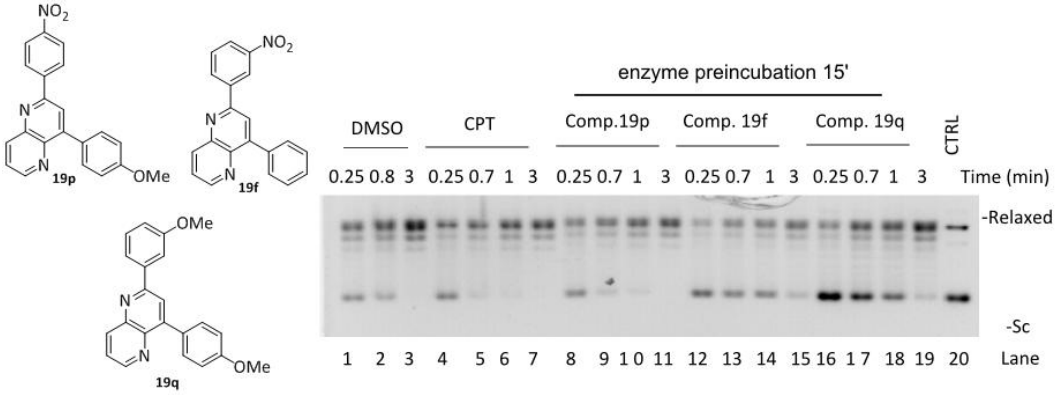

Figure 20.

Particularly interesting results are observed for the derivatives that bear a biphenyl group in its structure **19h-19l** (Table 4, entries 8-12). Thus, for compound **19i** (Figure 21) a very strong inhibitory effect can be observed in all cases, when preincubating compounds with DNA (lanes 12-15), when preincubating with the enzyme (lanes 16-16) and also without preincubation (lanes 8-11).

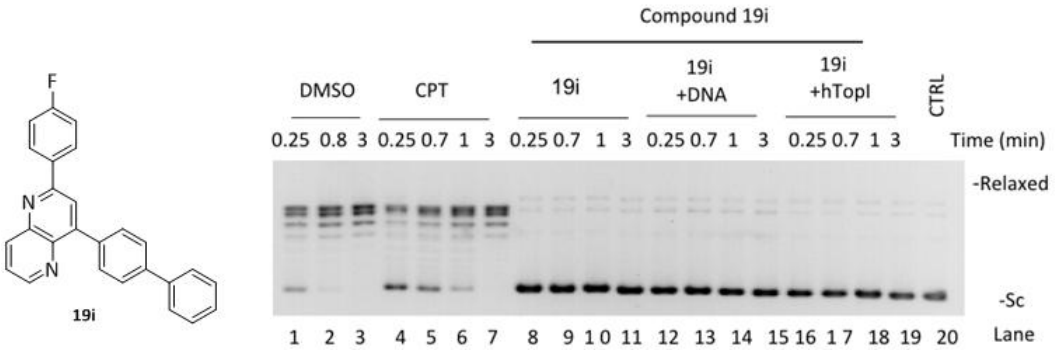

Figure 21.

In this section just some representative examples are shown. Nevertheless, the inhibitory effect of all the synthesized derivatives **19** was studied. These results are summarized in table 4.

Table 4. Inhibitory effect of derivatives **19** towards TopI.

Entry	Comp.	R	R^1	R^2	% Inhibition[a]			
					15 s	40 s	1 min	3 min
1			CPT		++	++	++	Θ
2	**19a**	Ph	H	Ph	++	+	+	Θ
3	**19b**	3,4-F_2-C_6H_3	H	Ph	++	NT	+	Θ
4	**19c**	4-CF_3-C_6H_4	H	Ph	+	NT	+	Θ
5	**19d**	4-F-C_6H_4	H	Ph	+++	NT	+	Θ
6	**19e**	4-NO_2-C_6H_4	H	Ph	++	++	++	+
7	**19f**	3-NO_2-C_6H_4	H	Ph	+++	+++	+++	+++
8	**19g**	3-OMe-C_6H_4	H	Ph	++	++	+	Θ
9	**19h**	4-CF_3-C_6H_4	H	C_6H_4Ph	+++	+++	+++	+++
10	**19i**	4-F-C_6H_4	H	C_6H_4Ph	+++	+++	+++	+++
11	**19j**	4-NO_2-C_6H_4	H	C_6H_4Ph	+++	+++	+++	+++
12	**19k**	3-NO_2-C_6H_4	H	C_6H_4Ph	+++	+++	+++	+++
13	**19l**	3-OMe-C_6H_4	H	C_6H_4Ph	+++	+++	+++	+++
14	**19m**	4-F-C_6H_4	H	6-OMe-Naphthyl	++	++	+	Θ
15	**19n**	4-CF_3-C_6H_4	H	4-OMe-C_6H_4	++	NT	++	Θ
16	**19o**	4-F-C_6H_4	H	4-OMeC_6H_4	++	++	++	+
17	**19p**	4-NO_2-C_6H_4	H	4-OMeC_6H_4	++	++	+	Θ
18	**19q**	3-OMe-C_6H_4	H	4-OMeC_6H_4	+++	+++	+++	+++
19	**19r**	4-CF_3-C_6H_4	H	4-CF_3-C_6H_4	+++	NT	++	+
20	**19s**	4-CF_3-C_6H_4	H	3-Thienyl	++	NT	+	Θ
21	**19t**	4-F-C_6H_4	H	3-Thienyl	++	++	++	Θ
22	**19u**	4-CF_3-C_6H_4	Me	Ph	++	NT	+	Θ

[a] TopI inhibitory activity was expressed semiquantitatively as follows: Θ, no activity; +, weaker activity than CPT; ++ similar activity to CPT; +++ stronger activity than CPT.

It can be observed that some of the derivatives show an inhibitory effect similar to that of CPT (Table 4, entries 1, 8, 14, 16, 17 and 21) when preincubating reaction mixture, TopI and compounds. Some naphthyridine derivatives **19** present a stronger inhibitory effect compared to CPT (Table 4, entries 7, 9, 10, 11, 12, 13 and 18) showing TopI full inhibition even at 3 minutes. This effect is shown when biphenyl group is present in the molecule (Table 4, entries 9-13), this fact could be that the lengthening of the molecule in this part could be an interesting challenge for further investigations.

On the basis of the results of the relaxation assays, we can conclude that all the tested compounds **19** were confirmed to inhibit TopI mediated DNA relaxation and in most of the cases in a stronger way than CPT (Table 4, entries 7, 9, 10, 11, 12, 13 and 18).

Therefore, not only indeno-1,5-naphthyridine derivatives **9**, **10**, **16** and **17** (Figure 3) but also 1,5-naphthyridine derivatives **19** act as topoisomerase I inhibitors as it can be deduced from the relaxation experiments. In terms of the inhibitory effect we observe different grades of inhibition depending on the different substituyents in the molecule. Some of the derivatives have a stronger effect in inhibiting topoisomerase I than CPT that is one of the reference inhibitors found in literature and which activity towards TopI is fully described. Moreover, in the same way that we have prepared two different families of compounds such as indeno-1,5-naphthyridines and 1,5-naphthyridines, in terms of TopI inhibition two different behaviors seems to be observed.

In addition, to the best of our knowledge there are no precedents of 1,5-naphthyridine derivatives that act as TopI inhibitors.

3.2. Cytotoxicity studies of the newly synthesized derivatives in different cancer cell lines

3.2.1. Cytotoxicity studies in cancer cell lines with indeno-1,5-naphthyridine derivatives 9, 10, 16 and 17 and lactams 14 and 15

The newly synthesized indeno-1,5-naphthyridine derivatives **9**, **10**, **16** and **17** were explored for antiproliferative activity against different human cancer cell lines: A549 (carcinomic human alveolar basal epithelial cell), BT20 (human breast cancer) and SKOV3 (human ovarian carcinoma).

Cell counting kit-8 (CCK-8) assay was employed to assess growth inhibition and cell proliferation inhibitory activities of all the synthesized compounds. CCK-8 allows sensitive colorimetric assays for the determination of cell viability in cell proliferation and cytotoxicity assays. A water-soluble tetrazolium salt **I**, is reduced by dehydrogenase activities in cells to give a yellow-color formazan dye **II**, which is soluble in the tissue culture media (Figure 22). The amount of the formazan dye, generated by the activities of dehydrogenases in cells, is directly proportional to the number of living cells.

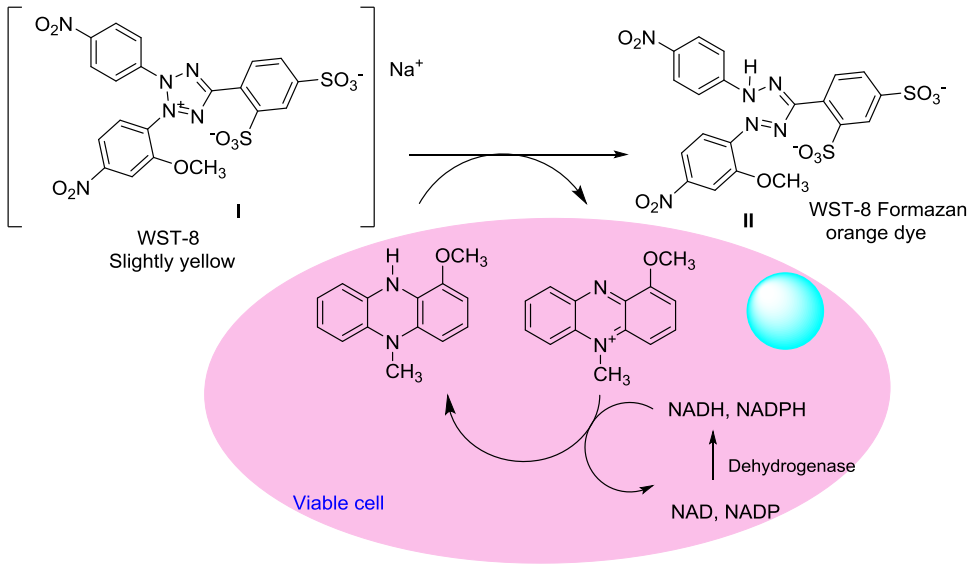

Figure 22. Cell viability detection mechanism with CCK-8

For these experiments an appropriate amount of cells are seeded in 96 well tissue plates. The following day cells were treated with the corresponding compounds at different concentrations (50, 30, 20, 10, 5, 2.5, 1 µM). Untreated cells were included in the assay. After 48h of compounds incubation, CCK-8 reagent was added (Figure 23, 1) and after 2h of incubation (Figure 23, 2), the absorbance was read by means of the optical density (O.D) at 450 nm (Figure 23, 3). The results were normalized to 100% survival for the untreated cells.

Figure 23. Cytotoxicity assay.

The cytotoxicity results are displayed in table 5 by means of IC_{50} values (µM)

Table 5. Antiproliferative activity of 1,5-indenonaphthyridines **9**, **10**,**14**, **15**, **16** and **17**.

Entry	Compound	R	Cytotoxicity IC_{50} (µM)[a]		
			breast BT20	lung A549	ovarian SKOV3
1	camptothecin		0.07±0.04	$(1.0±0.4)10^{-3}$	0.5±0.4
2	**9a**	Ph	>50	5.6±0.5	>50
3	**9b**	1-Naphthyl	>50	25.3±0.3	>50
4	**9c**	2-Naphthyl	>50	13.5±0.8	>50
5	**9d**	4-NO_2-C_6H_4	>50	10.5±0.3	>50
6	**9e**	4-Pyridyl	26.4±0.6	9.1±0.2	>50
7	**9f**	2,4-F_2-C_6H_3	>50	6.4±0.6	>50
8	**9g**	3,4-F2-C_6H_3	25.6±0.1	27.3±0.7	>50
9	**10a**	Ph	>50	>50	>50
10	**10b**	1-Naphthyl	>50	10.5±0.3	>50
11	**10c**	2-Naphthyl	>50	23.7±1.0	>50
12	**10d**	4-NO_2-C_6H_4	>50	5.7±0.6	>50
13	**10e**	4-Pyridyl	32.9±0.4	2.9±0.9	10.5±0.4
14	**10f**	2,4-F_2-C_6H_3	39.6±0.3	1.7±0.1	6.4±0.3
15	**10g**	3,4-F_2-C_6H_3	>50	18.6±0.5	>50
16	**14**	---	17.0±0.3	11.2±0.8	>50
17	**15**	---	>50	30.2±0.9	>50
18	**16a**	Ph	14.1±0.5	23.7±0.9	1.9±0.1
19	**16c**	2-Naphthyl	23.3±0.8	0.8±0.2	5.3±0.1
20	**16f**	2,4-F_2-C_6H_3	>50	34.1±0.9	>50
21	**17a**	Ph	>50	>50	>50
22	**17c**	2-Naphthyl	48.2±0.7	5.5±0.2	>50

[a] The cytotoxicity IC_{50} values listed are the concentrations corresponding to 50% growth inhibition. Each data represents mean ± S.D. from three different experiments performed in triplicate

It can be observed that the cytotoxicity values (Table 5) display a broad spectrum of antiproliferative activity against the cancer cell lines tested in culture. According to the data presented in table 5, we could come to the conclusion that from tetrahydro-indeno1,5-naphthyridines **9** the best cytotoxic result is found in lung cancer cell line (A549) for derivative **9f** (R= 2,4-$F_2C_6H_3$, Table 5, entry 7) containing two fluorine atoms in its structure with an IC_{50} of 6.4±0.6 µM. Furthermore, for the corresponding dehydrogenated compounds **10**, the fluorinated indeno[1,5]-naphthyridine derivative **10f** (R= 2,4-$F_2C_6H_3$, Table 5, entry 14) presents the highest cytotoxic effect, with an IC_{50} of 1.7±0.1 µM, against the A549 cell line *in vitro*, and a high cytotoxicity, with an IC_{50} of 6.4±0.3 µM against the SKOV3 cell line *in vitro*. On the other hand, indeno-1,5-naphthyridine derivative **10d** (R= 4-$NO_2C_6H_4$, Table 5, entry 12) and indeno-1,5-naphthyridine derivative **10e** (R= 4-pyridyl, Table 5, entry 13), showed high cytotoxicity against A549 cell line *in vitro*, with an IC_{50} of 5.7±0.6 and 2.9±0.9 µM, respectively. Regarding the derivatives with different structural modification as for example the carbonyl derivative **16c** (R= 2-Naphthyl, Table 5, entry 19) presents the better cytotoxic effect, with an IC_{50} of 0.8±0.02 µM towards lung cancer cell line. Moreover the corresponding hydroxyl derivative **17c** (R= 2-Naphthyl, Table 5, entry 22) shows an interesting IC_{50} of 5.5±0.02 µM in the same cell line tested *in vitro*.

Therefore, it is noticeable that lung cancer cell line is the most sensitive cell line towards the derivatives tested. All the compounds (Table 5, Figure 24) present better cytotoxic effect in lung cancer cell line whereas ovarian and breast cancer are not so sensitive to the synthesized derivatives.

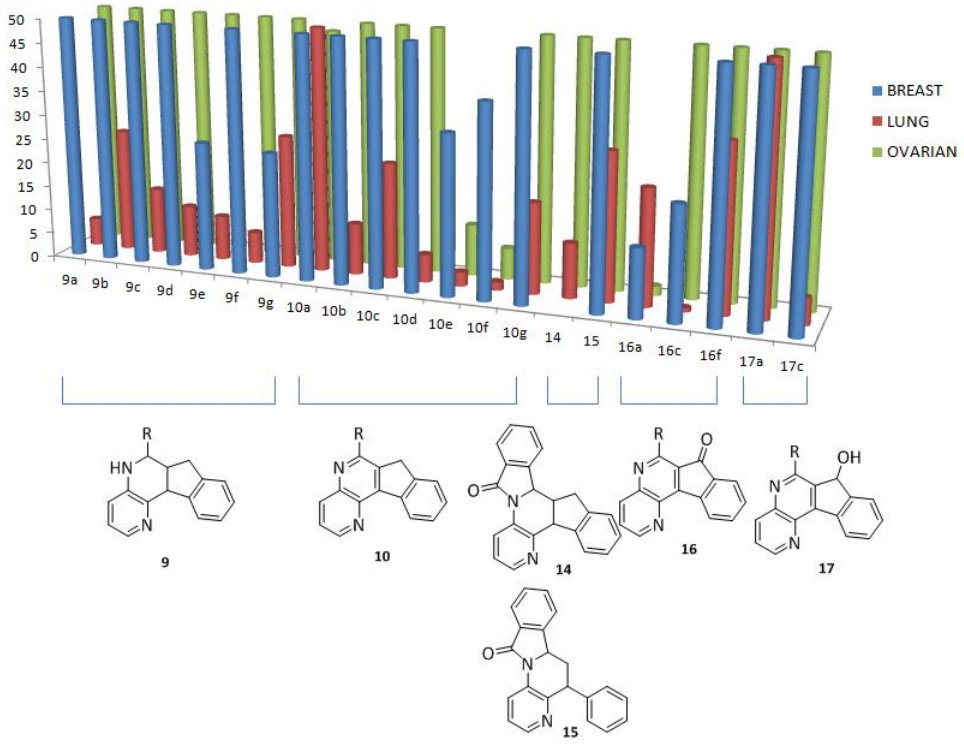

Figure 24. IC_{50} values comparison in the different three cancer cell lines.

Once that we found this sensitivity towards lung cancer cell lines we explored the cytotoxic effect of some of the synthesized derivatives in healthy lung cells, fibroblast lung cells (MRC 5). For this purpose, an appropriate amount of healthy lung cells was cultured in the corresponding culture media in multi well plates during 24 hours and then, some of the most cytotoxic compounds of each family were added at the IC_{50} concentration and double the IC_{50} concentration and then incubated for 48 hours. After this period of time, we took some photographs under the microscope. In all cases culture cells were compared to the control which are cells grown without the addition of any compound. For instance, the tetrahydroindenonaphthyridine **9f**, it clearly kills lung

cancer cells (A549, Figure 25, A) and at double the IC_{50} concentration there are almost none cells alive. Nevertheless, the addition of the same compound **9f** to normal lung cells (MRC 5) seems not to present any effect (Figure 25, B).

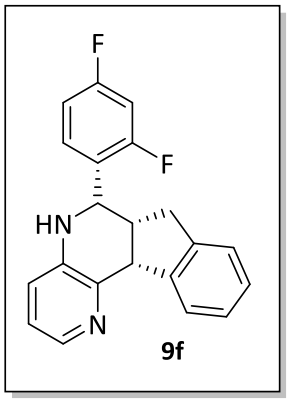

9f

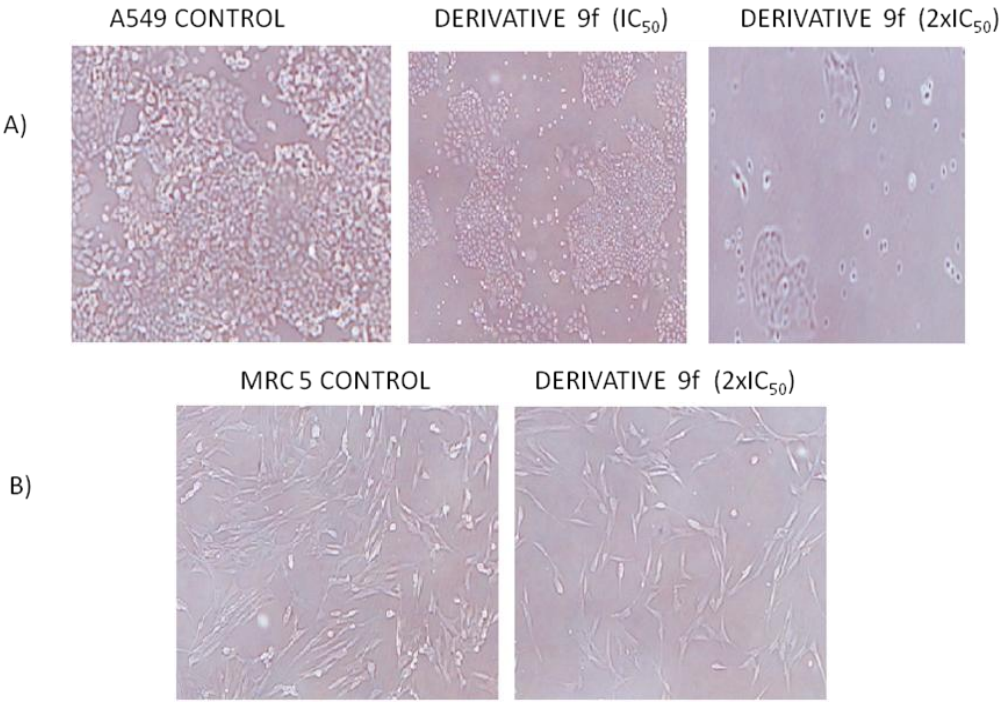

Figure 25.

In a similar way, when compound **10e** was evaluated it can be observed that lung cancer cells (A549, Figure 26, A) died but normal lung cells (MRC 5) did not die (Figure 26, B).

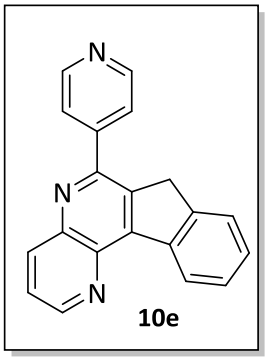

10e

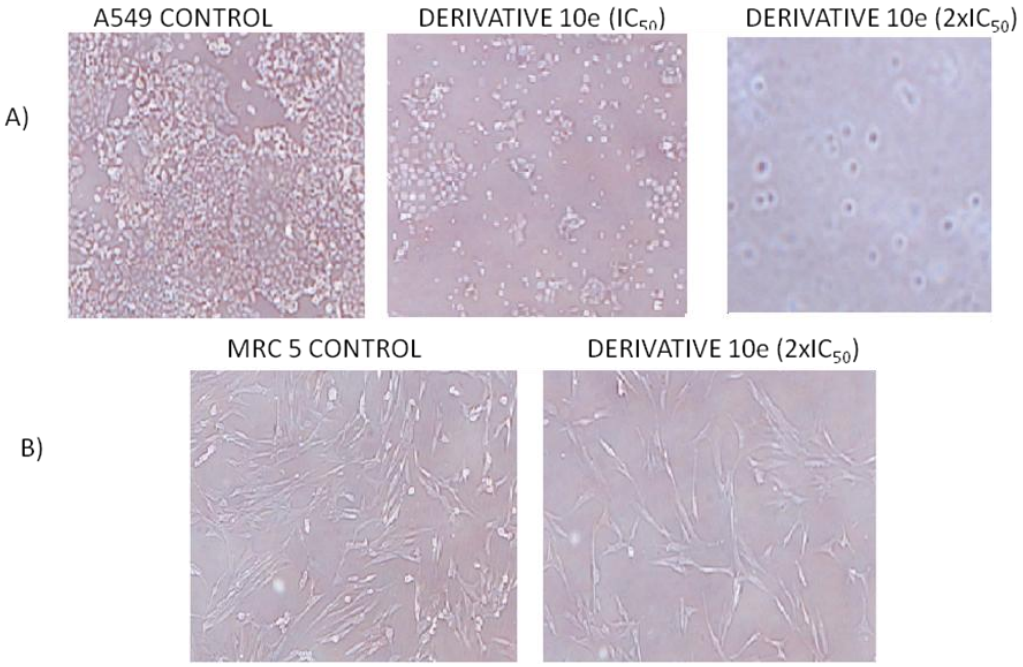

Figure 26.

Likewise, indenonaphthyridinone **16c** kill lung cancer cells (A549, Figure 27, A) whereas lung cells (MRC 5) seem not to be affected (Figure 27, B).

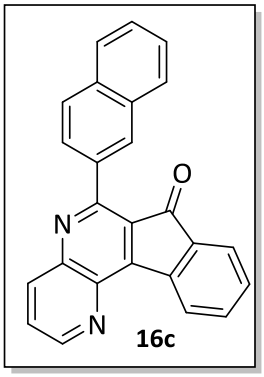

16c

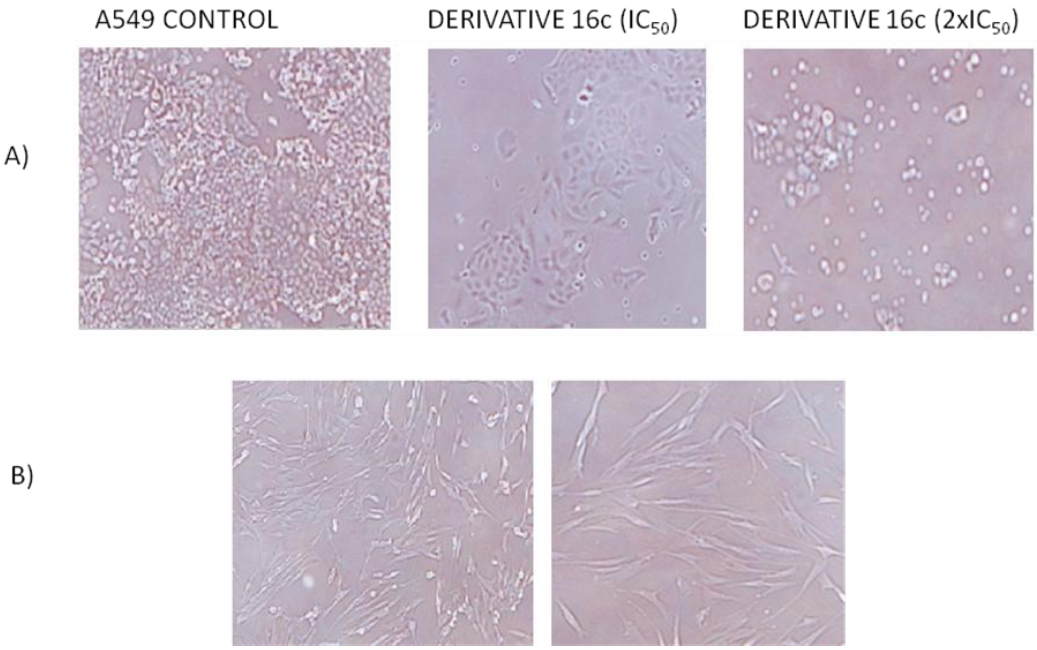

Figure 27.

These results may be very relevant, since if we observe the effect of CPT in normal lung cells (Figure 28) it clearly kills normal cells at the IC_{50} concentration. This fact is one of the main drawbacks of CPT because its toxicity is very high. This could be the starting point to think about studying bioavailability and to design *in vivo* experiments.

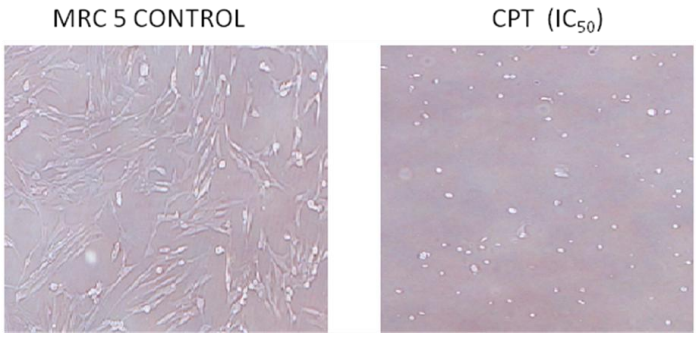

Figure 28.

We can conclude that the best candidate of this family is indenonaphthyridinone **16c** with an IC_{50}= 0.8±0.02 µM in lung cancer cells (A549) moreover, this derivative **16c** is able to kill lung cancer cells but it hardly affects normal lung cells (MRC 5) growth.

3.2.2. Cytotoxicity studies in cancer cell lines with 1,5-naphthyridine derivatives 19

Using the same protocol as for the indenonaphthyridine derivatives (**9**, **10**, **14**-**17**), the cytotoxicity of 1,5-naphthyridine derivatives **19** was studied (Table 6). The cancer cell lines studied were the same; A549 (carcinomic human alveolar basal epithelial cell), BT20 (human breast cancer) and SKOV3 (human ovarian carcinoma). Cells were incubated with compounds during 48 hours. Untreated cells were included in the assay, CCK-8 was used as the cytotoxicity assay (Figure 22 and 23) and the results were normalized to 100% survival for the untreated cells. Results are summarized in table 6.

Table 6. Cytotoxicity values of 1,5-naphthyridine derivatives **19**.

Entry	Comp.	R	R^1	R^2	Cytotoxicity IC_{50} (μM)[a]		
					breast BT20	lung A549	ovarian SKOV03
1		CPT			0.07±0.04	$(1.0\pm0.4)10^{-3}$	0.5±0.4
2	**19a**	Ph	H	Ph	>50	>50	>50
3	**19b**	3,4-F_2-C_6H_3	H	Ph	39.3±0.6	5.5±0.9	31.7±0.8
4	**19c**	4-CF_3-C_6H_4	H	Ph	>50	9.4±0.4	>50
5	**19d**	4-F-C_6H_4	H	Ph	49.9±0.8	20.7±0.4	>50
6	**19e**	4-NO_2-C_6H_4	H	Ph	>50	11.8±0.1	>50
7	**19f**	3-NO_2-C_6H_4	H	Ph	>50	6.6±0.5	28.7±0.4
8	**19g**	3-OMe-C_6H_4	H	Ph	>50	6.8±0.5	>50
9	**19h**	4-CF_3-C_6H_4	H	C_6H_4Ph	>50	40.2±0.8	>50
10	**19i**	4-F-C_6H_4	H	C_6H_4Ph	49.8±0.4	11.3±0.2	>50
11	**19j**	4-NO_2-C_6H_4	H	C_6H_4Ph	3.9±0.3	1.9±0.4	21.5±1.2
12	**19k**	3-NO_2-C_6H_4	H	C_6H_4Ph	19.2±0.3	7.4±0.5	40.3±0.3
13	**19l**	3-OMe-C_6H_4	H	C_6H_4Ph	31.6±0.4	9.8±0.4	>50
14	**19m**	4-F-C_6H_4	H	6-OMe-Naphthyl	12.6±0.1	2.8±0.2	44.5±0.5
15	**19n**	4-CF_3-C_6H_4	H	4-OMe-C_6H_4	>50	19.5±0.6	>50
16	**19o**	4-F-C_6H_4	H	4-OMeC_6H_4	>50	9.2±0.4	>50
17	**19p**	4-NO_2-C_6H_4	H	4-OMeC_6H_4	36.4±0.4	8.7±0.3	41.5±0.3
18	**19q**	3-OMe-C_6H_4	H	4-OMeC_6H_4	47.4±0.3	4.4±0.4	>50
19	**19r**	4-CF_3-C_6H_4	H	4-CF_3-C_6H_4	>50	27.4±0.7	47.9±0.7
20	**19s**	4-CF_3-C_6H_4	H	3-thienyl	>50	13.2±1.5	>50
21	**19t**	4-F-C_6H_4	H	3-Thienyl	>50	8.6±0.3	>50
22	**19u**	4-CF_3-C_6H_4	Me	Ph	>50	10.4±0.2	>50

[a] The cytotoxicity IC_{50} values listed are the concentrations corresponding to 50% growth inhibition. Each data represents mean ± S.D. from three different experiments performed in triplicate

In this case, cytotoxicity results show a great variety of antiproliferative activities too (Table 6). Compound **19j** (Table 6, entry 11) display the highest cytotoxic effect in

lung cancer cells (A549) with an IC_{50} of 1.9±0.4 µM. Derivatives with a fluorine atom in *para* position (Table 6, entries 14, 16 and 21) show good cytotoxicity values with IC_{50} of 2.8±0.2 µM, IC_{50} of 9.2±0.4 µM and IC_{50} of 8.6±0.3 µM, respectively. The *metha* substitution in the aromatic aldehydes seems to be interesting both in terms of TopI inhibitory effect and in terms of cytotoxicity. The cytotoxicity values for these derivatives (Table 6 entries 7, 8, 12, 13 and 18) are IC_{50}= 6.6±0.3 µM, IC_{50}= 6.8±0.5 µM, IC_{50}= 7.4±0.5 µM, IC_{50}= 9.8±0.4 µM and IC_{50}= 4.4±0.4 µM, respectively. The same compound **19j** that shows the best cytotoxic value in lung cancer cells display the better cytotoxic value in breast cancer cell line too with an IC_{50} of 3.9±0.3 µM (Table 6, entry 11).

It can be clearly visualized (Figure 29) that lung cancer cells are the most sensitive cells to the synthesized derivatives, whereas ovarian and breast cancer cells seem less affected by the tested derivatives.

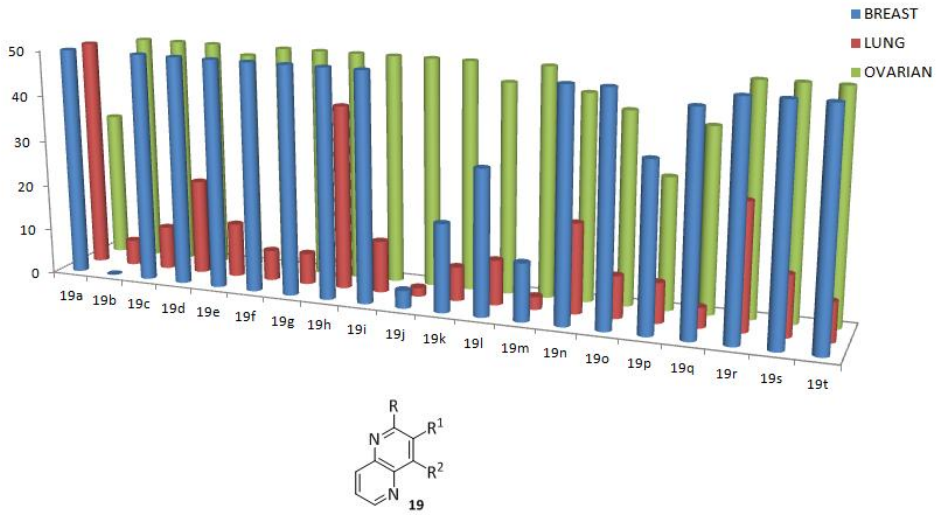

Figure 29. IC_{50} values comparison in the different three cancer cell lines.

Similarly as for the case of the indenonaphthyridine family, some of the most cytotoxic compounds were tested in normal lung cells (MRC 5). For instance, compound **19j** proved to kill lung cancer (A549, Figure 30, A) cells, whereas it hardly affects normal lung cells (MRC 5, Figure 30, B).

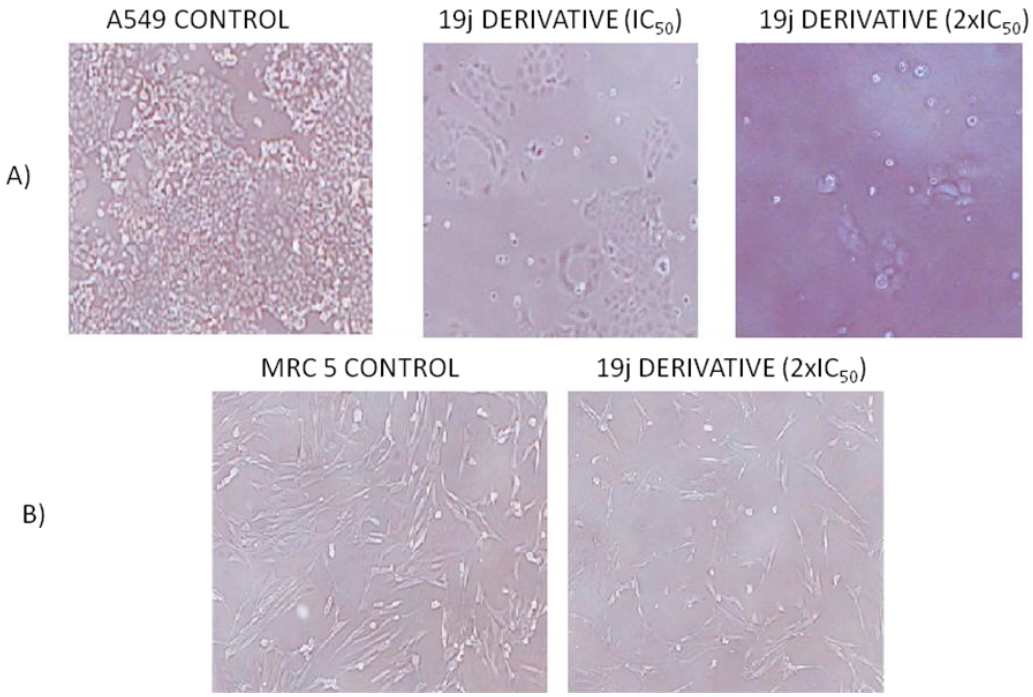

Figure 30.

If the effect of derivative **19j** in normal lung cells is compared to the effect that CPT has in this cells (Figure 28), we can conclude that while CPT shows a strong effect in normal cells, compound **19j** seems not to affect this cells.

In conclusion, we demonstrated that some of the synthesized compounds show promising cytotoxic effect towards the cancer cell lines tested (A549, BT20 and SKOV3). In this sense, further analysis can be made in terms of bioavalibilty and stability in the

bloodstream. Moreover, a deeper study in the structural modifications of the molecules could be made to improve the cytotoxicity effect. This work is a starting point, so the next step could be to study pharmacokinetics.

4. Addenda

Leishmaniasis and topoisomerase I

4.1. Background in Leishmania

Besides anticancer activity, antiviral activity is another outstanding property of CPT and many of its derivatives. Topoisomerase I activity has been associated with various retroviruses including Rous sarcoma virus,[183] equine infectious anemia virus, human immunodeficiency virus (HIV),[184] and Leishmaniasis[185]

Leishmaniasis is a complex disease caused by 17 different species of protozoan parasites belonging to the genus *Leishmania*, transmitted *via* the bite of plebotomine sand flies. This disease has worldwide distribution with important focus of infection in Central and South America, Southern Europe, North and East Africa, the Middle East and the Indian subcontinent.[186] This disease generally occurs in underdeveloped countries, where most patients do not avail themselves of a complete course of treatment because of the cost, availability, invasive route of administration, and long treatment duration, which, in turn, increases the chance of drug resistance.[187]

With increasing numbers of human immunodeficiency virus (HIV) coinfections, human migration, and resettlement, there is a possibility of resurgence of the disease.[188]

There are two major clinical forms of the disease, visceral (VL) and cutaneous leishmaniasis (CL). Apart from these two there are other cutaneous manifestations including mucocutaneous leishmaniasis (MCL), diffuse cutaneous leishmaniasis (DCL), recidivans leishmaniasis (LR), and post-kala-azar dermal leishmaniasis (PKDL).

---

[183] Weiss, R.; Teich, N.; Varmus, H.; Coffin, J. In: Molecular Biology of Tumor Viruses: RNA Tumor Viruses, 2nd ed. New York: Cold Spring Harbor; **1985**.

[184] Priel, E.; Showalter, S. D.; Roberts, M.; Oroszlan, S.; Segar, S.; Aboud, M.; Blair, D. G. *EMBO J.* **1990**, *12*, 4167-4172.

[185] Chakraborty, A. K. *Ind. J. Biochem. Biophys.* **1993**, *30*, 257-263.

[186] Goupil, L.; Mckerrow, J. *Chem. Rev.* **2014**, *114*, 11131-11137.

[187] Freitas-Junior, L. H.; Chatelain, E.; Andrade Kim, H.; Siqueira-Neto, J. L. *Int. J. Parasitol. Drugs Drug Resist*. **2012**, *2*, 11-19.

[188] Croft, S. L.; Sundar, S.; Fairlamb, A. H. *Clin. Microbiol. Rev*. **2006**, *19*, 111-126.

This generates the need for new treatment methods and the use of recent technologies to develop new chemotherapeutic agents that are easily available to, and affordable by, the affected population.

DNA topoisomerases recently have emerged as principal therapeutic targets with a group of targeting agents having a broad spectrum of anti-parasitic activity.[189] Because of emergence of drug resistance in *Leishmania*, improved drug therapy of *Leishmania* infections is still desirable and there is a genuine need for developing therapeutic agents to combat drug resistance. While topoisomerases are ubiquitous in all organisms, studies have shown that kinetoplastid topoisomerases have some distinguishing features that differentiate the parasite enzyme from its prokaryotic and eukaryotic counterparts.[189,190]

Leishmania donovani is an unicellular eukaryote having a well-defined nucleus and other cell organelles including a kinetoplast and a flagellum. Leishmania parasites have two morphological forms, termed amastigotes and promastigotes (Figure A1), which are found in the mammalian and sandfly hosts, respectively.[191]

[189] Das, A.; Dasgupta, A.; Sengupta, T.; Majumder, H. K. *Trends in Parasitol*. **2004**, *20*, 381-387.

[190] (a) Das, B. B.; Sen, N.; Dasgupta, S. B.; Ganguly, A.; Das, R.; Majumder, H. K. Indian *J. Med. Res.* **2006**, *123*, 221-232. (b) Jean-Moreno, V.; Rojas, R.; Goyeneche, D.; Coombs, G. H.; Walker, *J. Exp. Parasitol.* **2006**, *112*, 21-30.

[191] Bates, P. A.; Rogers, M. A. *Curr. Mol. Med*. **2004**, *4*, 601-609.

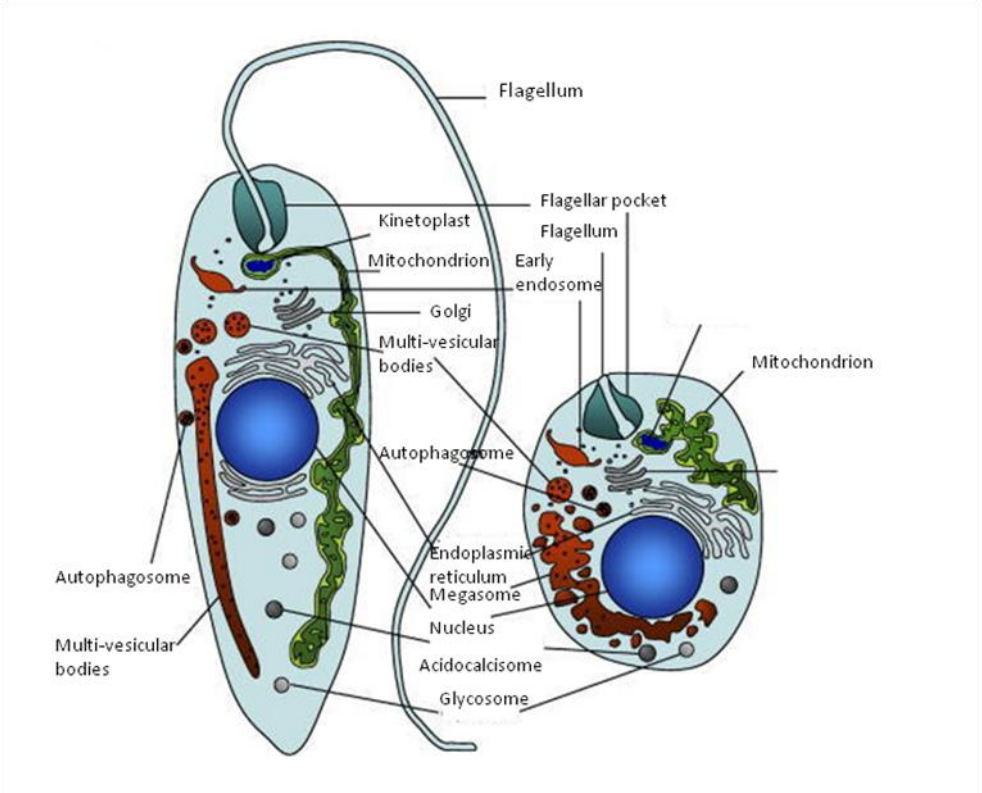

Figure A1. Intracellular organelles in leishmania promastigote (left) and amastigote (right) forms.

Promastigote is formed in the alimentary tract of the sandfly. It is an extracellular and motile form. A long flagellum is projected externally at the anterior end. The nucleus lies at the centre, and in front of which are kinetoplast and basal body (Figure A1).

Amastigote form is found in the mononuclear phagocyte and circulatory systems of humans. It is an intracellular and non-motile form, being devoid of external flagellum. The short flagellum is embedded in the anterior end without projecting out. It is oval in shape, and measures 3-6 µm in length and 1-3 µm in width. The kinetoplast and basal

body lie towards the anterior end. Amastigotes are largely intracellular stages that mainly live in the phagolysosomal system of macrophages, the predominant host cell.

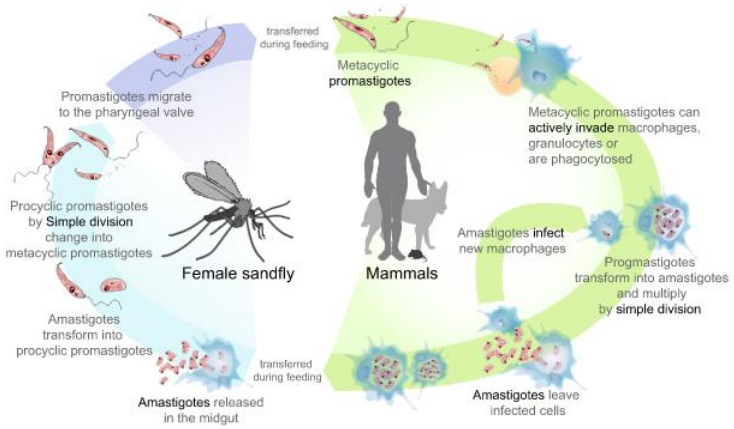

Figure A2. Life cycle of *Leishmania donovani*.

Macrophages are phagocytic and readily cover amastigotes, followed by phagosome-lysosome fusion, this microbial defence mechanism is lethal to most foreign organism, as it results in exposure to acidic pH of 4.5 to 5.5 and attack by a battery of lysosomal enzymes. However, *Leishmania* can survive this experience, and indeed grow in this environment.[192] Parasites within the phagolysosome grow and divide, such that an individual macrophage may eventually contain many tens of amastigotes. There is no specific scape mechanism known, and it is assumed that in most cases the host cell simply ruptures when it cannot accommodate any more parasites, which are taken up by further macrophages (Figure A2).

These parasites show variable genetic diversity in their life cycle, wherein DNA topoisomerases play a key role in cellular processes affecting the topology and organization of intracellular DNA. Kinetoplastid topoisomerases offer most attractive

[192] Zilberstein, D.; Shapira, M. *Annu. Rev. Microbiol*. **1994**, *48*, 449-470.

targets for their structural diversity from other eukaryotic counterpart and their indispensable function in cell biology. Therefore, understanding the biology of kinetoplastid topoisomerases and the components and steps involved in this complex process provide opportunities for target based drug design against protozoan parasitic diseases.

Type I DNA topoisomerase I was isolated from *L. donovani*.[185] The purified active enzyme (65-75 kDa) was ATP-independent and found to be sensitive to topoisomerase I specific inhibitor, camptothecin (CPT).[193] The first DNA sequence of a topoisomerase I-like gene from the kinetoplastid, *L. donovani* was reported by Broccoli and coworkers in 1999.[194] The deduced amino acid sequence of this gene showed an extensive degree of homology with the central core DNA binding domain of other eukaryotic type IB topoisomerase, including conserved motifs but having a variable *C*-terminal. The difference in the sensitivity of kinetoplastid topoisomerase I for camptothecin[195] prompted the search for topoisomerase I sequence from kinetoplastid parasites which uncovered the existence of unique topoisomerase I from the parasite.[196]

Starting from bacteria to human to viruses, topoisomerases I are encoded by a single gen that contains the highly conserved DNA-binding and catalytic domains on a single peptide. In kinetoplastid parasites however, topoisomerase I is encoded by two genes, which associate with each other to form a hetero-dimeric topoisomerase I enzyme within the parasite. Genetic analyses identify a gene for a large subunit, namely LdTopIL (Figure A3), on *L. donovani* chromosome 34, encoding for a 636-amino acid polypeptide with an estimated molecular mass of 73 kDa. This subunit is closely homologous to the core domain of human topoisomerase I. The gene for the small subunit LdTopIS encoding a 262 amino acid polypeptide with a predicted molecular mass of 28kDa, in turn is found on the *L. donovani* chromosome 4. The small subunit

---

[193] Bodley, A. L.; Shapiro, T. A. *Proc. Natl. Acad. Sci. USA* **1995**, *92*, 3726-3730.
[194] Broccoli, S.; Marquis, J. F.; Papadopaulou, B.; Olivier, M.; Drolet, M. *Nucleic Acids Res.* **1999**, *27*, 2745-2752.
[195] Bodley, A. L.; Shapiro, T. A. *Proc. Natl. Acad. Sci. USA* **1995**, *92*, 3726-3730.
[196] Villa, H.; OteroMarcos, A. R.; Reguera, R. M. *J. Biol. Chem*. **2003**, *278*, 3521-3526.

contains the phylogenetically conserved "SKXXY" motif placed at the *C*-terminal domain of all type I DNA topoisomerases, which conserves a tyrosine residue playing a role in DNA cleavage (Figure A3). LdTopIL shows about 54% identity with core subdomain of human TopI, including alignment of the conserved sequences surrounding the catalytic tyrosine residue. LdTopIL also deviates significantly from human topoisomerase I at loop regions bounded by LdTopIL residues Pro62-His 63, Asp114-His118 and Pro341-Asp342 which do not share the conserved sequences. Overall, the similarity indicates that the structure and catalytic machinery of the two enzymes are highly conserved, despite the fact that one is monomeric and the other is heterodimeric.

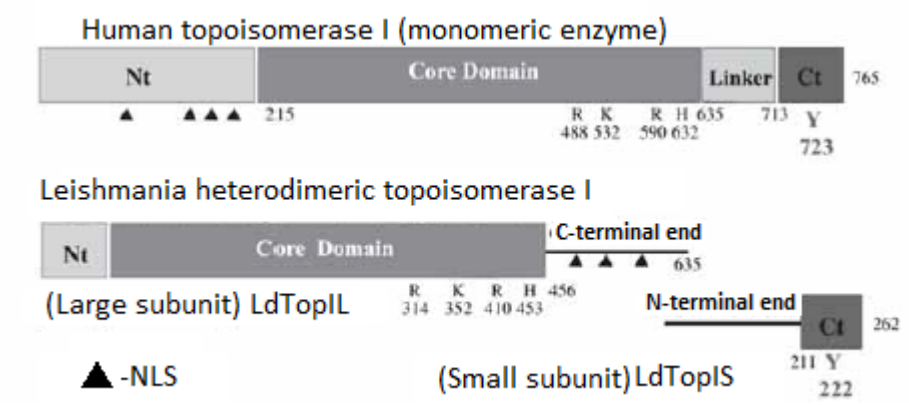

Figure A3. Domain organization of human TopI and *L. donovani* TopI.

Davies and coworkers reported a 2.72Å crystal structure[197] of an active truncated *L. donovani* TopIL/TopIS heterodimer bound to nicked double stranded DNA in the presence of vanadate (Figure A4). The vanadate forms covalent linkages between the catalytic tyrosine residue of the small subunit and the nicked ends of the scissile DNA strand. This study reveals that Arg410 (Arg490 in human topoisomerase I) activates Tyr222 residue of LdTopIS (Tyr723 in human topoisomerase I) for attack to the scissile

[197] Davies, D. R.; Mushtaq, A.; Interthal, H. Champoux, J. J.; Hol, W. G. *J. Mol. Biol.* **2006**, *357*, 1202-1210.

phosphate group, with water acting as specific base. Moreover, it was also observed that Lys352 of LdTopIL (Lys532 in human topoisomerase I) acts as general acid in the cleavage reaction. Comparison of LdTopILS to the structure of human topoisomerase I bond to the DNA containing topotecan reveals that all of the amino acids that form the drug binding pocket are completely conserved between the two species.

Figure A4. Crystal Structure of *L. donovani* topoisomerase I-vanadate-DNA complex (PDB: 2B9S).

Das and coworkers[198] reported, for the first time, the *in vitro* reconstitution of the two recombinant proteins, LdTopIL and LdTopIS and the localization of the active enzyme in both the nucleus and Kinetoplast.

[198] Das, B. B.; Sen, N.; Ganguly, A.; Majumder, H. K. *FEBS. Lett.* **2004**, *565*, 81-88.

4.1.1. Current treatments in Leishmaniasis

In ancient China, the crude extract of *Camptotheca acuminate* containing CPT has been used traditionally to control insect pests for centuries, and it is was reported to be a potent chemosterilant against the housefly and cabbage caterpillar.[199,200]

The most serious and severe form of this disease is visceral leishmaniasis (VL) caused by *Leishmania donovani* and *Leishmania infantum* and if untreated it is fatal in almost all cases.[201] VL patients are prone to suffer from bacterial coinfections including pneumonia, tuberculosis and gastrointestinal infections. Moreover, the risk of developing VL is about 100-2000- times greater in patients infected with HIV compared to non-HIV people.[202] Drugs that are nowadays in use for the treatment of VL are summarized in figure A5.

Antimony has been widely used as therapeutic agent for several centuries. Meglumine antimoniate (Figure A5) is a formulation of pentavalent antimonial used in CL treatment, due to its poor oral absorption this drug is administrate *via* intramuscular injections or intravenous infusions. The pentavalent antimonials sodium stibogluconate and meglumine antimoniate, the first line of drugs for visceral (VL) and cutaneous Leishmaniasis (CL), have variable efficacy and side effects.[203]

---

199 Liu, Y. Q.; Liu, Z. L.; Tian, X.; Yang, L. *Nat. Prod. Res*. **2010**, *24*, 509-514.

200 DeMilo, A. B.; Borkovec, A. B. *J. Econ. Entomol*. **1974**, *67*, 457-458.

201 Ejazi, S. A.; Ali, N. *Expert Rev. Anti Infect. Ther.* **2013**, *11*, 79-98.

202 (a) Rosenthal, E.; Marty, P.; Poizot-Martin, I.; Reynes, J.; Pralong, F.; Lafeuillade, A.; Jaubert, D.; Boulat, O.; Dereure, J.; Gambarelli, F.; Gastaut, J. A.; Dujardin, P.; Dellamonica, P.; Cassuto, J. P. *Trans. R. Soc. Trop. Med. Hyg.* **1995**, *89*, 159-162. (b) Gradoni, L.; Scalone, A.; Gramiccia, M.; Troiani, M. *AIDS* **1996**, *10*, 785-791. (c) Lopez-Velez, R.; Perez-Molina, J. A.; Guerrero, A.; Baquero, F.; Villarrubia, J.; Escribano, L.; Bellas, C.; Perez-Corral, F.; Alvar, J. *Am. J. Trop. Med. Hyg*. **1998**, *58*, 436-443.

203 (a) Thakur, C. P.; Kumar, M.; Kumar, P.; Mishra, B. N.; Pandey, A. K. *Br. Med. J*. **1998**, *296*, 1557-1561. (b) Lawn, S. D.; Armstrong, M.; Chilton, D.; Whitty, C. J. *Trans. R. Soc. Trop. Med. Hyg*. **2006**, *100*, 264-269.

Amphotericin B (Figure A5) is a polyene antiobiotic isolate from *Streptomyces nodosus* in 1995, which was identified due to its antifungal activity.[204] The first favorable treatment in patients with VL was reported in 1963. This drug was usually classified as second line treatment of VL but decreased efficacy of antimonials and pentamidine converted this drug as a first-line treatment. In the case of pentamidine (Figure A5), this was one of the first treatments[205] of VL but it had severe side-effects that reduce the utility of the treatments. Amphotericin B and pentamidines, referred as to second line drugs (Figure A5), although used clinically, are often of limited efficacy and are very toxic.[206]

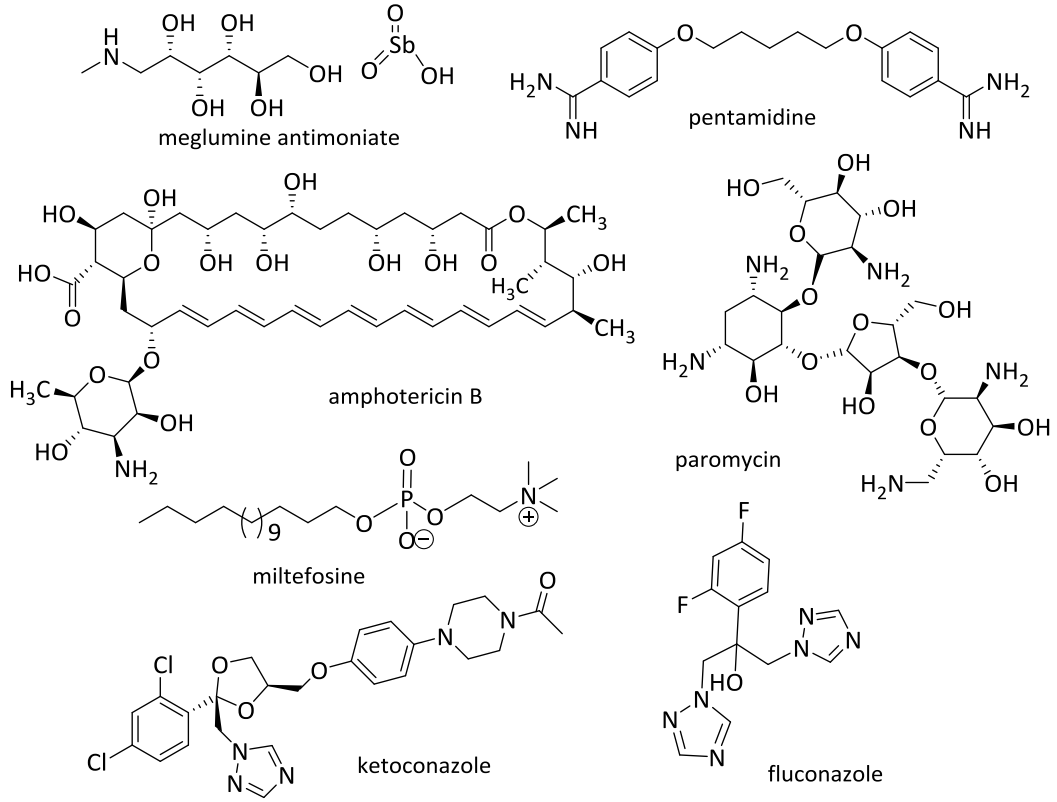

Figure A5. Current treatments in leishmaniasis.

[204] Gold, W.; Stout, H. A.; Pagano, J. F.; Donovick, R. *Antibiot. Annu.* **1955–56**, *3*, 579-585.
[205] Hazarika, A. N. *Ind. Med. Gaz*. **1949**, *84*, 140-145.
[206] Iwu, M. M.; Jackson, J. E.; Schuster, B. G. *Parasitol. Today* **1994**, *10*, 65-68.

Miltefosine (hexadecylphosphocholine, Figure A5), was first described as anticancer treatment and after that it was demonstrated that it has antileishmanial activity.[207] In 2002 it was approved as the first oral treatment for VL. The most common adverse effects are not as aggressive as in other cases.

Paromycin (Figure A5) is an aminoglycoside broad-spectrum antibiotic first isolated from *Streptomyces krestomuceticus* that was demonstrated to be appropriate for treatment of VL in 1990.[208] Azoles are considered oral antifungal drugs that could have antileishmanial activity. Ketoconazole (Figure A5) and fluconazole (Figure A5) belong to this azole family, however, only ketoconazole was found to be efficacious.

As it has been mentioned before leishmaniasis drugs often need to be used in economically depressed areas where hospitals are not set up to carry out long treatments. In this sense, treatment of leishmaniasis must be low cost and processes and of course with as less as side effects as possible.[209] Drug discovery for leishmaniasis is not an easy task since there are limited funds available. Due to these limitations repurposing drugs have gain great interest. This repurposing of drugs allows short and fast paths to reach patients and the cost of development is reduced. In fact, treatments such as pentamidine, amphotericin B, and miltefosine, were previously designed for different applications than that of leishmaniasis.[210,211] In the next lines some of the repurposing drugs studied for leishmaniasis are described (Figure A6).

---

[207] Croft, S. L.; Snowdon, D.; Yardley, V. *J. Antimicrob. Chemother*. **1996**, *38*, 1041-1047.

[208] Chunge, C. N.; Owate, J.; Pamba, H. O.; Donno, L. *Trans. R. Soc. Trop. Med. Hyg*. **1990**, *84*, 221-225.

[209] Nagle, A. S.; Khare, S.; Kumar, A. B.; Supek, F.; Buchynsky, A.; Mathison, C. J. N.; Chennamaneni, N. K.; Pendem, N.; Buckner, F. S.; Gelb, M. H.; Molteni, V. *Chem. Rev.* **2014**, *114*, 11305-11347.

[210] (a) Ashburn, T. T.; Thor, K. B. *Nat. Rev. Drug Discov*. **2004**, *3*, 673-683. (b) Novac, N. *Trends Pharmacol. Sci.* **2013**, *34*, 267-272.

[211] Shakya, N.; Bajpai, P.; Gupta, S. *J. Parasit. Dis.* **2011**, *35*, 104-112.

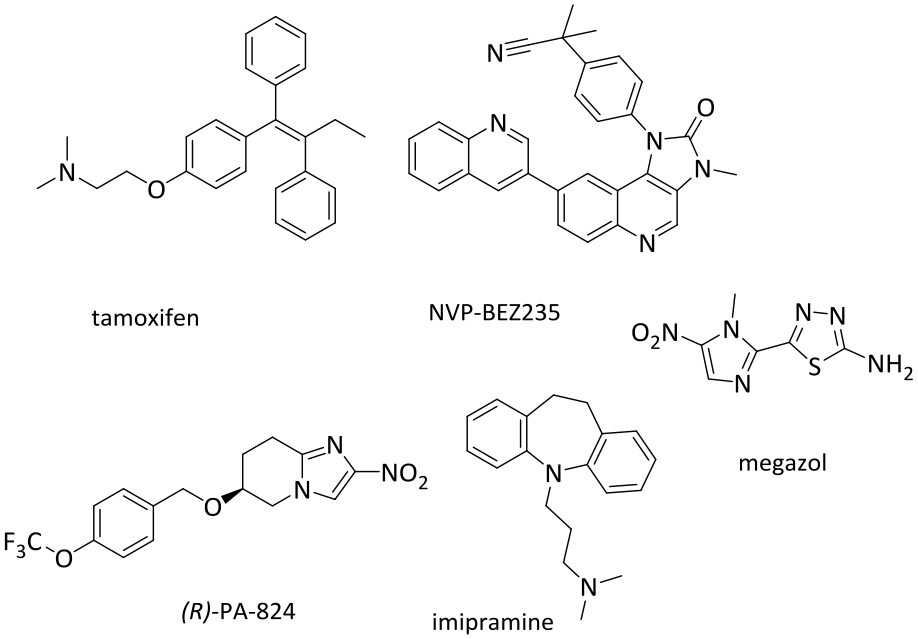

Figure A6. Repurposing drugs.

Tamoxifen (Figure A6) is an estrogen receptor antagonist which clinical use was for the treatment of breast cancer. Tamoxifen has *in vitro* activity against *Leishmania braziliensis* and *Leishmania infantum* intracellular amastigotes. Nevertheless, while tamoxifen is able to cure leishmaniasis in laboratory animals, it also causes important side effects to the male reproductive system in mouse models.[212] Parasites and humans express similar kinase enzymes, this is the reason why some phosphoinositide-3-kinase inhibitors have been studied as antileishmanial inhibitors. This is the case of NVP-BEZ235 (Figure A6) that shows potent antileishmanial activity in parasite cultures, however, no activity was observed *in vivo* mouse models.[213]

[212] Eissa, M. M.; Amer, E. I.; El Sawy, S. M. *Exp. Parasitol*. **2011**, *128*, 382-390.

[213] Diaz-Gonzalez, R.; Kuhlmann, F. M.; Galan-Rodriguez, C.; Madeira da Silva, L.; Saldivia, M.; Karver, C. E.; Rodriguez, A.; Beverley, S. M.; Navarro, M.; Pollastri, M. P. *PLoS Neglected Trop. Dis*. **2011**, *5*, 1297-1308.

Nitroimidazoles are known in the field of anaerobic bacterial and parasitic infections. The best candidate of this family against leishmaniasis was megazol (Figure A6) but its development was finally stopped due to mutagenicity.[214] Thus, the bicyclic nitroimidazole derivative *(R)*-PA-824 (Figure A6) has demonstrated to be a potent inhibitor for late lead optimization for visceral leishmaniasis.[215] Imipramine (Figure A6) is a cationic amphiphilic drug commonly used for the treatment of depression in humans. Preliminary studies have shown that this derivative is able to decrease mitochondrial transmembrane potential of *L. donovani* promastigotes.[216]

4.1.2. Targeting Topoisomerase I in Leishmaniasis

Leishmaniasis is one of the most neglected tropical diseases (NTDs) in terms of drug discovery and current therapies are inadequate. Improved drug therapy of leishmanial infections is still desirable and the need for new molecular targets on which to base future treatment strategies is clear and justified. Currently DNA topoisomerases have been recognized as potential chemotherapeutic targets for antitumor and antiparasitic agents.[217]

[214] Enanga, B.; Ariyanayagam, M. R.; Stewart, M. L.; Barrett, M. P. *Antimicrob. Agents Chemother*. **2003**, *47*, 3368-3370.

[215] Patterson, S.; Wyllie, S.; Stojanovski, L.; Perry, M. R.; Simeons, F. R.; Norval, S.; Osuna-Cabello, M.; De Rycker, M.; Read, K. D.; Fairlamb, A. H. *Antimicrob. Agents Chemother*. **2013**, *57*, 4699-4706.

[216] Zilberstein, D.; Liveanu, V.; Gepstein, A. *Biochem. Pharmacol.* **1990**, *39*, 935-940.

[217] Das, B. B.; Ganguly, A.; Majunder, H. K. Drug Targets in Kinetoplastid Parasites. Landes Biosciences, **2007**.

4.1.2.1. Camptothecin derivatives

Based on the success of CPT as anticancer agent, camptothecin analogues used in this therapy were evaluated for antileishmanial activity.[209] Topotecan, gimatecan, irinotecan and SN-38 (Figure A7) were evaluated against *L. infantum*. Gimatecan and CPT were the most potent in *L. infantum* promastigotes. Sean and coworkers[218] demonstrated that CPT induces programmed cell death both in the amastigotes and promastigotes from *L. donovani* parasite. The inhibitory efficacy of CPT derivatives on recombinant *L. infantum* topoisomerase IB demonstrated that all compounds affected topoisomerase I activity, being gimatecan the most potent preventing the relaxation of supercoiled DNA.[219]

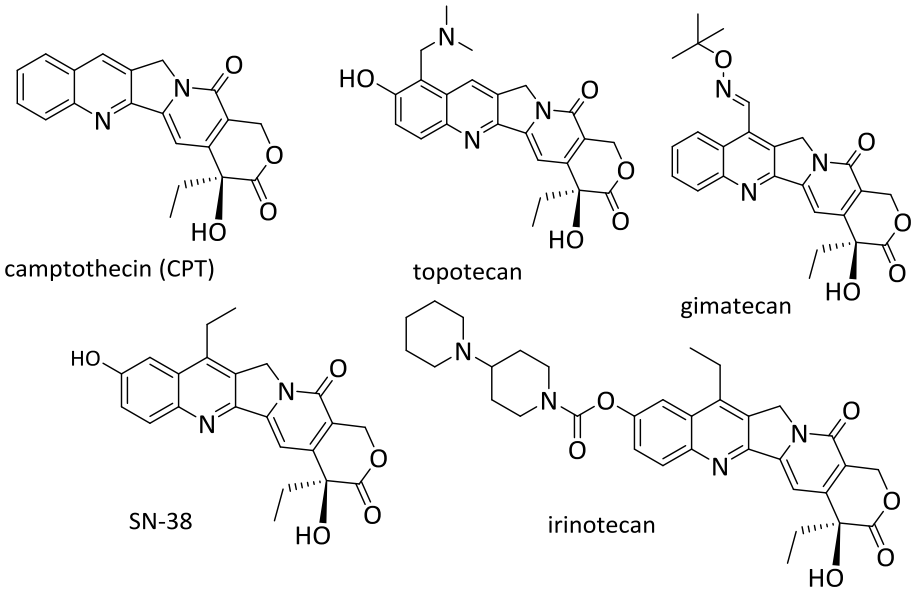

Figure A7. Representative examples of Leishmania TopI inhibitors

[218] Sen, N.; Das, B. B.; Ganguly, A.; Mukherjee, T.; Bandyopadhyay, S.; Majumder, H. K. *J. Biol. Chem*. **2004**, *279*, 52366-52375.

[219] Prada, C. F.; Álvarez-Velilla, R., Balaña-Fouce, R.; Prieto, C.; Calvo-Álvarez, E.; Escudero-Martínez, J. M.; Requena, J. M.; Ordóñez, C.; Desideri, A.; Pérez-Pertejo, Y.; Reguera, R. M. *Biochem. Pharmacol.* **2013**, *10*, 1433-1440.

Werbovetz and coworkers[220] further examined CPT and 10,11-methylenedioxy analogs (Figure A8) against the pathogenic protozoan *Leishmania donovani in vitro.* Compared with CPT, 10,11-methylenedioxy-CPT (Figure A8) exhibited 90-fold greater antileishmanial activity, whereas, introduction of difluoro substitution at the methylene position (10,11-difluoromethylenedioxy-CPT) reduced the activity.

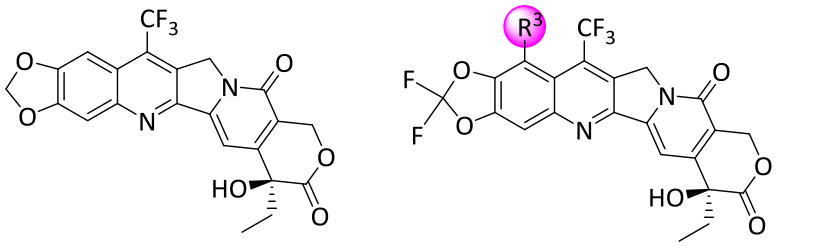

10,11-methylenedioxy-CPT

10,11-difluoromethylenedioxy-CPT

Figure A8. CPT analogs showing antileishmanial activity.

4.1.2.2. Non-camptothecin derivatives

It is possible to find non-CPT leishmania TopI inhibitors, as for example, heterocyclic derivatives as is the case of mitonafide (Figure A9) that inhibits both nuclear and mitochondrial topoisomerase of *Leishmania* with preferential targeting of the mitochondrial enzyme over the nuclear enzyme.[221]

[220] Werbovetz, K. A.; Bhattacharjee, A. K.; Brendle, J. J.; Scovill, J. P. *Bioorg. Med. Chem*. **2000**, *8*, 1741-1747.

[221] Slunt, K. M.; Grace, J. M.; Macdonal, T. L. *Antimicrob. Agents Chemother.* **1996**, *40*, 706-709.

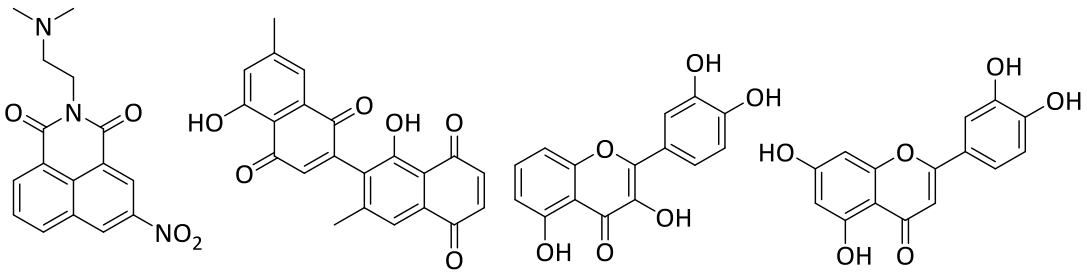

Figure A9. Heterocyclic compounds as antileishmanial inhibitors.

Moreover, quinone derivatives such as diospyrin (Figure A9), a bisnapthoquinone isolated from *Diospyros Montana*, has been reported to be a potent inhibitor of leishmania topoisomerase I with no effect on topoisomerase II. It exhibits significant inhibitory effect on the growth of *L. donovani* promastigotes.[222] This compound inhibits the catalytic activity of DNA topoisomerase I of the parasite. Preincubation of topoisomerase I with diospyrin before the addition of DNA in the relaxation reaction increases this inhibition. Results suggest that this bis-naphthoquinone compound exerts its inhibitory effect by binding with the enzyme and stabilizing the topoisomerase I-DNA cleavable complex.

In addition, it has been suggested that TopI from *L. Donovani* may be a promising target for the flavonoid family of drugs. For instance, quercetin and luteolin (Figure A9), already mentioned as anticancer agents, have potent anti-leishmanial effect. The flavonoids inhibited the growth of *L. donovani* promastigotes and amastigotes. They arrested cell cycle progression in *L. donovani* promastigotes leading to apoptosis and reduced parasite burden in animal models.[223]

[222] Ray, S. ; Hazra, B. ; Mittra, B. ; Das, A. ; Majumder, H. K. *Mol. Pharmacol.* **1998**, *54*, 994-999.
[223] Mishra, A.; Vinayagam, J.; Saha, S.; Chowdhury, S.; Roychowdhury, S.; Jaishankar, P.; Majumder, H. K. *Mol. Med*. **2000**, *6*, 527-541.

Indenoisoquinoline derivatives, another known human topoisomerase inhibitors, namely AM13-55 and indotecan (Figure A10) were evaluated as antileishmanial inhibitors and both showed potent inhibitory effect in *L. infantum.*[224]

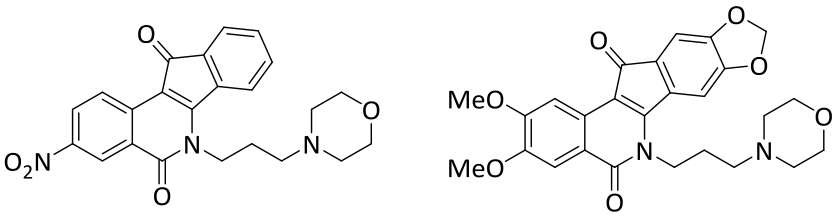

Figure A10. Anti-leishmanial TopI inhibitors with isoquinoline core.

Dihydrobetulinic acid (DHBA, Figure A11), a derivative of betulinic acid that exhibits anti-HIV activity, is another excellent inhibitor of *leishmania* DNA topoisomerase I with the potential to become lead therapeutic compound.[225] DHBA is a potent anti-leishmanial agent that induces apoptosis by primarily targeting parasitic topoisomerases.

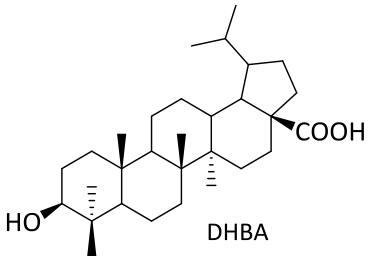

Figure A11. Dihydrobetulinic acid (DHBA).

[224] Balaña-Fouce, R.; Prada, C. F.; Requena, J. M.; Cushman, M.; Pommier, Y.; Álvarez-Velilla, R.; Escudero-Martinez, J. M.; Calvo-Álvarez, E.; Perez-Pertejo, Y.; Reguera, R. M. *Antimicrob. Agents Chemother.* **2012**, *56*, 5264-5270.

[225] Chowdhury, A. R.; Mandal, S.; Goswami, A.; Ghosh, M.; Mandal, L.; Chakraborty, D.; Ganguly, A.; Tripathi, G.; Mukhopadhyay, S.; Bandyopadhyay, S.; Majumder, H. K. *Mol. Med*. **2003**, *9*, 26-36.

Unfortunately, because of a lack of commercial interest, few new drugs are being developed or introduced against this deadly disease. Currently, no effective vaccines have been developed and the control of leishmaniasis primarily relies on chemotherapy. Most anti-leishmanial drugs available are highly toxic, present resistance issues or require hospitalization for their use; therefore, they are not suitable for being used in most of the affected countries.[226]

With these antecedents we considered that the new families of heterocycles prepared with 1,5-naphthyridine skeleton that have been revealed to inhibit human topoisomerase I, could also be good candidates as antileishmanial agents.

[226] Rajasekaran, R.; Phoebe Chen, Y. P. *Drug Discov. Today* **2015**, 20, 958-968.

4.2. Evaluation of the antileishmanial activity of the naphthyridine derivatives

It was described beforehand that, TopI is a well-known target against Leishmaniasis.[¡Error! Marcador no definido.,198] Thus, in view of the results of the synthesized compounds against human topoisomerase I, we decided to explore the antileishmanial activity of our derivatives.

The experiments related to the inhibition and cytotoxic effect against TopI of *Leishmania donovani* were performed in the group of Prof. Rafael Balaña in the Department of Biomedical Sciences in León University.

The effect of the compounds on one subunit of type IB topoisomerase of *L. donovani* (LdTopILs) was examined by pSK plasmid DNA relaxation assay and reaction products were resolved in agarose gel and subsequently visualized by ethidium bromide staining.

The relaxation assay using the tetrahydroindenonaphthyridine **9d** (Figure A12) and CPT was made using 100 μM concentration of compound **9d** and CPT, and compound was preincubated on ice for 15 min prior to the addition of the plasmid. The result shows a clear inhibition of LdTopIB activity until 1 min (lanes 8 and 9) and the inhibitory effect of compound **9d** is stronger than the effect of CPT (compare lanes 8-10 with lanes 5-7). Control (C, lane 1) is the reaction mixture plus 10% DMSO.

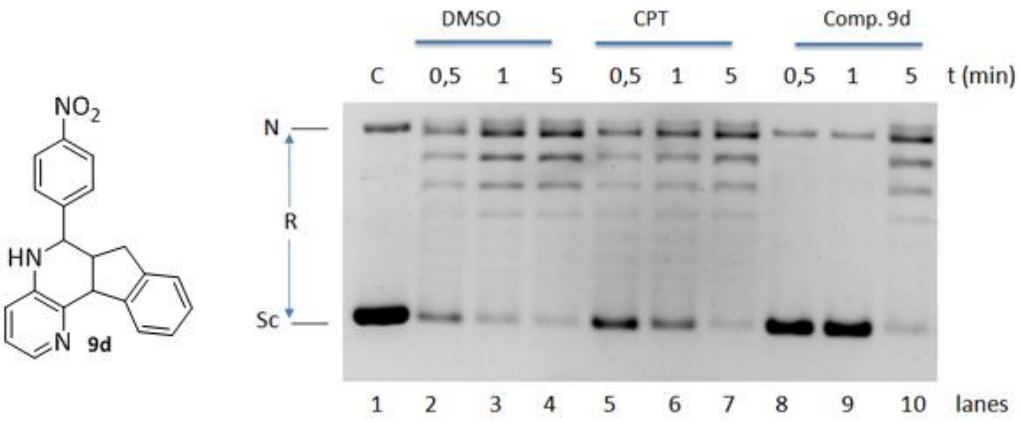

Figure A12. Inhibition of the relaxation activity of LdTopIB by **9d**.

When the inhibitory effect of the indenonaphthyridine **10d** (Figure A13, Table A1, entry 6), was evaluated, it can be observed that compound **10d** is able to inhibit LdTopIB activity (lanes 8-10) and the inhibition is more persistent along the time than in the case of CPT (compare lanes 7 and 10).

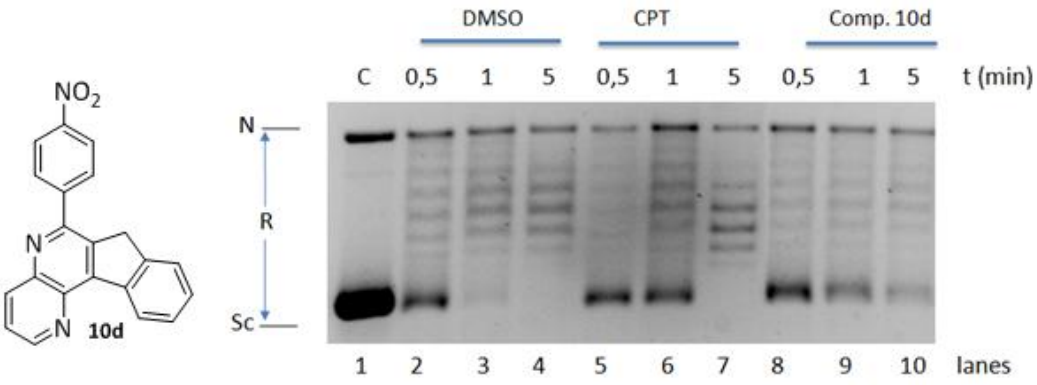

Figure A13. Inhibition of the relaxation activity of LdTopIB by **10d**.

For the cytotoxicity experiments, it is important to bear in mind that compounds must kill the intracellular parasite without damaging the cell. Regarding the results of the cytotoxicity values in *L. donovani* of indeno-1,5-naphthyridine derivatives **9**, **10** and **16** (Table A2), it can be deduced that the selectivity indexes (SI) are very low meaning that the compounds kill the macrophage and thus are not interesting in terms of antileishmanial activity.

Table A1.

Entry	Comp.	R	Cytotoxicity IC_{50} (μM)		
			IC_{50} (macrophage)	IC_{50} (amastigote)	SI (IC_m/IC_a)
1	**9d**	4-NO_2-C_6H_4	124.4±44.3	7.41±0.43	>1.09
2	**9e**	4-Pyridyl	82.47±1.78	65.28±1.36	1.45
3	**9f**	2,4-F_2-C_6H_3	32.1±1.1	0.67±0.06	47.9
4	**9g**	3,4-F_2-C_6H_3	86.81±3.24	76.23±1.36	1.02
5	**10c**	2-Naphthyl	75.8±7.7	11.90±2.8	6.4
6	**10d**	4-NO_2-C_6H_4	68.26±1.96	88.11±0.18	1.29
7	**10e**	4-Pyridyl	33.9±3.0	un	un
8	**10f**	2,4-F_2-C_6H_3	un	6.07±1.45	12.7
9	**10g**	3,4-F_2-C_6H_3	86.12±3.69	78.15±3.94	0.95
10	**16c**	2-Naphthyl	20.6±1.5	4.55±0.69	4.5
11	**16f**	2,4-F_2-C_6H_3	78.1±8.9	13.34±0.91	5.9

In the case of the relaxation activity of the 1,5-naphthyridine derivatives, compound **19d** is shown as an example of LdTopIB relaxation assay (Figure A14, Table A2, entry 3). It can be deduced from the experiments that compound **19d** inhibits the relaxation of LdTopIB in a strong way (lanes 6-8) and the inhibition is more stable along the time than that of CPT (compare lanes 5 and 8).

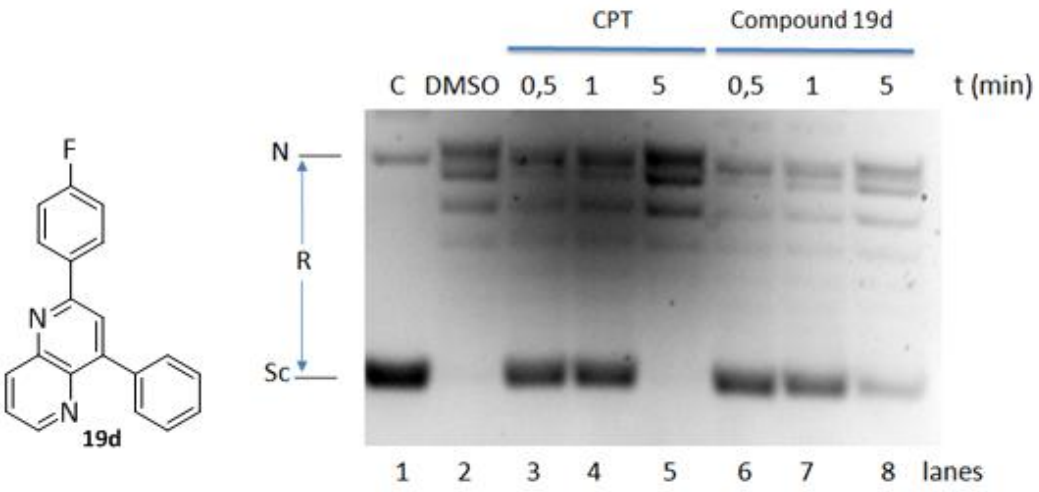

Figure A14. Inhibition of the relaxation activity of LdTopIB by **19d**.

Nevertheless, the 1,5-naphthyridines results (Table A2), are more interesting since higher SI values were found. Compound **19d** seems to be the best candidate of the tested compounds with and SI value of 139,8 µM meaning that the compound selectively kills the parasite without killing the cell.

Table A2.

Entry	Comp.	R	R^1	R^2	Cytotoxicity IC_{50} (μM)		
					IC_{50} (macrophage)	IC_{50} (amastigote)	SI (IC_m/IC_a)
1	**19a**	Ph	H	Ph	54.8±6.1	8.42±1.9	6.5
2	**19b**	3,4-F_2-C_6H_3	H	Ph	21.7±4.8	2.82±0.76	7.7
3	**19c**	4-CF_3-C_6H_4	H	Ph	65.7±5.4	0.47±0.98	139.8
4	**19d**	*p*-F-C_6H_4	H	Ph	124.4±44.3	7.41±0.4	16.7
5	**19h**	4-CF_3-C_6H_4	H	C_6H_4Ph	105.4±33.6	11.65±2.37	9.1
6	**19j**	4-NO_2-C_6H_4	H	C_6H_4Ph	111.3±6.8	1.23±0.32	90,5
7	**19n**	4-CF_3-C_6H_4	H	*p*-OMe-C_6H_4	151.6±89.7	2.26±0.45	67.1
8	**19r**	4-CF_3-C_6H_4	H	*p*-CF_3-C_6H_4	178.4±63.2	9.47±0.12	18.8
9	**19s**	4-CF_3-C_6H_4	H	3-thienyl	181.4±51.5	3.67±0.16	49.4
10	**19u**	4-CF_3-C_6H_4	Me	Ph	126.1±39.6	2.37±0.12	53.2

These preliminary results are very interesting, especially in the case of 1,5-naphthyridines **19** that shows better results in terms of cytotoxicity. Likewise, this information will provide us information to make structural modification in order to find more candidates with better antileishmanial activity.

It is noteworthy to emphasize that, the synthesized compounds show inhibitory effect towards hTopIB and LdTopIB and not necessarily the best candidates in cancer show the best results in Leishmania. Thus, it is possible that we will find certain selectivity among the synthesized compounds and the application of them.

5. Conclusions

5. Conclusions

The [4+2] cycloaddition reaction (Povarov reaction) of aldimines derived from 3-aminopyridine and different aromatic aldehydes with indene as dienophile, using BF3·Et2O as Lewis acid, via *endo* transition state, allows the preparation of tetrahydro-7*H*-indeno[2,1-*c*][1,5]-naphthyridines with a regio- and stereoselective control of the three stereocenters. Moreover, the same indeno-1,5-naphthyridine derivatives can be prepared using the multicomponent version of the [4+2] cycloaddition in shorter reaction times and better yields. In the special case of using the imine **3l** derived from methyl 2-formylbenzoate as the starting aldehyde (R=2-MeO_2C-C_6H_4), the products obtained from the [4+2] cycloaddition reaction with indene or styrene are the polycyclic lactams.

The dehydrogenation of the tetrahydro-7*H*-indeno-[2,1-*c*][1,5]-naphthyridine derivatives with DDQ yields the corresponding 7*H*-indeno-[2,1-*c*][1,5]-naphthyridines. In order to increase the diversity of the polycyclic derivatives the methylene group of compounds can be transformed into a carbonyl group by oxidation with $Mn(OAc)_3$ in a microwave reactor in acetic acid to yield the corresponding 7*H*-indeno-[1,5]-naphthyridin-7-ones. The carbonyl group present in these derivatives can be reduced to the hydroxyl group to obtain the hydroxylated derivatives.

With the aim of synthesizing aromatic flat compounds in only one step, the [4+2] cycloaddition reaction between aldimines and acetylenes in the presence of $BF_3{\cdot}Et_2O$ as Lewis acid was explored and the desired 1,5-naphthyridines were obtained in good yields. However, if the process is performed in the presence of a Bronsted acid (diphenylphosponic acid) the reaction of imine **3h** (R = 4-CF_3-C_6H_4) with 4-methoxyphenylacetylene led to the formation of propargylamine. In the special case of using the functionalized imine **3l** (R=2-MeO_2C-C_6H_4) the product formed rather than the

tetracyclic lactam, as it was described for olefins, the oxo-*N*-pyridylactams were obtained. These results may suggest a step-by-step mechanism instead of a concerted one, as happened in the case of employing olefins as the dienophiles for the Povarov reaction.

All the synthesized derivatives were subjected to biological evaluation as topoisomerase I inhibitors and to *in vitro* cytotoxicity experiments in different cancer cell lines.

The indeno-[1,5]-naphthyridine derivatives, the dehydrogenated forms, the carbonyl derivatives and hydroxyl derivatives act as Topoisomerase I inhibitors and their effect is stronger than CPT. Likewise, 1,5-naphthyridines also act as Topoisomerase I inhibitors and different grades of inhibition were observed depending on the different substituents in the molecule. The *metha* substitution of the aromatic ring in the position 2 of the naphthyridine has a positive effect in terms of inhibition. When a biphenyl group is present in the position 4, the 1,5-naphthyridines present a stronger inhibitory effect compared to CPT, showing TopI full inhibition even at 3 minutes.

The newly synthesized indeno[1,5]-naphthyridine derivatives were explored for antiproliferative activity against different human cancer cell lines: A549 (carcinomic human alveolar basal epithelial cell), BT20 (human breast cancer) and SKOV3 (human ovarian carcinoma). A broad spectrum of antiproliferative activity against the cancer cell lines tested in culture can be observed. For tetrahydro-indeno1,5-naphthyridines the best cytotoxic result is found in lung cancer cell line (A549) for derivative **9f** (R= 2,4-F2C6H3) containing two fluorine atoms in its structure with an IC50 of 6.4±0.6 µM. Furthermore, for the corresponding dehydrogenated compounds, the fluorinated indeno-[1,5]-naphthyridine derivative **10f** (R= 2,4-$F_2C_6H_3$) presents the highest cytotoxic effect, with an IC50 of 1.7±0.1 µM, against the A549 cell line *in vitro*, and a high cytotoxicity, with an IC_{50} of 6.4±0.3 µM against the SKOV3 cell line *in vitro*. On the other hand, indeno-1,5-naphthyridine derivatives **10d** (R= 4-NO2C6H4) and indeno-1,5-

naphthyridine derivative **10e** (R= 4-pyridyl), showed high cytotoxicity against A549 cell line *in vitro*, with an IC_{50} of 5.7±0.6 and 2.9±0.9 μM, respectively. Regarding the derivatives with different structural modification, as for example the carbonyl derivative **16c** (R= 2-Naphthyl) presents the better cytotoxic effect, with an IC_{50} of 0.8±0.02 μM towards lung cancer cell line. Moreover the corresponding hydroxyl derivative **17c** (R= 2-Naphthyl) shows an interesting IC_{50} of 5.5±0.02 μM in the same cell line tested *in vitro*.

Lung cancer cell line is the most sensitive cell line towards the derivatives tested. All the compounds present better cytotoxic effect in lung cancer cell line (A549) whereas ovarian and breast cancer are not so sensitive to the synthesized derivatives. Some of the most cytotoxic compounds were tested in healthy lung cells (MRC 5) and they proved to kill lung cancer (A549) cells, whereas it hardly affects normal lung cells. The best candidate (indeno-1,5-naphthyridinone **16c** with an IC_{50}= 0.8±0.02 μM in lung cancer cell line (A549), is able to kill lung cancer cells but it hardly affects normal lung cells (MRC 5) growth.

The cytotoxicity of 1,5-naphthyridine derivatives was also studied in the same human cancer cell lines and the results showed a great variety of antiproliferative activities. Compound **19j** with a 4-$NO_2C_6H_4$ group in the position 2 and a biphenyl group in position 4 shows the best cytotoxic value in lung cancer cells with an IC_{50} of 1.9±0.4 μM and in breast cancer cell line too with an IC_{50} of 3.9±0.3 μM. Derivatives with a fluorine atom in *para* position **19m**, **19o** and **19t** show good cytotoxicity values with IC_{50} of 2.8±0.2 μM, IC_{50} of 9.2±0.4 μM and IC_{50} of 8.6±0.3 μM, respectively. Moreover, the *metha* substitution in the aromatic aldehydes seems to be interesting both in terms of TopI inhibitory effect and in terms of cytotoxicity. The cytotoxicity values for these derivatives **19f**, **19g**, **19k** and **19q** are IC_{50}= 6.6±0.3 μM, IC_{50}= 6.8±0.5 μM, IC_{50}= 7.4±0.5 μM, IC_{50}= 9.8±0.4 μM and IC_{50}= 4.4±0.4 μM, respectively. Similarly as for the case of the indeno-[1,5]-naphthyridine derivatives, some of the most cytotoxic compounds were tested in normal lung cells (MRC 5) and they proved to kill lung cancer cells (A549), whereas it hardly affects normal lung cells.

6. Experimental Section

6.1. General analytical techniques

6.1.1. Analytic techniques

NMR spectra were recorded with Varian Unity Plus (300 MHz) and Bruker Avance 400 (400MHz) spectrometers and recorded at 25°C. NOESY, HMQC, HMBC and COSY experiments were performed in Bruker Avance 400 (400 MHz) spectrometer. The solvent used for the NMR experiments is deuterium chloroform ($CDCl_3$). Chemical shifts for ^{1}H NMR spectra are reported in ppm downfield from TMS, chemical shifts for ^{13}C NMR spectra are recorded in ppm relative to the internal chloroform reference (δ = 77.2 ppm for ^{13}C), chemical shifts for ^{19}F NMR are reported in ppm downfield from fluorotrichloromethane ($CFCl_3$). Coupling constants (*J*) are reported in Hertz. The terms m, s, d, t, q refer to multiplet, singlet, doublet, triplet, quartet. ^{13}C NMR and ^{19}F NMR were broadband decoupled from hydrogen nuclei.

Infrared spectra (IR) were recorded with the Nicolet iS10 infrared spectrometer, by means of absorbance frequencies given at maximum of intensity in cm^{-1}.

MS spectra were obtained in a Hewlett-Packard 5973 chromatographic spectrometer and HRMS spectra were obtained in a LC/Q-TOF spectrometer (serial num US93620455) at 70 eV with ionization source Agilent Jet Stream with the following conditions:

Mobile phase: 0.1% formic acid: 0.1% methanol and formic acid (50:50)

Ionization: Gas T= 325°C

Drying gas 5 ml/min

Nebulizer 40 psi

Shealt gas T. 375°C

Shealt gas flow 11 l/min

Vcap: 4000 V

Melting points were determined with an Electrothermal Digital Melting Point Apparatus, Büchi MPB-540, without correction.

6.1.2. Solvents and reagents

The solvents used for chromatography, recrystalizations and extractions possess high purity, so it was not necessary to distillate beforehand. All solvents employed in the reactions were dried over molecular sieves (4Å) prior to their use.

All reagents from commercial suppliers were used without further purification. All other reagents were recrystallized or distilled when necessary. Reactions were performed under a nitrogen dried atmosphere.

Analytical TLCs were performed with silica gel 60 F254 or neutral alumina plates. Visualization was accomplished by UV light. Column chromatography was carried out using silica gel 60 (230-400 mesh ASTM).

Column chromatography was carried out using silica gel 60 (230-400 mesh ASTM) or neutral alumina (70-290 mesh ASTM).

6.2. Experimental Section-Synthesis of compounds

6.2.1. Synthesis of imines 3

General procedure

To a solution of 3-aminopyridine **1** (5 mmol, 0.471 g) in $CHCl_3$ (10 ml) the corresponding aldehydes **2** (5 mmol) were added under nitrogen atmosphere and in the presence of molecular sieves (4Å). The mixture was stirred at the opportune temperature until consumption of starting materials was checked by ^{1}H-NMR, ^{13}C-NMR and ^{19}F NMR spectroscopy. In all cases, products were used *in situ* for further reactions.

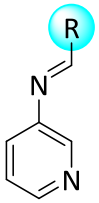

3

N-(Phenylmethylene)-3-pyridinamine (3a)

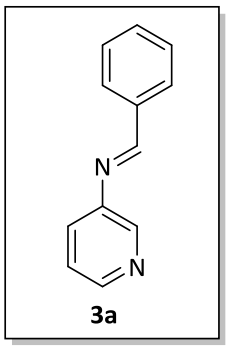

3a

The general procedure for the synthesis of imines was followed using benzaldehyde (5 mmol, 0.508 ml) and the reaction mixture was stirred for 48 hours at room temperature.

^{1}H NMR (300 MHz, $CDCl_3$) δ = 7.30-7.34 (m, $1H_{arom}$), 7.49-7.56 (m, $4H_{arom}$), 7.87-7.94 (m, $2H_{arom}$), 8.47-8.50 (m, $2H_{arom}$ and HC=N) ppm.

^{13}C NMR (75 MHz, $CDCl_3$) δ = 123.5(HC_{arom}), 126.7 (HC_{arom}), 128.4 ($2HC_{arom}$), 129.5 ($2HC_{arom}$),130.5 (HC_{arom}), 136.3 (C_{arom}), 142.3 (HC_{arom}), 143.6 (C_{arom}), 148.5 (HC_{arom}), 160.3 (HC=N) ppm.

N-(1-Naphthalenylmethylene)-3-pyridinamine (3b)

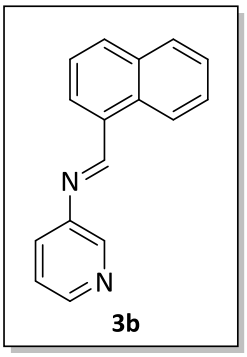

3b

The general procedure for the synthesis of imines was followed using 1-naphthaldehyde (5 mmol, 0.679 ml) and the reaction mixture was stirred for 48 hours at refluxing chloroform.

^{1}H NMR (300 MHz, $CDCl_3$) δ = 7.20-7.29 (m, 1H, H_{arom}), 7.40-7.65 (m, 2H, H_{arom}), 7.80-8.17 (m, 4H, H_{arom}), 8.42-8.61 (m, 2H, H_{arom}), 8.84-9.18 (m, 3H, 2 H_{arom} and HC=N) ppm.

^{13}C NMR (75 MHz, $CDCl_3$) δ = 123.9 (HC_{arom}), 124.5 (HC_{arom}), 125.1 (HC_{arom}), 125.5 (HC_{arom}), 126.6 (HC_{arom}), 128.0 (C_{arom}), 128.1 ($2HC_{arom}$), 129.1 (HC_{arom}), 131.0 (C_{arom}), 132.8 (HC_{arom}), 135.5 (C_{arom}), 136.9 (HC_{arom}), 142.9 (C_{arom}), 147.4 (HC_{arom}), 162.8 (HC=N) ppm.

N-(2-Naphthalenylmethylene)-3-pyridinamine (3c)

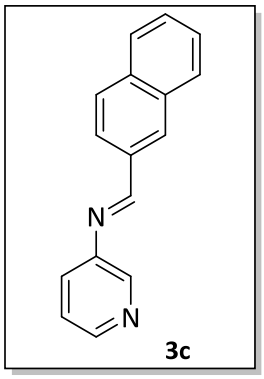

3c

The general procedure for the synthesis of imines was followed using 2-naphthaldehyde (5 mmol, 0.781 g) and the reaction mixture was stirred for 24 hours at refluxing chloroform.

^{1}H NMR (300 MHz, $CDCl_3$) δ = 7.17-7.25 (m, 1H, H_{arom}), 7.46-7.54 (m, 3H, H_{arom}), 7.78-7.93 (m, 3H, H_{arom}), 8.00-8.22 (m, 2H, H_{arom}), 8.40-8.50 (m, 3H, 2 H_{arom} and HC=N) ppm.

^{13}C NMR (75 MHz, $CDCl_3$) δ = 123.4 (HC_{arom}), 126.5 (HC_{arom}), 127.5 (HC_{arom}), 127.6 (HC_{arom}), 127.7 ($2HC_{arom}$), 128.5 (HC_{arom}), 128.6 ($2HC_{arom}$), 131.6 (HC_{arom}), 132.7 (HC_{arom}), 133.1 (C_{arom}), 134.9 (C_{arom}), 142.4 (C_{arom}), 146.8 (C_{arom}), 161.7 (HC=N) ppm.

N-[(4-Nitrophenyl)methylene]-3-pyridinamine (3d)

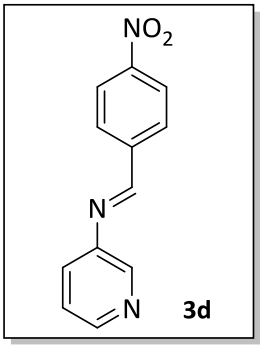

3d

The general procedure for the synthesis of imines was followed using 4-nitrobenzaldehyde (5 mmol, 0.756 g) and the reaction mixture was stirred for 18 hours at refluxing chloroform.

^{1}H NMR (300 MHz, $CDCl_3$) δ = 7.24-7.38 (m, 1H, H_{arom}), 7.46-7.63 (m, 1H, H_{arom}), 8.03 (d, $^{3}J_{HH}$ = 8.2 Hz, 2H, H_{arom}), 8.28 (d, $^{3}J_{HH}$ = 8.2 Hz, 2H, H_{arom}), 8.37-8.50 (m, 3H, 2 H_{arom} and HC=N) ppm.

^{13}C NMR (75 MHz, $CDCl_3$) δ = 124.0 ($2HC_{arom}$), 127.8 (HC_{arom}), 129.6 ($2HC_{arom}$), 141.1 (C_{arom}), 142.8 (HC_{arom}), 146.7 (C_{arom}), 148.2 ($2HC_{arom}$), 149.6 (C_{arom}), 159.5 (HC=N) ppm.

N-(4-Pyridinylmethylene]-3-pyridinamine (3e)

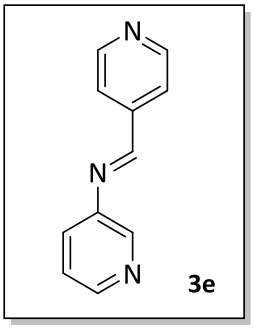

3e

The general procedure for the synthesis of imines was followed using 4-pyridinecarboxaldehyde (5 mmol, 0.471 ml) and the reaction mixture was stirred for 48 hours at refluxing chloroform.

^{1}H NMR (300 MHz, $CDCl_3$) δ = 7.35-7.79 (m, 2H, H_{arom}), 7.77 (d, $^{3}J_{HH}$ = 6.0 Hz, 2H, H_{arom}), 8,48-8.56 (m, 3H, H_{arom} and HC=N), 8.79 (d, $^{3}J_{HH}$ = 6.0 Hz, 2H, H_{arom}) ppm.

^{13}C NMR (75 MHz, $CDCl_3$) δ = 122.3 ($2HC_{arom}$), 123.7 (HC_{arom}), 127.8 (HC_{arom}), 142.1 (C_{arom}), 142.5 (HC_{arom}), 146.7 (C_{arom}), 148.1 (HC_{arom}), 150.7 ($2HC_{arom}$), 159.8 (HC=N) ppm.

N-[(2,4-Difluorophenyl)methylene]-3-pyridinamine(3f)

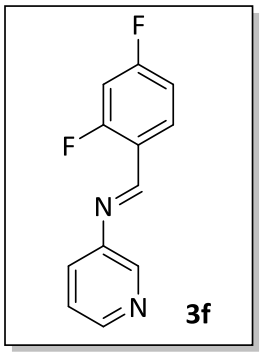

3f

The general procedure for the synthesis of imines was followed using 2,4-difluorobenzaldehyde (5 mmol, 0.547 ml) and the reaction mixture was stirred for 20 hours at refluxing chloroform.

^{1}H NMR (300 MHz, $CDCl_3$) δ = 6.76-6.92 (m, 2H, $H_{arom.}$), 7.24 (d, $^{3}J_{HH}$ = 8.1 Hz, 1H, H_{arom}), 7.43 (d, $^{3}J_{HH}$ = 8.1 Hz, 1H, H_{arom}), 8.07-8.14 (m, 1H, H_{arom}), 8.42-8.87 (m, 3H, 3H, H_{arom} and HC=N) ppm.

^{13}C NMR (75 MHz, $CDCl_3$) δ = 104.4 (dd, $^2J_{CF}$ = 25.4 Hz, $^2J_{CF}$ = 25.4 Hz, HC_{arom}), 112.6 (dd, $^2J_{CF}$ = 21.8 Hz, $^4J_{CF}$ = 3.8 Hz, HC_{arom}), 120.4 (dd, $^2J_{CF}$ = 9.3 Hz, $^4J_{CF}$ = 3.8 Hz, C_{arom}), 123.8 (C_{arom}), 127.8 (HC_{arom}), 129.7 (dd, $^3J_{CF}$ = 10.1 Hz, $^3J_{CF}$ = 3.8 Hz, HC_{arom}), 143.1 (HC_{arom}), 147.6 ($2HC_{arom}$), 154.1 (dd, $^3J_{CF}$ = 4.5 Hz, $^5J_{CF}$ = 1.9 Hz, HC=N), 163.4 (dd, $^1J_{CF}$ = 256.8 Hz, $^3J_{CF}$ = 12.6 Hz, C_{arom}), 165.8 (dd, $^1J_{CF}$ = 254.8 Hz, $^3J_{CF}$ = 12.6 Hz, C_{arom}) ppm.

^{19}F NMR (376 MHz, $CDCl_3$) δ = -103.6 (d, $^4J_{FF}$ = 7.5 Hz), -117.2 (d, $^4J_{FF}$ = 7.5 Hz) ppm.

N-[(3,4-Difluorophenyl)methylene]-3-pyridinamine(3g)

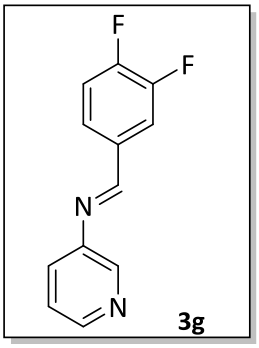

3g

The general procedure for the synthesis of imines was followed using 3,4-difluorobenzaldehyde (5 mmol, 0.552 ml) and the reaction mixture was stirred for 20 hours at refluxing chloroform.

^{1}H NMR (300 MHz, $CDCl_3$) δ = 7.09-7.90 (m, 5H, $H_{arom.}$), 8.33 (s, 1H, H_{iminic}), 8.36-8.41 (m, 2H, H_{arom}) ppm.

^{13}C NMR (75 MHz, $CDCl_3$) δ = 116.9 (dd, $^2J_{CF}$ = 85.8 Hz, $^4J_{CF}$ = 17.3 Hz, $2HC_{arom}$), 123.5 (HC_{arom}), 125.8 (dd, $^3J_{CF}$ = 7.1Hz, $^4J_{CF}$ = 3.6 Hz, HC_{arom}), 127.4 (HC_{arom}), 132.7 (dd, $^3J_{CF}$ = 5.6 Hz, $^4J_{CF}$ = 3.7 Hz, C_{arom}), 142.1 (HC_{arom}), 146.7 (HC_{arom}), 147.2 (C_{arom}), 150.5 (dd, $^1J_{CF}$ = 250.4 Hz, $^2J_{CF}$ = 13.6 Hz, C_{arom}), 152.3 (dd, $^1J_{CF}$ = 256.0 Hz, $^2J_{CF}$ = 13.6 Hz, C_{arom}), 160.0 (HC=N) ppm.

^{19}F NMR (376 MHz, $CDCl_3$) δ = -131.8 (d, $^3J_{FF}$ = 21.4 Hz), -133.6 (d, $^3J_{FF}$ = 21.4 Hz) ppm.

N-[(4-Trifluoromethyl)phenylmethylene]-3-pyridinamine(3h)

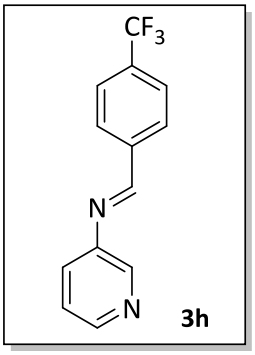

The general procedure for the synthesis of imines was followed using 4-trifluorobenzaldehyde (5mmol, 0.68ml) and the reaction mixture was stirred for 30 hours at room temperature. Compound **3h** was obtained as a white solid after evaporation.

^{1}H NMR (300 MHz, $CDCl_3$) δ = 7.35 (dd, $^{3}J_{HH}$ = 7.9 Hz, $^{3}J_{HH}$ = 4.0 Hz, 1H, H_{arom}), 7.55 (d, $^{3}J_{HH}$ = 8.1 Hz, 1H, H_{arom}), 7.75 (d, $^{3}J_{HH}$ = 8.2 Hz, 2H, H_{arom}), 8.04 (d, $^{3}J_{HH}$ = 8.09 Hz, 2H, H_{arom}), 8.53 (m, 3H, H_{arom} and HC=N) ppm.

^{13}C NMR (75 MHz,$CDCl_3$) δ = 120.5 ($2HC_{arom}$), 123.9 (HC_{arom}), 126.1 (q, $^{2}J_{CF}$ = 3.7 Hz, C-CF_3), 128.1 (HC_{arom}), 129.4 ($3HC_{arom}$), 142.8 ($2C_{arom}$), 142.9 (q, $^{1}J_{CF}$ = 435 Hz, HC_{arom}), 148.0 (HC_{arom}), 160.4 (HC=N) ppm.

^{19}F NMR (282 MHz, $CDCl_3$) δ = -63.3 ppm.

N-[(4-Fluorophenyl)methylene]-3-pyridinamine(3i)

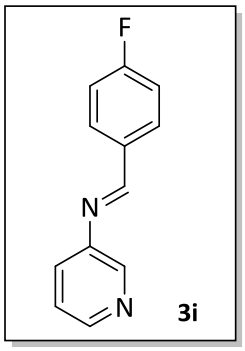

The general procedure for the synthesis of imines was followed using 4-fluorobenzaldehyde (5 mmol, 0.536 ml) and the reaction mixture was stirred for 30 hours at room temperature.

^{1}H NMR (300 MHz, $CDCl_3$) δ = 7.16-7.22 (m, 2H, H_{arom}.), 7.33 (dd, $^{3}J_{HH}$ = 4.9 Hz, $^{3}J_{HH}$ = 7.5 Hz, 1H, H_{arom}), 7.52 (dd, $^{3}J_{HH}$ = 8.1 Hz, $^{4}J_{HH}$ = 1.5 Hz, 1H, H_{arom}), 7.91-7.96 (m, 2H, H_{arom}), 8.44 (d, $^{4}J_{HH}$ = 1.5 Hz, 1H, H_{arom}), 8.50 (s, 1H, HC=N) ppm

^{19}F NMR (282 MHz, $CDCl_3$) δ = -107.4 ppm.

N-[(3-Nitrophenyl)methylene]-3-pyridinamine(3j)

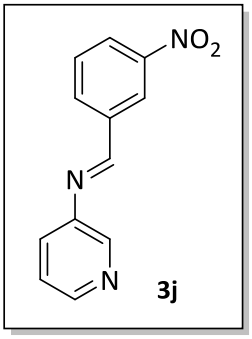

3j

The general procedure for the synthesis of imines was followed using 3-nitrobenzaldehyde (5 mmol, 0.756 g) and the reaction mixture was stirred for 15 hours at room temperature.

^{1}H NMR (300 MHz, $CDCl_3$) δ = 7.26-7.29 (m, 1H, H_{arom}), 7.47-7.50 (m, 1H, H_{arom}), 7.59-7.63 (t, $^{3}J_{HH}$ = 8.1 Hz, 1H, H_{arom}), 8.18 (d, $^{3}J_{HH}$ = 8.2 Hz, 2H, H_{arom}), 8.25-8.28 (m, 1H, H_{arom}), 8.43-8.45 (m, 1H, H_{arom}), 8.48 (s, 1H, HC=N), 8.67-8.68 (m, H, $2H_{arom}$) ppm.

^{13}C NMR (75 MHz, $CDCl_3$) δ = 123.5 (HC_{arom}), 123.7 (HC_{arom}), 126.0 (HC_{arom}), 127.8 (HC_{arom}), 129.9 (HC_{arom}), 134.2 (HC_{arom}), 137.2 (C_{arom}), 144.4 (HC_{arom}), 146.6 (C_{arom}), 148.0 (HC_{arom}), 148.7 (C_{arom}), 159.0 (HC=N) ppm.

N-[(3-Methoxyphenyl)methylene]-3-pyridinamine(3k)

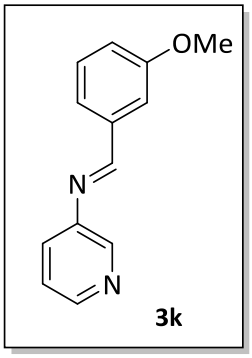

3k

The general procedure for the synthesis of imines was followed using 3-methoxybenzaldehyde (5 mmol, 0.609 ml) and the reaction mixture was stirred for 12 hours at refluxing chloroform.

^{1}H NMR (300 MHz,$CDCl_3$) δ = 3.8 (s, 3H, OCH_3), 7.18-7.23 (m, 1H, H_{arom}), 7.31-7.34 (m, 3H, H_{arom}), 7.41-7.44 (m, 2H, H_{arom}), 8.33 (s, 1H, HC=N), 8.38-8.41 (m, 2H, H_{arom}) ppm.

^{13}C NMR (75 MHz,$CDCl_3$) δ = 55.1 (OCH_3), 111.7 (HC_{arom}), 118.5 (HC_{arom}), 122.3 (HC_{arom}), 123.4 (HC_{arom}), 127.5 (HC_{arom}), 129.5 (HC_{arom}), 136.8 (C_{arom}), 142.4 (HC_{arom}), 146.9 (HC_{arom}), 147.4 (C_{arom}), 159.7 (C_{arom}), 161.7 (HC=N) ppm.

2-[(3-Pyridinyl)iminomethyl]benzoic acid methyl ester (3l)

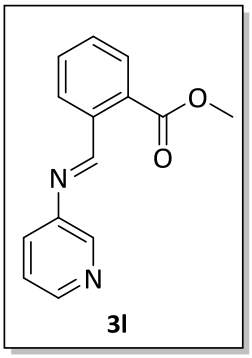

3l

The general procedure for the synthesis of imines was followed using methyl 2-formylbenzoate (5 mmol, 0.695 ml) and the reaction mixture was stirred for 12 hours at refluxing chloroform.

^{1}H NMR (300 MHz,$CDCl_3$) δ = 3.93 (s, 3H, CH_3), 7.28-7.39 (m, 1H, H_{arom}), 7.56-7.69 (m, 3H, H_{arom}), 8.02 (d, $^{3}J_{HH}$ = 7.7 Hz, 1H, H_{arom}), 8.25 (d, $^{3}J_{HH}$ = 7.7 Hz, 1H, H_{arom}), 8.48-8.59 (m, 2H, H_{arom}), 9.27 (s, 1H, HC=N) ppm.

^{13}C NMR (75 MHz,$CDCl_3$) δ = 52.7 (CH_3), 123.9 (HC_{arom}), 128.1 (HC_{arom}), 128.7 (HC_{arom}), 130.7 ($2HC_{arom}$), 130.9 (C_{arom}), 131.1 (HC_{arom}), 132.7 (HC_{arom}), 136.9 (C_{arom}), 143.4 (HC_{arom}), 147.6 (HC_{arom}), 147.9 (C_{arom}), 161.9 (HC=N), 167.3 (COO) ppm.

6.2.2. Synthesis of tetrahydro-7H-indeno[2,1-c][1,5]-naphthyridine derivatives 9

General procedure A

Indene (7.5mmol, 0.868 ml) and $BF_3{\cdot}Et_2O$ (10mmol, 1.230 ml) were added to a solution of the previously prepared aldimines **3** (5 mmol) in $CHCl_3$ (10 ml). The mixture was stirred at the appropriate temperature until TLC and ^1H NMR spectroscopy indicated the disappearance of imine **3** signals. The reaction mixture was washed with 2M aqueous solution of NaOH (20 ml) and water (20 ml), extracted with dichloromethane (20 ml) and dried over anhydrous $MgSO_4$. The removal of the solvent under vacuum led to an oil or solid that was purified by flash chromatography on silica gel flash column chromatography (eluent: Hexane/AcOEt) to afford the desired products **9**.

General procedure B

A mixture of 3-aminopyridine (5 mmol, 0.471 g), freshly destiled aldehydes (5 mmol) in $CHCl_3$ (10 ml), indene (7.5 mmol, 0.868 ml) and two equivalents of $BF_3{\cdot}Et_2O$ (10 mmol, 1.230 ml) in the presence of molecular sieves (4 Å) was stirred and heated to reflux until TLC and ^1H NMR spectroscopy analysis indicated the consumption of the starting materials. The molecular sieves were removed by filtration and the resulting solution was diluted with methylene chloride (20 ml), washed with a solution of NaOH 2M (25 ml), extracted with methylene chloride (2 x 15 ml) and dried over $MgSO_4$. Removal of the solvent under vacuum led to an oil or solid that was purified by flash chromatography on silica gel using a gradient of elution of 10-40% ethyl acetate in hexane to afford compounds **9**.

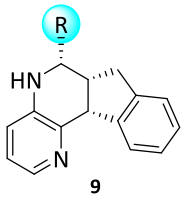

9

6-Phenyl-6,6a,7,11b-tetrahydro-5H-indeno[2,1-c][1,5]naphthyridine (9a)

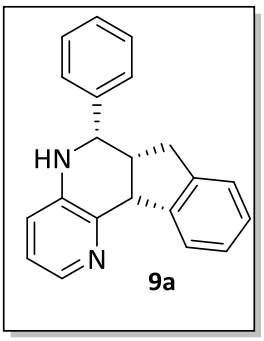

9a

The general procedure A was followed using imine **3a,** prepared *in situ*, and the reaction mixture was stirred at refluxing chloroform for 48 h affording a mixture of compounds **9a**/**10a**. Compound **9a** and **10a** were obtained as yellow solids after purification by flash chromatography (1.119 g, 75% and 0.191 g, 13%, respectively). When the general procedure B was followed using benzaldehyde (5 mmol, 0.508 ml) for 21h a mixture of compounds **9a**/**10a** (1.044 g, 70% and 0.103 g, 7%, respectively) was obtained.*

m.p.(°C) 55-56 (ethyl acetate/hexane).

IR νmax 3356, 3021, 2912, 1574, 1457 cm^{-1}.

^{1}H NMR (300 MHz, $CDCl_3$) δ = 2.46 (dd, $^2J_{HH}$ = 20.2 Hz, $^3J_{HH}$ = 12.6 Hz, 1H, CH_2), 3.27-3.34 (m, 2H, HC_{6a}-$C\underline{H}_2$), 3.84 (s, 1H, NH), 4.70 (d, $^3J_{HH}$ = 7.4 Hz, 1H, HC_{11b}), 4.80 (s, 1H, HC_6), 6.84-6.93 (m, $3H_{arom}$), 7.08-7.79 (m, $8H_{arom}$), 8.06 (d, $^3J_{HH}$ = 4.4 Hz, $1H_{arom}$) ppm.

^{13}C NMR (75 MHz, $CDCl_3$) δ = 31.4 (CH_2), 47.8 (HC_{6a}), 49.1 (HC_{11b}), 57.6 (HC_6), 121.7 (HC_{arom}), 122.1 (HC_{arom}), 124.3 (HC_{arom}), 126.3 (HC_{arom}), 126.5 (HC_{arom}), 126.7 (HC_{arom}), 127.1 (HC_{arom}), 127.6 (HC_{arom}), 128.7 (HC_{arom}), 140.6 (HC_{arom}), 141.4 (C_{arom}), 141.9 (C_{arom}), 142.5 (C_{arom}), 144.6 (C_{arom}), 145.1 (C_{arom}) ppm.

HRMS (CI): calculated for $C_{21}H_{18}N_2$ $[M]^+$ 298.1470 found 298.1466.

See data for compound **10a in section 6.2.4.*

6-(1-Naphtalenyl)-6,6a,7,11b-tetrahydro-5H-indeno[2,1-c][1,5]naphthyridine (9b)

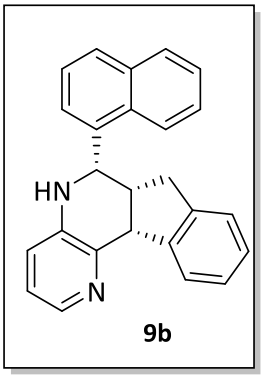

9b

The general procedure A was followed using imine **3b,** prepared *in situ*, and the reaction mixture was heated at refluxing chloroform for 48 h affording a mixture of compounds **9b**/**10b** (12%/60%). Compounds **9b** and **10b** were obtained as yellow solids after purification by flash chromatography (1.045 g, 60% and 0.207 g, 12%, respectively). *

m.p.(°C) 121-122 (ethyl acetate/hexane).

IR νmax 3040, 2980, 1748, 1222, 1182 cm^{-1}.

^{1}H NMR (300 MHz, $CDCl_3$) δ = 2.26 (dd, $^{2}J_{HH}$ = 15.7 Hz, $^{3}J_{HH}$ = 8.1 Hz, 1H, CH_2), 3.28-3.67 (m, 2H, HC_{6a}-$C\underline{H}_2$), 3.81 (s, 1H, NH), 4.83 (d, $^{3}J_{HH}$ = 8.1 Hz, 1H, HC_{11b}), 5.56 (s, 1H, HC_6), 6.93-7.20 (m, 4H, H_{arom}), 7.53-7.62 (m, 4H, H_{arom}), 7.81-7.97 (m, 4H, H_{arom}), 8.10-8.17 (m, 2H, H_{arom}) ppm.

^{13}C NMR (75 MHz, $CDCl_3$) δ = 32.0 (CH_2), 45.7 (HC, C_{6a}), 49.2 (HC, C_{11b}), 53.4 (HC, C_6), 121.9 (HC_{arom}), 122.6 (HC_{arom}), 122.7 (HC_{arom}), 123.0 (HC_{arom}), 124.5 (HC_{arom}), 125.7 (HC_{arom}), 126.0 (HC_{arom}), 126.5 (HC_{arom}), 126.6 (HC_{arom}), 126.9 (HC_{arom}), 127.3 (HC_{arom}), 128.3 (HC_{arom}), 129.4 (HC_{arom}), 130.7 (C_{arom}), 134.1 (C_{arom}), 137.5 (C_{arom}), 140.8 (HC_{arom}), 142.2 (C_{arom}), 142.6 (C_{arom}), 144.8 (C_{arom}), 145.6 (C_{arom}) ppm.

HRMS (CI): calculated for $C_{25}H_{20}N_2$ $[M]^+$ 348.1626 found 348.1622.

See data for compound **10b in section 6.2.4*.

6-(2-Naphtalenyl)-6,6a,7,11b-tetrahydro-5H-indeno[2,1-c][1,5]naphthyridine (9c)

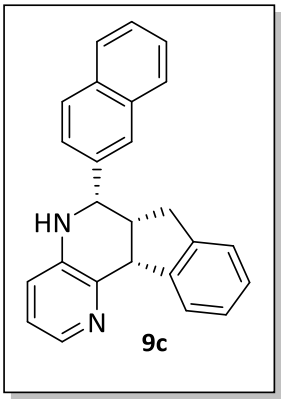

9c

The general procedure A was followed using imine **3c**, prepared *in situ*, and the reaction mixture was stirred at refluxing chloroform for 48 h affording a mixture of compounds **9c**/**10c**. Compounds **9c** and **10c** were obtained as yellowish solids after purification by flash chromatography (0.348 g, 20% and 0.947 g, 55%, respectively). When the general procedure B was followed using 2-naphthaldehyde (5 mmol, 0.781 g) for 36 h a mixture of compounds **9c**/**10c** (0.871 g, 50% and 0.172 g, 10%, respectively) was obtained.*

m.p.(°C) 115-117 (ethyl acetate/hexane).

IR νmax 3062, 1584, 1420, 1284, 900, 790 cm^{-1}.

^{1}H NMR (300 MHz, $CDCl_3$) δ = 2.31 (dd, $^2J_{HH}$ = 14.3 Hz, $^3J_{HH}$ = 8.3 Hz, 1H, CH_2), 3.19-3.28 (m, 2H, HC_{6a}-$C\underline{H}_2$), 3.85 (s, 1H, NH), 4.61- 4.64 (m, 1H, HC_{11b}), 4.81 (s, 1H, HC_6), 6.76-6.83 (m, 2H, H_{arom}), 6.92-7.10 (m, 3H, H_{arom}), 7.41-7.49 (m, 3H, H_{arom}), 7.70 (d, $^3J_{HH}$ = 7.4 Hz, 1H, H_{arom}), 7.77-7.81 (m, 3H, H_{arom}), 7.87 (s, 1H), 7.98 (dd, $^4J_{HH}$ = 2.3 Hz, $^3J_{HH}$ = 4.1 Hz, 1H, H_{arom}) ppm.

^{13}C NMR (75 MHz, $CDCl_3$) δ δ = 31.5 (CH_2), 47.6 (HC, C_{6a}), 49.1 (HC, C_{11b}), 57.5 (HC, C_6), 121.6 (HC_{arom}), 122.1 (HC_{arom}), 124.3 (HC_{arom}), 124.7 (HC_{arom}), 124.9 (HC_{arom}), 125.9 (HC_{arom}), 126.3 (2 HC_{arom}), 126.7 (HC_{arom}), 127.0 (HC_{arom}), 127.7 (HC_{arom}), 127.9 (HC_{arom}), 128.3 (HC_{arom}), 132.9 (C_{arom}), 133.4 (C_{arom}), 139.3 (C_{arom}), 140.6 (HC_{arom}), 141.3 (C_{arom}), 142.4 (C_{arom}), 144.6 (C_{arom}), 145.1 (C_{arom}) ppm.

HRMS (CI): calculated for $C_{25}H_{20}N_2$ $[M]^+$ 348.1626 found 348.1631.

See data for compound **10b in section 6.2.4.*

6-(4-Nitrophenyl)-6,6a,7,11b-tetrahydro-5H-indeno[2,1-c][1,5]naphthyridine (9d)

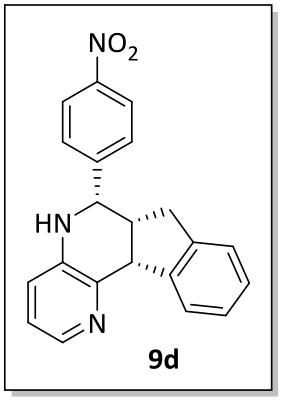

9d

The general procedure A was followed using imine **3d**, prepared *in situ*, and the reaction mixture was stirred at refluxing chloroform for 36 h affording compound **9d** as a yellow solid after purification by flash chromatography (1.200 g, 70%). When general procedure B was followed using 4-nitrobenzaldehyde (5 mmol, 0.756 g) for 36 h compound **9d** was obtained as a yellow solid (1.149 g, 67%).

m.p.(°C) 178-179 (ethyl acetate/hexane).

IR νmax 2960, 2925, 1724, 1344, 795 cm^{-1}.

^{1}H NMR (300 MHz, $CDCl_3$) δ = 2.38 (dd, $^{2}J_{HH}$ = 14.0 Hz, $^{3}J_{HH}$ = 6.5 Hz, 1H, CH_2), 3.21-3.31 (m, 2H, HC_{6a}-C$\underline{H}_2$), 3.89 (s, 1H, NH), 4.72 (d, $^{3}J_{HH}$ = 8.1 Hz, 1H, HC_{11b}), 4.89 (s, 1H, HC_6), 6.94-7.22 (m, 6H, H_{arom}), 7.68 (d, $^{3}J_{HH}$ = 8.6 Hz, 2H, H_{arom}), 8.09-8.11 (m, 1H, H_{arom}), 8.29 (d, $^{3}J_{HH}$ = 8.6 Hz, 2H, H_{arom}) ppm.

^{13}C NMR (75 MHz, $CDCl_3$) δ = 31.2 (CH_2), 47.2 (HC_{6a}), 48.8 (HC_{11b}), 57.1 (HC_6), 121.8 (HC_{arom}), 122.4 (HC_{arom}), 124.2 ($2HC_{arom}$), 124.3 (HC_{arom}), 126.4 (HC_{arom}), 126.7 (HC_{arom}), 127.2 (HC_{arom}), 127.4 ($2HC_{arom}$), 140.5 (C_{arom}), 141.2 ($2C_{arom}$), 141.7 (HC_{arom}), 144.1 (C_{arom}), 144.5 (C_{arom}), 147.4 (C_{arom}), 149.3 (C_{arom}) ppm.

HRMS (CI): calculated for $C_{21}H_{17}N_3O_2$ $[M]^+$ 343.1321 found 343.1320.

6-(Pyridin-4-yl)-6,6a,7,11b-tetrahydro-5H-indeno[2,1-c][1,5]naphthyridine (9e)

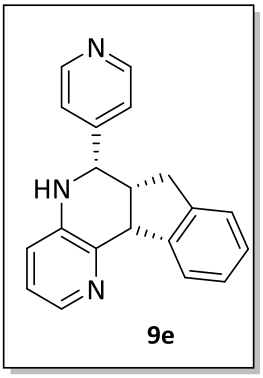

9e

The general procedure A was followed using imine **3d**, prepared *in situ*, and the reaction mixture was stirred at refluxing chloroform for 30 h affording compound **9e** as a white solid after purification by flash chromatography (0.897 g, 60%). When general procedure B was followed using 4-pyridinecarboxaldehyde (5 mmol, 0.471 ml) for 60 h compounds **9e** was obtained as a white solid (1.046 g, 70%).

m.p.(°C) 175-176 (ethyl acetate/hexane).

IR νmax 2970,1780, 1650, 960, 820 cm^{-1}.

^{1}H NMR (300 MHz, $CDCl_3$) δ = 2.35 (dd, $^2J_{HH}$ = 14.7 Hz, $^3J_{HH}$ = 7.5 Hz, 1H, CH_2), 3.13-3.28 (m, 3H, HC_{6a}-C<u>H</u>$_2$, NH), 4.62-4.72 (m, 2H, HC_{11b}, HC_6), 6.81-7.18 (m, 5H, H_{arom}), 7.36-7.43 (m, 2H, H_{arom}), 7.72 (d, $^3J_{HH}$ = 7.3 Hz, 1H, H_{arom}), 7.96-7.99 (m, 1H, H_{arom}), 8.55 (dd, $^4J_{HH}$ = 4.7 Hz, $^3J_{HH}$ = 1.1 Hz, 2H, H_{arom}) ppm.

^{13}C NMR (75 MHz, $CDCl_3$) δ= 31.5 (CH_2), 47.3 (HC_{6a}), 48.7 (HC_{11b}), 56.6 (HC_6), 122.1 ($2HC_{arom}$), 122.3 (HC_{arom}), 123.3 (HC_{arom}), 124.6 (HC_{arom}), 126.6 (HC_{arom}), 126.8 (HC_{arom}), 127.5 (HC_{arom}), 140.5 (HC_{arom}), 141.1 (C_{arom}), 142.0 (C_{arom}), 144.0 (C_{arom}), 144.6 (C_{arom}), 149.7 ($2HC_{arom}$), 151.6 (C_{arom}) ppm.

HRMS (CI): calculated for $C_{20}H_{17}N_3$ $[M]^+$ 299.1422 found 299.1428.

***6-(2,4-Difluorophenyl)-6,6a,7,11b-tetrahydro-5H-indeno[2,1c][1,5]naphthyridin* (9f)**

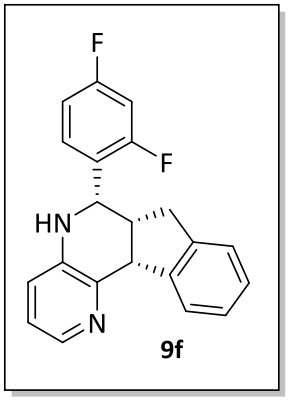

9f

The general procedure A was followed using imine **3f**, prepared *in situ*, and the reaction mixture was stirred at refluxing chloroform for 24 h affording compound **9f** as a white solid after purification by flash chromatography (1.203 g, 75%). When general procedure B was followed using 2,4-difluorobenzaldehyde (5 mmol, 0.547 ml) for 24 h compounds **9f** was obtained as a white solid (1.337 g, 80%).

m.p.(°C) 185-186 (ethyl acetate/hexane).

IR νmax 3350, 3071, 2940, 1617, 1480, 1450, 940, 743 cm^{-1}.

^{1}H NMR (300 MHz, $CDCl_3$) δ= 2.32 (dd, $^{2}J_{HH}$ = 15.0 Hz, $^{3}J_{HH}$ = 7.8 Hz, 1H, CH_2), 3.08-3.28 (m, 2H, HC_{6a}-C<u>H</u>$_2$), 3.55 (s, 1H, NH), 4.56 (d, $^{3}J_{HH}$ = 8.3 Hz, 1H, HC_{11b}), 4.93 (s, 1H, HC_6), 6.73-8.01 (m, 7H, H_{arom}), 7.50 (dd, $^{2}J_{HH}$ = 15.0 Hz, $^{3}J_{HH}$ = 7.8 Hz, 1H, H_{arom}), 7.60 (d, $^{3}J_{HH}$ = 7.0 Hz, 1H, H_{arom}), 7.95 (dd, $^{3}J_{HH}$ = 4.0 Hz, $^{4}J_{HH}$ = 1.1 Hz, 1H, H_{arom}) ppm.

^{13}C NMR (75 MHz, $CDCl_3$) δ = 31.7 (CH_2), 45.4 (HC_{6a}), 48.7 (HC_{11b}), 50.7 (d, $^{3}J_{CF}$ = 8.3 Hz, HC_6), 104.2 (dd, $^{2}J_{CF}$ = 25.4 Hz, $^{2}J_{CF}$ = 25.4 Hz, HC_{arom}), 111.5 (dd, $^{2}J_{CF}$ = 21.1 Hz, $^{4}J_{CF}$ = 3.5 Hz, HC_{arom}), 122.0 (HC_{arom}), 122.3 (HC_{arom}), 124.3 (HC_{arom}), 124.6 (dd, $^{2}J_{CF}$ = 13.9 Hz, $^{4}J_{CF}$ = 3.7 Hz, C_{arom}), 126.3 (HC_{arom}), 126.7 (HC_{arom}), 127.0 (HC_{arom}), 128.2 (dd, $^{3}J_{CF}$ = 9.6 Hz, $^{3}J_{CF}$ = 6.1 Hz, HC_{arom}),140.8 (HC_{arom}), 141.1 (C_{arom}), 141.9 (C_{arom}), 144.9 (C_{arom}), 159.8 (dd, $^{1}J_{CF}$ = 249.2 Hz, $^{3}J_{CF}$ = 11.7 Hz, FC_{arom}), 162.3 (dd, $^{1}J_{CF}$ = 248.4 Hz, $^{4}J_{CF}$ = 12.3 Hz, FC_{arom}) ppm.

^{19}F NMR (376 MHz, $CDCl_3$) δ =-111.6 (d, $^{4}J_{FF}$ = 7.5 Hz), -115.2 (d, $^{4}J_{FF}$ = 7.5 Hz) ppm.

HRMS (CI): calculated for $C_{21}H_{16}F_2N_2$ $[M]^+$ 334.1282 found 334.1286.248.

***6-(3,4-Difluorophenyl)-6,6a,7,11b-tetrahydro-5H-indeno[2,1c][1,5]naphthyridin* (9g)**

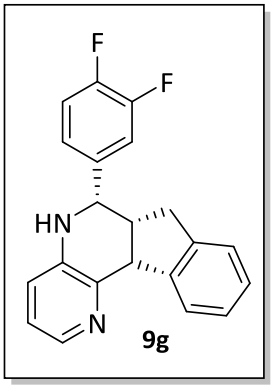

9g

The general procedure A was followed using imine **3g**, prepared *in situ*, and the reaction mixture was stirred at refluxing chloroform for 36 h affording compound **9g** as a white solid after purification by flash chromatography (1.171 g, 70%). When general procedure B was followed using 3,4-difluorobenzaldehyde (5 mmol, 0.551 ml) for 36 h compounds **9g** was obtained as a white solid (1.221 g, 73%).

m.p.(°C) 171-172 (ethyl acetate/hexane).

IR ν_{max} 3350, 2941, 1617, 1520, 1286, 964, 744 cm^{-1}.

^{1}H NMR (300 MHz,$CDCl_3$) δ = 2.44 (dd, $^2J_{HH}$ = 12.7 Hz, $^3J_{HH}$ = 7.6 Hz, 1H, CH_2), 3.20-3.30 (m, 2H, HC_{6a}-C<u>H</u>$_2$), 3.78 (s, 1H, NH), 4.67 (d, $^3J_{HH}$ = 7.7 Hz, 1H, HC_{11b}), 4.73 (s, 1H, HC_6), 6.87-6.94 (m, 2H, H_{arom}), 7.06-7.24 (m, 5H, H_{arom}), 7.31-7.38 (m, 1H, H_{arom}), 7.78 (d, $^3J_{HH}$ = 7.1 Hz, 1H, H_{arom}), 8.08 (dd, $^3J_{HH}$ = 4.4 Hz, $^4J_{HH}$ = 1.5 Hz, 1H, H_{arom}) ppm.

^{13}C NMR (75 MHz,$CDCl_3$) δ = 31.6 (CH_2), 47.8 (HC_{6a}), 49.1 (HC_{11b}), 56.8 (HC_6), 115.3 (d, $^2J_{CF}$ = 18.0 Hz, HC_{arom}), 117.4 (d, $^2J_{CF}$ = 22.5 Hz, HC_{arom}), 121.7 (HC_{arom}), 122.3 (HC_{arom}), 122.4 (dd, $^3J_{CF}$ = 9.0 Hz, $^4J_{CF}$ = 3.7 Hz, HC_{arom}), 124.6 (HC_{arom}), 126.3 (HC_{arom}), 126.8 (HC_{arom}), 127.2 (HC_{arom}), 138.9 (dd, $^3J_{CF}$ = 8.0 Hz, $^4J_{CF}$ = 3.7 Hz, C_{arom}), 140.8 (C_{arom}), 140.9 (C_{arom}), 141.9 (HC_{arom}), 144.4 (C_{arom}), 144.8 (C_{arom}), 149.4 (dd, $^1J_{CF}$ = 249.0 Hz, $^2J_{CF}$ = 12.7 Hz, FC_{arom}), 150.3 (dd, $^1J_{CF}$ =248.2 Hz, $^2J_{CF}$ = 12.0 Hz, FC_{arom}) ppm.

^{19}F NMR (376 MHz, $CDCl_3$) δ=-137.0 (d, $^3J_{FF}$ = 21.4 Hz), -139.3 (d, $^3J_{FF}$ = 21.4 Hz) ppm.

HRMS (CI): calculated for $C_{21}H_{16}F_2N_2$ $[M]^+$ 334.1282 found 334.1285.

6.2.3. Synthesis of derivatives 14 and 15

General procedure

Indene (7.5 mmol, 0.868 ml) or styrene (7.5 mmol, 0.862 ml) and $BF_3 \cdot Et_2O$ (10 mmol, 1.230 ml) were added to a solution of the previously prepared aldimine **3l** (5 mmol) in $CHCl_3$ (10 ml). The mixture was stirred at the appropriate temperature until TLC and ^1H NMR spectroscopy indicated the disappearance of imine **3l** signals. The reaction mixture was washed with 2M aqueous solution of NaOH (20 ml) and water (20 ml), extracted with dichloromethane (20 ml), and dried over anhydrous $MgSO_4$. The removal of the solvent under vaccum affored an oil or solid that were purified by silica gel flash column chromatography (eluent: Hexane/AcOEt) to afford the desired products **14** or **15**.

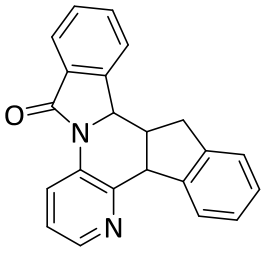

14

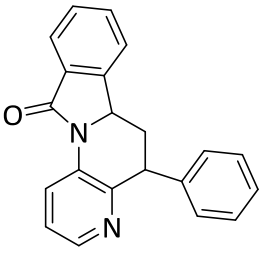

15

*4b,14b,14c,15-Tetrahydro-10H-indeno[2,1-c]isoindolo[2,1-a][1,5]naphthyridin-10-one (***14**)

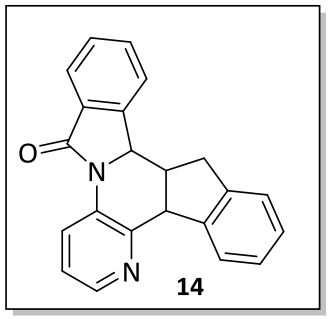

14

The general procedure was followed using indene, and the reaction mixture was stirred at room temperature for 24 h. Compound **14** was obtained as a white solid after purification by flash chromatography (1.377 g, 85%).

m.p.(°C) 223-224 (ethyl acetate/hexane).

IR νmax 3051, 2940, 1691, 1426, 755 cm^{-1}.

^{1}H NMR (300 MHz,$CDCl_3$) δ = 2.24 (m, 2H, CH_2), 3.70-3.78 (m, 1H, $\underline{H}C\text{-}CH_2$), 470 (d, $^{3}J_{HH}$ = 8.4 Hz, 1H), 5.11 (s, 1H, HC-N), 6.88-6.90 (m, 1H, H_{arom}), 7.00-7.18 (m, 3H, H_{arom}), 7.45-7.61 (m, 3H, H_{arom}), 7.69-7.86 (m, 1H, H_{arom}), 7.88-7.97 (m, 1H, H_{arom}), 8.27-8.29 (m, 1H, H_{arom}), 8.56 (d, $^{3}J_{HH}$ = 8.3 Hz, 1H, H_{arom}) ppm.

^{13}C NMR (75 MHz,$CDCl_3$) δ = 31.4 (CH_2), 41.9 (HC), 48.3 (HC), 58.8 (HC-N), 121.8 (HC_{arom}), 122.1 (HC_{arom}), 124.3 ($2HC_{arom}$), 126.6 (HC_{arom}), 126.7 (HC_{arom}), 127.3 (HC_{arom}), 127.5 (HC_{arom}), 128.8 (HC_{arom}), 132.1 (HC_{arom}), 132.6 (C_{arom}), 132.7 (HC_{arom}), 141.1 (C_{arom}), 142.9 (C_{arom}), 143.6 (C_{arom}), 145.5 (C_{arom}), 148.8 (C_{arom}), 166.7 (C=O) ppm.

HRMS (CI): calculated for $C_{26}H_{16}N_2O$ $[M]^+$ 324.1263 found 324.1265.

5-Phenyl-6,6a-dihydroisoindolo[2,1-a][1,5]naphthyridin-11(5H)-one **(15)**

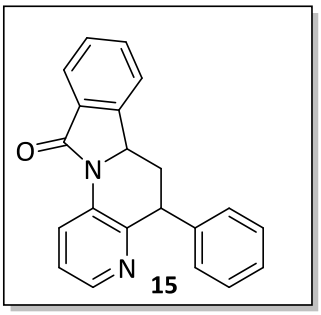

15

The general procedure was followed using styrene, and the reaction mixture was stirred at chloroform reflux for 24 h. Compound **15** was obtained as a white solid after purification by flash chromatography (1.248 g, 80%).

m.p.(°C) 242-243 (ethyl acetate/hexane).

IR νmax 3026, 2877, 1693, 1493, 1370, 769 cm^{-1}.

^{1}H NMR (300 MHz,$CDCl_3$) δ = 1.85 (ddd, $^{2}J_{HH}$ = 12.4 Hz, $^{3}J_{HH}$ = 12.4 Hz, $^{3}J_{HH}$ = 12.4 Hz, 1H, CH_2), 2.86 (ddd, $^{2}J_{HH}$ = 12.4 Hz, $^{3}J_{HH}$ =6.3 Hz, $^{3}J_{HH}$ = 2.5 Hz, 1H, CH_2), 4.46 (dd, $^{3}J_{HH}$ = 12.4 Hz, $^{3}J_{HH}$ =6.3 Hz, 1H, HC_5), 4.90 (dd, $^{2}J_{HH}$ = 12.4 Hz, $^{3}J_{HH}$ =2.5 Hz, 1H, HC_{6a}), 7.05-7.07 (m, 2H, H_{arom}), 7.13-7.26 (m, 4H, H_{arom}), 7.42-7.56 (m, 3H, H_{arom}), 7.88 (d, $^{3}J_{HH}$ =7.6 Hz, 1H, H_{arom}), 8.24 (dd, $^{3}J_{HH}$ = 4.6 Hz, $^{4}J_{HH}$ =1.6 Hz, 1H, H_{arom}), 8.81 (dd, $^{3}J_{HH}$ = 8.3 Hz, $^{4}J_{HH}$ =1.6 Hz, 1H, H_{arom}), ppm.

^{13}C NMR (75 MHz,$CDCl_3$) δ = 38.6 (CH_2), 47.4 (HC_5), 58.6 (HC_{6a}), 122.2 (HC_{arom}), 122.5 (HC_{arom}), 124.6 (HC_{arom}), 127.1 (HC_{arom}), 127.4 (HC_{arom}), 128.8 ($2HC_{arom}$), 129.0 ($2HC_{arom}$), 129.1 (HC_{arom}), 132.3 (C_{arom}), 132.8 (HC_{arom}), 133.6 (C_{arom}), 144.1 (C_{arom}), 144.2 (C_{arom}), 145.3 (HC_{arom}), 149.1 (C_{arom}), 166.8 (C=O) ppm.

HRMS (CI): calculated for $C_{21}H_{16}N_2O$ $[M]^+$ 312.1263 found 312.1265.

6.2.4. Synthesis of 7H-indeno[2,1-c][1,5]-naphthyridines 10.

General procedure

To a solution of the corresponding tetrahydro-5*H*-indeno[2,1-*c*][1,5]-naphthyridine **9** (1 mmol) in toluene (20 ml) DDQ (1 mmol, 0.227 g) was added and the mixture was irradiated with microwave at 150 W at 25°C for 2 h. The formed solid was filtered off, the solvent of the resulting solution removed under vacuum leading to an oil that was purified by column chromatography on alumina (ethyl acetate / hexane 1:20) to afford compounds **10**.

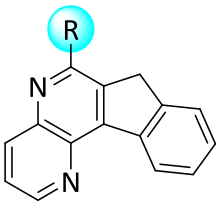

10

6-(Phenyl)- 7H-indeno[2,1-c][1,5]-naphthyridine (10a)

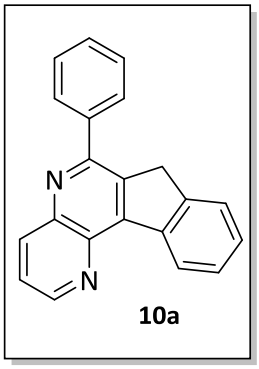

10a

The general procedure for the dehydrogenation reaction was followed using the tetrahydronaphthyridine **9a** (1 mmol, 0.298 g) affording compound **10a** as a yellow solid after purification by flash chromatography on alumina (0.200 g, 68%).

m.p.(°C) 157-158 (ethyl acetate/hexane).

IR νmax 3060, 2925, 1488, 1257, 726 cm^{-1}.

^{1}H NMR (300 MHz,$CDCl_3$) δ = 4.13 (s, 2H, CH_2), 7.37-7.61 (m, 7H, H_{arom}), 7.87-7.90 (m, 2H, H_{arom}), 8.43-8.46 (m, 1H, H_{arom}), 8.98-9.00 (m, 1H, H_{arom}), 9.06 (d, $^{3}J_{HH}$ = 7.0 Hz, 1H, H_{arom}) ppm.

^{13}C NMR (75 MHz,$CDCl_3$) δ = 38.3 (CH_2), 124.1 (HC_{arom}), 124.6 (HC_{arom}), 127.2 (HC_{arom}), 127.7 (HC_{arom}), 128.9 ($3HC_{arom}$), 129.2 ($2HC_{arom}$), 129.3 (HC_{arom}), 137.5 (C_{arom}), 137.7 (HC_{arom}), 140.2 (C_{arom}), 140.3 (C_{arom}), 140.7 (C_{arom}), 143.5 (C_{arom}), 144.6 (C_{arom}), 146.7 (C_{arom}), 150.4 (HC_{arom}), 157.0 (C_{arom}) ppm.

HRMS (CI): calculated for $C_{21}H_{14}N_2O$ $[M]^+$ 294.1157 found 294.1162.

6-(1-Naphtyl)-7H-indeno[2,1-c][1,5]-naphthyridine (10b)

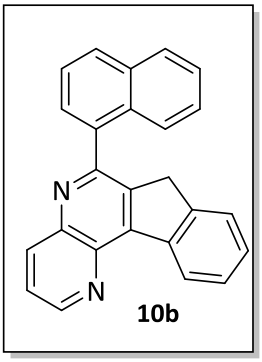

10b

The general procedure for the dehydrogenation reaction was followed using tetrahydronaphthyridine **9b** (1 mmol, 0.348 g) affording compound **10b** as a white solid after purification by flash chromatography on alumina (0.206 g, 60%).

m.p.(°C) 145-146(ethyl acetate/hexane).

IR νmax 3012, 2930, 1729, 1360, 820, 735 cm^{-1}.

^{1}H NMR (300 MHz, $CDCl_3$) δ = 4.34 (s, 2H, CH_2), 7.50-7.60 (m, 4H, H_{arom}), 7.66-7.75 (m, 3H, H_{arom}), 7.93-8.05 (m, 3H, H_{arom}), 8.12-8.19 m, 1H, H_{arom}), 8.48 (s, 1H, H_{arom}), 8.62 (d, $^3J_{HH}$ = 8.6 Hz, 1H, H_{arom}), 9.12 (dd, $^3J_{HH}$ = 4.1 Hz, $^4J_{HH}$ = 1.8 Hz, 1H, H_{arom}), 9.20 (d, $^3J_{HH}$ = 7.7 Hz, 1H, H_{arom}) ppm.

^{13}C NMR (75 MHz,$CDCl_3$) δ = 38.5 (CH_2), 123.8 (HC_{arom}), 124.3 (HC_{arom}), 125.6 ($2HC_{arom}$), 126.7 (HC_{arom}), 127.5 (HC_{arom}), 127.9 (HC_{arom}), 128.3 (HC_{arom}), 128.5 (HC_{arom}), 128.6 (HC_{arom}), 128.9 (HC_{arom}), 130.5 (HC_{arom}), 132.9 (C_{arom}), 133.8 (C_{arom}), 136.5 (C_{arom}), 137.2 (HC_{arom}), 137.9 (C_{arom}), 140.2 (C_{arom}), 140.8 (C_{arom}), 142.7 (C_{arom}), 143.3 (C_{arom}), 146.5 (C_{arom}), 151.4 (HC_{arom}), 155.6 (C_{arom}) ppm.

HRMS (CI): calculated for $C_{25}H_{16}N_2$ $[M]^+$ 344.1313 found 344.1317.

6-(2-Naphtyl)-7H-indeno[2,1-c][1,5]-naphthyridine (10c)

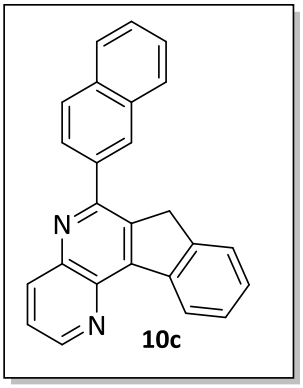

10c

The general procedure for the dehydrogenation reaction was followed using tetrahydronaphthyridine **9c** (1 mmol, 0.348 g) affording compound **10c** as a white solid after purification by flash chromatography on alumina (0.206 g, 60%).

m.p.(°C) 158-159(ethyl acetate/hexane).

IR νmax 3025, 2916, 1730, 1352, 1128, 800, 735 cm^{-1}.

^{1}H NMR (300 MHz,$CDCl_3$) δ = 4.04 (s, 2H, CH_2), 7.32-7.36 (m, 1H, H_{arom}), 7.44-7.49 (m, 3H, H_{arom}), 7.53 (dd, $^3J_{HH}$ = 8.6 Hz, $^4J_{HH}$ = 4.1 Hz, 1H, H_{arom}), 7.81-7.96 (m, 4H, H_{arom}), 8.00 (dd, $^3J_{HH}$ = 8.5 Hz, $^4J_{HH}$ = 1.8 Hz, 1H, H_{arom}), 8.30 (s, 1H, H_{arom}), 8.41 (dd, $^3J_{HH}$ = 8.5 Hz, $^4J_{HH}$ = 1.8 Hz, 1H, H_{arom}), 8.93 (dd, $^3J_{HH}$ = 4.1 Hz, $^4J_{HH}$ = 1.8 Hz, 1H, H_{arom}), 9.01 (d, $^3J_{HH}$ = 7.5 Hz, 1H, H_{arom}) ppm.

^{13}C NMR (75 MHz,$CDCl_3$) δ = 38.3 (CH_2), 124.1 (C_{arom}), 124.6 (HC_{arom}), 126.6 ($2HC_{arom}$), 127.0 (HC_{arom}), 127.1 (HC_{arom}), 127.6 (HC_{arom}), 128.0 (HC_{arom}), 128.6 (HC_{arom}), 128.7 (HC_{arom}), 128.8 (HC_{arom}), 128.9 (HC_{arom}), 133.4 (C_{arom}), 133.7 (C_{arom}), 137.4 (C_{arom}), 137.5 (HC_{arom}), 137.6 (C_{arom}), 140.1 (C_{arom}), 140.6 (C_{arom}), 143.5 (C_{arom}), 144.6 (C_{arom}), 146.9 (C_{arom}), 150.4 (HC_{arom}), 156.6 (C_{arom}) ppm.

HRMS (CI): calculated for $C_{25}H_{16}N_2$ $[M]^+$ 344.1313 found 344.1318.

6-(4-Nitrophenyl)-7H-indeno[2,1-c][1,5]-naphthyridine (10d)

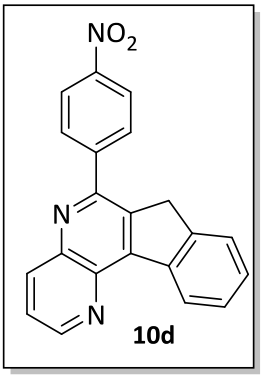

10d

The general procedure for the dehydrogenation reaction was followed using tetrahydronaphthyridine **9d** (1 mmol, 0.343 g) affording compound **10d** as a yellow solid after purification by flash chromatography on alumina (0.153 g, 45%).

m.p.(°C) 121-122 (ethyl acetate/hexane).

IR νmax 3015, 2925, 1724, 1344, 1108, 810, 725 cm^{-1}.

^{1}H NMR (300 MHz, $CDCl_3$) δ = 4.15 (s, 2H, CH_2), 7.42-7.53 (m, 2H, H_{arom}), 7.59-7.63 (m, 2H, H_{arom}), 7.66-7.71 (m, 1H, H_{arom}), 8. 12 (d, $^3J_{HH}$ = 8.7 Hz, 2H, H_{arom}), 8.38 (d, $^3J_{HH}$ = 8.7 Hz, 2H, H_{arom}), 8.51 (dd, $^3J_{HH}$ = 8.6 Hz, $^4J_{HH}$ = 1.5 Hz, 1H, H_{arom}), 9.03-9.11 (m, 1H, H_{arom}) ppm.

^{13}C NMR (75 MHz,$CDCl_3$) δ = 38.1 (CH_2), 124.1 ($2HC_{arom}$), 124.3 (HC_{arom}), 124.5 (HC_{arom}), 127.1 (HC_{arom}), 127.7 (HC_{arom}), 129.2 (HC_{arom}), 130.2 ($2HC_{arom}$), 136.8 (C_{arom}), 137.7 (HC_{arom}), 139.6 (C_{arom}), 140.4 (C_{arom}), 143.4 (C_{arom}), 144.1 (C_{arom}), 145.6 (C_{arom}), 147.5 (C_{arom}), 148.1 (C_{arom}), 151.1 (HC_{arom}), 154.0 (C_{arom}) ppm.

HRMS (CI): calculated for $C_{21}H_{13}N_3O_2$ $[M]^+$ 339.10089 found 339.1011.

6-(Pyridin-4-yl)-7H-indeno[2,1-c][1,5]-naphthyridine (10e)

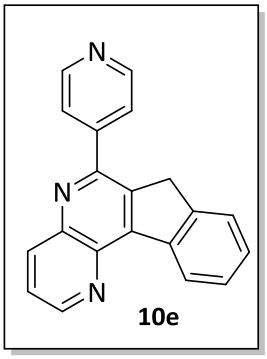

10e

The general procedure for the dehydrogenation reaction was followed using tetrahydronaphthyridine **9e** (1 mmol, 0.304g) affording compound **10e** as a white solid after purification by flash chromatography on alumina (0.118 g, 40%).

m.p.(°C) 145-146 (ethyl acetate/hexane).

IR νmax 3025, 2899, 1600, 1489, 1259, 822, 760 cm^{-1}.

^{1}H NMR (300 MHz, $CDCl_3$) δ = 4.13 (s, 2H, CH_2), 7.42-7.50 (m, 2H, H_{arom}), 7.55-7.61 (m, 1H, H_{arom}), 7.67 (dd, $^3J_{HH}$ = 8.6 Hz, $^3J_{HH}$ = 4.1 Hz, 1H, H_{arom}), 7.84-7.90 (m, 2H, H_{arom}),8.44 (d, $^3J_{HH}$ = 8.6 Hz, 1H, H_{arom}), 8.68-8.73 (m, 2H, H_{arom}), 9.00-9.06 (m, 2H, H_{arom}) ppm.

^{13}C NMR (75 MHz,$CDCl_3$) δ = 48.4 (CH_2), 123.4 ($2HC_{arom}$), 124.2 ($2HC_{arom}$), 126.7 (HC_{arom}), 127.3 (HC_{arom}), 129.0 (HC_{arom}), 136.6 (C_{arom}), 136.9 (HC_{arom}), 139.0 (C_{arom}), 140.1 (C_{arom}), 142.9 (C_{arom}), 143.9 (C_{arom}), 147.4 (C_{arom}), 147.5 (C_{arom}), 149.3 ($2HC_{arom}$), 150.9 (HC_{arom}), 153.1 (C_{arom}) ppm.

HRMS (CI): calculated for $C_{20}H_{13}N_3$ $[M]^+$ 295.1109 found 295.1113.

6-(2,4-Difluorophenyl)-7H-indeno[2,1-c][1,5]-naphthyridine (10f)

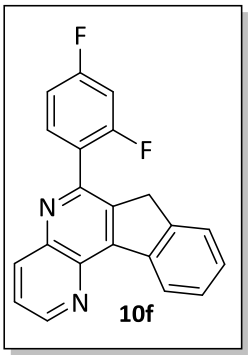

10f

The general procedure for the dehydrogenation reaction was followed using tetrahydronaphthyridine **9f** (1 mmol, 0.334 g) affording compound **10f** as a white solid after purification by flash chromatography on alumina (0.178 g, 54%).

m.p.(°C) 181-182 (ethyl acetate/hexane).

IR νmax 3069, 1564, 1475, 1350, 1260, 815, 725 cm^{-1}.

^{1}H NMR (300 MHz, $CDCl_3$) δ = 4.13 (s, 2H, CH_2), 7.00-7.27 (m, 2H, H_{arom}), 7.55-7.73 (m, 5H, H_{arom}), 8.53 (d, $^{3}J_{HH}$ = 8.5 Hz, 1H, H_{arom}), 9.03-9.09 (m, 2H, H_{arom}) ppm.

^{13}C NMR (75 MHz,$CDCl_3$) δ = 36.7 (CH_2), 103.9 (dd, $^{2}J_{CF}$ = 25.7 Hz, $^{2}J_{CF}$ = 25.7 Hz, HC_{arom}), 111.5 (dd, $^{2}J_{CF}$ = 21.1 Hz, $^{4}J_{CF}$ = 3.5 Hz, HC_{arom}), 123.6 (HC_{arom}), 124.0 (HC_{arom}), 124.1 (dd, $^{2}J_{CF}$ = 14 Hz, $^{4}J_{CF}$ = 3.6 Hz, C_{arom}), 126.6 (HC_{arom}), 127.0 (HC_{arom}), 128.5 (HC_{arom}), 132.1 (dd, $^{3}J_{CF}$ = 9.8 Hz, $^{3}J_{CF}$ = 5.1 Hz, HC_{arom}), 137.5 (HC_{arom}), 138.8 (C_{arom}), 139.8 (C_{arom}), 140.5 (C_{arom}), 143.4 (C_{arom}), 144.5 (C_{arom}), 146.4 (C_{arom}), 150.5 (HC_{arom}), 152.2 (C_{arom}), 160.7 (dd, $^{1}J_{CF}$ = 250.8 Hz, $^{3}J_{CF}$ = 12.1 Hz, C_{arom}), 163.9 (dd, $^{1}J_{CF}$ = 251.1 Hz, $^{3}J_{CF}$ = 11.8 Hz, C_{arom}) ppm.

^{19}F NMR (376 MHz, $CDCl_3$) δ: -108.6 (d, $^{4}J_{FF}$ = 7.5 Hz), -109.5 (d, $^{4}J_{FF}$ = 7.5 Hz) ppm.

HRMS (CI): calculated for $C_{21}H_{12}F_2N_2$ $[M]^+$ 330.0969 found 330.0973.

6-(3,4-Difluorophenyl)-7H-indeno[2,1-c][1,5]-naphthyridine (10g)

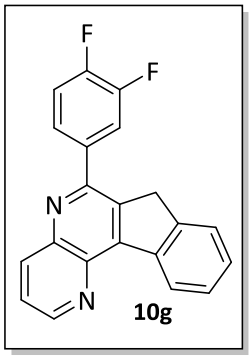

10g

The general procedure for the dehydrogenation reaction was followed using tetrahydronaphthyridine **9g** (1 mmol, 0.334 g) affording compound **10g** as a white solid after purification by flash chromatography on alumina (0.228 g, 69%).

m.p.(°C): 192-193 (ethyl acetate/hexane).

IR νmax: 3048, 2960, 1735, 1540, 1480, 1230, 970, 735 cm^{-1}.

^{1}H NMR (300 MHz, $CDCl_3$) δ= 4.06 (s, 2H, CH_2), 7.17-7.78 (m, 7H, H_{arom}), 8.40 (d, $^{3}J_{HH}$ = 8.3Hz, 1H, H_{arom}), 9.01 (dd, $^{3}J_{HH}$ = 4.1 Hz, $^{4}J_{HH}$ = 1.7 Hz, 1H, H_{arom}), 9.05 (d, $^{3}J_{HH}$ = 7.7Hz, 1H, H_{arom}) ppm.

^{13}C NMR (75 MHz,$CDCl_3$) δ= 37.5 (CH_2), 117.5 (dd, $^{2}J_{CF}$ = 15.5 Hz, $^{3}J_{CF}$ = 2.6 Hz, HC_{arom}), 117.7 (dd, $^{2}J_{CF}$ = 17.5 Hz, $^{3}J_{CF}$ = 2.0 Hz, HC_{arom}), 123.6 (HC_{arom}), 123.9 (HC_{arom}), 125.1(dd, $^{3}J_{CF}$ = 9.0 Hz, $^{4}J_{CF}$ = 4.0 Hz, C_{arom}), 126.5 (HC_{arom}), 127.1 (HC_{arom}), 128.4 (HC_{arom}), 136.6 (C_{arom}), 136.8 (dd, $^{3}J_{CF}$ = 10.0 Hz, $^{4}J_{CF}$ = 4.0 Hz, HC_{arom}), 137.4 (HC_{arom}), 139.7 (C_{arom}), 140.3 (C_{arom}), 143.2 (C_{arom}), 144.1 (HC_{arom}), 147.2 (C_{arom}), 150.4 (dd, $^{1}J_{CF}$ = 250.8 Hz, $^{2}J_{CF}$ = 14.8 Hz, FC_{arom}), 150.5 (C_{arom}), 151.1 (dd, $^{1}J_{CF}$ = 253.1 Hz, $^{2}J_{CF}$ = 14.5 Hz, FC_{arom}), 154.1 (C_{arom}) ppm.

^{19}F NMR (376 MHz, $CDCl_3$): δ: -137.7 (d, $^{3}J_{FF}$ = 22.0 Hz), -137.4 (d, $^{3}J_{FF}$ = 22.0 Hz) ppm.

HRMS (CI): calculated for $C_{21}H_{12}F_2N_2$ $[M]^+$ 330.0969 found 330.0972.

6.2.5. Synthesis of 7H-indeno[2,1-c][1,5]-naphthyridine-7-ones 16.

General procedure

To a solution of 7*H*-indeno[2,1-*c*][1,5]-naphthyridine **10** (1 mmol) in acetic acid (10 ml) $Mn(AcO)_3$ (3 mmol, 0.804 g) was added. The mixture was subjected to microwave irradiation at 150 W and 80°C during 30 min. The formed manganese diacetate was filtered off, the reaction mixture was poured into water, neutralized by $NaHCO_3$, extracted with methylene chloride (20 ml) and dried over anhydrous sodium sulphate. The solvent of the resulting solutions was removed under vacuum leading to an oil that was purified by column chromatography on alumina (ethyl acetate / hexane 1:10) to afford compounds **16**.

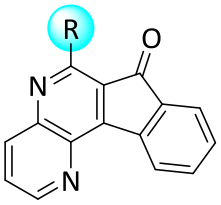

16

6-Phenyl-7H-indeno[2,1-c][1,5]-naphthyridine-7-one (16a)

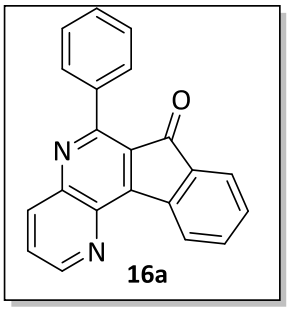

16a

The general procedure was followed using compound **10a** (1 mmol, 0.294 g). Compound **16a** was obtained as a yellow solid after purification by flash chromatography on alumina (0.157 g, 51%).

m.p.(°C) 163-165 (ethyl acetate/hexane) .

IR νmax 2951, 1717, 1490, 1228, 731 cm^{-1}.

^{1}H NMR (300 MHz, $CDCl_3$) δ = 7.46-7.75 (m, 7H, H_{arom}), 7.89-7.92 (m, 2H, H_{arom}), 8.43 (dd, $^{3}J_{HH}$ = 8.7 Hz, $^{3}J_{HH}$ = 1.7 Hz, 1H, H_{arom}), 8.84 (d, $^{3}J_{HH}$ = 7.5 Hz, 1H, H_{arom}), 9.08 (dd, $^{4}J_{HH}$ = 1.7 Hz, $^{3}J_{HH}$ = 4.1 Hz, 1H, H_{arom}) ppm.

^{13}C NMR (75 MHz,$CDCl_3$) δ = 124.0 (HC_{arom}), 124.7 (C_{arom}), 126.6 (HC_{arom}), 127.5 (HC_{arom}), 127.9 ($2HC_{arom}$), 129.7 (HC_{arom}), 129.8 ($2HC_{arom}$), 131.4 (HC_{arom}), 133.2 (C_{arom}), 134.8 (HC_{arom}), 137.1 (C_{arom}), 137.6 (HC_{arom}), 139.1 (C_{arom}), 141.1 (C_{arom}), 148.0 (C_{arom}), 151.9 (HC_{arom}), 153.3 (C_{arom}), 157.3 (C_{arom}), 192.5 (C=O) ppm.

HRMS (CI): calculated for $C_{21}H_{12}N_2O$ $[M]^+$ 308.09450 found 308.0951.

6-(2-Naphthyl)-7H-indeno[2,1-c][1,5]-naphthyridine-7-one (16c)

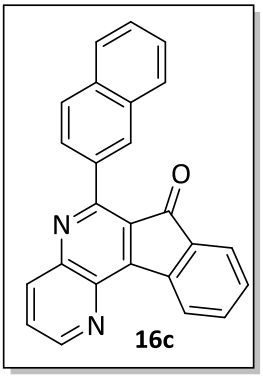

16c

The general procedure was followed using compound **10c** (1 mmol, 0.344 g). Compound **16c** was obtained as a yellow solid after purification by flash chromatography on alumina (0.107 g, 30%).

m.p.(°C) 215-216 (ethyl acetate/hexane) .

IR νmax 3059, 1460, 1560, 1463, 896, 741 cm^{-1}.

^{1}H NMR (300 MHz, $CDCl_3$) δ = 7.30-7.39 (m, 3H, H_{arom}), 7.40-7.63 (m, 3H, H_{arom}), 7.80- 7.92 (m, 4H, H_{arom}), 8.35- 8.41 (m, 2H, H_{arom}), 8.80 (d, $^{3}J_{HH}$ = 7.2 Hz, 1H, H_{arom}), 9.01-9.03 (m, 1H, H_{arom}) ppm.

^{13}C NMR (75 MHz,$CDCl_3$) δ = 124.5 (HC_{arom}), 124.9 (C_{arom}), 126.4 (HC_{arom}), 126.9 (C_{arom}), 127.1 (C_{arom}), 127.4 (HC_{arom}), 127.7 (HC_{arom}), 128.9 (HC_{arom}), 130.0 (HC_{arom}), 131.4 (HC_{arom}), 132.9 (HC_{arom}), 133.2 (C_{arom}), 133.3 (C_{arom}), 134.3 (HC_{arom}), 134.7 (HC_{arom}), 134.8 (HC_{arom}), 135.0 (HC_{arom}), 137.6 (HC_{arom}), 138.0 (HC_{arom}), 139.4 (C_{arom}), 141.4 (C_{arom}), 148.0 (C_{arom}), 152.2 (HC_{arom}), 153.7 (C_{arom}), 157.5 (C_{arom}), 192.6 (C=O) ppm.

HRMS (CI): calculated for $C_{25}H_{14}N_2O$ $[M]^+$ 358.1106 found 358.1114.

6-(2,4-Difluorophenyl)-7H-indeno[2,1-c][1,5]-naphthyridine-7-one (16f)

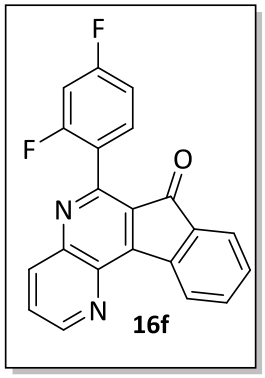

16f

The general procedure was followed using compound **10f** (1 mmol, 0.330 g). Compound **16f** was obtained as a white solid after purification by flash chromatography on alumina (0.120 g, 35%).

m.p.(°C) 221-222 (ethyl acetate/hexane) .

IR νmax 3040, 1540, 1670, , 890, 730 cm^{-1}.

^{1}H NMR (300 MHz, $CDCl_3$) δ = 6.90-7.03 (m, 3H, H_{arom}), 7.43 (t, $^{3}J_{HH}$ = 7.5 Hz, 1H, H_{arom}), 7.53- 7.69 (m, 2H, H_{arom}), 7.73 (dd, $^{3}J_{HH}$ = 8.7 Hz, $^{4}J_{HH}$ = 4.1 Hz, 1H, H_{arom}), 8.36 (dd, $^{3}J_{HH}$ = 8.7 Hz, $^{4}J_{HH}$ = 4.1 Hz, 1H, H_{arom}), 8.74 (d, $^{3}J_{HH}$ = 7.5 Hz, 1H, H_{arom}), 9.06 (dd, $^{3}J_{HH}$ =4.1 Hz, $^{4}J_{HH}$ = 1.7 Hz, 1H, H_{arom}) ppm.

^{13}C NMR (75 MHz,$CDCl_3$) δ = 104.1 (ddt, $^{2}J_{CF}$ = 26.0 Hz, $^{2}J_{CF}$ = 26.0 Hz, HC_{arom}), 111.8 (dd, $^{2}J_{CF}$ = 22.0 Hz, $^{4}J_{CF}$ = 3.7 Hz, HC_{arom}), 121.9 (dd, $^{2}J_{CF}$ = 15.0 Hz, $^{4}J_{CF}$ = 3.7 Hz, C_{arom}), 124.3 (HC_{arom}), 126.0 (C_{arom}), 127.1 (HC_{arom}), 132.1 (HC_{arom}), 132.2 (dd, $^{3}J_{CF}$ = 10.5 Hz, $^{3}J_{CF}$ = 6.0 Hz, HC_{arom}), 132.3 (C_{arom}), 133.9 (C_{arom}), 135.2 (HC_{arom}), 137.4 (HC_{arom}), 139.4 (C_{arom}), 141.2 (C_{arom}), 148.4 (C_{arom}), 150.6 (C_{arom}),152.7 ($2HC_{arom}$), 160.8 (dd, $^{1}J_{CF}$ = 252.0 Hz, $^{3}J_{CF}$ = 12.4 Hz, FC_{arom}), 164.5 (dd, $^{1}J_{CF}$ = 251.3 Hz, $^{3}J_{CF}$ = 12.1 Hz, FC_{arom}), 192.6 (C=O) ppm.

^{19}F NMR ($CDCl_3$) δ = 107.9 (d, $^{3}J_{FF}$ = 9.0 Hz), - 109.9 (d, $^{3}J_{FF}$ = 9.0 Hz) ppm.

HRMS (CI): calculated for $C_{21}H_{10}F_2N_2O$ $[M]^+$ 344.0761 found 344.0773.

6.2.6. Synthesis of 7H-indeno[2,1-c][1,5]-naphthyridine-7-ols 17.

General procedure

$NaBH_4$ (1 mmol, 0.085 g) was added to a solution of 7*H*-indeno[2,1-*c*][1,5]-naphthyridin-7-one **16** (1 mmol) in methanol (10 ml) and the mixture was stirred at room temperature until TLC and ^1H NMR analysis indicated the consumption of starting materials. The resulting solution was washed with water, extracted with methylene chloride (2 x 20 ml), and dried over ($MgSO_4$). Removal of solvent under vacuum led to a solid which was purified by recrystallization.

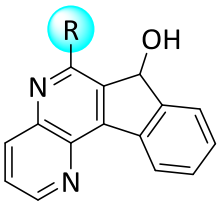

17

6-Phenyl-7H-indeno[2,1-c][1,5]-naphthyridine-7-ol (17a)

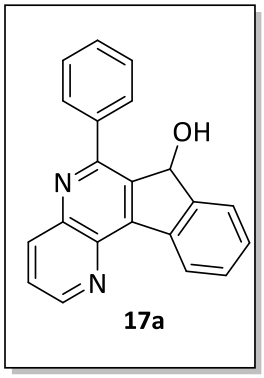

17a

The general procedure was followed using compound **16a** (1 mmol, 0.308 g) during 30 min to afford compound **17a** as a yellowish solid after purification by recrystallization (0.279 g, 90%).

m.p.(°C) 226-227 (ethyl acetate/hexane) .

IR νmax 3334, 3064, 2924, 1976, 1490, 1027, 737 cm^{-1}.

^{1}H NMR (300 MHz, $CDCl_3$) δ = 2.14 (s, 1H, OH), 6.15 (s, 1H, CH), 7.44-7.69 (m, 7H, H_{arom}), 8.04-8.07 (m, 2H, H_{arom}), 8.47 (dd, $^{3}J_{HH}$ = 8.5 Hz, $^{4}J_{HH}$ = 1.5 Hz, 1H, H_{arom}), 8.94 (d, $^{3}J_{HH}$ = 7.6 Hz, 1H, H_{arom}), 9.04 ((dd, $^{3}J_{HH}$ = 4.0 Hz, $^{4}J_{HH}$ = 1.5 Hz, 1H, H_{arom}) ppm.

^{13}C NMR (75 MHz, $CDCl_3$) δ = 74.8 (HC-OH), 124.5 (HC_{arom}), 124.6 (HC_{arom}), 127.2 (HC_{arom}), 127.9 (C_{arom}), 128.8 ($2HC_{arom}$), 128.9 ($2HC_{arom}$), 129.4 (HC_{arom}), 129.5 (HC_{arom}), 129.9 (HC_{arom}), 137.5 (HC_{arom}), 137.8 (C_{arom}), 138.8 (C_{arom}), 139.2 (C_{arom}), 139.9 (C_{arom}), 144.7 (C_{arom}), 146.2 (C_{arom}), 150.7 (HC_{arom}), 156.8 (C_{arom}) ppm.

HRMS (CI): calculated for $C_{21}H_{14}N_2O$ $[M]^+$ 310.1106 found 310.1112.

6-(2-Naphthyl)-7H-indeno[2,1-c][1,5]-naphthyridine-7-ol (17c)

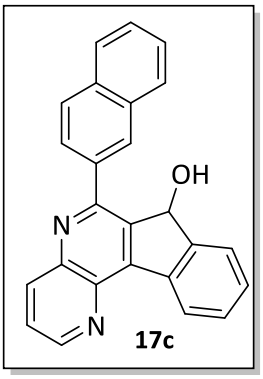

17c

The general procedure was followed using compound **16c** (1 mmol, 0.358 g). Compound **17c** was obtained as a yellowish solid after purification by recrystallization (0.108 g, 30%).

m.p.(°C) 206-207 (ethyl acetate/hexane) .

IR νmax 3330, 3024, 2959, 1967, 1380, 960, 717 cm^{-1}.

^{1}H NMR (300 MHz, $CDCl_3$) δ = 2.19 (s, 1H, OH), 6.16 (s, 1H, CH), 7.27-7.28 (m, 1H, H_{arom}), 7.51-7.58 (m, 3H, H_{arom}), 7.65-7.75 (m, 4H, H_{arom}), 8.00-8.02 (m, 3H, H_{arom}), 8.44-8.49 (m, 1H, H_{arom}), 8.86-8.90 (m, 1H, H_{arom}), 9.11-9.12 (m, 1H, H_{arom}) ppm.

^{13}C NMR (75 MHz, $CDCl_3$) δ = 74.8 (HC-OH), 124.8 (HC_{arom}), 125.0 (HC_{arom}), 126.4 (HC_{arom}), 127.1 (HC_{arom}), 127.2 (HC_{arom}), 127.9 ($2HC_{arom}$), 128.5 (HC_{arom}), 128.9 (HC_{arom}), 129.0(HC_{arom}), 129.5 (HC_{arom}), 130.1 (HC_{arom}), 133.4 (C_{arom}), 133.7 (C_{arom}), 136.6 (C_{arom}), 137.2 (HC_{arom}), 137.8 (C_{arom}), 139.6 (C_{arom}), 140.1 (C_{arom}), 146.8(C_{arom}), 144.6 (C_{arom}), 147.2 (C_{arom}), 151.0 (HC_{arom}), 157.4 (C_{arom}) ppm.

HRMS (CI): calculated for $C_{25}H_{16}N_2O$ $[M]^+$ 360.4214 found 360.4218.

6.2.7. Synthesis of [1,5]-naphthyridines 19.

General procedure

To a solution imines **3** (5 mmol) in chloroform the corresponding acetylenes **18** (7 mmol) and $BF_3{\cdot}Et_2O$ (10 mmol, 1.23 ml) were added and the mixture was stirred at the opportune temperature until TLC and ^1H NMR spectroscopy indicated the disappearance of the starting materials. The reaction mixture was washed with 2M aqueous solution of NaOH (20 ml) and water (20 ml), extracted with dichloromethane (20 ml), and dried over anhydrous $MgSO_4$. The removal of the solvent under vaccum and purification by silica gel flash column chromatography (eluent: Hexane/AcOEt) afford the desired products **19**.

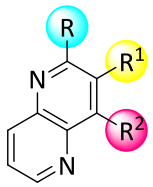

19

2,4-Diphenyl-1,5-naphthyridine (19a)

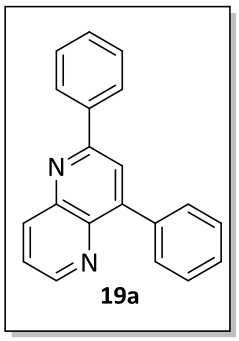

19a

The general procedure was followed using imine **3a** (5 mmol, 0.911 g) and phenylacetylene (7 mmol, 0.768 ml) and the reaction mixture was stirred at refluxing chloroform for 24 h. Compound **19a** was obtained as a white solid after purification by flash chromatography (1.057 g, 75%).

m.p.(°C) 122-124 (ethyl acetate/hexane) .

IR νmax 3058, 1587, 1482, 1360, 691 cm^{-1}.

^{1}H NMR (300 MHz, $CDCl_3$) δ = 7.37-7.47 (m, 6H, H_{arom}), 7.52 (dd, $^{3}J_{HH}$ = 8.4 Hz, $^{3}J_{HH}$ = 4.0 Hz, 1H, H_{arom}), 7.71 (d, $^{3}J_{HH}$ = 7.6 Hz, 2H, H_{arom}), 8.00 (s, 1H, HC), 8.10(d, $^{3}J_{HH}$ = 7.8 Hz, 2H, H_{arom}), 8.40 (d, $^{3}J_{HH}$ = 7.9 Hz, 1H, H_{arom}), 8.86 (d, $^{3}J_{HH}$ = 4.0 Hz, 1H, H_{arom}) ppm.

^{13}C NMR (75 MHz, $CDCl_3$) δ = 122.2 (HC_{arom}), 124.2 (HC_{arom}), 127.6 ($2HC_{arom}$), 128.3 ($2HC_{arom}$), 128.7 (HC_{arom}), 128.9 ($2HC_{arom}$), 129.7 (HC_{arom}), 130.4 ($2HC_{arom}$), 137.0 (C_{arom}), 137.7 (HC_{arom}), 138.9 (C_{arom}),141.2 (C_{arom}), 144.3 (C_{arom}), 148.9 (C_{arom}), 150.4 (HC_{arom}), 157.7 (C_{arom}) ppm.

HRMS (CI): calculated for $C_{20}H_{14}N_2$ $[M]^+$ 282.1157 found 282.1165.

2-(3,4-Difluorophenyl)-4-phenyl-1,5-naphthyridine (19b)

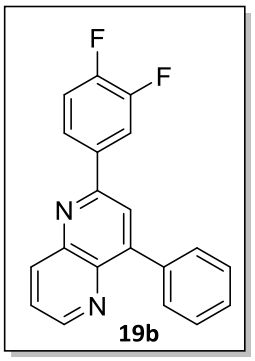

19b

The general procedure was followed using imine **3g** (5 mmol, 1.091 g) and phenylacetylene (7 mmol, 0.768 ml) and the reaction mixture was stirred at refluxing chloroform for 24 h. Compound **19b** was obtained as a white solid after purification by flash chromatography (0.954 g, 60%).

m.p.(°C) 221-222 (ethyl acetate/hexane) .

IR νmax 3040, 1575, 1460, 1370, 890, 750 cm^{-1}.

^{1}H NMR (300 MHz, $CDCl_3$) δ = 7.19-7.29 (m, 1H, H_{arom}), 7.44-7.52 (m, 3H, H_{arom}), 7.61 (dd, $^{3}J_{HH}$ = 8.5 Hz, $^{3}J_{HH}$ = 4.2 Hz, 1H, H_{arom}), 7.72-7.75 (m, 2H, H_{arom}), 7.83-7.89 (m, 1H, H_{arom}), 7.98 (s, 1H, HC),8.01-8.09 (m, 1H, H_{arom}), 8.41 (dd, $^{3}J_{HH}$ = 8.5 Hz, $^{4}J_{HH}$ = 1.7 Hz, 1H, H_{arom}), 8.92 (dd, $^{3}J_{HH}$ = 4.1 Hz, $^{4}J_{HH}$ = 1.7 Hz, 1H, H_{arom}) ppm.

^{13}C NMR (75 MHz, $CDCl_3$) δ = 117.3 (d, $^{2}J_{CF}$ = 67.8 Hz, HC_{arom}), 117.6 (d, $^{2}J_{CF}$ = 67.8 Hz, HC_{arom}), 121.7 (HC_{arom}), 123.9 (dd, $^{3}J_{CF}$ = 6.8 Hz, $^{4}J_{CF}$ = 3.7 Hz, HC_{arom}), 124.8 (HC_{arom}), 128.6 ($2HC_{arom}$), 129.2 (HC_{arom}), 130.7 ($2HC_{arom}$), 136.2 (dd, $^{3}J_{CF}$ = 8.5 Hz, $^{4}J_{HH}$ = 4.2 Hz, C_{arom}), 136.2 (dd, $^{3}J_{CF}$ = 6.2 Hz, $^{4}J_{CF}$ = 4.1 Hz, C_{arom}), 137.1 (C_{arom}), 138.0 (HC_{arom}), 144.6 (C_{arom}), 149.7 (C_{arom}), 151.1 (HC_{arom}), 151.1 (dd, ^{1}JCF = 247.4 Hz, $^{2}J_{CF}$ = 12.1 Hz, FC_{arom}), 151.8 (dd, $^{1}J_{CF}$ = 250.4 Hz, $^{2}J_{CF}$ = 10.1 Hz, FC_{arom}), 155.5 (C_{arom}) ppm.

^{19}F NMR ($CDCl_3$) δ: - 136.5(d, $^{3}J_{FF}$ = 21.4 Hz), - 137.2 (d, $^{3}J_{FF}$ = 21.4 Hz) ppm.

HRMS (CI): calculated for $C_{20}H_{12}F_2N_2$ $[M]^+$ 318.0989 found 318.0989.

4-Phenyl-2-(4-(trifluoromethyl)phenyl)-1,5-naphthyridine (19c)

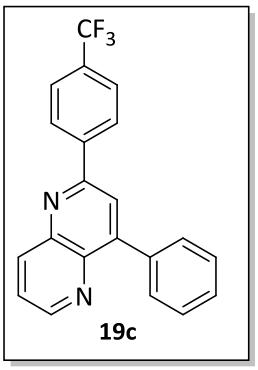

19c

The general procedure was followed using imine **3h** (5 mmol, 1.250 g) and phenylacetylene (7 mmol, 0.768 ml) and the reaction mixture was stirred at refluxing chloroform for 18 h. Compound **19c** was obtained as a yellowish solid after purification by flash chromatography (1.050 g, 60%).

m.p.(°C) 164-165 (ethyl acetate/hexane) .

IR νmax 3040, 1560, 1470, 1365, 890, 775 cm^{-1}.

^{1}H NMR (300 MHz, $CDCl_3$) δ = 7.42-7.50 (m, 3H, H_{arom}), 7.57 (dd, $^{3}J_{HH}$ = 8.5 Hz, $^{3}J_{HH}$ = 4.1 Hz, 1H, H_{arom}), 7.68-7.74 (m, 4H, H_{arom}), 8.00 (s, 1H, HC), 8.22 (d, $^{3}J_{HH}$ = 8.5 Hz, 2H, H_{arom}), 8.41 (dd, $^{3}J_{HH}$ = 8.5 Hz, $^{4}J_{HH}$ = 1.7 Hz, 1H, H_{arom}), 8.91 (dd, $^{3}J_{HH}$ = 4.1 Hz, $^{4}J_{HH}$ = 1.7 Hz, 1H, H_{arom}) ppm.

^{13}C NMR (75 MHz, $CDCl_3$) δ = 122.3 (HC_{arom}), 124.5 (q, $^{1}J_{CF}$ = 270.1 Hz, CF_3), 124.8 (HC_{arom}), 126.1 (q, $^{3}J_{CF}$ = 4.5 Hz, HC_{arom}), 128.2 ($2HC_{arom}$), 128.6 ($2HC_{arom}$), 129.2 (HC_{arom}), 130.7 ($2HC_{arom}$), 131.6 (q, $^{2}J_{CF}$ = 32.5 Hz, C-CF_3), 137.0 (C_{arom}), 138.1 (HC_{arom}), 141.6 (C_{arom}), 142.5 (C_{arom}), 144.7 (C_{arom}), 149.7 (C_{arom}), 151.2 ($2HC_{arom}$), 156.3(C_{arom}) ppm.

^{19}F NMR ($CDCl_3$) δ= - 63.0 ppm.

HRMS (CI): calculated for $C_{21}H_{13}F_3N_2$ $[M]^+$ 350.1031 found 350.1037.

2-(4-Fluorophenyl)-4-phenyl-1,5-naphthyridine (19d)

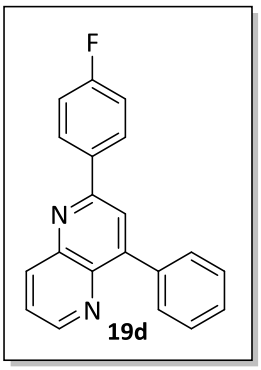

19d

The general procedure was followed using imine **3i** (5 mmol, 1.006 g) and phenylacetylene (7 5 mmol, 0.768 ml) and the reaction mixture was stirred at refluxing chloroform for 36 h. Compound **19d** was obtained as a white solid after purification by flash chromatography (1.125 g, 75%).

m.p.(°C) 164-165 (ethyl acetate/hexane) .

IR νmax 3070, 1680, 1354, 930, 720 cm^{-1}.

^{1}H NMR (300 MHz, $CDCl_3$) δ = 7.21-7.24 (m, 4H, H_{arom}), 7.53-7.60 (m, 2H, H_{arom}), 7.68 (dd, $^{3}J_{HH}$ = 8.5 Hz, $^{3}J_{HH}$ = 4.1 Hz, 1H, H_{arom}), 7.81-7.84 (m, 1H, H_{arom}), 8.08 (s, 1H, HC), 8.20-8.25 (m, 2H, H_{arom}), 8.51 (dd, $^{3}J_{HH}$ = 8.5 Hz, $^{4}J_{HH}$ = 1.8 Hz, 1H, H_{arom}), 9.0 (dd, $^{3}J_{HH}$ = 4.1 Hz, $^{4}J_{HH}$ = 1.0 Hz, 1H, H_{arom}) ppm.

^{13}C NMR (75 MHz, $CDCl_3$) δ = 116.1 (d, $^{2}J_{CF}$ = 22.0 Hz, $2HC_{arom}$), 122.2 (HC_{arom}), 124.8 (HC_{arom}), 128.6 ($2HC_{arom}$), 129.1 (HC_{arom}), 129.8 (d, $^{3}J_{CF}$ = 9.5 Hz, $2HC_{arom}$), 130.6 ($2HC_{arom}$), 135.2 (C_{arom}), 137.2 (C_{arom}), 137.8 (HC_{arom}), 141.3 (C_{arom}), 144.5 (C_{arom}), 149.6 (C_{arom}), 150.8 (HC_{arom}), 156.8 (C_{arom}), 164.3 (d, $^{1}J_{CF}$ = 250.6 Hz, FC_{arom}) ppm.

^{19}F NMR ($CDCl_3$) δ= - 112.0 ppm.

HRMS (CI): calculated for $C_{20}H_{13}FN_2$ $[M]^+$ 300.1096 found 300.1075.

2-(4-Nitrophenyl)-4-phenyl-1,5-naphthyridine (19e)

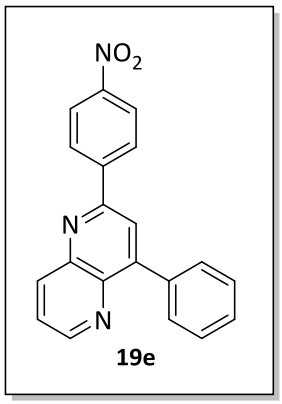

19e

The general procedure was followed using imine **3d** (5 mmol, 1.136 g) and phenylacetylene (7 mmol, 0.768 ml) and the reaction mixture was stirred at room temperature for 50 h. Compound **19e** was obtained as a yellow solid after purification by flash chromatography (0.817 g, 50%).

m.p.(°C) 178-179 (ethyl acetate/hexane) .

IR νmax 3080, 1575, 1780, 930, 725 cm^{-1}.

^{1}H NMR (300 MHz, $CDCl_3$) δ = 7.53-7.66 (m, 2H, H_{arom}), 7.78-7.85 (m, 2H, H_{arom}), 8.05 (d, $^{3}J_{HH}$ = 7.7 Hz, 2H, H_{arom}), 8.16 (s, 1H, HC), 8.30 (d, $^{3}J_{HH}$ = 8.6 Hz, 2H, H_{arom}),8.42 (s, 1H, H_{arom}), 8.56 (dd, $^{3}J_{HH}$ = 8.6 Hz, $^{4}J_{HH}$ = 1.7 Hz, 1H, H_{arom}), 9.05 (dd, $^{3}J_{HH}$ = 4.1 Hz, $^{4}J_{HH}$ = 1.7 Hz, 1H, H_{arom}) ppm.

^{13}C NMR (75 MHz, $CDCl_3$) δ = 121.2 (HC_{arom}), 122.1 (HC_{arom}), 123.5 (HC_{arom}), 124.8 (HC_{arom}), 127.2 ($2HC_{arom}$), 128.5 (HC_{arom}), 130.6 ($2HC_{arom}$), 130.7 (HC_{arom}), 132.8 (HC_{arom}), 136.9 (C_{arom}), 138.1 (HC_{arom}), 155.5 (C_{arom}), 140.86 (C_{arom}), 141.67 (C_{arom}), 144.70 (C_{arom}), 150.26 (C_{arom}), 151.5 (HC_{arom}), 155.25 (C_{arom}) ppm.

HRMS (CI): calculated for $C_{20}H_{13}N_3O_2$ $[M]^+$ 327.1008 found 327.1013.

2-(3-Nitrophenyl)-4-phenyl-1,5-naphthyridine (19f)

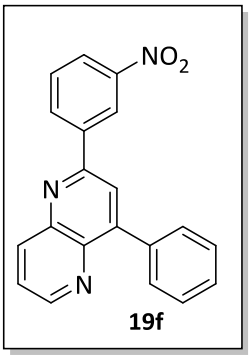

19f

The general procedure was followed using imine **3j** (5 mmol, 1.136 g) and phenylacetylene (7 mmol, 0.768 ml) and the reaction mixture was stirred at chloroform reflux for 15 h. Compound **19f** was obtained as a white solid after purification by flash chromatography (0.572 g, 35%).

m.p.(°C) 177-178 (ethyl acetate/hexane) .

IR νmax 3087, 1589, 1529, 1348, 909, 742 cm^{-1}.

^{1}H NMR (300 MHz, $CDCl_3$) δ = 7.74-7.52 (m, 3H, H_{arom}), 7.63-7.67 (m, 2H, H_{arom}), 7.74-7.77 (m, 2H, H_{arom}), 8.09 (s, 1H, HC), 8.26-8.29 (m, 1H, H_{arom}), 8.50-8.53 (m, 1H, H_{arom}), 8.96 (dd, $^{3}J_{HH}$ = 4.2 Hz, $^{4}J_{HH}$ = 1.8 Hz, 1H, H_{arom}), 9.03-9.04 (m, 1H, H_{arom}) ppm.

^{13}C NMR (75 MHz, $CDCl_3$) δ = 121.8 (HC_{arom}), 122.8 (HC_{arom}), 124.4 (HC_{arom}), 125.0 (HC_{arom}), 128.7 ($2HC_{arom}$), 129.3 (HC_{arom}), 130.2 (HC_{arom}), 130.7 ($2HC_{arom}$), 133.6 (HC_{arom}), 136.9 (C_{arom}), 138.1 (HC_{arom}), 155.5 (C_{arom}), 140.86 (C_{arom}), 141.67 (C_{arom}), 144.70 (C_{arom}), 150.26 (C_{arom}), 151.5 (HC_{arom}), 155.25 (C_{arom}) ppm.

HRMS (CI): calculated for $C_{20}H_{13}N_3O_2$ $[M]^+$ 327.1008 found 327.1018.

2-(3-Methoxyphenyl)- 4-phenyl -1,5-naphthyridine (19g)

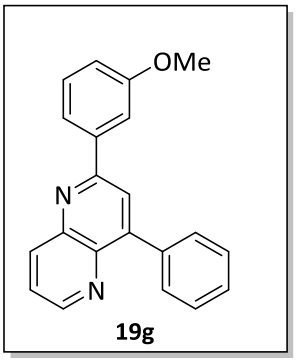

19g

The general procedure was followed using imine **3K** (5 mmol, 1.062 g) and phenylacetylene (7 mmol, 0.768 ml) and the reaction mixture was stirred at refluxing chloroform for 20 h. Compound **19g** was obtained as yellowish oil after purification by flash chromatography (0.783 g, 50%).

Rf 0.67 (50:50 ethyl acetate/hexane) .

IR νmax 3082, 1610, 1532, 134, 1253, 910, 756 cm^{-1}.

^{1}H NMR (300 MHz, $CDCl_3$) δ = 3.95 (s, 3H, OCH_3), 7.06 (d, $^{3}J_{HH}$ = 8.3 Hz, 1H, H_{arom}), 7.43-7.55 (m, 4H, H_{arom}), 7.63-7.68 (m, 1H, H_{arom}), 7.76-7.86 (m, 5H, H_{arom}), 8.12 (s, 1H, HC), 8.53 (d, $^{3}J_{HH}$ = 8.6 Hz, 1H, H_{arom}), 8.99-9.00 (m, 1H, H_{arom}) ppm.

^{13}C NMR (75 MHz, $CDCl_3$) δ =55.7 (OCH_3), 113.0 (HC_{arom}), 116.0 (HC_{arom}), 120.3 (HC_{arom}), 124.6 (HC_{arom}), 122.6 (HC_{arom}), 128.5 ($2HC_{arom}$), 129.0 (HC_{arom}), 130.1 (HC_{arom}), 130.7 ($2HC_{arom}$), 137.3 (C_{arom}), 138.0 (HC_{arom}), 140.7 (C_{arom}), 141.6 (C_{arom}), 144.5 (C_{arom}), 149.2 (C_{arom}), 150.7 (HC_{arom}), 157.7 (C_{arom}), 160.4 (C_{arom}) ppm.

HRMS (CI): calculated for $C_{21}H_{16}N_2O$ $[M]^+$ 312.1263 found 312.1269.

4-([1,1'-Biphenyl]-4-yl)-2-(4-trifluoromethylphenyl)-1,5-naphthyridine (19h)

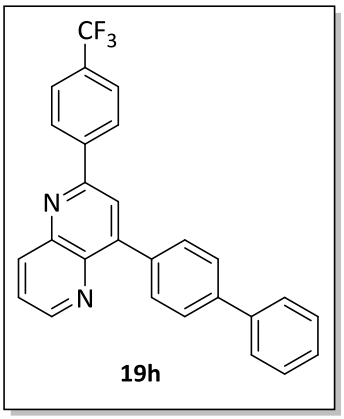

19h

The general procedure was followed using imine **3h** (5 mmol, 1.250 g) and 4-ethynylbiphenyl (7 mmol, 1.248 g) and the reaction mixture was stirred at room temperature for 48 h. Compound **19h** was obtained as a white solid after purification by flash chromatography (1.278 g, 60%).

m.p.(°C) 198-199 (ethyl acetate/hexane) .

IR νmax 3060, 2970 1570, 1325, 885, 732 cm^{-1}.

^{1}H NMR (300 MHz, $CDCl_3$) δ = 7.30-7.34 (m, 1H, H_{arom}), 7.38-7.45 (m, 2H, H_{arom}), 7.60-7.65 (m, 3H, H_{arom}), 7.70-7.76 (m, 4H, H_{arom}), 7.82-7.87 (m, 2H, H_{arom}), 8.10 (s, 1H, HC), 8.27 (d, $^{3}J_{HH}$ = 8.5 Hz, 2H, H_{arom}), 8.46 (dd, $^{3}J_{HH}$ = 8.5 Hz, $^{4}J_{HH}$ = 1.7 Hz, 1H, H_{arom}), 8.97 (dd, $^{3}J_{HH}$ = 4.2 Hz, $^{4}J_{HH}$ = 1.7 Hz, 1H, H_{arom}) ppm.

^{13}C NMR (75 MHz, $CDCl_3$) δ = 121.9 (HC_{arom}), 124.7 (HC_{arom}), 125.8 (HC_{arom}), 126.1 (q, $^{3}J_{CF}$ = 4.5 Hz, $2HC_{arom}$), 126.8 (q, $^{1}J_{CF}$ = 272.1 Hz, CF_3), 127.2 (HC_{arom}), 127.3 ($2HC_{arom}$), 127.7 ($2HC_{arom}$), 127.9 (HC_{arom}), 128.9 ($2HC_{arom}$), 130.9 (HC_{arom}), 131.5 (q, $^{2}J_{CF}$ = 32.3 Hz, C-CF_3), 135.7 (C_{arom}), 138.0 (HC_{arom}), 140.7 (C_{arom}), 141.4 (C_{arom}), 141.9 (C_{arom}), 142.3 (C_{arom}), 144.5 (C_{arom}), 149.1(C_{arom}), 151.1 (HC_{arom}), 156.2(C_{arom}) ppm.

^{19}F NMR ($CDCl_3$) δ= - 63.0 ppm.

HRMS (CI): calculated for $C_{27}H_{17}F_3N_2$ $[M]^+$ 426.1344 found 426.1357.

4-([1,1'-Biphenyl]-4-yl)-2-(4-fluorophenyl)-1,5-naphthyridine (19i)

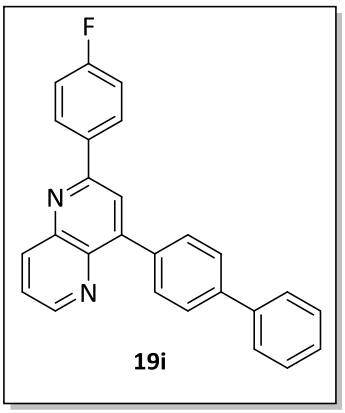

19i

The general procedure was followed using imine **3i** (5 mmol, 1.006 g) and 4-ethynylbiphenyl (7 mmol, 1.248 g) and the reaction mixture was heated at refluxing chloroform for 36 h. Compound **19i** was obtained as a white solid after purification by flash chromatography (1.034 g, 55%).

m.p.(°C) 206-207 (ethyl acetate/hexane) .

IR νmax 3059, 3029, 1596, 1483, 910, 837 cm^{-1}.

^{1}H NMR (300 MHz, $CDCl_3$) δ = 7.17-7.19 (m, 2H, H_{arom}), 7.31-7.34 (m, 1H, H_{arom}), 7.40-7.43 (m, 2H, H_{arom}), 7.58-7.63 (m, 3H, H_{arom}), 7.71-7.73 (m, 2H, H_{arom}), 7.83-7.86 (m, 2H, H_{arom}), 8.03 (s, 1H, HC), 8.41-8.44 (m, 2H, H_{arom}), 8.43 (dd, $^{3}J_{HH}$ = 8.6 Hz, $^{4}J_{HH}$ = 1.7 Hz, 1H, H_{arom}), 8.90 (dd, $^{3}J_{HH}$ = 4.1 Hz, $^{4}J_{HH}$ = 1.7 Hz, 1H, H_{arom}) ppm.

^{13}C NMR (75 MHz, $CDCl_3$) δ = 116.0 (d, $^{2}J_{CF}$ = 21.9 Hz, $2HC_{arom}$), 121.7 (HC_{arom}), 124.4 (HC_{arom}), 127.1 ($2HC_{arom}$), 127.2 ($2HC_{arom}$), 127.5 (HC_{arom}), 128.8 ($2HC_{arom}$), 129.5 (d, $^{3}J_{CF}$ = 8.5 Hz, $2HC_{arom}$), 130.8 ($2HC_{arom}$), 135.2 (C_{arom}), 135.8 (C_{arom}), 137.7 (HC_{arom}), 140.6 (C_{arom}), 141.2 (C_{arom}), 141.7 (C_{arom}), 144.3 (C_{arom}). 148.7 (C_{arom}), 150.4 (HC_{arom}), 156.6 (C_{arom}), 163.8 (d, $^{1}J_{CF}$ = 250.1 Hz, FC_{arom}) ppm.

^{19}F NMR ($CDCl_3$) δ= - 111.9 ppm.

HRMS (CI): calculated for $C_{26}H_{17}FN_2$ $[M]^+$ 376.1376 found 376.1383.

4-([1,1'-Biphenyl]-4-yl)-2-(4-nitrophenyl)-1,5-naphthyridine (19j)

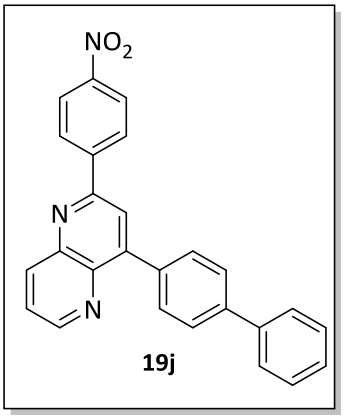

19j

The general procedure was followed using imine **3d** (5 mmol, 1.136 g) and 4-ethynylbiphenyl (7 mmol, 1.248 g) and the reaction mixture was stirred at room temperature for 24 h. Compound **19j** was obtained as a yellowish solid after purification by flash chromatography (1.007 g, 50%).

m.p.(°C) 195-196 (ethyl acetate/hexane) .

IR νmax 3059, 3045, 1660, 1470, 919, 820 cm^{-1}.

^{1}H NMR (300 MHz, $CDCl_3$) δ = 7.42-7.44 (m, 1H, H_{arom}), 7.47-7.54 (m, 3H, H_{arom}), 7.69-7.72 (m, 3H, H_{arom}), 7.82 (d, $^{3}J_{HH}$ = 8.4 Hz, 3H, H_{arom}), 7.90 (d, $^{3}J_{HH}$ = 7.6 Hz, 2H, H_{arom}), 8.22 (s, 1H, HC), 8.43 (s, 2H, H_{arom}), 8.57 (dd, $^{3}J_{HH}$ = 8.4 Hz, $^{4}J_{HH}$ = 1.7 Hz, 1H, H_{arom}), 9.07 (dd, $^{3}J_{HH}$ = 4.0 Hz, $^{4}J_{HH}$ = 1.7 Hz, 1H, H_{arom}) ppm.

^{13}C NMR (75 MHz, $CDCl_3$) δ = 124.5 ($2HC_{arom}$), 125.9 (HC_{arom}), 127.5 (HC_{arom}), 127.6 ($2HC_{arom}$), 127.7 ($2HC_{arom}$), 128.7 (HC_{arom}), 129.1 (HC_{arom}), 129.2 ($2HC_{arom}$), 129.3 ($2HC_{arom}$), 129.5 ($2HC_{arom}$), 131.3 (C_{arom}), 136.4 (C_{arom}), 137.7 (C_{arom}), 139.9 (C_{arom}), 141.3 (C_{arom}), 141.8 (HC_{arom}), 144.0 (C_{arom}), 146.4 (C_{arom}), 148.8 (C_{arom}), 155.0 (C_{arom}) ppm.

HRMS (CI): calculated for $C_{26}H_{17}N_3O_2$ $[M]^+$ 403.1321 found 403.1334.

4-([1,1'-Biphenyl]-4-yl)-2-(3-nitrophenyl)-1,5-naphthyridine (19k)

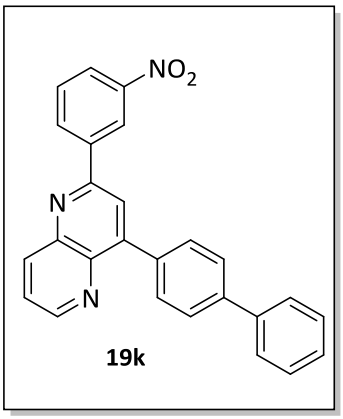

19k

The general procedure was followed using imine **3j** (5 mmol, 1.136 g) and 4-ethynylbiphenyl (7 mmol, 1.248 g) and the reaction mixture was stirred at chloroform reflux for 24 h. Compound **19k** was obtained as a yellowish solid after purification by flash chromatography (0.604 g, 30%).

m.p.(°C) 197-198 (ethyl acetate/hexane) .

IR νmax 3050, 3035, 1580, 1465, 920, 820 cm^{-1}.

^{1}H NMR (300 MHz, $CDCl_3$) δ = 7.18-7.19 (m, 1H, H_{arom}), 7.31-7.36 (m, 1H, H_{arom}), 7.40-7.45 (m, 2H, H_{arom}), 7.60-7.64 (m, 2H, H_{arom}), 7.65-7.68 (m, 1H, H_{arom}), 7.72-7.76 (m, 2H, H_{arom}), 7.80-7.84 (m, 2H, H_{arom}), 8.14 (s, 1H, H_{arom}), 8.29 (dd, $^{3}J_{HH}$ = 8.4 Hz, $^{4}J_{HH}$ = 2.3 Hz, 1H, H_{arom}), 8.49 (dd, $^{3}J_{HH}$ = 8.4 Hz, $^{4}J_{HH}$ = 1.8 Hz, 1H, H_{arom}), 8.52-8.55 (m, 1H, H_{arom}), 8.99 (dd, $^{3}J_{HH}$ = 4.1 Hz, $^{4}J_{HH}$ = 1.8 Hz, 1H, H_{arom}), 9.05 (t, $^{4}J_{HH}$ = 1.8 Hz, 1H, H_{arom}) ppm.

^{13}C NMR (75 MHz, $CDCl_3$) δ = 121.4 (HC_{arom}), 122.5 ($2HC_{arom}$), 124.3 (HC_{arom}), 124.8 (HC_{arom}), 127.2 ($2HC_{arom}$), 127.6 ($2HC_{arom}$), 128.8 ($2HC_{arom}$), 129.9 (HC_{arom}), 130.9 ($2HC_{arom}$), 133.3 (C_{arom}), 135.5 (HC_{arom}), 138.0 (HC_{arom}), 140.5 (C_{arom}), 140.6 (C_{arom}), 141.4 (C_{arom}), 142.0 (C_{arom}), 144.4 (C_{arom}), 148.9 (C_{arom}), 149.4 (C_{arom}), 151.2 (HC_{arom}), 154.8 (C_{arom}) ppm.

HRMS (CI): calculated for $C_{26}H_{17}N_3O_2$ $[M]^+$ 403.1321 found 403.1334.

4-([1,1'-Biphenyl]-4-yl)-2-(3-methoxyphenyl)-1,5-naphthyridine (19l)

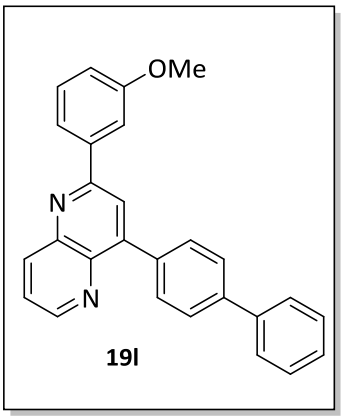

19l

The general procedure was followed using imine **3k** (5 mmol, 1.062 g) and 4-ethynylbiphenyl (7 mmol, 1.248 g) and the reaction mixture was stirred at refluxing chloroform for 48 h. Compound **19l** was obtained as a yellowish solid after purification by flash chromatography (1.068 g, 55%).

m.p.(°C) 185-186 (ethyl acetate/hexane) .

IR νmax 3030, 1168, 1450, 850, 775 cm^{-1}.

^{1}H NMR (300 MHz, $CDCl_3$) δ = 3.87 (s, 3H, OCH_3), 7.02 (d, $^{3}J_{HH}$ = 8.3 Hz, 1H, H_{arom}), 7.32-7.37 (m, 2H, H_{arom}), 7.39-7.43 (m, 4H, H_{arom}), 7.62-7.74 (m, 4H, H_{arom}), 7.83-7.83 (m, 3H, H_{arom}), 8.08 (s, 1H, H_{arom}), 8.46 (dd, $^{3}J_{HH}$ = 8.5 Hz, $^{4}J_{HH}$ = 1.7 Hz, 1H, H_{arom}), 8.94 (dd, $^{3}J_{HH}$ = 4.2 Hz, $^{4}J_{HH}$ = 1.7 Hz, 1H, H_{arom}) ppm.

^{13}C NMR (75 MHz, $CDCl_3$) δ = 55.5 (OCH_3), 112.8 (HC_{arom}),115.8 (HC_{arom}), 120.0 (HC_{arom}), 122.2 (HC_{arom}), 124.4 (HC_{arom}), 127.1 ($2HC_{arom}$), 127.2 ($2HC_{arom}$), 127.5 (HC_{arom}), 128.8 ($2HC_{arom}$), 129.9 (HC_{arom}), 130.8 ($2HC_{arom}$), 135.9 (C_{arom}), 137.8 (HC_{arom}), 140.5 (C_{arom}), 140.7 (C_{arom}), 141.4 (C_{arom}), 141.7 (C_{arom}), 144.3 (C_{arom}), 148.5 (C_{arom}), 150.5 (HC_{arom}), 157.6 (C_{arom}), 160.2 (C_{arom}) ppm.

HRMS (CI): calculated for $C_{27}H_{20}N_2O$ $[M]^+$ 388.4689 found 388.4684.

2-(4-Fluorophenyl)-4-(6-methoxynaphthalen-2-yl)-1,5-naphthyridine (19m)

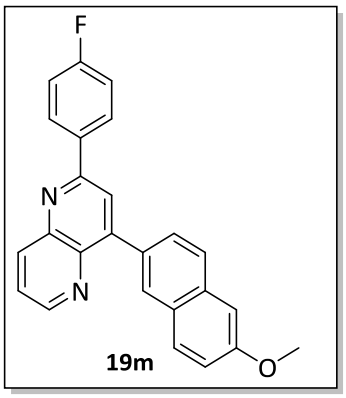

19m

The general procedure was followed using imine **3i** (5 mmol, 1.006 g) and 2-ethynyl-6-methoxynaphtalene (7 mmol, 1.275 g) and the reaction mixture was heated at refluxing chloroform for 24 h. Compound **19m** was obtained as a white solid after purification by flash chromatography (0.950 g, 50%).

m.p.(°C) 208-209 (ethyl acetate/hexane) .

IR νmax 3040, 3030, 1570, 1480, 880, 780 cm^{-1}.

^{1}H NMR (300 MHz, $CDCl_3$) δ = 3.90 (s, 3H, OCH_3), 7.13-7.19 (m, 4H, H_{arom}), 7.60 (dd, $^{3}J_{HH}$ = 8.5 Hz, $^{3}J_{HH}$ = 4.1 Hz, 1H, H_{arom}), 7.77-7.87 (m, 3H, H_{arom}), 8.07 (s, 1H, H_{arom}), 8.14-8.17 (m, 3H, H_{arom}), 8.43 (dd, $^{3}J_{HH}$ = 8.6 Hz, $^{4}J_{HH}$ = 1.8 Hz, 1H, H_{arom}), 8.92 (dd, $^{3}J_{HH}$ = 4.1 Hz, $^{4}J_{HH}$ = 1.8 Hz, 1H, H_{arom}) ppm.

^{13}C NMR (75 MHz, $CDCl_3$) δ = 55.6 (OCH_3), 105.9 (HC_{arom}), 116.1 (d, $^{2}J_{CF}$ = 21.3 Hz, $2HC_{arom}$), 119.4 (HC_{arom}), 122.2 (HC_{arom}), 124.7 (HC_{arom}), 126.9 (HC_{arom}), 128.9 (HC_{arom}), 129.0 (HC_{arom}), 129.7 (HC_{arom}), 129.8 (d, $^{3}J_{CF}$ = 8.4 Hz, $2HC_{arom}$), 130.3 (HC_{arom}), 132.6 (C_{arom}), 135.0 (C_{arom}), 135.5 (C_{arom}), 137.9 (HC_{arom}), 141.7 (C_{arom}), 144.6 (C_{arom}), 149.5 (C_{arom}), 150.7 (HC_{arom}). 156.9 (C_{arom}), 158.6 (C_{arom}), 162.6 (C_{arom}), 165.9 (C_{arom}) ppm.

^{19}F NMR ($CDCl_3$) δ= - 112.1 ppm.

HRMS (CI): calculated for $C_{27}H_{17}FN_2O$ $[M]^+$ 380.1096 found 380.1075.

4-(4-Methoxyphenyl)-2-(4-(trifluoromethyl)phenyl)-1,5-naphthyridine (19n)

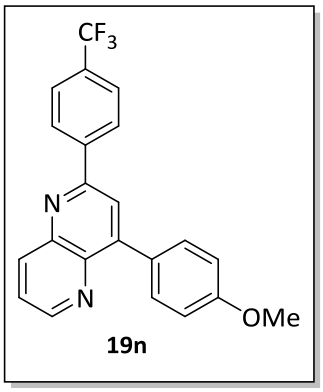

19n

The general procedure was followed using imine **3h** (5 mmol, 1.250 g) and 4-methoxyphenylacetylene (7 mmol, 0.908 ml) and the reaction mixture was stirred at refluxing chloroform for 36 h. Compound **19n** was obtained as a white solid after purification by flash chromatography (1.140 g, 60%).

m.p.(°C) 165-166 (ethyl acetate/hexane) .

IR νmax 3030, 1675, 1525, 1330, 885, 750 cm^{-1}.

^{1}H NMR (300 MHz, $CDCl_3$) δ = 3.84 (s, 3H, OCH_3), 7.01-7.07 (m, 2H, H_{arom}), 7.61 (dd, $^{3}J_{HH}$ = 8.5 Hz, $^{3}J_{HH}$ = 4.3 Hz, 1H, H_{arom}), 7.69-7.77 (m, 4H, H_{arom}), 8.04 (s, 1H, H_{arom}), 8.26 (d, $^{3}J_{HH}$ = 8.5 Hz, 2H, H_{arom}), 8.44 (dd, $^{3}J_{HH}$ = 8.5 Hz, $^{4}J_{HH}$ = 1.8 Hz, 1H, H_{arom}), 8.95 (dd, $^{3}J_{HH}$ = 4.3 Hz, $^{4}J_{HH}$ = 1.8 Hz, 1H, H_{arom}) ppm.

^{13}C NMR (75 MHz, $CDCl_3$) δ = 55.4 (OCH_3), 114.3 ($2HC_{arom}$), 121.5 (HC_{arom}), 124.5 (HC_{arom}), 125.8 (q, $^{3}J_{CF}$ = 4.1 Hz, $2HC_{arom}$), 126.3 (q, $^{1}J_{CF}$ = 274.5 Hz, CF_3), 127.9 ($2HC_{arom}$), 128.9 (C_{arom}), 131.4 (q, $^{2}J_{CF}$ = 33.5 Hz, C-CF_3), 131.8 ($2HC_{arom}$), 137.9 (HC_{arom}), 141.5 (C_{arom}), 142.4 (C_{arom}), 144.5 (C_{arom}), 148.9 (C_{arom}), 150.8 (HC_{arom}), 156.1 (C_{arom}), 160.3 (C_{arom}) ppm.

^{19}F NMR ($CDCl_3$) δ= - 63.1 ppm.

HRMS (CI): calculated for $C_{22}H_{15}F_3N_2O$ $[M]^+$ 380.1136 found 380.1136.

2-(4-Fluorphenyl)-4-(4-methoxyphenyl)-1,5-naphthyridine (19o)

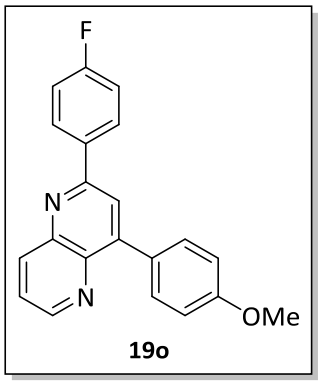

19o

The general procedure was followed using imine **3i** (5 mmol, 1.006 g) and 4-methoxyphenylacetylene (7 mmol, 0.908 ml) and the reaction mixture was heated at refluxing chloroform for 24 h. Compound **19o** was obtained as a white solid after purification by flash chromatography (0.495 g, 30%).

m.p.(°C) 174-175 (ethyl acetate/hexane) .

IR νmax 3045, 1667, 1520, 1345, 909, 845, 737 cm^{-1}.

^{1}H NMR (300 MHz, $CDCl_3$) δ = 3.83 (s, 3H, OCH_3), 7.02-7.05 (m, 2H, H_{arom}), 7.15-7.18 (m, 1H, H_{arom}), 7.57 (dd, $^{3}J_{HH}$ = 8.6 Hz, $^{3}J_{HH}$ = 4.3 Hz, 1H, H_{arom}), 7.72-7.74 (m, 2H, H_{arom}), 7.98 (s, 1H, H_{arom}), 8.11-8.15 (m, 2H, H_{arom}), 8.39 (dd, $^{3}J_{HH}$ = 8.6 Hz, $^{4}J_{HH}$ = 1.7 Hz, 1H, H_{arom}), 8.90 (dd, $^{3}J_{HH}$ = 4.3 Hz, $^{4}J_{HH}$ = 1.7 Hz, 1H, H_{arom}) ppm.

^{13}C NMR (75 MHz, $CDCl_3$) δ = 55.0 (OCH_3), 114.2 ($2HC_{arom}$), 116.0 (d, $^{2}J_{CF}$ = 22.0 Hz, $2HC_{arom}$), 121.7 (HC_{arom}), 124.6 (HC_{arom}), 129.5 (C_{arom}), 129.7 (q, $^{3}J_{CF}$ = 8.4 Hz, $2HC_{arom}$), 132.0 ($2HC_{arom}$), 135.6 (C_{arom}), 137.9 (HC_{arom}), 141.6 (C_{arom}), 144.6 (C_{arom}), 148.9 (C_{arom}), 150.5 (HC_{arom}), 156.9 (C_{arom}), 160.5 (C_{arom}), 164.3(d, $^{1}J_{CF}$ = 248.4 Hz, C_{arom}) ppm.

^{19}F NMR ($CDCl_3$) δ= - 112.1 ppm.

HRMS (CI): calculated for $C_{21}H_{15}FN_2O$ $[M]^+$ 330.1168 found 330.1176.

2-(4-Nitrophenyl)-4-(4-methoxyphenyl)-1,5-naphthyridine (19p)

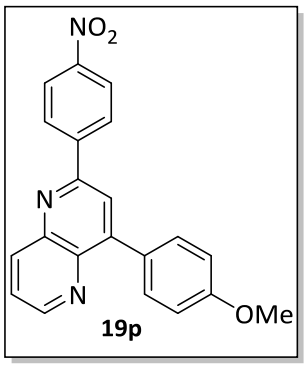

19p

The general procedure was followed using imine **3d** (5 mmol, 1.136 g) and 4-methoxyphenylacetylene (7 mmol, 0.908 ml) and the reaction mixture was heated at refluxing chloroform for 18 h. Compound **19p** was obtained as a white solid after purification by flash chromatography (1.071 g, 60%).

m.p.(°C) 134-135 (ethyl acetate/hexane).

IR νmax 1600, 1518, 1485, 1255, 848, 818.

^{1}H NMR (300 MHz, $CDCl_3$) δ = 3.84 (s, 3H, OCH_3), 7.03 (d, $^{3}J_{HH}$ = 8.7 Hz, 3H, H_{arom}),7.60 (dd, $^{3}J_{HH}$ = 8.5 Hz, $^{3}J_{HH}$ = 4.1 Hz, 1H, H_{arom}), 7.75 (d, $^{3}J_{HH}$ = 8.7 Hz, 3H, H_{arom}), 8.05 (s, 1H, HC), 8.33 (s, 4H, H_{arom}), 8.44 (dd, $^{3}J_{HH}$ = 8.5 Hz, $^{4}J_{HH}$ = 1.8 Hz, 1H, H_{arom}), 8.96 (dd, $^{3}J_{HH}$ = 4.1 Hz, $^{4}J_{HH}$ = 1.8 Hz, 1H, H_{arom}) ppm.

^{13}C NMR (75 MHz, $CDCl_3$) δ = 55.7 (OCH_3), 114.3 ($2HC_{arom}$), 121.8 (HC_{arom}), 124.3 ($2HC_{arom}$), 124.9 (HC_{arom}), 128.7 ($2HC_{arom}$), 132.1 ($2HC_{arom}$), 135.6 (C_{arom}), 138.2 (HC_{arom}), 141.8 (C_{arom}), 144.8 (C_{arom}), 145.2 (C_{arom}), 149.5(C_{arom}), 151.5 (HC_{arom}), 151.4 (C_{arom}), 155.3 (C_{arom}), 160.8(C_{arom}) ppm.

HRMS (CI): calculated for $C_{16}H_{13}NO_4$ $[M]^+$ 357.3712 found 357.3717.

2-[(3-(Methoxyphenyl)-4-(4-methoxyphenyl)]-1,5-naphthyridine (19q)

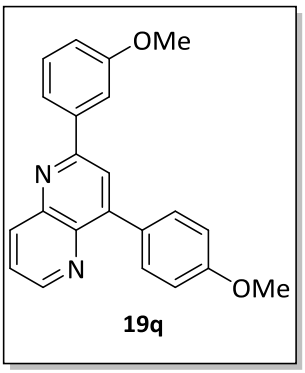

19q

The general procedure was followed using imine **3k** (5 mmol, 1.062 g) and 4-methoxyphenylacetylene (7mmol, 0.908 ml) and the reaction mixture was stirred at refluxing chloroform for 70 h. Compound **19q** was obtained as a white solid after purification by flash chromatography (0.684 g, 40%).

m.p.(°C) 193-194 (ethyl acetate/hexane).

IR νmax 3082, 1610, 1532, 1348, 1253, 910, 756.

^{1}H NMR (300 MHz, $CDCl_3$) δ = 3.85 (s, 6H, OCH_3), 7.04 (d, $^{3}J_{HH}$ = 8.8 Hz, 2H, H_{arom}), 7.61-7.66 (m, 3H, H_{arom}), 7.76 (d, $^{3}J_{HH}$ = 8.8 Hz, 1H, H_{arom}), 8.08 (s, 1H, H_{arom}), 8.28 (ddd, $^{3}J_{HH}$ = 8.1 Hz, $^{4}J_{HH}$ = 2.2 Hz, $^{4}J_{HH}$ = 1.1 Hz, 2H, H_{arom}), 8.66 (d, $^{3}J_{HH}$ = 8.8 Hz, 1H, H_{arom}), 8.96 (dd, $^{3}J_{HH}$ = 8.6 Hz, $^{3}J_{HH}$ = 4.0 Hz, 1H, H_{arom}),9.03 (t, $^{4}J_{HH}$ = 1.7 Hz, 1H, H_{arom}) ppm.

^{13}C NMR (75 MHz, $CDCl_3$) δ = 55.4 ($2OCH_3$), 114.0 ($2HC_{arom}$), 121.0 (HC_{arom}), 122.5 (HC_{arom}), 124.2 (HC_{arom}), 124.7 (HC_{arom}), 128.8 (C_{arom}), 129.9 (HC_{arom}), 131.9 ($2HC_{arom}$), 133.3 (HC_{arom}), 137.8 (HC_{arom}), 140.6 (C_{arom}), 141.5 (C_{arom}), 144.5 (C_{arom}), 148.8 (C_{arom}), 149.4 (C_{arom}), 150.9 (HC_{arom}), 154.8 (C_{arom}), 160.4 (C_{arom}) ppm.

HRMS (CI): calculated for $C_{22}H_{18}F_3N_2O_2$ $[M]^+$ 342.4005 found 342.4009.

2,4-(4-Trifluoromethyl)phenyl-1,5-naphthyridine (19r)

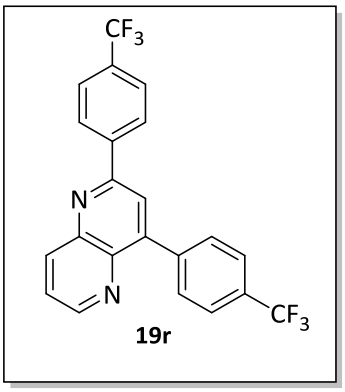

19r

The general procedure was followed using imine **3h** (5 mmol, 1.250 g) and 4-trifluoromethylphenylacetylene (7 mmol, 1.190 g) and the reaction mixture was stirred at refluxing chloroform for 36 h. Compound **19r** was obtained as a white solid after purification by flash chromatography (1.251 g, 60%).

m.p.(°C) 191-192 (ethyl acetate/hexane).

IR νmax 3020, 2850, 1780, 1250, 880 cm^{-1}.

^{1}H NMR(300 MHz, $CDCl_3$) δ = 7.65 (dd, $^{3}J_{HH}$ = 8.5 Hz, $^{3}J_{HH}$ = 4.1 Hz, 1H, H_{arom}), 7.73-7.77 (m, 4H, H_{arom}), 7.85-7.87 (m,2H, H_{arom}), 8.05 (s, 1H, H_{arom}), 8.26 (d, $^{3}J_{HH}$ = 8.6 Hz, 2H, H_{arom}), 8.48 (dd, $^{3}J_{HH}$ = 8.5 Hz, $^{4}J_{HH}$ = 1.8 Hz, 1H, H_{arom}), 8.94 (dd, $^{3}J_{HH}$ = 4.1 Hz, $^{4}J_{HH}$ = 1.8 Hz, 1H, H_{arom}) ppm.

^{13}C NMR (75 MHz, $CDCl_3$) δ = 121.7 (HC_{arom}), 122.4 (q, $^{3}J_{CF}$ = 272.8 Hz, CF_3), 122.8 (q, $^{3}J_{CF}$ = 272.3 Hz, CF_3), 124.7 (HC_{arom}), 125.0 (q, $^{3}J_{CF}$ = 4.0 Hz, HC_{arom}), 125.6 (q, $^{3}J_{CF}$ = 4.0 Hz, HC_{arom}), 127.6 ($2HC_{arom}$), 130.5 ($2HC_{arom}$), 130.6 (q, $^{2}J_{CF}$ = 31.7 Hz, C-CF_3), 131.4 (q, $^{2}J_{CF}$ = 33.7 Hz, C-CF_3), 137.7 (HC_{arom}), 140.1 (HC_{arom}), 140.6 (C_{arom}), 141.6 (C_{arom}), 144.2 (C_{arom}), 147.7 (C_{arom}), 151.0 (HC_{arom}), 155.9 (C_{arom}) ppm.

^{19}F NMR ($CDCl_3$) δ= - 63.1 ppm.

HRMS (CI): calculated for $C_{22}H_{12}F_6N_2$ $[M]^+$ 418.0905 found 418.0908.

4-(Thiophen-3-yl)-2-(4-(trifluoromethyl)phenyl)-1,5-naphthyridine (19s)

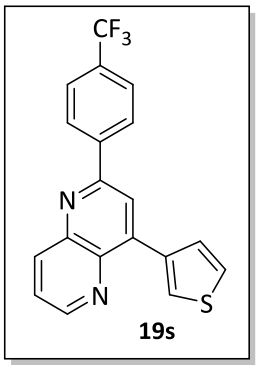

19s

The general procedure was followed using imine **3h** (5 mmol, 1.250 g) and 3-ethynyltiophene (7 mmol, 0.693 ml) and the reaction mixture was stirred at refluxing chloroform for 40 h. Compound **19s** was obtained as a yellowish solid after purification by flash chromatography (0.890 g, 50%).

m.p.(°C) 195-196 (ethyl acetate/hexane) .

IR νmax 3030, 2870, 1770, 1240, 870, 773 cm^{-1}.

^{1}H NMR (300 MHz, $CDCl_3$) δ = 7.45 (dd, $^{3}J_{HH}$ = 5.0 Hz, $^{3}J_{HH}$ = 3.0 Hz, 1H, H_{arom}), 7.6 (dd, $^{3}J_{HH}$ = 8.5 Hz, $^{3}J_{HH}$ = 4.1 Hz, 1H, H_{arom}), 7.68-7.76 (m, 3H, H_{arom}), 8.14 (s, 1H, H_{arom}), 8.19-8.26 (m, 2H, H_{arom}), 8.40 (dd, $^{3}J_{HH}$ = 8.5 Hz, $^{4}J_{HH}$ = 1.7 Hz, 1H, H_{arom}), 8.92 (dd, $^{3}J_{HH}$ = 4.1 Hz, $^{4}J_{HH}$ = 1.7 Hz, 1H, H_{arom}) ppm.

^{13}C NMR (75 MHz, $CDCl_3$) δ = 120.8 (HC_{arom}), 123.9 (q, $^{1}J_{CF}$ = 271.8 Hz, CF_3), 124.9 (HC_{arom}), 125.9 (HC_{arom}), 126.1 (q, $^{3}J_{CF}$ = 3.8 Hz, $2HC_{arom}$), 128.1 ($2HC_{arom}$), 128.4 (HC_{arom}), 129.2 (HC_{arom}), 131.7 (q, $^{2}J_{CF}$ = 32.9 Hz C-CF_3), 137.0 (C_{arom}), 138.2 (HC_{arom}), 141.4 (C_{arom}), 142.6 (C_{arom}), 143.4 (C_{arom}), 144.9 (C_{arom}), 150.9 (HC_{arom}), 156.6 (C_{arom}) ppm.

^{19}F NMR ($CDCl_3$) δ= - 63.0 ppm.

HRMS (CI): calculated for $C_{19}H_{11}F_3N_2S$ $[M]^+$ 356.0595 found 356.0592.

2-(4-Fluorophenyl)-4-(thiophen-3-yl)-1,5-naphthyridine (19t)

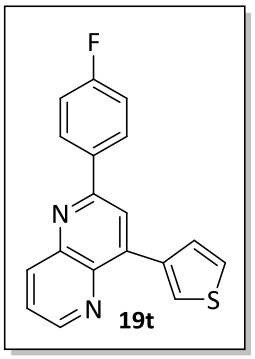

19t

The general procedure was followed using imine **3i** (5 mmol, 1.006 g) and 3-ethynyltiophene (7 mmol, 0.693 ml) and the reaction mixture was heated at refluxing chloroform for 48 h. Compound **19t** was obtained as a white solid after purification by flash chromatography (0.459 g, 30%).

m.p.(°C) 106-107 (ethyl acetate/hexane) .

IR νmax 3035, 2980, 1760, 1250, 880, 765 cm^{-1}.

^{1}H NMR(300 MHz, $CDCl_3$) δ = 7.25-7.27 (m, 2H, H_{arom}), 7.50-7.53 (m, 1H, H_{arom}), 7.65-7.70 (m, 1H, H_{arom}), 7.79-7.81 (m, 3H, H_{arom}), 8.08 (s, 1H, H_{arom}), 8.30-8.32 (m, 1H, H_{arom}), 8.47 (dd, $^{3}J_{HH}$ = 8.6 Hz, $^{4}J_{HH}$ = 1.8 Hz, 1H, H_{arom}), 9.00 (dd, $^{3}J_{HH}$ = 4.0 Hz, $^{4}J_{HH}$ = 1.8 Hz, 1H, H_{arom}) ppm.

^{13}C NMR (75 MHz, $CDCl_3$) δ = 116.0 (d, $^{2}J_{CF}$ = 21.7 Hz, $2HC_{arom}$), 120.7 (HC_{arom}), 124.7 (HC_{arom}), 125.7 (HC_{arom}), 128.1 (HC_{arom}), 129.2 (HC_{arom}), 129.7 (d, $^{3}J_{CF}$ = 8.9 Hz, $2HC_{arom}$), 135.5 (C_{arom}), 137.3 (C_{arom}), 138.0 (HC_{arom}), 141.2 (C_{arom}), 143.1 (C_{arom}), 144.7 (C_{arom}), 150.5 (HC_{arom}), 157.2 (C_{arom}), 164.3 d, $^{1}J_{CF}$ = 252.3 Hz, C_{arom}) ppm.

^{19}F NMR ($CDCl_3$) δ= - 112.1 ppm.

HRMS (CI): calculated for $C_{18}H_{11}FN_2S$ $[M]^+$ 306.0627 found 306.0633.

4-Phenyl-3-methyl-2(4-trifluoromethylphenyl)-1,5-naphthyridine (19u)

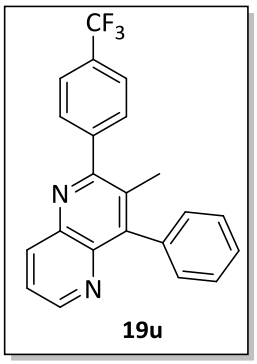

19u

The general procedure was followed using imine **3h** (5 mmol, 1.250 g) and propyl-1-yl-benzene (7 mmol, 0.802 ml) and the reaction mixture was heated at refluxing chloroform for 58 h. Compound **19u** was obtained as a yellowish solid after purification by flash chromatography (0.910 g, 50%).

m.p.(°C) 189-190 (ethyl acetate/hexane) .

IR νmax 3030, 1778, 1250, 860, 773 cm^{-1}.

^{1}H NMR (300 MHz, $CDCl_3$) δ = 2.1 (CH_3), 7.27-7.29 (m, 2H, H_{arom}), 7.36-7.41 (m, 1H, H_{arom}), 7.44-7.49 (m, 3H, H_{arom}), 7.67 (q, $^{3}J_{HH}$ = 8.5 Hz, 4H, H_{arom}), 8.33 (dd, $^{3}J_{HH}$ = 8.5 Hz, $^{4}J_{HH}$ = 1.8 Hz, 1H, H_{arom}), 8.83 (dd, $^{3}J_{HH}$ = 4.1 Hz, $^{4}J_{HH}$ = 1.8 Hz, 1H, H_{arom}) ppm.

^{13}C NMR (75 MHz, $CDCl_3$) δ = 18.91 (CH_3), 123.6 (HC_{arom}), 124.0 (q, $^{1}J_{CF}$ = 275.0 Hz, CF_3), 125.3 (q, $^{3}J_{CF}$ = 3.7 Hz, $2HC_{arom}$), 127.9 (HC_{arom}), 128.3 ($2HC_{arom}$), 129.3 ($2HC_{arom}$), 129.5 ($2HC_{arom}$), 130.2 (C_{arom}), 130.4 (q, $^{2}J_{CF}$ = 32.5 Hz, C-CF_3), 136.5 (C_{arom}), 137.1 (HC_{arom}), 141.6 (C_{arom}), 142.0 (C_{arom}), 144.0 (C_{arom}), 149.1 (C_{arom}), 151.1 (HC_{arom}), 160.1 (C_{arom}) ppm.

^{19}F NMR ($CDCl_3$) δ= - 62.9 ppm.

HRMS (CI): calculated for $C_{22}H_{15}F_3N_2$ $[M]^+$ 364.1187 found 364.1189.

6.2.8. Reaction between aldehydes and acetylenes

3-(4-Nitrophenyl)-1-phenylprop-2-en-1-one

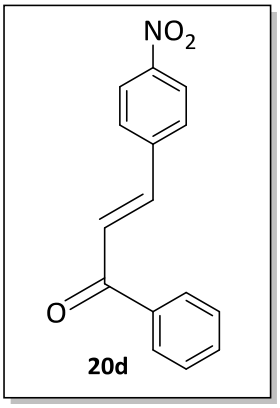

20d

A solution of 4-nitrobenzaldehyde (5 mmol, 0.775 g) and phenylacetylene (7mmol, 0.768 ml) was stirred at refluxing chloroformfor (10 ml) for 20 h. Compound **20d** was obtained as a white solid after purification by flash chromatography (1.075 g, 85%).

m.p.(°C) 128-129 (ethyl acetate/hexane) .

IR νmax 3040, 1760, 1450, 850, 775 cm^{-1}.

^{1}H NMR (300 MHz, $CDCl_3$) δ = 7.50-7.59 (m, 3H, $2H_{arom}$ and 1CH=), 7.61-7.66 (m, 2H, H_{arom}), 7.76-7.83 (m, 3H, $2H_{arom}$,1CH=), 8.01-8.09 (m, 2H, H_{arom}), 8.26-8.32 (m, 2H, H_{arom}) ppm.

^{13}C NMR (75 MHz, $CDCl_3$) δ = 124.5 ($2HC_{arom}$), 125.7 (CH), 128.6 ($2HC_{arom}$), 128.8 ($2HC_{arom}$), 128.9 ($2HC_{arom}$), 133.3 (HC_{arom}), 137.5 (C_{arom}), 141.0 (C_{arom}), 141.5 (CH), 148.6 (C_{arom}), 189.6 (C=O) ppm.

HRMS (CI): calculated for $C_{15}H_{11}NO_3$ $[M]^+$ 253.0744 found 253.0746.

1-(4-Methoxyphenyl)-3-(4-nitrophenyl)prop-2-en-1-one

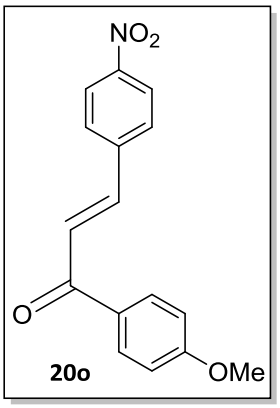

A solution of 4-nitrobenzaldehyde (5 mmol, 0.775 g) and 4-methoxyphenylacetylene (7 mmol, 0.908 ml) was stirred at refluxing chloroformfor (10 ml) for 24 h. Compound **20o** was obtained as a yellow solid after purification by flash chromatography (0.773 g, 55%).

m.p.(°C) 130-131 (ethyl acetate/hexane) .

IR νmax 3030, 1765, 1420, 870, 778 cm^{-1}.

^{1}H NMR (300 MHz, $CDCl_3$) δ = 7.50-7.59 (m, 3H, $2H_{arom}$ and 1CH=), 7.61-7.66 (m, 2H, H_{arom}), 7.76-7.83 (m, 3H, $2H_{arom}$,1CH=), 8.01-8.09 (m, 2H, H_{arom}), 8.26-8.32 (m, 2H, H_{arom}) ppm.

^{13}C NMR (75 MHz, $CDCl_3$) δ = 55.3 (OCH_3), 114.0 ($2HC_{arom}$), 123.6 ($2HC_{arom}$), 124.3 (CH), 128.1 ($2HC_{arom}$), 129.8 ($2HC_{arom}$), 131.5 (C_{arom}), 138.2 (C_{arom}), 140.2 (=HC), 148.1 (C_{arom}), 163.3 ($2C_{arom}$), 187.8 (C=O) ppm.

HRMS (CI): calculated for $C_{17}H_{13}F_3O_2$ $[M]^+$ 283.2874 found 283.2879.

1-(4-Methoxyphenyl)-3-(4-(trifluoromethyl)phenyl)prop-2-en-1-one

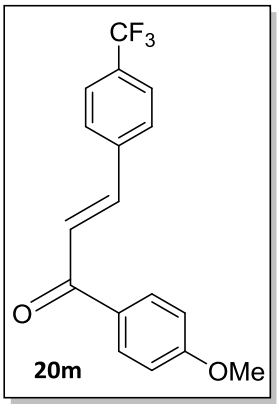

20m

A solution of 4-(trifluoromethyl)benzaldehyde (5 mmol, 0.721 ml) and 4-methoxyphenylacetylene (7mmol, 0.908 ml) was stirred at refluxing chloroformfo (10 ml) for 24 h. Compound **20m** was obtained as a white solid after purification by flash chromatography (1.150 g, 75%).

m.p.(°C) 139-140 (ethyl acetate/hexane) .

IR νmax 3050, 1770, 1460, 870, 775 cm^{-1}.

^{1}H NMR (300 MHz, $CDCl_3$) δ = 3.91 (s, 3H, OCH_3), 7.01 (d, $^{3}J_{HH}$ = 8.8 Hz, 2H, $2H_{arom}$), 7.58-7.81 (m, 6H, H_{arom}), 8.06 (d, $^{3}J_{HH}$ = 8.8 Hz, 2H, $2H_{arom}$) ppm.

^{13}C NMR (75 MHz, $CDCl_3$) δ = 55.5 (OCH_3), 113.9 (HC_{arom}), 124.1 (CH), 125.8 ($2HC_{arom}$), 125.9 (q, $^{3}J_{CF}$ = 3.8 Hz, $2HC_{arom}$), 126.8 (q, $^{1}J_{CF}$ = 260.1 Hz, CF_3), 127.9 (q, $^{2}J_{CF}$ = 32.4 Hz, C-CF_3), 128.4 ($2HC_{arom}$), 130.9 (HC_{arom}), 138.5 (C_{arom}), 141.9 (CH), 163.7 ($2C_{arom}$), 188.1 (C=O) ppm.

^{19}F NMR ($CDCl_3$) δ= -63.2, ppm.

HRMS (CI): calculated for $C_{17}H_{13}F_3O_2$ $[M]^+$ 306.0868 found 306.0874.

6.2.9. Reaction between imine 3l and acetylenes

General procedure

The corresponding acetylenes (7 mmol) and $BF_3{\cdot}Et_2O$ (10 mmol, 1.230 ml) were added to a solution of the previously prepared aldimine **3l** (5 mmol, 1.201 g) in $CHCl_3$ (10 ml). The mixture was stirred at the appropriate temperature until TLC and ^1H NMR spectroscopy indicated the disappearance of imine **3l** signals. The reaction mixture was washed with 2M aqueous solution of NaOH (20 ml) and water (20 ml), extracted with dichloromethane (20 ml), and dried over anhydrous $MgSO_4$. The removal of the solvent under vaccum affored compounds **21** that were purified by silica gel flash column chromatography (eluent: Hexane/AcOEt) to afford the desired products **21**.

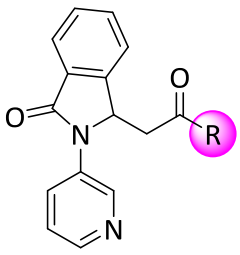

21

2-(pyridin-3-yl)-3-(2-Oxo-2-phenylethyl)isoindolin-1-one

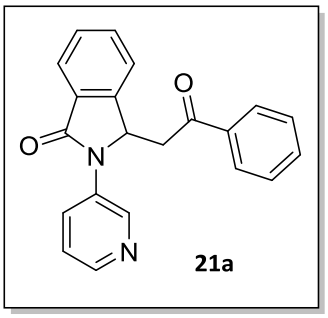

21a

The general procedure was followed using phenylacetylene (7 mmol, 0.768 ml), and the reaction mixture was stirred at chloroform reflux during 48 h. Compound **21a** was obtained as a white solid after purification by flash chromatography (0.820 g, 50%).

m.p.(°C) 152-153 (ethyl acetate/hexane) .

IR νmax 3390, 3056, 2902, 1698, 1579, 1483, 1145, 985, 751 cm^{-1}.

^{1}H NMR (300 MHz, $CDCl_3$) δ = 3.18 (dd, $^{2}J_{HH}$ = 17.2 Hz, $^{3}J_{HH}$ = 9.8 Hz, 1H, CH_2), 3.44 (dd, $^{2}J_{HH}$ = 17.2 Hz, $^{4}J_{HH}$ = 3.0 Hz, 1H, CH_2), 5.94 (dd, $^{2}J_{HH}$ =9.8 Hz, $^{3}J_{HH}$ = 3.0Hz, 1H, HC-CH_2), 7.27-7.37 (m, 3H, H_{arom}), 7.39-7.51 (m, 4H, H_{arom}), 7.74-7.79 (m, 2H, H_{arom}), 7.81-7.86 (m, 1H, H_{arom}), 8.00-8.06 (m, 1H, H_{arom}), 8.36 (dd, $^{3}J_{HH}$ = 4.8 Hz, $^{4}J_{HH}$ = 1.7 Hz, 1H, H_{arom}), 8.79-8.80 (d, $^{3}J_{HH}$ = 2.7 Hz, 1H, H_{arom}) ppm.

^{13}C NMR (75 MHz, $CDCl_3$) δ = 41.7 (CH_2), 56.3 (HC), 123.3 (HC_{arom}), 123.8 (HC_{arom}), 124.2 (HC_{arom}), 128.1 ($2HC_{arom}$), 128.8 ($2HC_{arom}$), 128.9 (HC_{arom}), 130.0 (HC_{arom}), 131.0 (C_{arom}), 132.9 (HC_{arom}), 133.6 (C_{arom}), 134.0 (HC_{arom}), 136.1 (C_{arom}), 143.8 (HC_{arom}), 145.2 (C_{arom}), 146.3 (HC_{arom}), 167.2 (C=O), 197.1 (C=O) ppm.

HRMS (CI): calculated for $C_{21}H_{16}N_2O_2$ $[M]^+$ 328.1212 found 328.1215.

3-[2-(1,1'-Biphenyl]-4-yl-2-oxoethyl]-2-(pyridin-3-yl)isoindolin-1-one

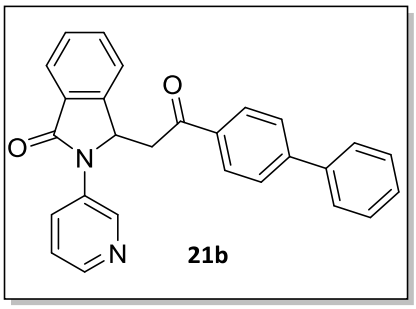

21b

The general procedure was followed using 4-ethynylbiphenyl (7 mmol, 1.248 g), and the reaction mixture was stirred at chloroform reflux during 50 h. Compound **21b** was obtained as an orange solid after purification by flash chromatography (1.010 g, 50%).

m.p.(°C) 180-181 (ethyl acetate/hexane) .

IR νmax 3040, 2932, 1570, 1453, 1120, 885, 750 cm^{-1}.

^{1}H NMR (300 MHz, $CDCl_3$) δ = 3.30 (dd, $^{2}J_{HH}$ = 17.4 Hz, $^{3}J_{HH}$ = 9.3 Hz, 1H, CH_2), 3.57 (d, $^{2}J_{HH}$ = 17.2 Hz, 1H, CH_2), 6.02 (d $^{3}J_{HH}$ = 9.3 Hz, 1H,HC-CH_2), 7.39-7.472 (m, 4H, H_{arom}), 7.56-7.65 (m, 6H, H_{arom}), 7.64-7.69(m, 3H, H_{arom}), 7.93-7.96 (m, 2H, H_{arom}), 8.12-8.21 (m, 1H, H_{arom}), 8.48 (d, $^{3}J_{HH}$ = 4.4 Hz, 1H, H_{arom}), 8.91 (s, 1H, H_{arom}) ppm.

^{13}C NMR (75 MHz, $CDCl_3$) δ = 42.0 (CH_2), 56.6 (CH), 123.5 (HC_{arom}), 124.1 (HC_{arom}), 124.5 (HC_{arom}), 127.6 ($2HC_{arom}$), 127.6 ($2HC_{arom}$), 128.7 (HC_{arom}), 128.9 ($2HC_{arom}$), 129.2 ($2HC_{arom}$), 129.3 (HC_{arom}), 130.2 (HC_{arom}), 131.3 (C_{arom}), 133.1 (HC_{arom}), 133.8 (C_{arom}), 135.0 (C_{arom}), 139.7 (C_{arom}), 144.0 (HC_{arom}), 145.4 (C_{arom}), 146.6 (HC_{arom}), 146.8 (C_{arom}), 167.4 (C=O), 196.9 (C=O) ppm.

HRMS (CI): calculated for $C_{27}H_{20}N_2O_2$ $[M]^+$ 404.1525 found 404.1521.

2-(pyridin-3-yl)-3-[2-Oxo-2-(4-methoxyphenylethyl)ethyl]isoindolin-3-one

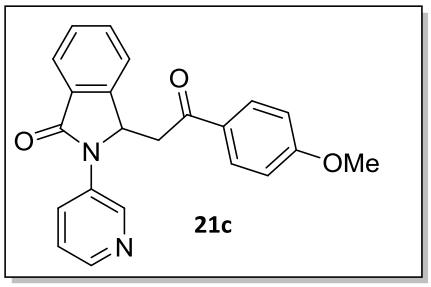

21c

The general procedure was followed using 4-methoxybenzaldehyde (7 mmol, 0.908 ml), and the reaction mixture was stirred at chloroform refux during 40 h. Compound **21c** was obtained as a white solid after purification by flash chromatography (0.984 g, 55%).

m.p.(°C) 167-168 (ethyl acetate/hexane) .

IR ν_{max} 3070, 2922, 1688, 1585, 1361, 1140, 980, 752 cm^{-1}.

^{1}H NMR (300 MHz, $CDCl_3$) δ = 3.11 (dd, $^{2}J_{HH}$ = 17.7 Hz, $^{3}J_{HH}$ = 9.7 Hz, 1H, CH_2), 3.37 (dd, $^{2}J_{HH}$ = 17.7 Hz, $^{3}J_{HH}$ = 3.0 Hz, 1H,CH_2), 5.93 (d, $^{3}J_{HH}$ =9.7 Hz, 1H, HC-N), 7.25-7.32 (m, 1H, H_{arom}), 7.39-7.48 (m, 3H, H_{arom}), 7.72-7.76 (m, 2H, H_{arom}), 7.80-7.86 (m, 1H, H_{arom}), 8.00-8.07 (m, 1H, H_{arom}), 8.36 (d, $^{3}J_{HH}$ = 4.7 Hz, 1H, H_{arom}), 8.81 (d, $^{4}J_{HH}$ = 2.7 Hz, 1H, H_{arom}) ppm.

^{13}C NMR (75 MHz, $CDCl_3$) δ = 25.5 (CH_2), 26.6 (HC-CH_2), 55.6 (OCH_3), 113.8 (HC_{arom}), 114.1 ($2HC_{arom}$), 124.2 (HC_{arom}), 124.9 (HC_{arom}), 129.2 (HC_{arom}), 130.9 ($2HC_{arom}$), 132.0 ($2HC_{arom}$), 136.9 (HC_{arom}), 141.1 (C_{arom}), 144.0 (C_{arom}), 148.2 (C_{arom}), 149.8 (HC_{arom}), 159.9 (C_{arom}), 160.4 (C_{arom}), 163.7 (C=O), 196.97 (C=O) ppm.

HRMS (CI): calculated for $C_{22}H_{18}N_2O_3$ $[M]^+$ 358.1317 found 358.1322.

6.2.10. Formation of propargylamine 27

N-[3-(4-methoxyphenyl)-1-(-trifluoromethylphenyl)prop-2-yn-1-yl]pyridin-3-amine 27

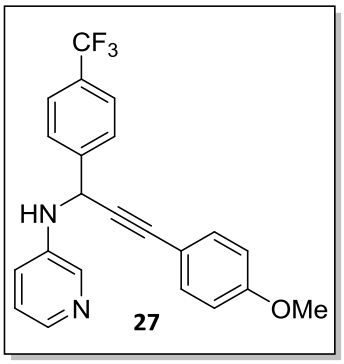

To a solution imine **3h** (5 mmol, 1.250 g) in chloroform, 4-methoxyphenylacetylene **18d** (7 mmol, 0.908 ml) and diphenylphosphonic acid (10 mmol, 2.5 ml) were added and the mixture was stirred in chloroform for 24 h. The reaction mixture was washed with 2M aqueous solution of NaOH (20 ml) and water (20 ml), extracted with dichloromethane (20 ml), and dried over anhydrous $MgSO_4$. Purification by silica gel flash column chromatography (eluent: Hexane/AcOEt) afforded the desired products **27** as an orange oil (0.955 g, 50%).

Rf 0.54 (50:50 ethyl acetate/hexane) .

^{1}H NMR (300 MHz, $CDCl_3$) δ = 3.82 (s, 3H, OCH_3), 5.55 (d, $^3J_{HH}$ = 7.2 Hz, 1H, HC-NH), 6.83 (d, $^3J_{HH}$ = 9.0 Hz, 2H, H_{arom}), 7.00-7.15 (m, 2H,NH and H_{arom}), 7.27 (s, 1H, H_{arom}), 7.35 (d, $^3J_{HH}$ = 9.0 Hz, 2H, H_{arom}), 7.68 (dd, $^3J_{HH}$ = 8.6 Hz, 2H, H_{arom}), 7.78 (dd, $^3J_{HH}$ = 8.2 Hz, 2H, H_{arom}), 8.06-8.08 (m, 1H, H_{arom}), 8.17-8.18(m, 1H, H_{arom}) ppm.

^{13}C NMR (75 MHz, $CDCl_3$) δ = 50.1 (HC-NH), 55.3 (OCH_3), 85.1 (C), 86.3 (C), 114.0 ($2HC_{arom}$), 120.2 (HC_{arom}), 123.7 (HC_{arom}), 125.9 (q, $^3J_{CF}$ = 3.9 Hz, $2HC_{arom}$), 127.6 ($2HC_{arom}$), 130.5 (q, $^2J_{CF}$ = 33.1 Hz, C-CF_3), 133.1 (q, $^1J_{CF}$ = 247.1 Hz, CF_3), 133.2 ($2HC_{arom}$), 137.2 (HC_{arom}), 140.3 (HC_{arom}), 142.2 ($2C_{arom}$), 143.1 (C_{arom}), 159.9 (C_{arom}) ppm.

^{19}F NMR ($CDCl_3$) δ= - 63.0 ppm.

HRMS (CI): calculated for $C_{27}H_{17}F_3N_2O$ $[M]^+$ 382.1293 found 382.1297.

6.3. Experimental Section- Biological Assays

6.3.1. Enzyme and materials

Human TopI was supplied by Prof. Birgitta Knudsen (Department of Molecular Biology and Genetics, Aarhus) DMSO and camptothecin (CPT) were purchased from Sigma-Aldrich. CPT was dissolved in 99.9 % DMSO at 10 mM and stored at -20 °C.

6.3.2. Relaxation assay

Relaxation reactions were carried out in either 80 µl (drug titrations) or 20 µl (kinetics) reaction volumes in the presence of 10 mM Tris-HCl (pH 7.5), 1 mM EDTA, 5 mM $MgCl_2$, 5 mM$CaCl_2$, and 150 mM or 50 mM NaCl. The enzyme storage buffer additionally provided 2.5% glycerol, 0.25 mM Tris-HCl (pH 7.5), and 0.025 mM EDTA to the reaction. When indicated, different concentrations of CPT and compounds dissolved in DMSO (2.5 % (v/v) final concentration) were added. Control reactions with no addition of drug were supplied with DMSO (2.5 % (v/final concentration).

A total of 800 fmol (drug titrations) or 200 fmol (kinetics) of pUC18 were incubated with 32 fmol (drug titrations) or 8 fmol (kinetics) purified TopI at 37°C for the indicated time intervals. When indicated, drugs were preincubated with purified TopI or pUC18 at 37°C for 15 minutes prior to the beginning of the enzymatic reactions. Reactions were terminated by the addition of SDS to a final concentration of 0.2% (w/v). Samples were subjected to proteolytic digestion by 0.8 µg/µl proteinase K at 37°C for 1 hour prior to separation of relaxation products in a 1 % agarose gel. DNA was visualized by staining of the gel with 0.5 µg/ml ethidium bromide and the gel was analyzed using the UV transilumator.

6.3.3. Assay for Topoisomerase I-mediated cleavage and ligation

Synthetic DNA substrates-Oligodeoxynucleotides for construction of suicide cleavage substrate and DNA ligator were synthesized by DNA Technology (Risskov, Denmark). The sequences of the oligonucleotides are as follows:

AS88:5'-GCCTGCAGGTCGACTCTAGAGGATCTAAAAGACTTAGA-3'

AS90:5'-AAAAATTTTTCTAAGTCTTTTAGATCCTCTAGAGTCGACCTGCAGGC-3'

AS91:5'-AGAAAAATTTTT

The oligodeoxynucleotide representing the cleavable strand (AS88) was 5'-radiolabelled prior to hybridization to the non-cleavable strand (AS90) by employing the T4 polynucleotide kinase reaction using [γ-^{32}P]ATP as phosphoryl donor. Unreacted [γ-^{32}P]ATP was removed by spin dialysis on a G-50 column (GE-healthcare). For hybridization, 10 pmol of AS88 oligodeoxynucleotide was mixed with 20 pmol of AS90 in 10 mM Tris-HCl (pH 7.5), 1 mM EDTA, heated to 95°C for 5 minutes, and cooled slowly to room temperature. In order to prevent ligation of the 5'-OH of the non-cleavable strand, AS90 was phosphorylated with unlabeled ATP at the 5'-OH prior to annealing.

Topoisomerase I-mediated cleavage - Prior to the cleavage reaction 990 fmol TopI was preincubated with a final concentration of 80 µM CPT dissolved in DMSO (3 % (v/v) final concentration), or 80 µM MG226 dissolved in DMSO (3 % (v/v) final concentration) for 10 minutes at 37 °C in a 30 µl reaction volume containing 10 mM Tris-HCl (pH 7.5), 1 mM EDTA, 5 mM $MgCl_2$, 5 mM $CaCl_2$, and 100 mM NaCl, as indicated. Control samples with no addition of drug were supplied with an equal volume of DMSO. Cleavage reactions were initiated by addition of 20 nM radiolabelled suicide DNA substrate AS88/AS90 in a final reaction volume of 30 µl. 5 µl aliquots of the reaction mixture were terminated after given periods of time by the addition of 0.7 % (w/v) SDS (final concentration). DNA was precipitated by the addition of 300 mM of NaCl and 3

volumes of 96 % ethanol. The precipitated samples were digested with 5 µl 1 mg/mL Trypsin for 30 min at 37°C and mixed with an appropriate volume of loading buffer (80 % (v/v) deionized formamide, 50 mM Tris-borate (pH8.3), 1 mM EDTA, 0.05 % (w/v) bromophenol blue, 0.05 % (w/v) Xylene xyanol) prior to loading on a 12 % denaturing polyacrylamide gel and run in TBE (48 mM Tris, 45.5 mM Boric Acid, 1Mm EDTA) for analysis. The gel was dried and radiolabelled DNA was visualized by PhosphorImager (Bio-Rad). The extent of cleavage was quantified using the QuantityOne software from Bio-Rad. Alternatively, reactions were stopped with SDS stop dye (2 % SDS, 2 mM β-mercaptoethanol, 4 % (v/v) glycerol, 50 mM Tris-HCl pH 7, 0.05 % Bromophenol blue) and blotted onto Hybond-C nitrocellulose membranes (Amersham Biosciences, USA) using a manifold dotblot apparatus. The nitrocellulose membrane was subsequently washed twice in TBS + Tween 20 buffer (20 mM Tris pH 7.5, 0.5 M NaCl, 0.25 % Tween 20) for 10 minutes and twice in 2x SSC for 10 minutes. Radiolabelled DNA was visualized by PhosphorImaging (Personal Molecular Imager, Bio-Rad) and the extent of cleavage was quantified using the QuantityOne software from Bio-Rad. The degree of cleavage was calculated as the ratio between cleaved and uncleaved substrate. The results were normalized to 100 % cleavage for the reaction performed in presence of DMSO after 1 minute of incubation and graphed. The results are plotted as the average of three experiments and error bars indicate standard deviations.

Topoisomerase I-mediated ligation **-** Active TopI-DNA cleavage complexes were generated by incubating 20 nM of suicide DNA substrate AS88/AS91 with 275 fmol of TopI at room temperature for 30 minutes following 15 minutes inbubation at 37 °C in a 25µl reaction volume containing 10 mM Tris-HCl (pH 7.5), 1 mM EDTA, 5 mM MgCl2, 5 mM CaCl2, and 100 mM NaCl. Prior to single strand ligation, the generated TopI-DNA cleavage complexes were preincubated with 80 µM CPT dissolved in DMSO (4 % (v/v) final concentration), or 80 µM drugs dissolved in DMSO (4 % v/v) final concentration) for 5 min, as indicated. Control samples with no addition of drug were supplied with an equal volume of DMSO. The ligation reaction was initiated by addition of 2µM ligator (AS91) to the reaction mixture. Aliquots of the reaction (5 µL) were terminated after given periods of time by the addition of 0.7 % (w/v) SDS (final concentration). Samples

were precipitated, trypsin digested, and analyzed as described for TopI mediated cleavages. The degree of religation was calculated as the ratio between religated substrate and the sum of religated and cleaved substrate. The results were normalized to 100 % religation for the reaction performed in presence of DMSO after 1 minute of incubation and graphed. The results are plotted as the average of three experiments and error bars indicate standard deviations.

6.3.4. Nicking assay

Nicking activities were measured in 20µl reaction volumes in the presence of 10 mM Tris-HCl (pH 7.5), 1 mM EDTA, 5 mM $MgCl_2$, 5 mM $CaCl_2$, and 50 mM NaCl. When indicated 80 µM CPT dissolved in DMSO (2.5 % (v/v) final concentration) or 80 µM **16c** compound dissolved in DMSO (2.5 % (v/v) final concentration) was added preincubated with 330 fmol purified TopI at 37 °C for 10 min as indicated. Control samples with no addition of drug were supplied with DMSO (2.5% (v/v) final concentration). Reactions were initiated by the addition of a total of 200 fmol pUC18 and incubated at 37°C for indicated time intervals. Reactions were terminated by the addition of SDS to a final concentration of 0.2 % (w/v). Samples were subjected to proteolytic digestion by 0.8 µg/µl proteinase K at 37 °C for 1 hour prior to separation of products in a 1 % agarose gel containing 0.5 µg/ml ethidium bromide and the gel was analyzed using the Bio-Rad Gel XR+ System.

6.3.5. Cell culture

A549 cells were grown in F-12K MEDIUM supplemented with 10 % FBS, (ATCC*).*

BT20 cells were grown in ATCC-formulated Eagle's Minimum Essential Medium (EMEM) supplemented with 10 % FBS (ATCC*).*

SKOV3 cells were grown ATCC-formulated McCoy's 5a Medium Modified supplemented with 10 % FBS (ATCC*).*

MCR5 cells were grown in ATCC-formulated Eagle's Minimum Essential Medium (EMEM) supplemented with 10 % FBS (ATCC*).*

All cell lines were maintained in a humidified incubator (5 % CO_2/ 95 % humidity at 37°C). Cells were plated into culture flask from teknovas. Cells were harvested by trypsin treatment (Trypsin-EDTA (0.25%), phenol red) from Gibco followed by consecutive wash with PBS and stored at -80 °C until further analysis.

6.3.6. CCK-8 cytotoxicity assay

The cytotoxic effect of the compounds was determined by CCK-8 colorimetric assay. A549, BT20 and SKOV3 cells were grown to 80 % confluence, trypsinized, and seeded in 96 well tissue plates at a concentration of 2.5 x 10^3 (A549 cells), 3.5 x 10^3 (BT20 cells) and 3.0 x 10^3 (SKOV3 cells) in 100 µl of complete growth media. After 24h the compounds were added at different concentrations (50, 30, 20, 10, 5, 2.5 and 1 µM final concentration) in the corresponding wells. After 48 hours of incubation, 10µl of CCK-8 reagent was added to each well and incubation was continued in the incubator (5 % CO_2/ 95 % air atmosphere at 37°C) for 2 additional hours in the dark. The absorbance of each well was analyzed at 450 nm using a microplate reader. The results were graphically represented in a dose-dependent graph to obtain IC_{50} values.

The electrophoretic agarose gels performed for all the derivatives in order to evaluate Topoisomerase I activity are shown below.

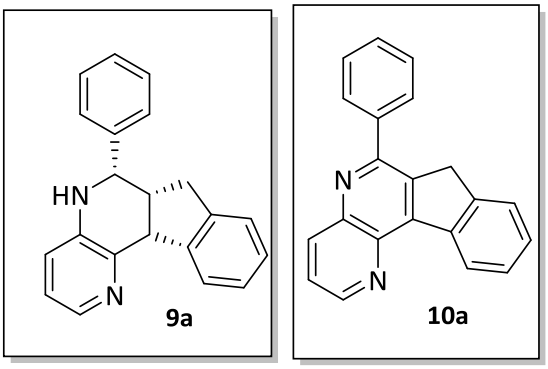

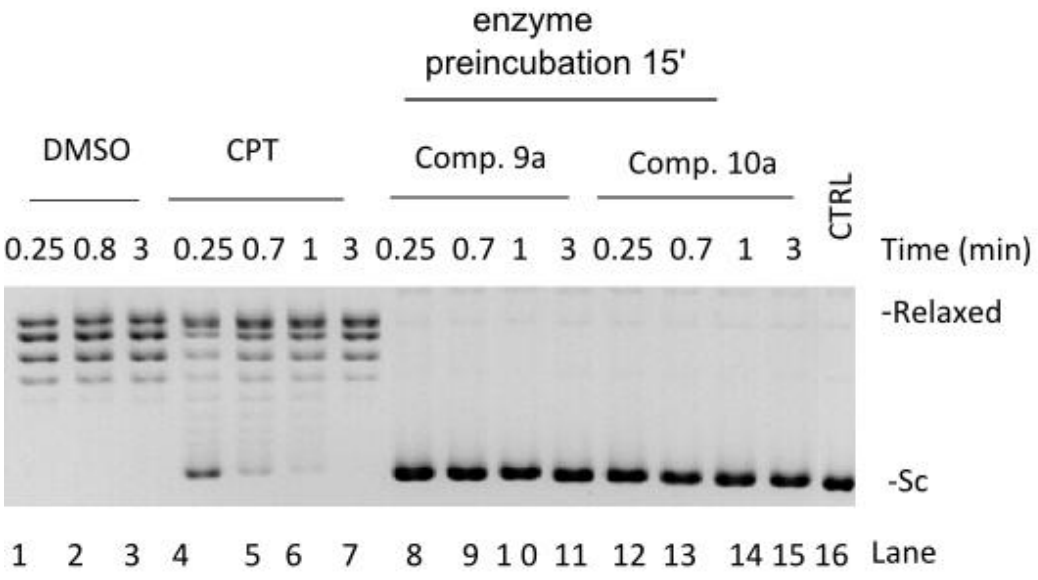

Compound **9a**

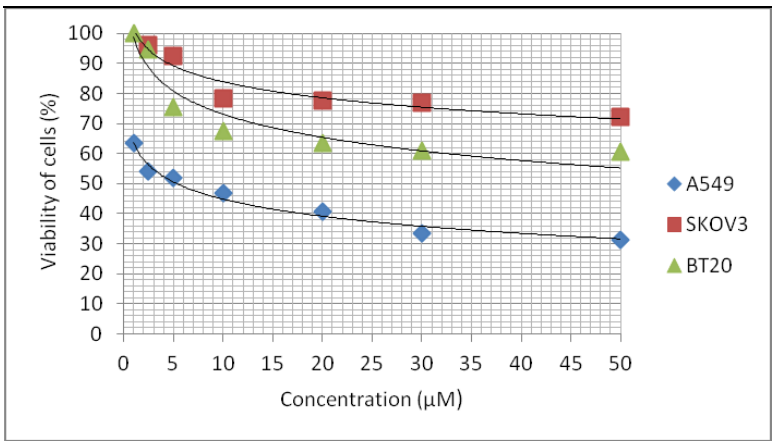

IC_{50} (A549): 5.6±0.45 µM; IC_{50} (SKOV3): >50 µM; IC_{50} (BT20): >50 µM.

Compound **10a**

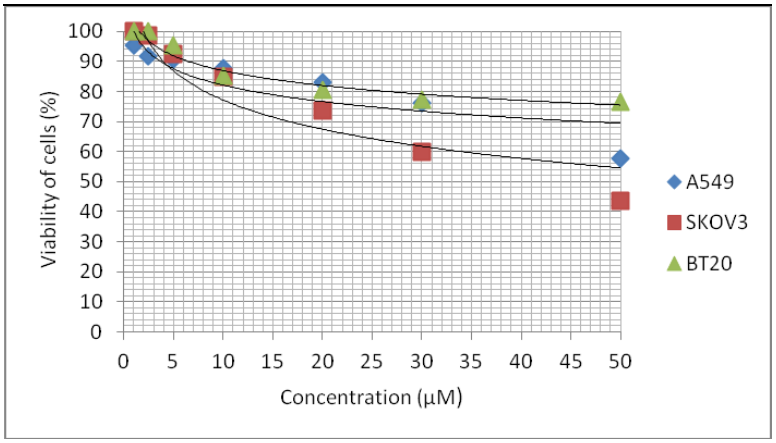

IC_{50} (A549): >50 µM; IC_{50} (SKOV3): >50 µM; IC_{50} (BT20): >50 µM.

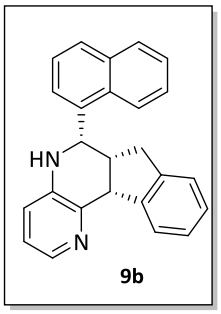

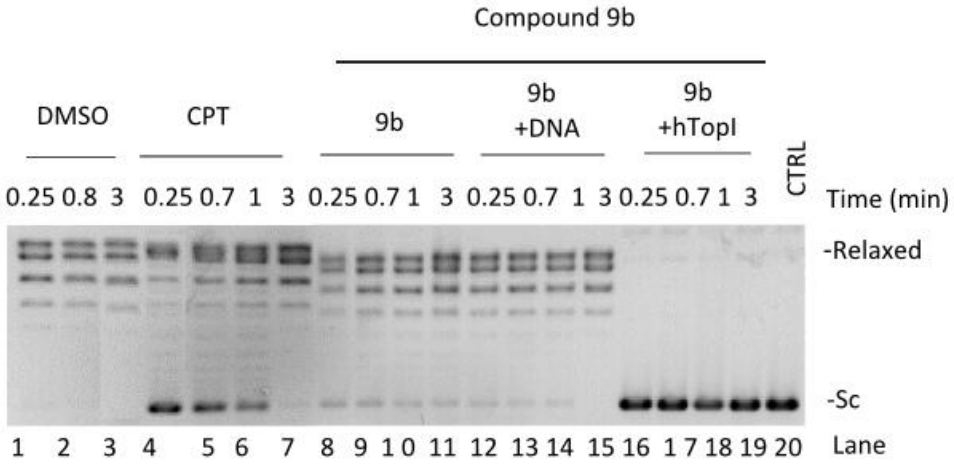

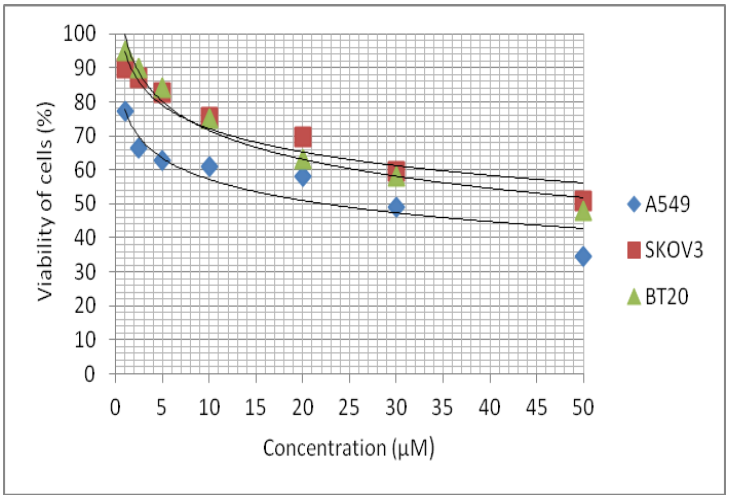

IC_{50} (A549): 25.3±0.3 µM; IC_{50} (SKOV3): >50 µM; IC_{50} (BT20): >50 µM.

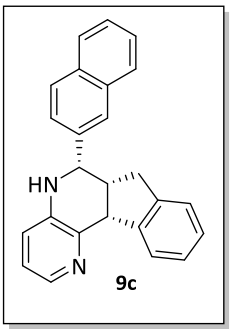

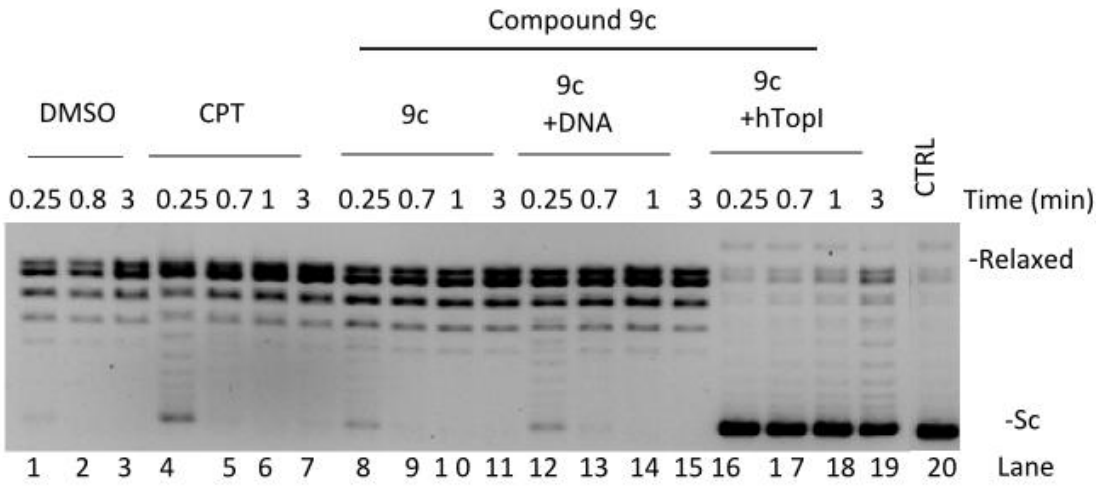

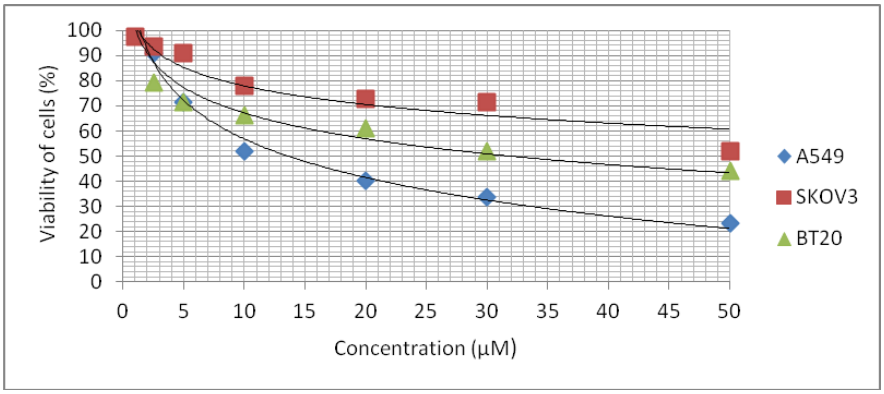

IC_{50} (A549): 13.5±0.8 μM; IC_{50} (SKOV3): >50 μM; IC_{50} (BT20): >50 μM.

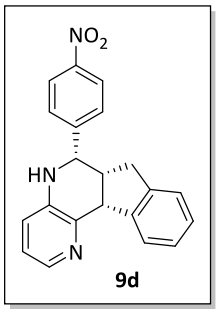

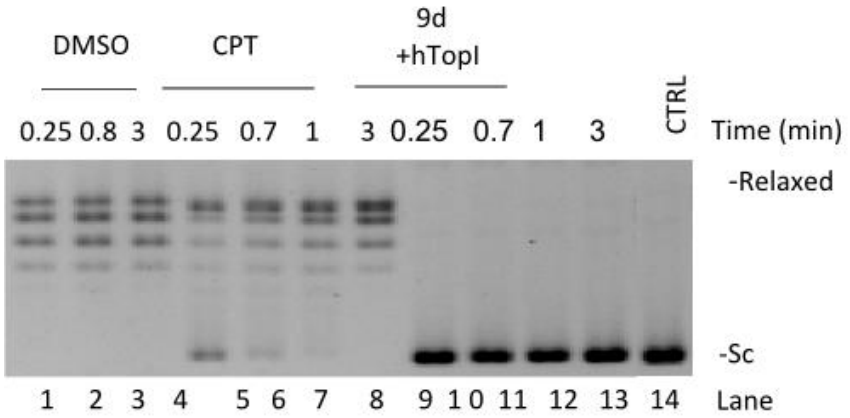

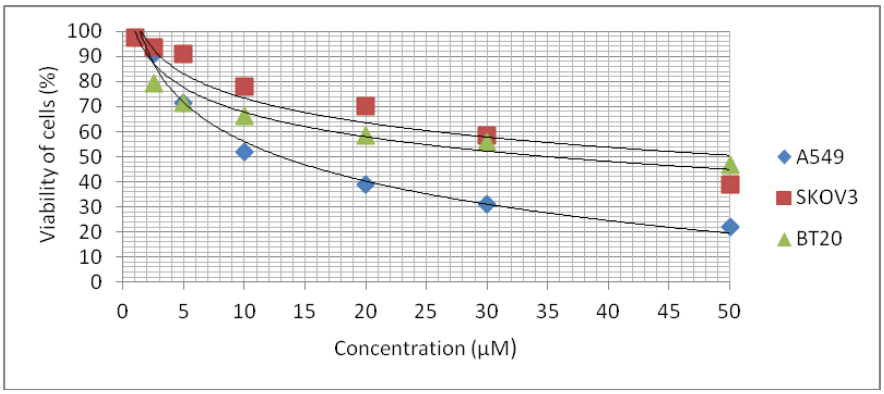

IC_{50} (A549): 10.5±0.3 μM; IC_{50} (SKOV3): >50 μM; IC_{50} (BT20): >50 μM.

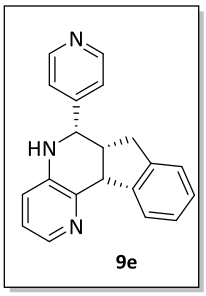

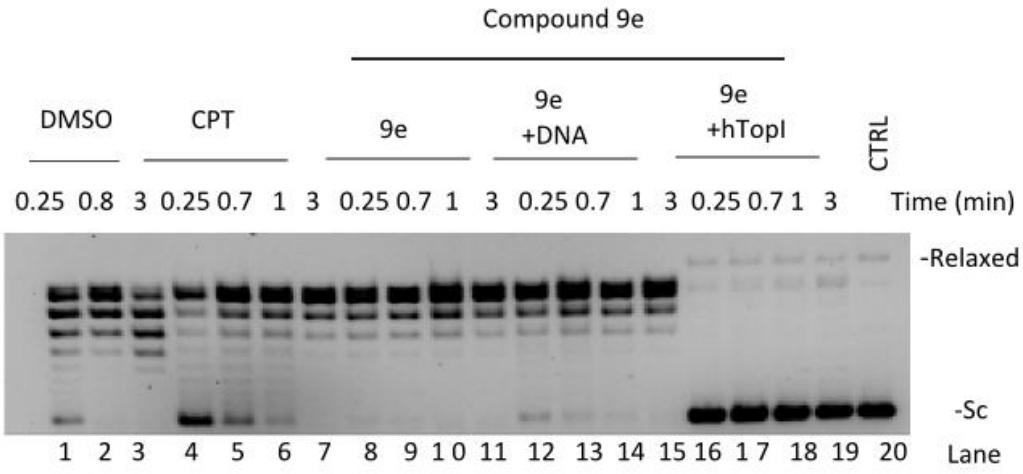

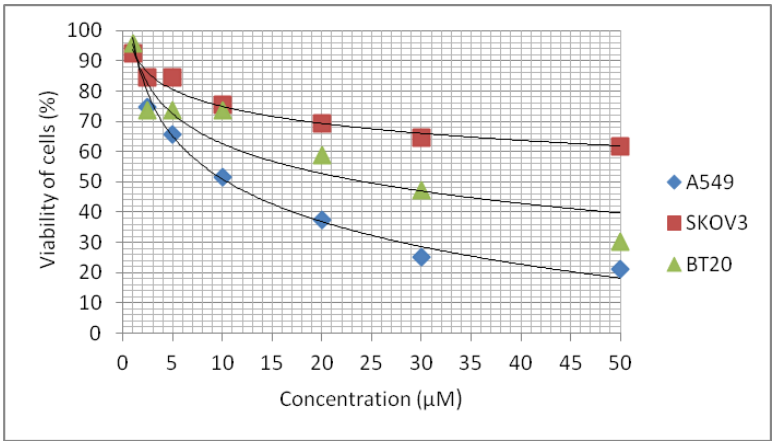

IC_{50} (A549): 9.1±0.2 μM; IC_{50} (SKOV3): >50 μM; IC_{50} (BT20): 26.4±0.6 μM.

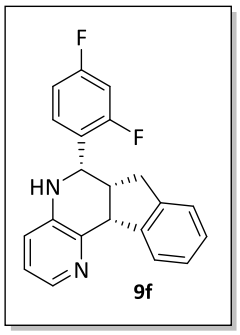
F
F
HN
N
9f

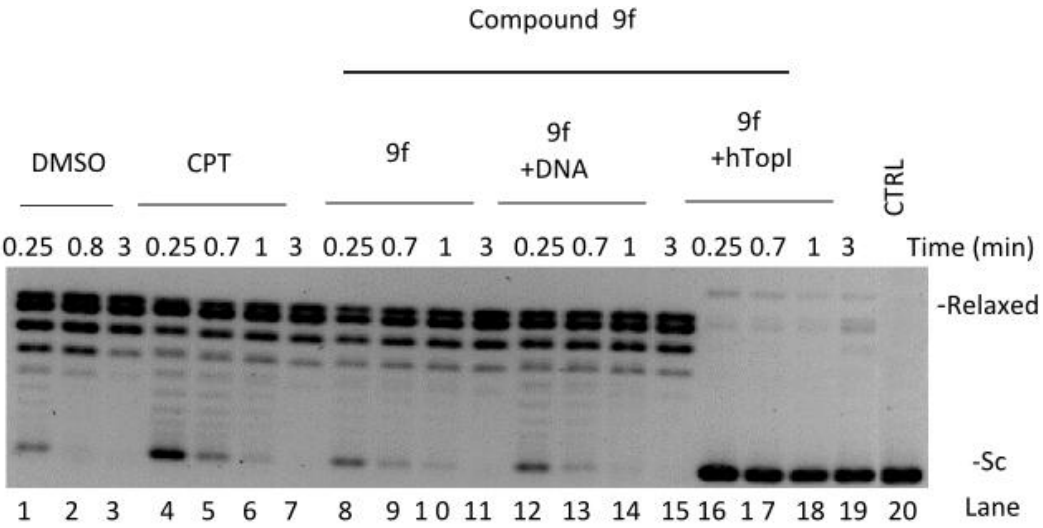
Compound 9f
DMSO
CPT
9f
9f +DNA
9f +hTopI
CTRL
0.25 0.8 3 0.25 0.7 1 3 0.25 0.7 1 3 0.25 0.7 1 3 0.25 0.7 1 3
Time (min)
-Relaxed
-Sc
1 2 3 4 5 6 7 8 9 10 11 12 13 14 15 16 17 18 19 20
Lane

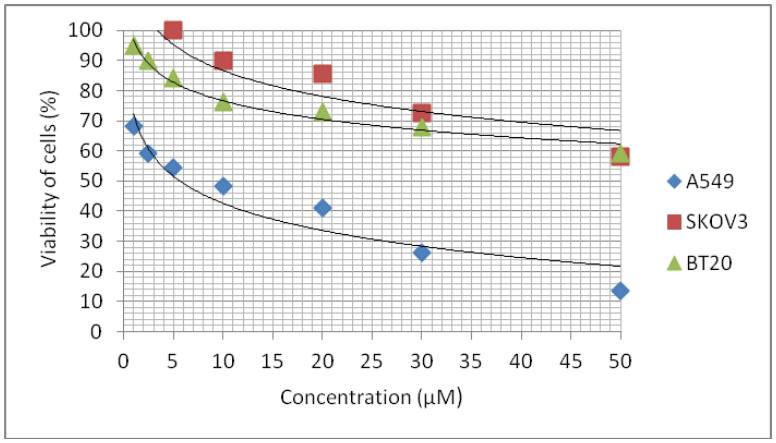
Viability of cells (%)
100
90
80
70
60
50
40
30
20
10
0
0 5 10 15 20 25 30 35 40 45 50
Concentration (µM)
A549
SKOV3
BT20

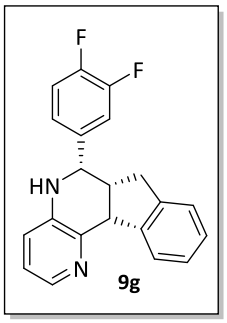

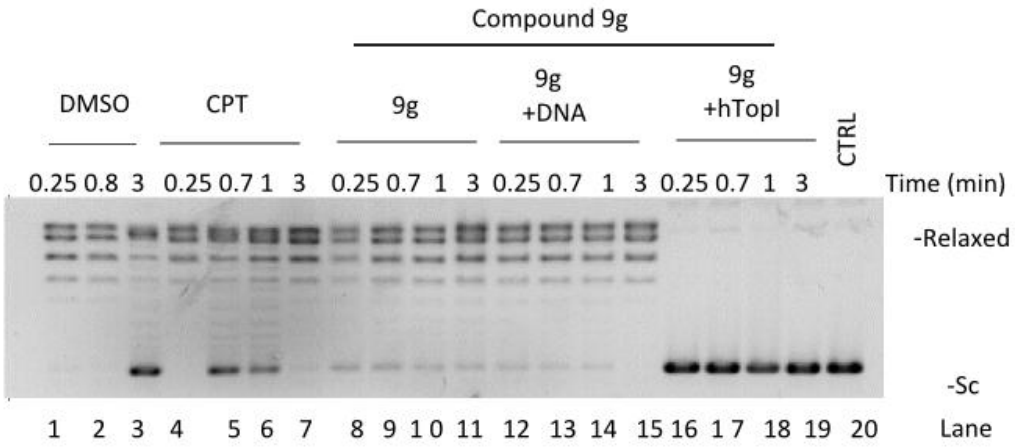

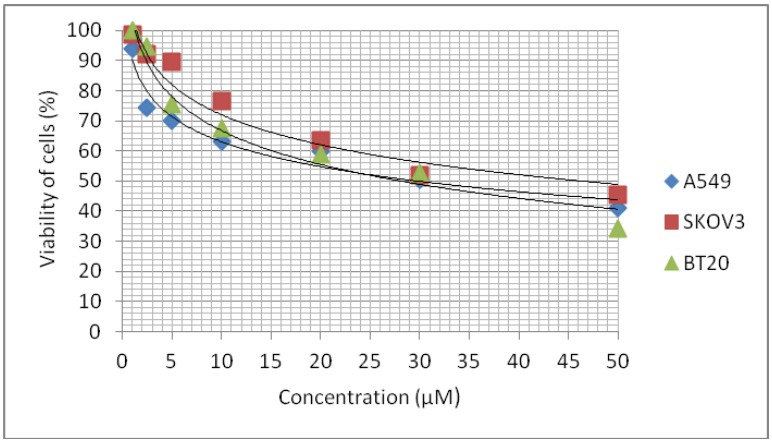

IC_{50} (A549): 27.3±0.7 μM; IC_{50} (SKOV3): >50 μM; IC_{50} (BT20): 25.6±0.1 μM.

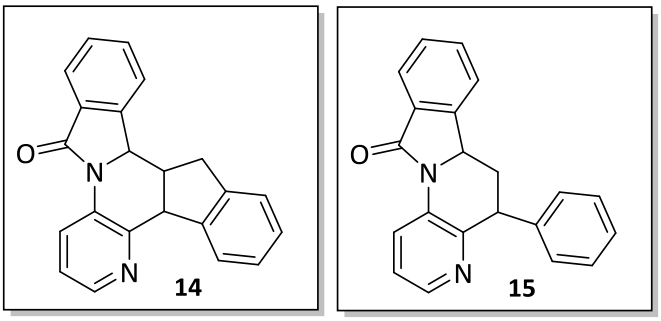
O
N
N
14
O
N
N
15

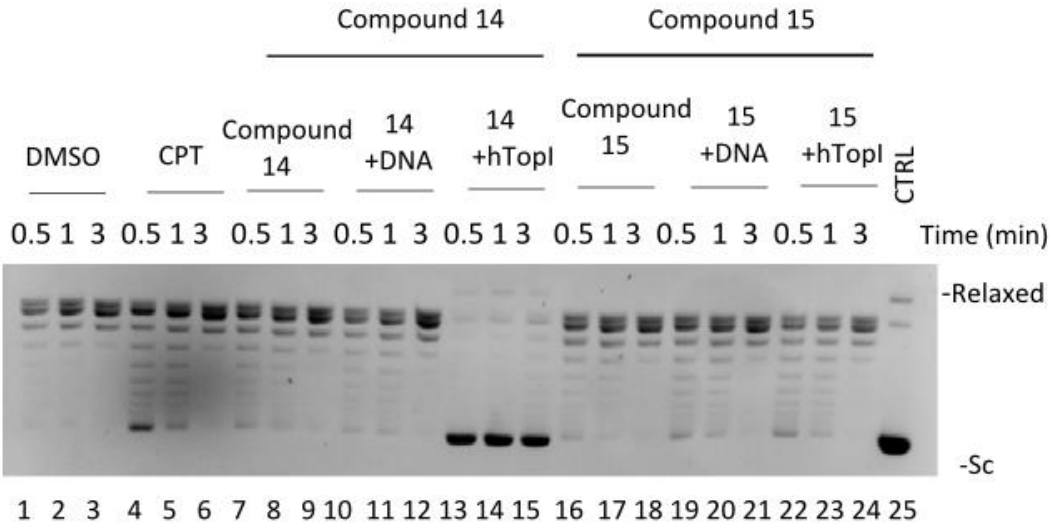
Compound 14
Compound 15
DMSO
CPT
Compound 14
14 +DNA
14 +hTopI
Compound 15
15 +DNA
15 +hTopI
CTRL
0.5 1 3 0.5 1 3 0.5 1 3 0.5 1 3 0.5 1 3 0.5 1 3 0.5 1 3 0.5 1 3
Time (min)
-Relaxed
-Sc
1 2 3 4 5 6 7 8 9 10 11 12 13 14 15 16 17 18 19 20 21 22 23 24 25

Compound **14**

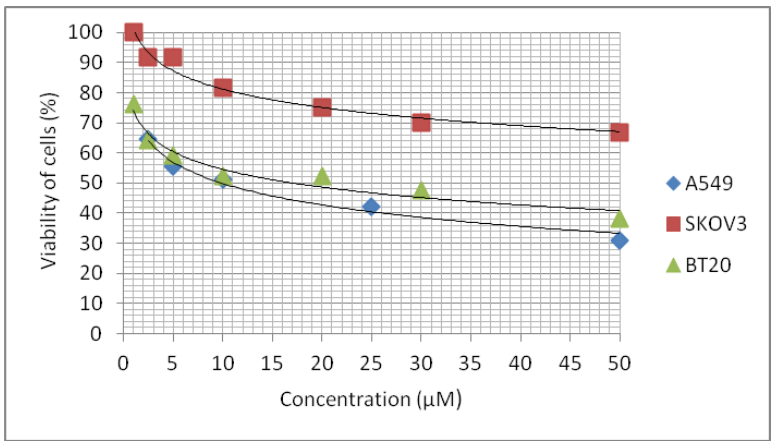

IC_{50} (A549): 11.2±0.8 µM; IC_{50} (SKOV3): >50 µM; IC_{50} (BT20): 17.0±0.3 µM.

Compound **15**

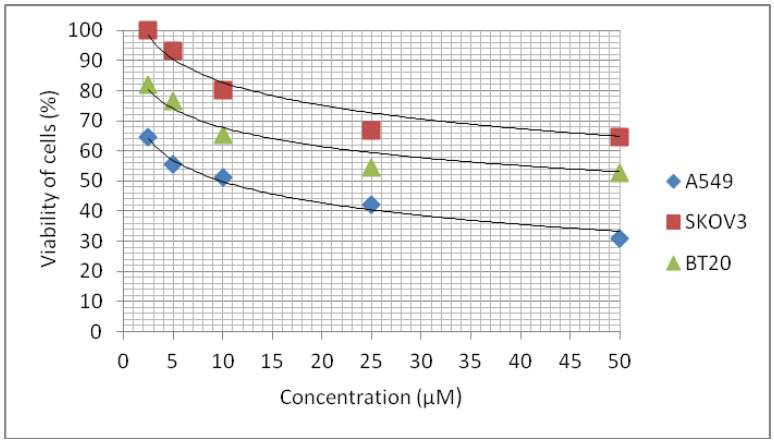

IC_{50} (A549): 30.2±0.9 µM; IC_{50} (SKOV3): >50 µM; IC_{50} (BT20): >50 µM.

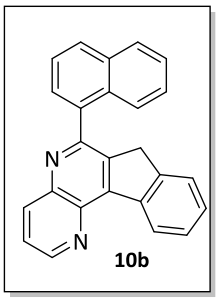

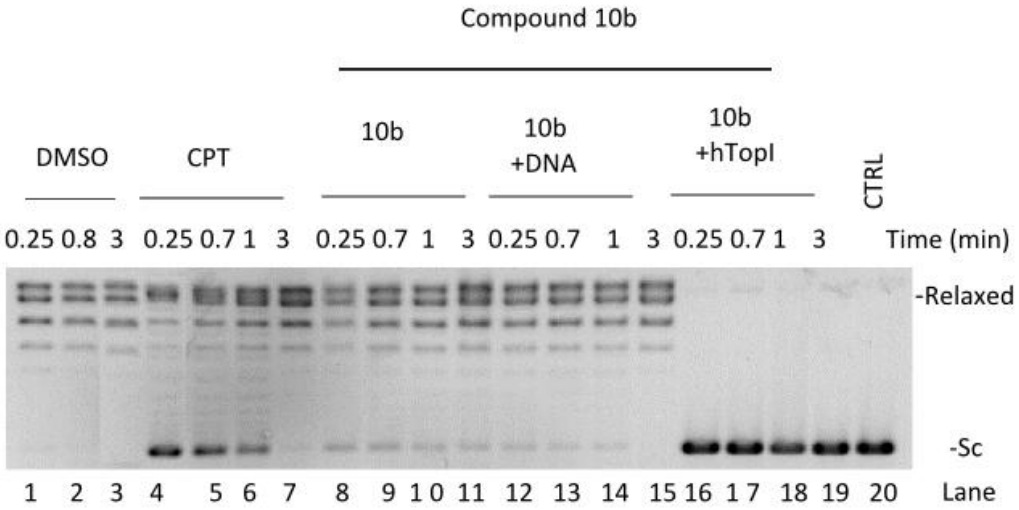

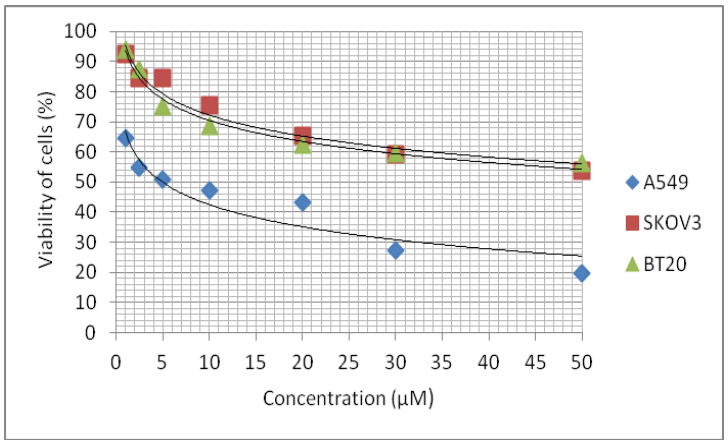

IC_{50} (A549): 10.5±0.3 µM; IC_{50} (SKOV3): >50 µM; IC_{50} (BT20): >50 µM.

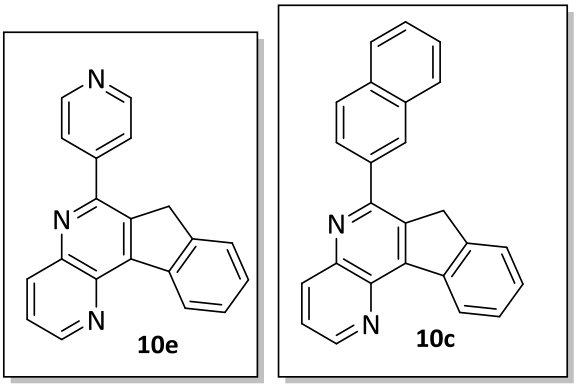
N
N
N
10e
N
N
N
10c

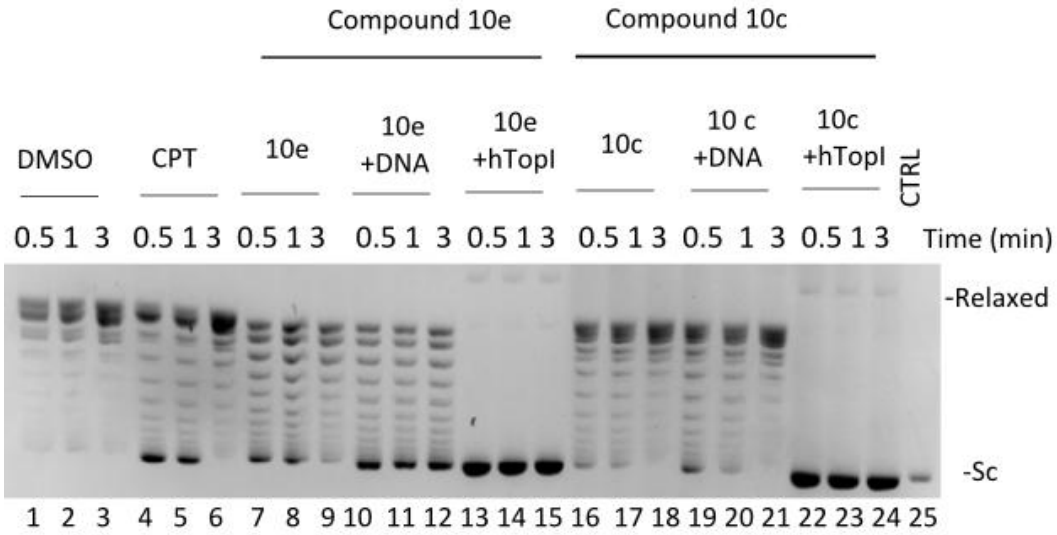
Compound 10e
Compound 10c
DMSO
CPT
10e
10e +DNA
10e +hTopI
10c
10 c +DNA
10c +hTopI
CTRL
0.5 1 3 0.5 1 3 0.5 1 3 0.5 1 3 0.5 1 3 0.5 1 3 0.5 1 3 0.5 1 3
Time (min)
-Relaxed
-Sc
1 2 3 4 5 6 7 8 9 10 11 12 13 14 15 16 17 18 19 20 21 22 23 24 25

Compound **10e**

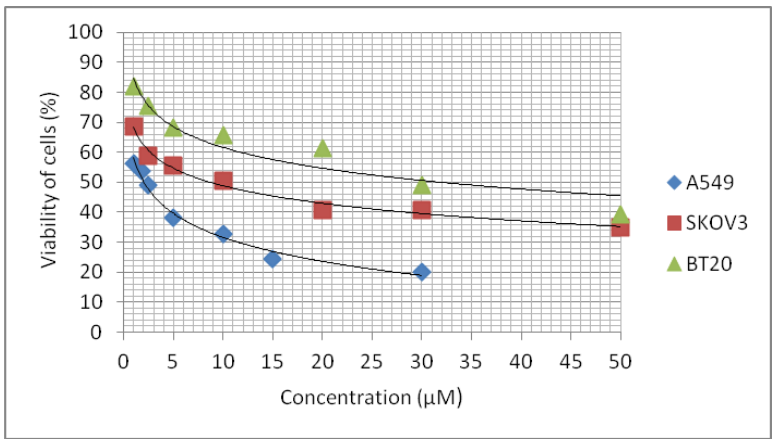

IC_{50} (A549): 2.9±0.9 µM; IC_{50} (SKOV3): 10.5±0.4 µM; IC_{50} (BT20): 32.9±0.4 µM.

Compound **10c**

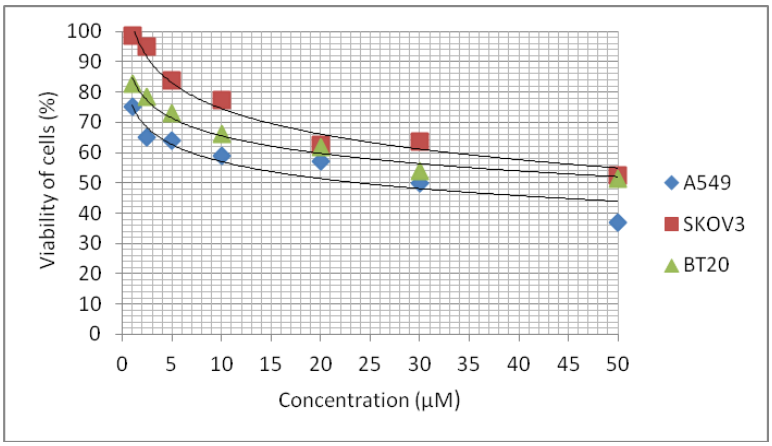

IC_{50} (A549): 23.7±1.0 µM; IC_{50} (SKOV3): >50 µM; IC_{50} (BT20): >50 µM.

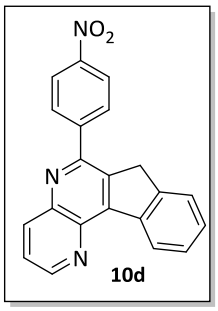

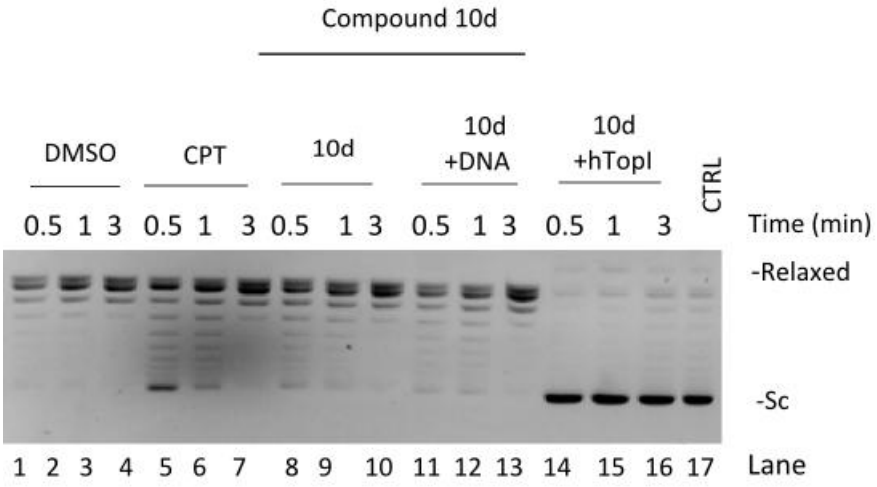

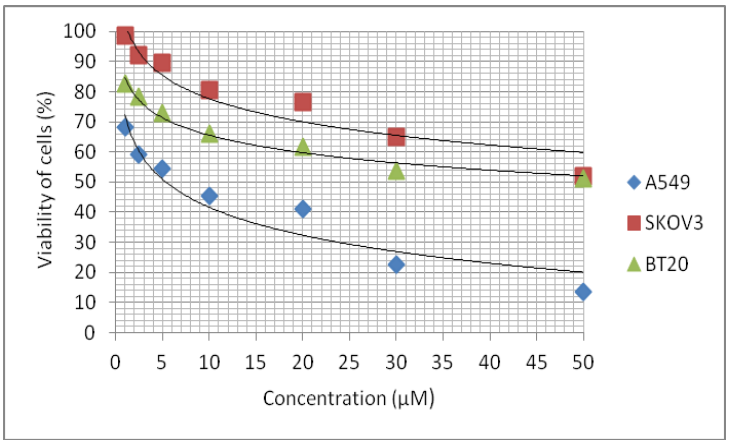

IC_{50} (A549): 5.7±0.6 μM; IC_{50} (SKOV3): >50μM; IC_{50} (BT20): >50 μM.

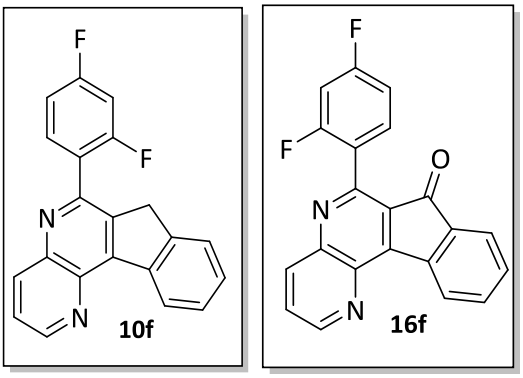
F
F
N
N
10f
F
F
O
N
N
16f

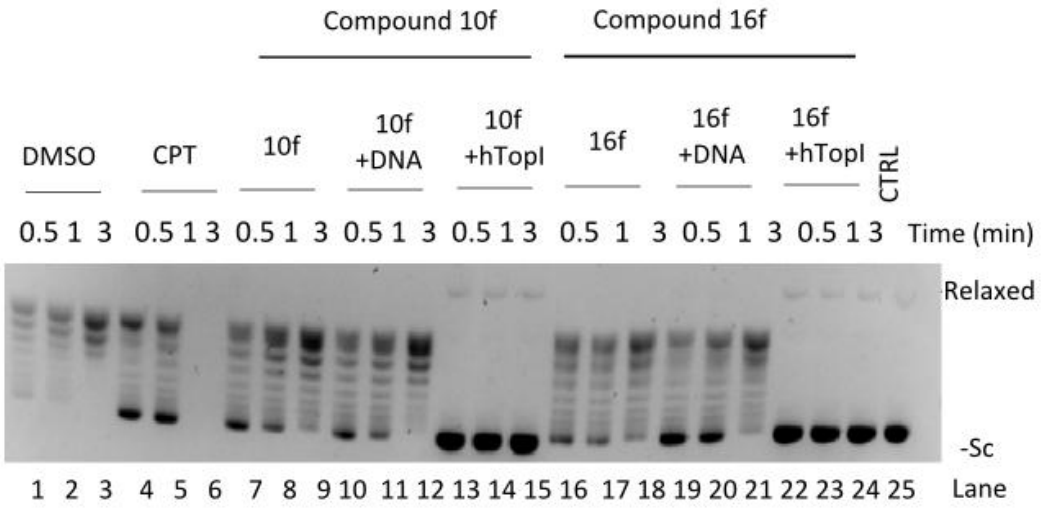
Compound 10f
Compound 16f
DMSO
CPT
10f
10f +DNA
10f +hTopI
16f
16f +DNA
16f +hTopI
CTRL
0.5 1 3 0.5 1 3 0.5 1 3 0.5 1 3 0.5 1 3 0.5 1 3 0.5 1 3 0.5 1 3 Time (min)
Relaxed
-Sc
1 2 3 4 5 6 7 8 9 10 11 12 13 14 15 16 17 18 19 20 21 22 23 24 25 Lane

Compound **10f**

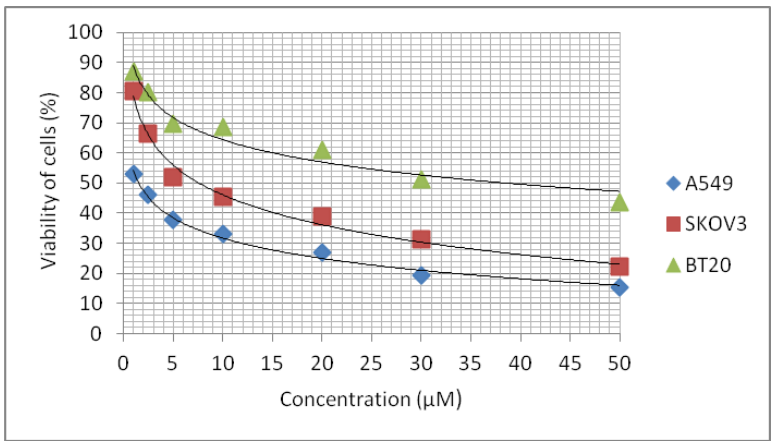

IC_{50} (A549): 1.7±0.1 µM; IC_{50} (SKOV3): 6.4±0.3 µM; IC_{50} (BT20): 39.6±0.3 µM.

Compound **16f**

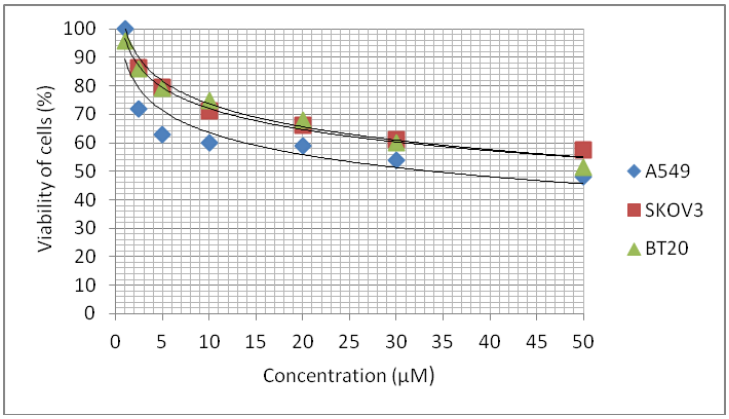

IC_{50} (A549): 34.1±0.9 µM; IC_{50} (SKOV3): >50 µM; IC_{50} (BT20): >50 µM.

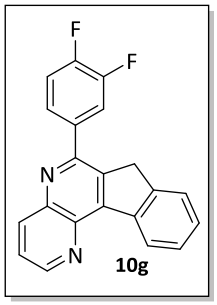

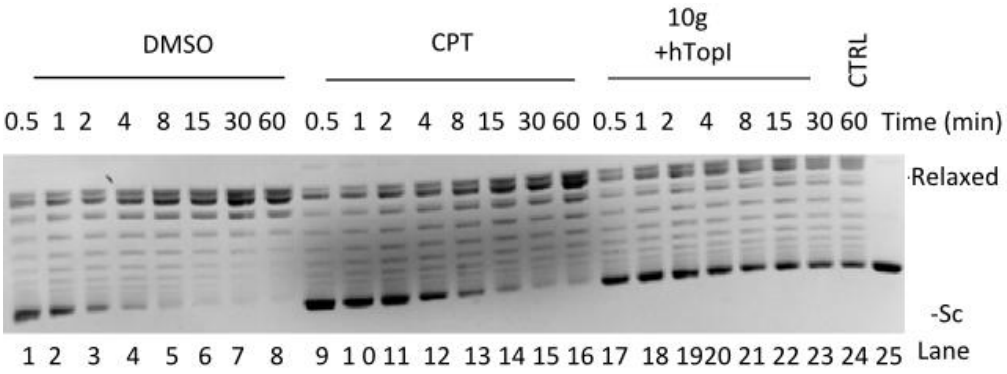

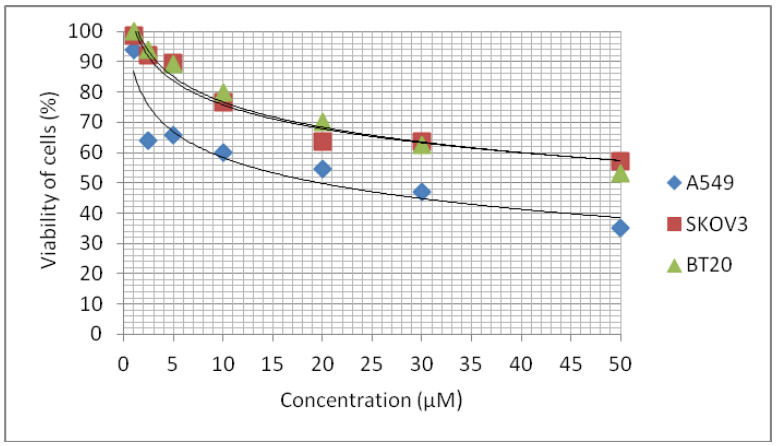

IC_{50} (A549): 18.6±0.5 µM; IC_{50} (SKOV3): >50 µM; IC_{50} (BT20): >50 µM.

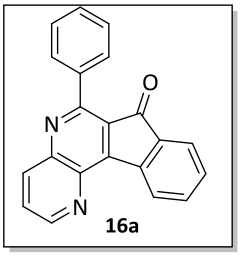

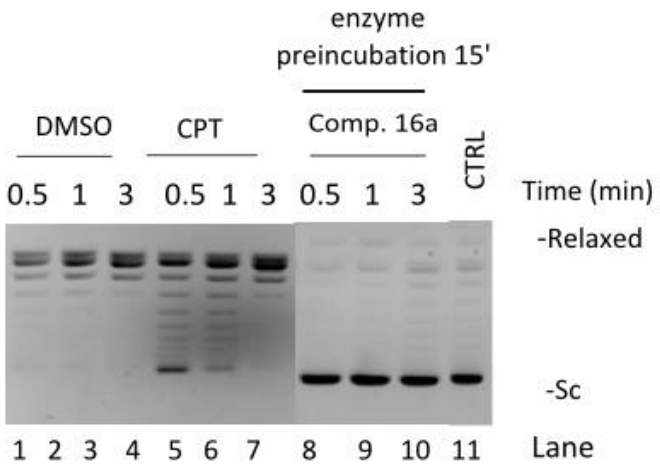

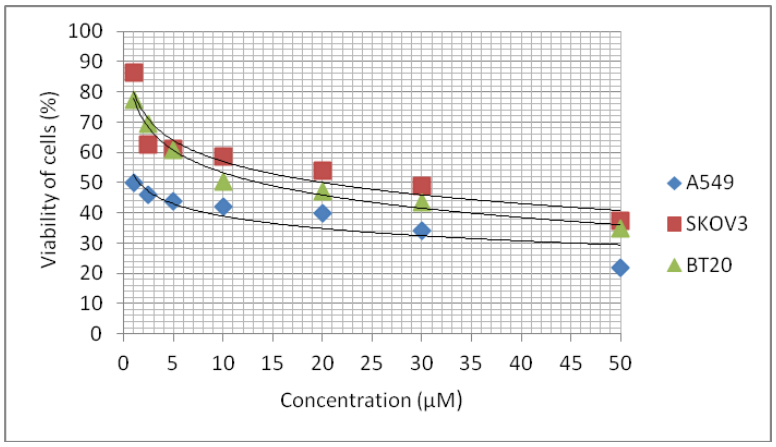

IC_{50} (A549): 1.9±0.1 μM; IC_{50} (SKOV3): 21.5±1.2 μM; IC_{50} (BT20): 14.1±0.5 μM.

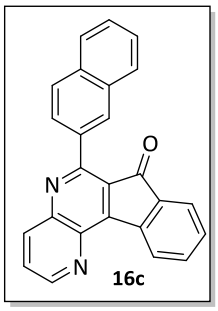

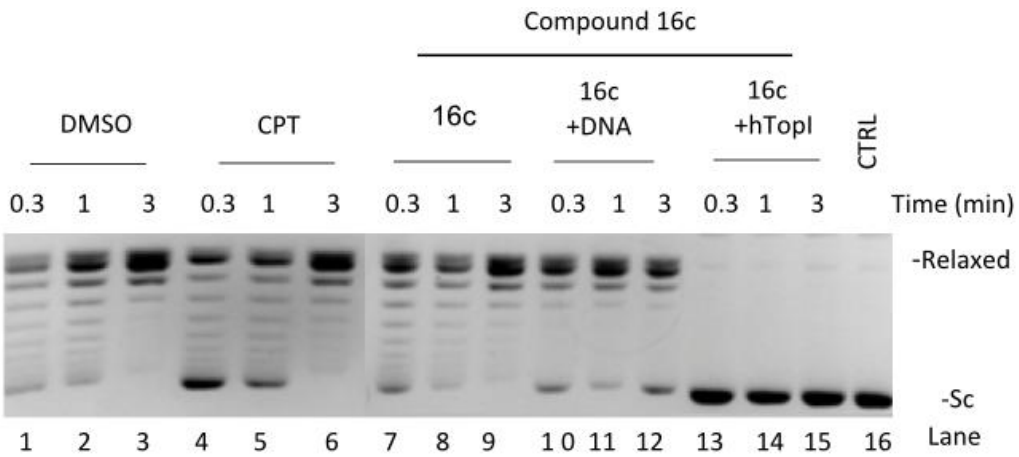

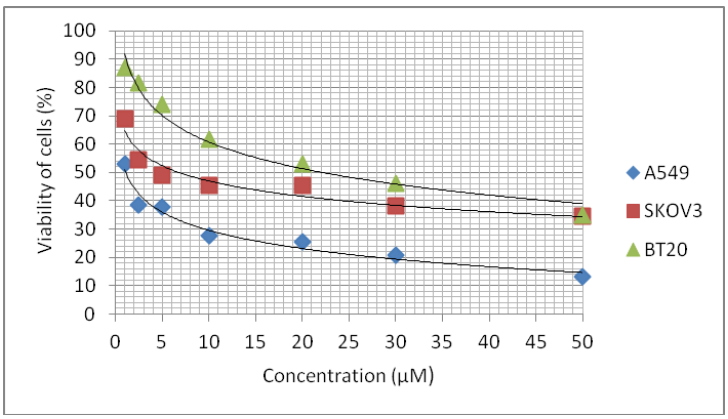

IC_{50} (A549): 0.8±0.2 µM; IC_{50} (SKOV3): 5.3±0.1 µM; IC_{50} (BT20): 23.3±0.8 µM.

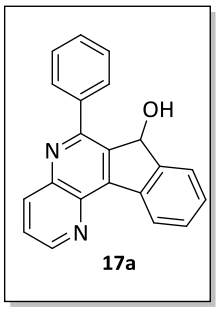

17a

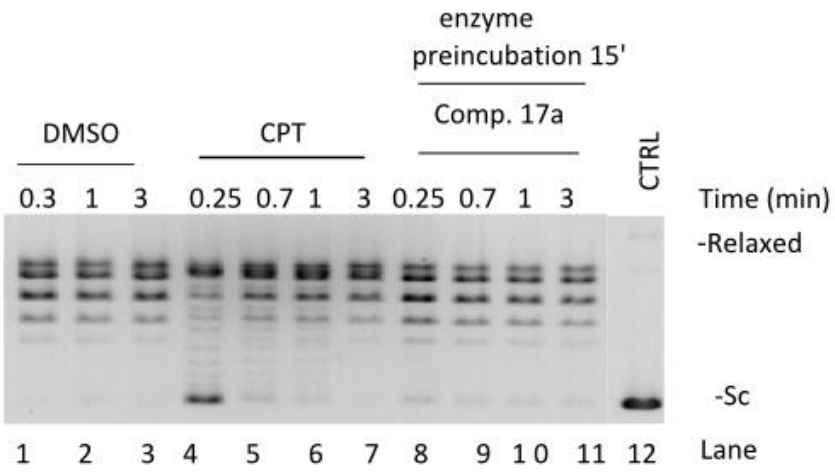

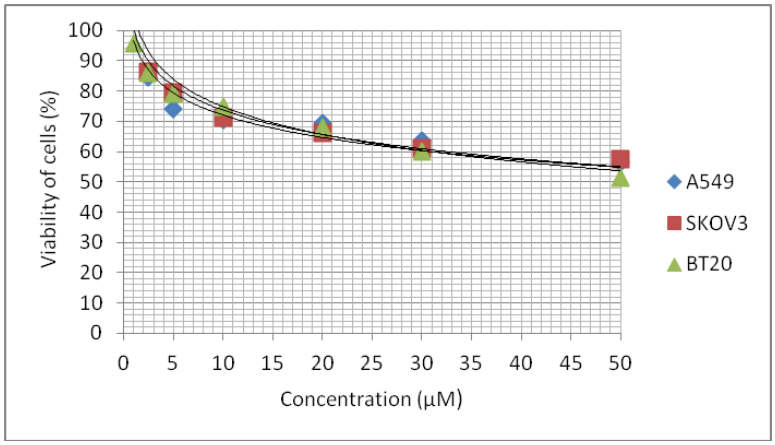

IC_{50} (A549): >50 µM; IC_{50} (SKOV3): >50 µM; IC_{50} (BT20): >50 µM.

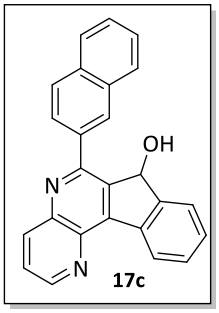

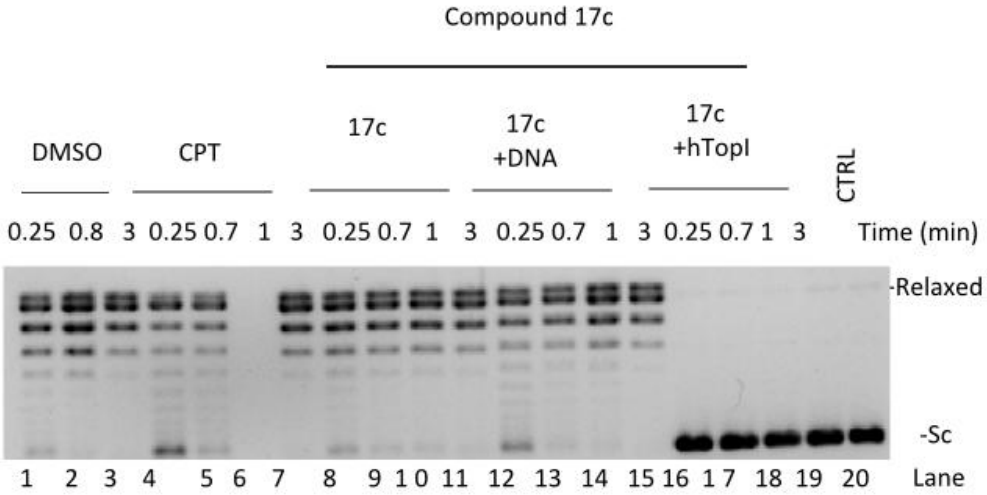

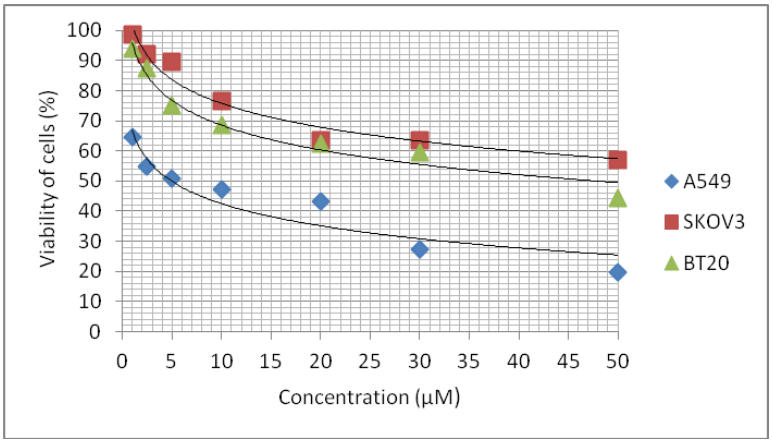

IC_{50} (A549): 5.5±0.2 μM; IC_{50} (SKOV3): >50 μM; IC_{50} (BT20): 48.2±0.7 μM.

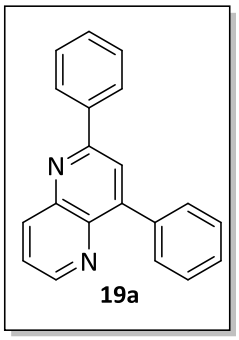

19a

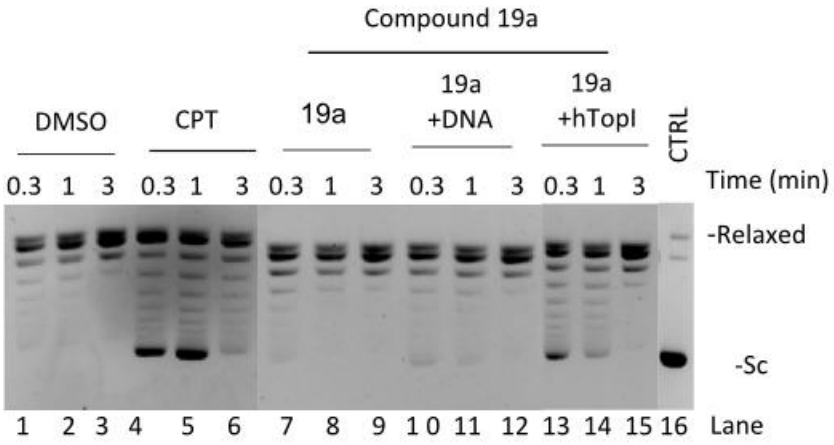

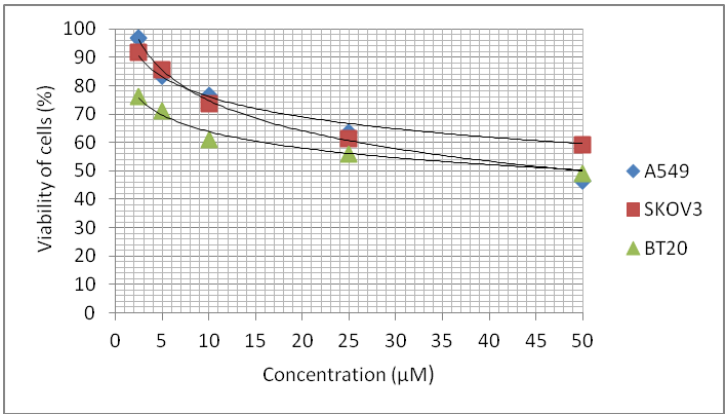

IC_{50} (A549): >50 µM; IC_{50} (SKOV3): >50 µM; IC_{50} (BT20): >50 µM.

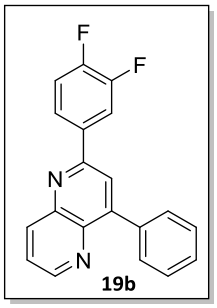

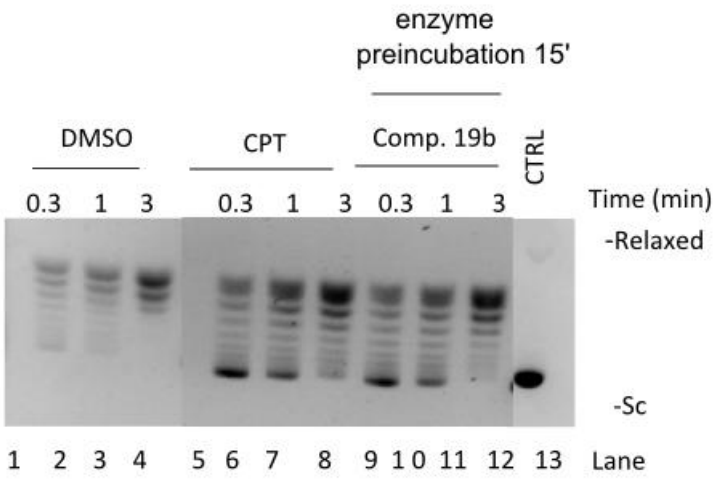

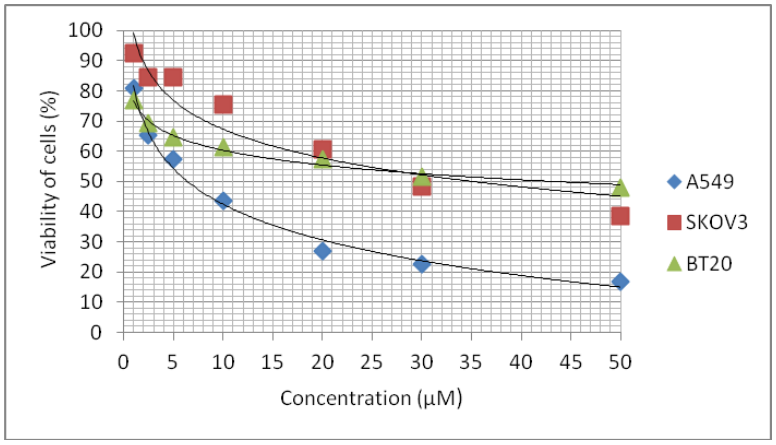

IC_{50} (A549): 5.5±0.9 µM; IC_{50} (SKOV3): 31.7±0.8 µM; IC_{50} (BT20): 39.3±0.6 µM.

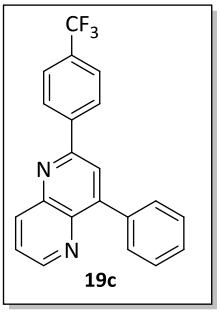

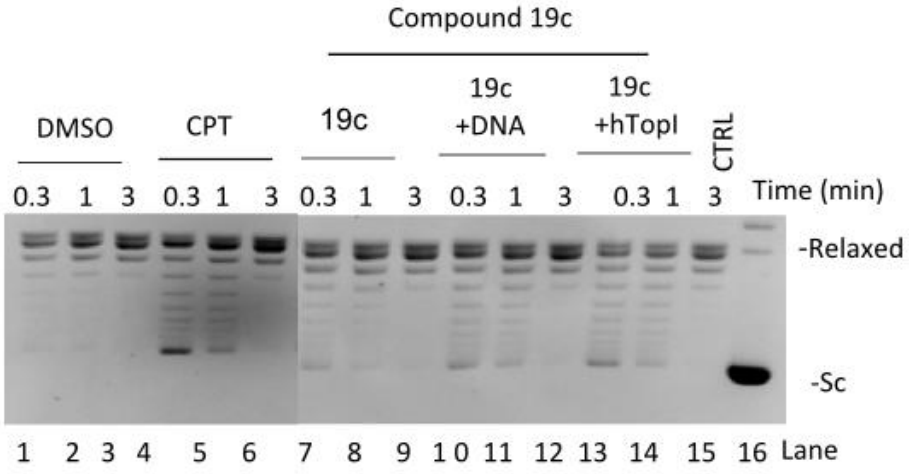

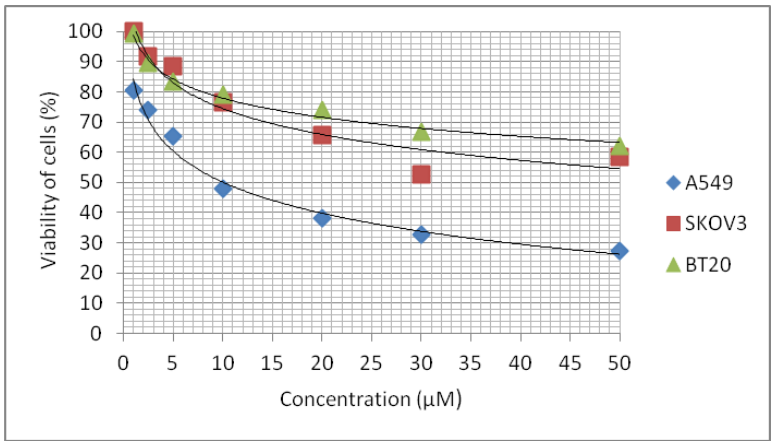

IC_{50} (A549): 9.4±0.4μM; IC_{50} (SKOV3): >50 μM; IC_{50} (BT20): >50 μM.

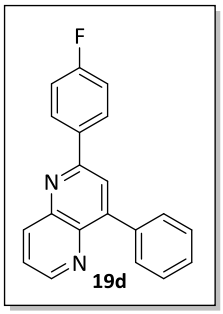

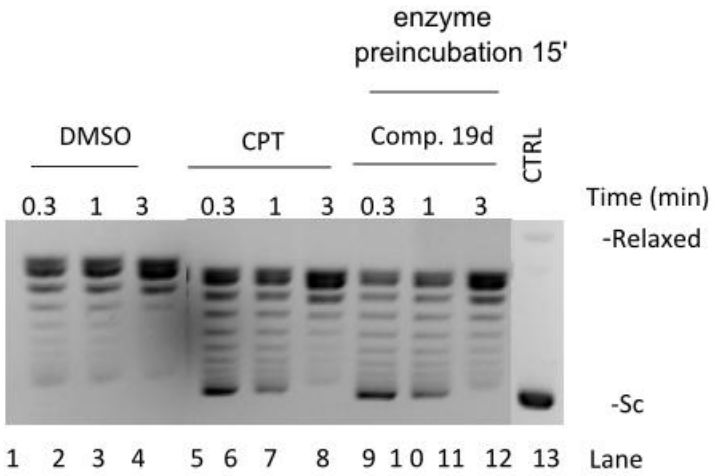

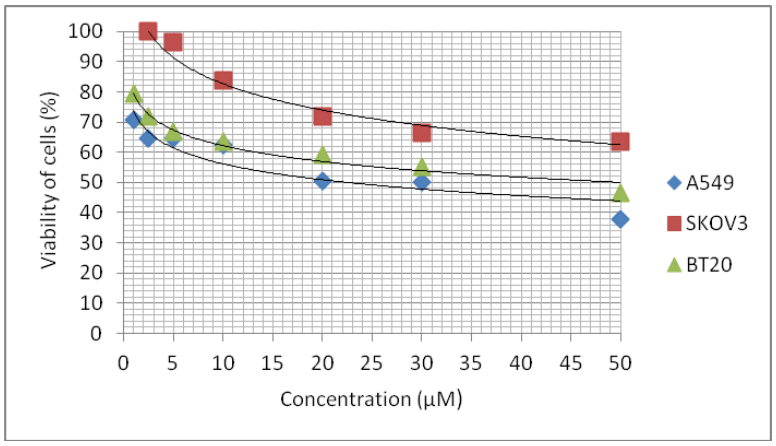

IC_{50} (A549): 20.7±0.4µM; IC_{50} (SKOV3): >50 µM; IC_{50} (BT20): 49.9±0.8µM.

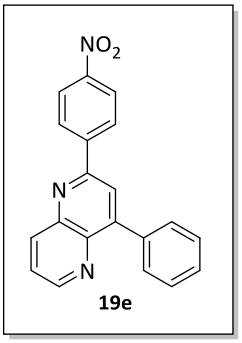

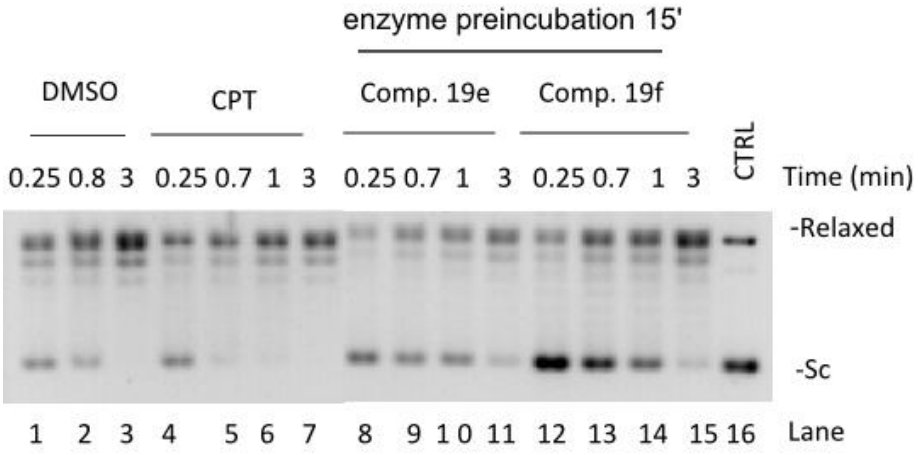

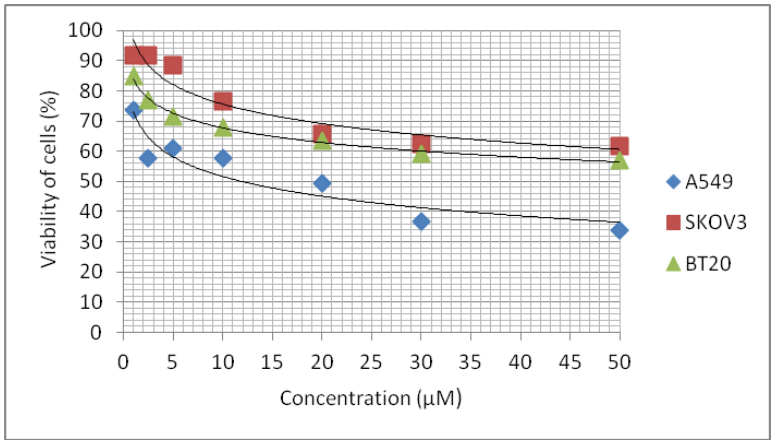

IC_{50} (A549): 11.8±0.1µM; IC_{50} (SKOV3): >50 µM; IC_{50} (BT20): >50 µM.

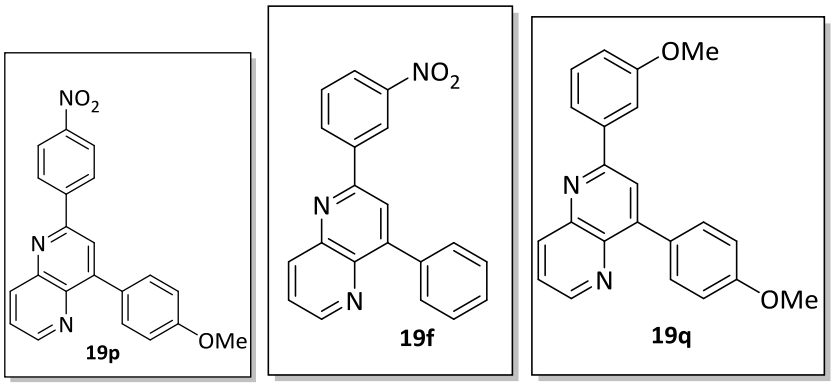

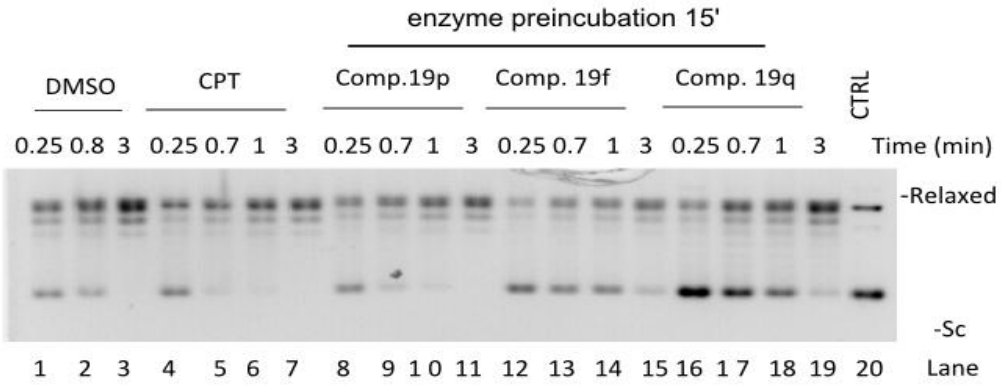

Compound **19f**

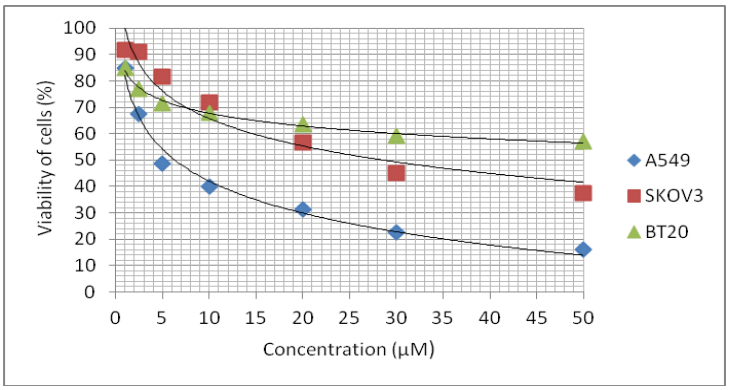

IC_{50} (A549): 6.6±0.5µM; IC_{50} (SKOV3): 28.7±0.4 µM; IC_{50} (BT20): >50 µM.

Compound **19p**

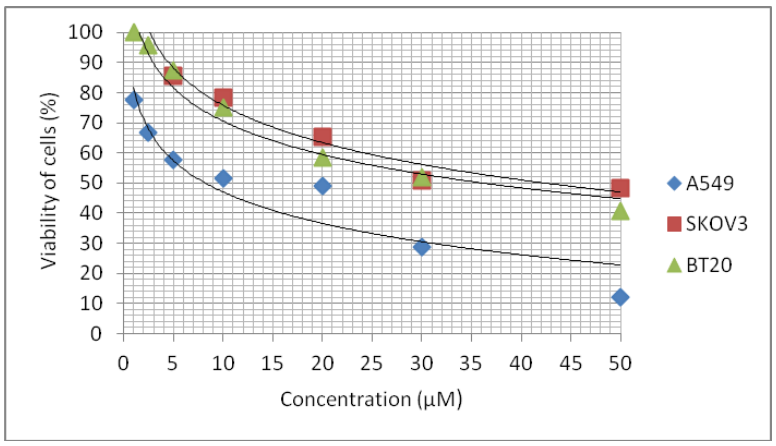

IC_{50} (A549): 8.7±0.3 µM; IC_{50} (SKOV3): 41.5±0.3 µM; IC_{50} (BT20): 36.4±0.4 µM.

Compound **19q**

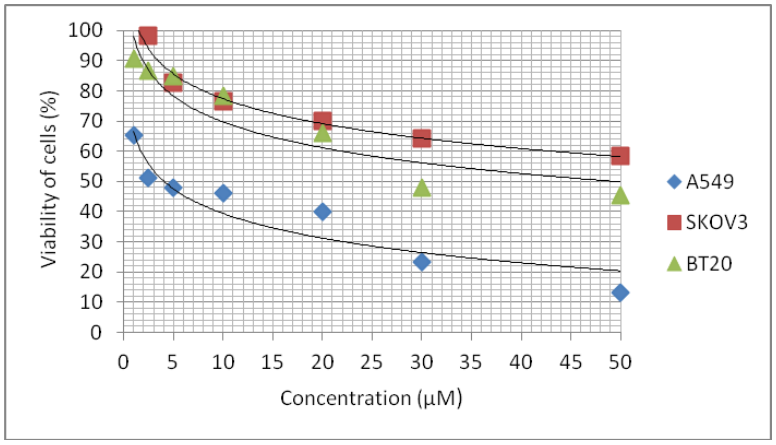

IC_{50} (A549): 4.4±0.4µM; IC_{50} (SKOV3):>50 µM; IC_{50} (BT20): 47.4±0.3 µM.

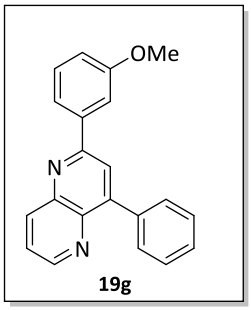

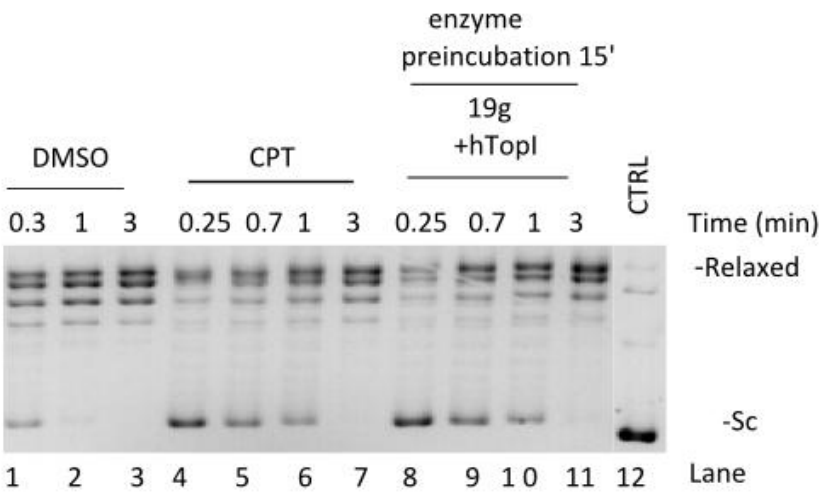

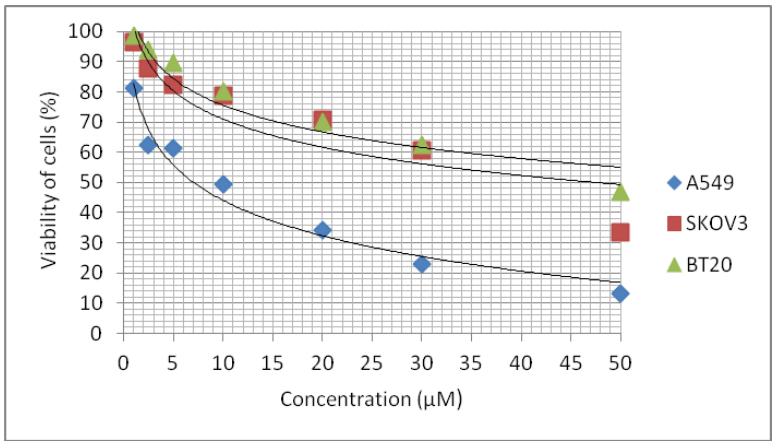

IC_{50} (A549): 6.8±0.5 μM; IC_{50} (SKOV3): >50 μM; IC_{50} (BT20): >50 μM.

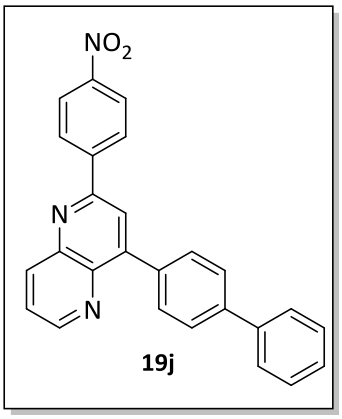
NO2
N
N

19j

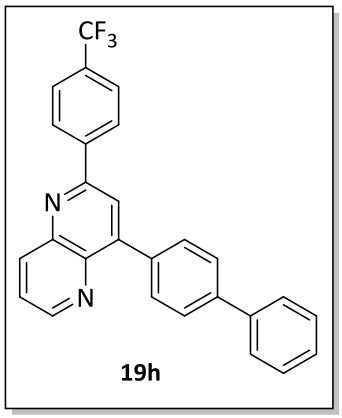
CF3
N
N

19h

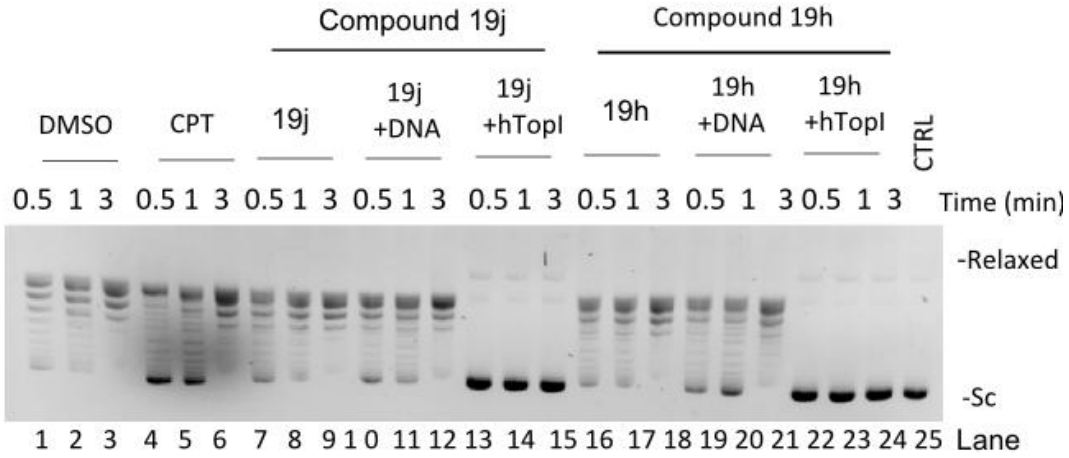
Compound 19j
Compound 19h
DMSO
CPT
19j
19j +DNA
19j +hTopI
19h
19h +DNA
19h +hTopI
CTRL
0.5 1 3 0.5 1 3 0.5 1 3 0.5 1 3 0.5 1 3 0.5 1 3 0.5 1 3 0.5 1 3 Time (min)
-Relaxed
-Sc
1 2 3 4 5 6 7 8 9 10 11 12 13 14 15 16 17 18 19 20 21 22 23 24 25 Lane

Compound **19j**

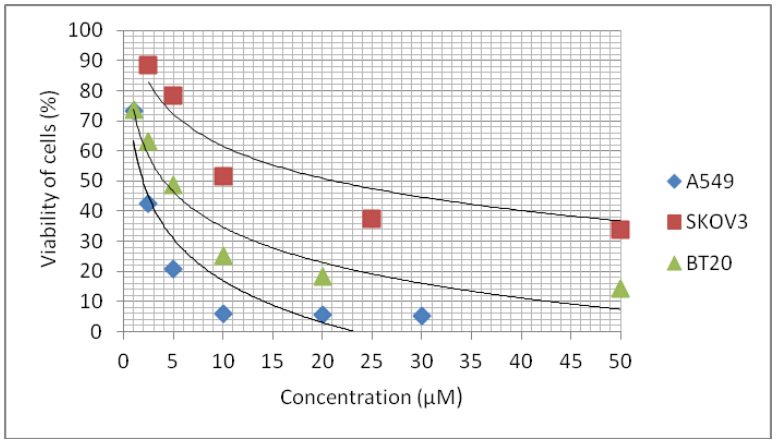

IC_{50} (A549): 1.9±0.4 µM; IC_{50} (SKOV3): 21.5±1.2 µM; IC_{50} (BT20): 3.9±0.3 µM.

Compound **19h**

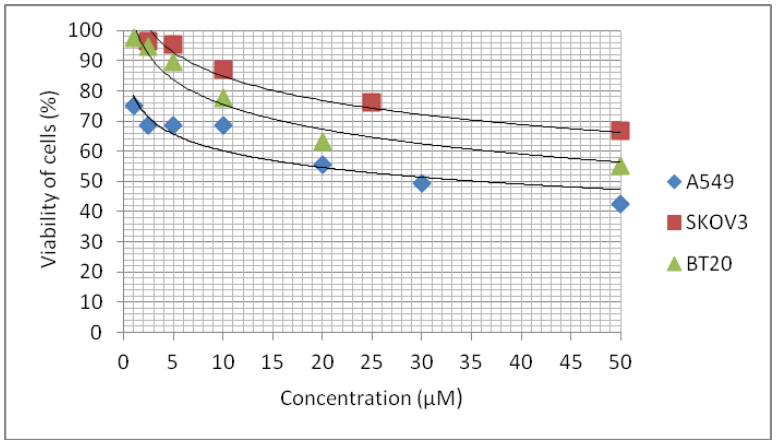

IC_{50} (A549): 40.2±0.8 µM; IC_{50} (SKOV3): >50 µM; IC_{50} (BT20): >50 µM.

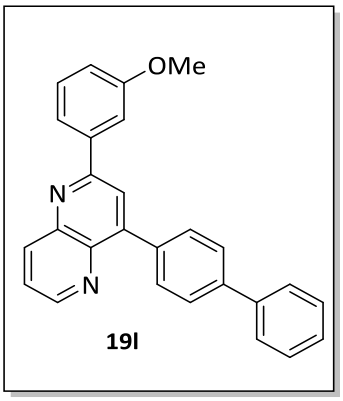
OMe
N
N

19l

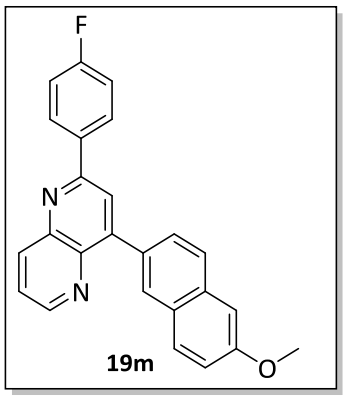
F
N
N
O

19m

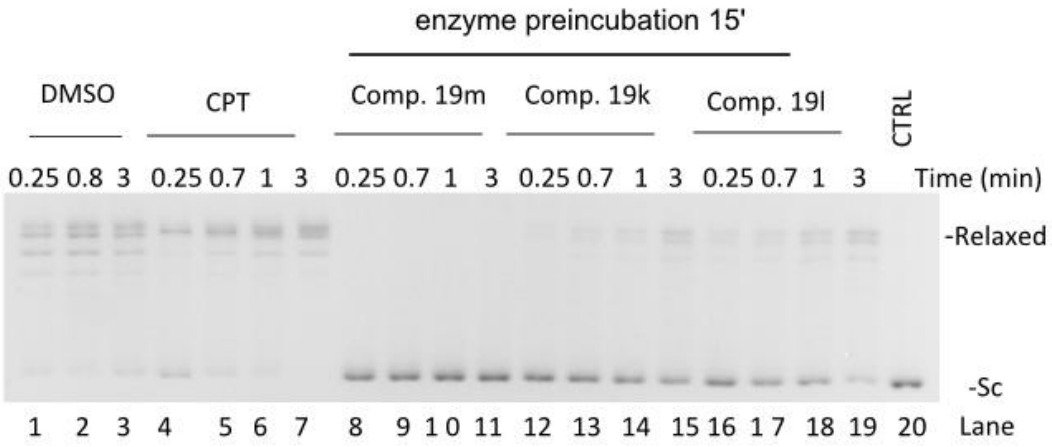
enzyme preincubation 15'
DMSO
CPT
Comp. 19m
Comp. 19k
Comp. 19l
CTRL
0.25 0.8 3 0.25 0.7 1 3 0.25 0.7 1 3 0.25 0.7 1 3 0.25 0.7 1 3
Time (min)
-Relaxed
-Sc
1 2 3 4 5 6 7 8 9 10 11 12 13 14 15 16 17 18 19 20
Lane

Compound **19l**

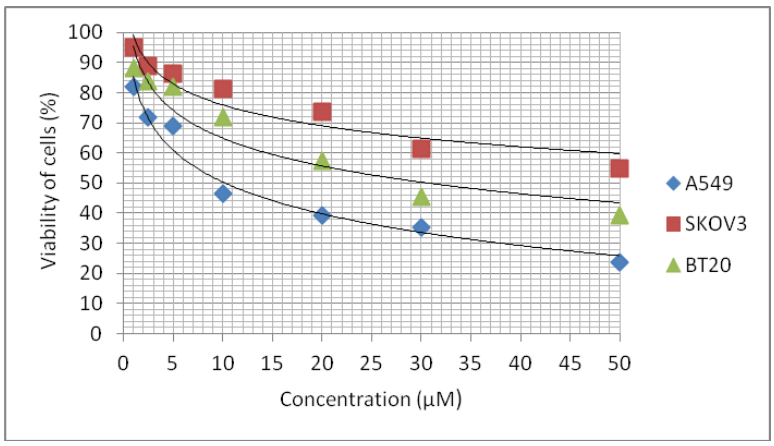

IC_{50} (A549): 9.8±0.4 µM; IC_{50} (SKOV3): >50 µM; IC_{50} (BT20): 31.6±0.4 µM.

Compound **19m**

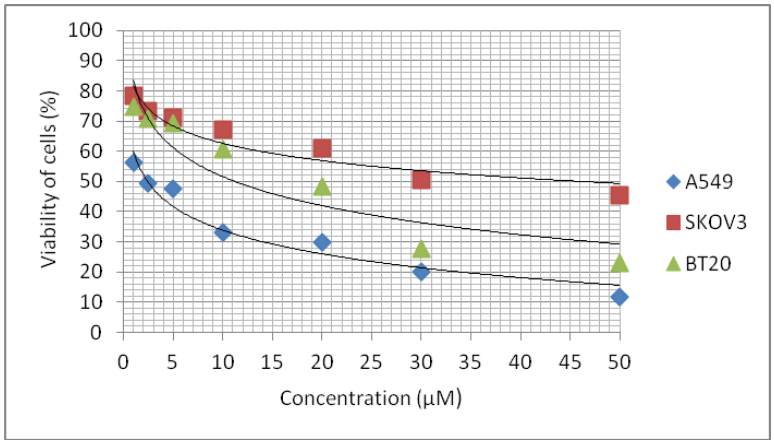

IC_{50} (A549): 2.8±0.6 µM; IC_{50} (SKOV3): 44.5±0.5 µM; IC_{50} (BT20): 12.6±0.1 µM.

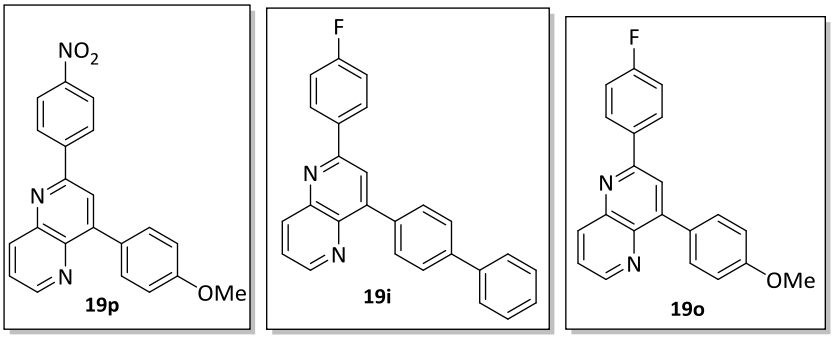

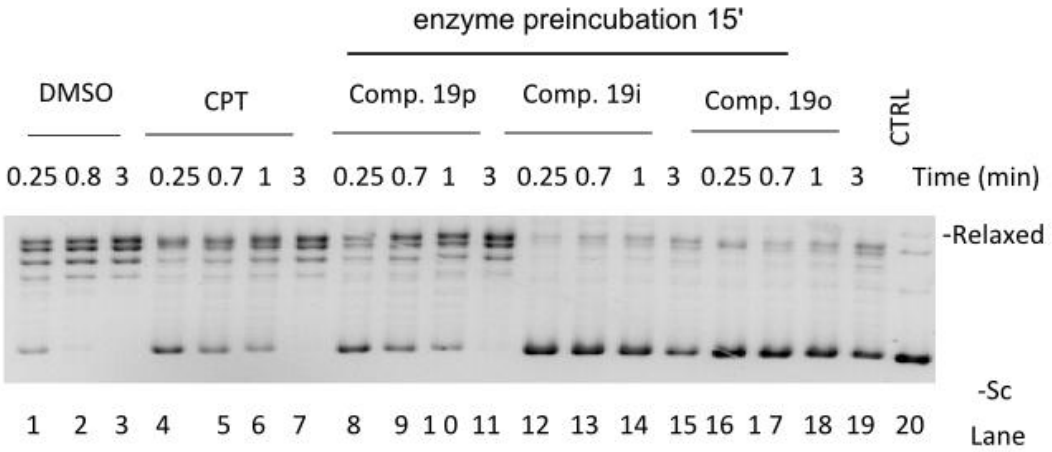

Compound **19p**

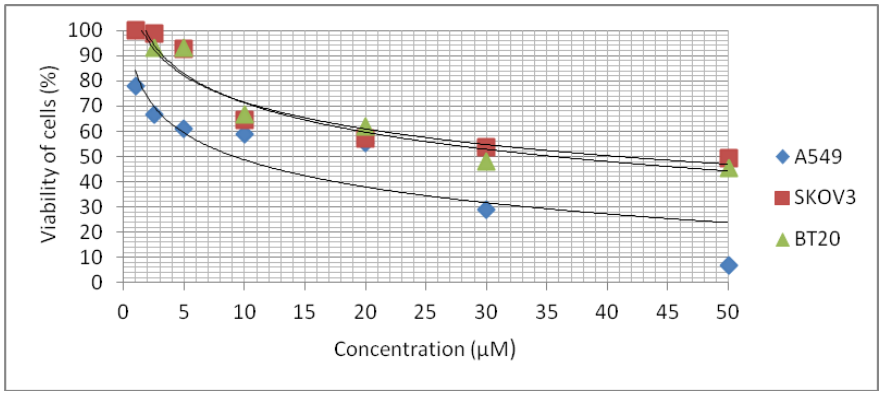

IC_{50} (A549): 8.7±0.3 µM; IC_{50} (SKOV3): 41.5±0.3 µM; IC_{50} (BT20): 36.4±0.4 µM.

Compound **19i**

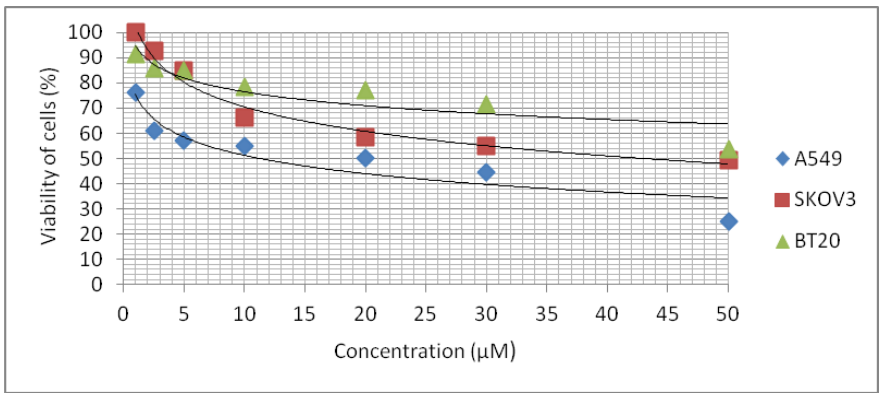

IC_{50} (A549): 11.3±0.2 µM; IC_{50} (SKOV3): >50µM; IC_{50} (BT20): 49.8±0.4 µM.

Compound **19o**

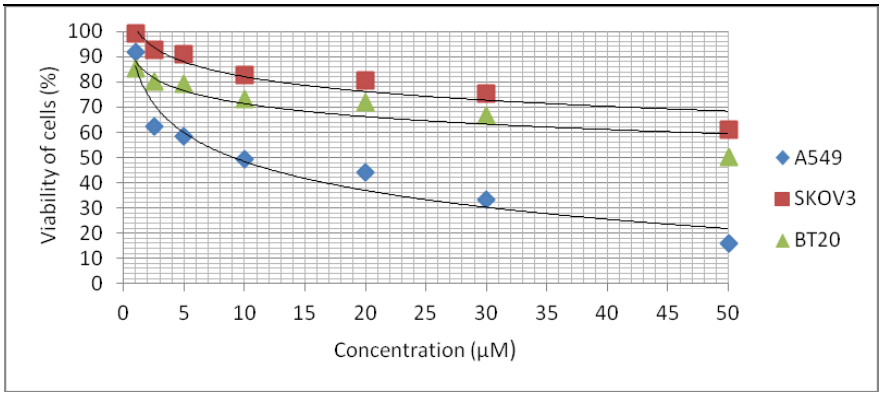

IC_{50} (A549): 9.2±0.4 µM; IC_{50} (SKOV3): >50 µM; IC_{50} (BT20): >50 µM.

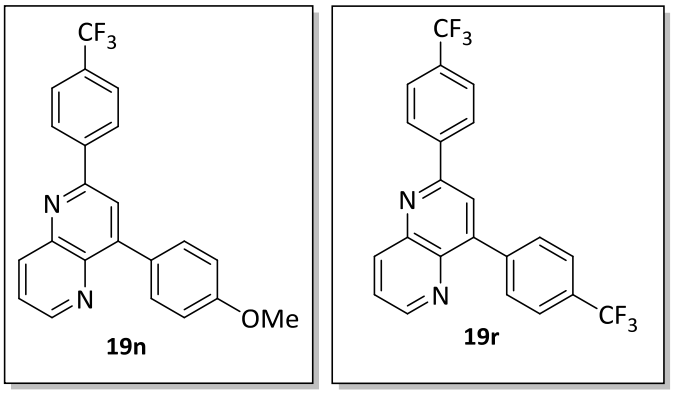
CF3
N
N
OMe
19n
CF3
N
N
CF3
19r

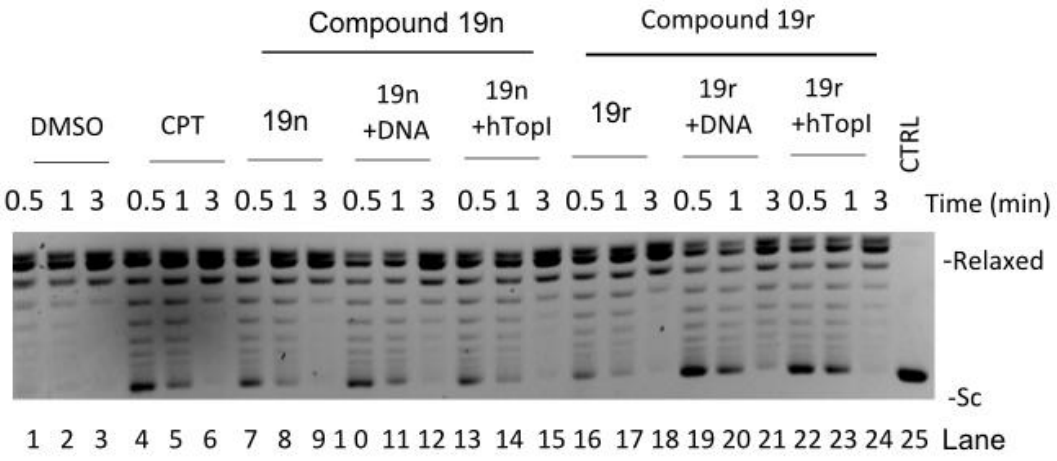
Compound 19n
Compound 19r
DMSO
CPT
19n
19n +DNA
19n +hTopI
19r
19r +DNA
19r +hTopI
CTRL
0.5 1 3 0.5 1 3 0.5 1 3 0.5 1 3 0.5 1 3 0.5 1 3 0.5 1 3 0.5 1 3
Time (min)
-Relaxed
-Sc
1 2 3 4 5 6 7 8 9 10 11 12 13 14 15 16 17 18 19 20 21 22 23 24 25
Lane

Compound **19n**

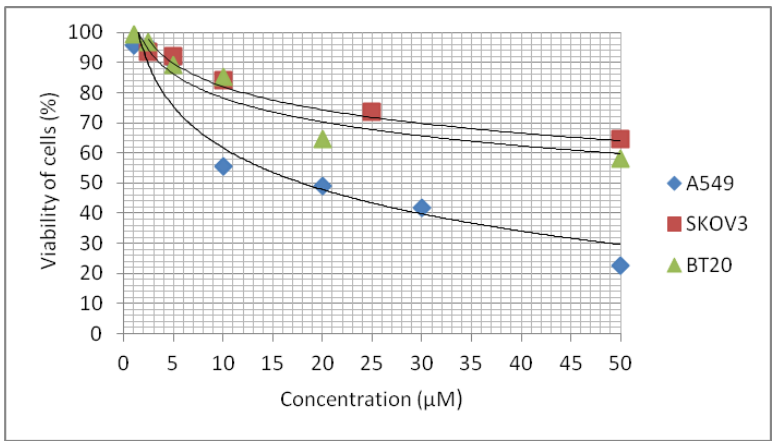

IC_{50} (A549): 19.5±0.6 µM; IC_{50} (SKOV3):>50 µM; IC_{50} (BT20): >50 µM.

Compound **19r**

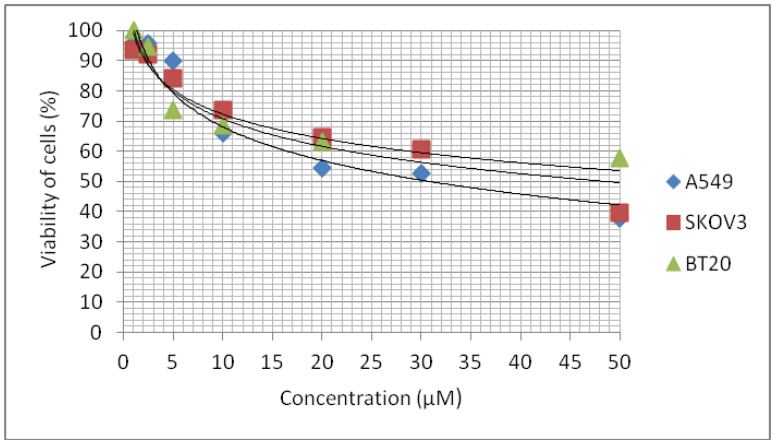

IC_{50} (A549): 27.4±0.7 µM; IC_{50} (SKOV3): 47.9±0.7 µM; IC_{50} (BT20): >50 µM.

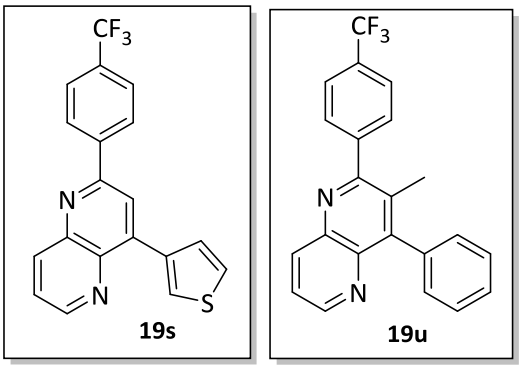
CF3
N
N
S
19s
CF3
N
N
19u

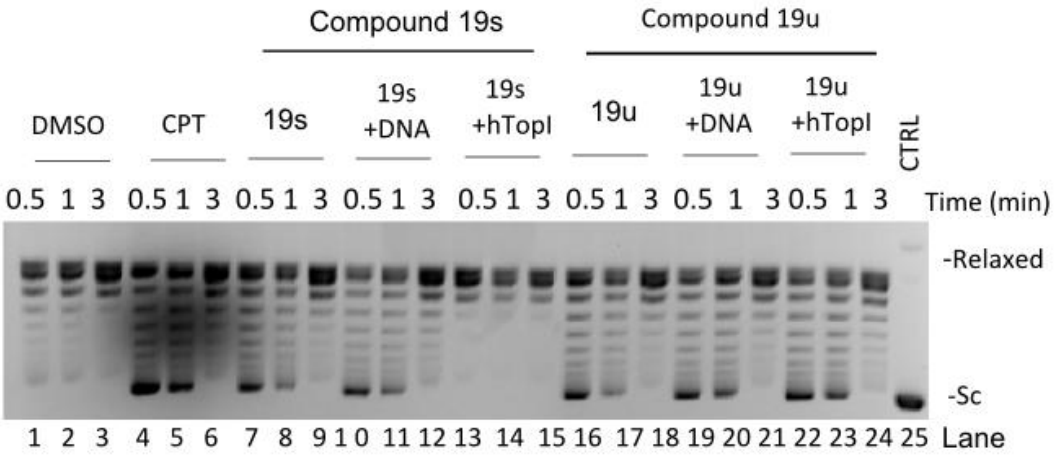
Compound 19s
Compound 19u
DMSO
CPT
19s
19s +DNA
19s +hTopI
19u
19u +DNA
19u +hTopI
CTRL
0.5 1 3 0.5 1 3 0.5 1 3 0.5 1 3 0.5 1 3 0.5 1 3 0.5 1 3 0.5 1 3
Time (min)
-Relaxed
-Sc
1 2 3 4 5 6 7 8 9 10 11 12 13 14 15 16 17 18 19 20 21 22 23 24 25
Lane

Compound **19s**

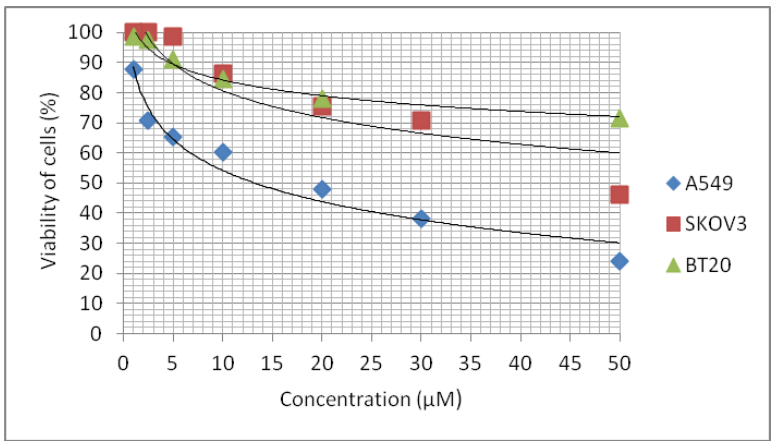

IC_{50} (A549): 13.2±1.5 µM; IC_{50} (SKOV3): >50 µM; IC_{50} (BT20): >50 µM.

Compound **19u**

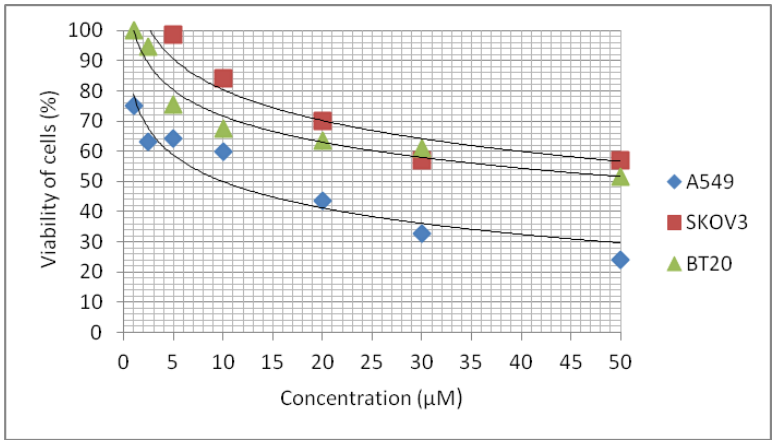

IC_{50} (A549): 10.4±0.2 µM; IC_{50} (SKOV3): >50 µM; IC_{50} (BT20): >50 µM.

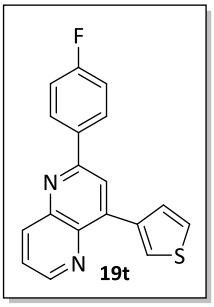

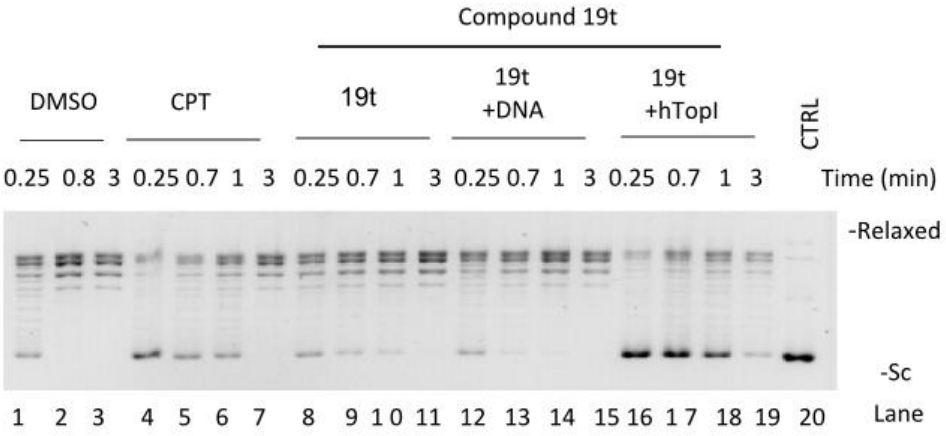

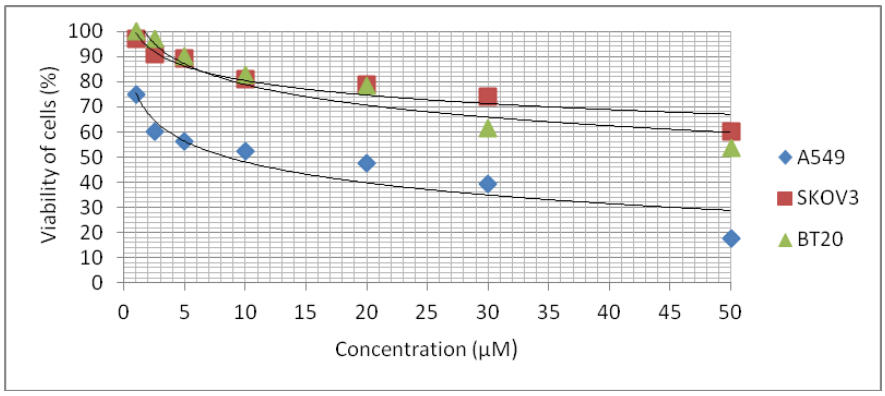

IC_{50} (A549): 8.6±0.3 μM; IC_{50} (SKOV3): >50 μM; IC_{50} (BT20): >50 μM.